Exploring human cortical disease trajectories in ALS using snRNA-seq

Zeynep İrem Güneş

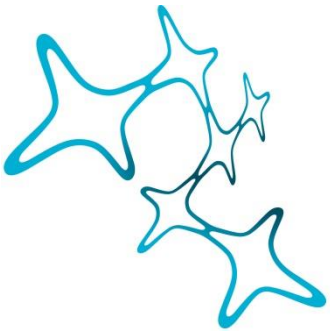

Graduate School of Systemic Neurosciences

LMU Munich

Dissertation at the
Graduate School of Systemic Neurosciences
Ludwig-Maximilians-Universität München

November 2023

Supervisor
Prof. Dr. med. Sabine Liebscher, PhD
Institute of Clinical Neuroimmunology
Biomedical Center (BMC)
Ludwig Maximilian University of Munich

First Reviewer: Prof. Dr. med. Sabine Liebscher, PhD
Second Reviewer: Prof. Dr. med. Dieter Edbauer
External Reviewer: Prof. Dr. Karin Danzer

Date of Submission: November 17, 2023
Date of Defense: April 23, 2024

七転八起

"Nana Korobi Ya Oki"

Table of Contents

List of Abbreviations 1

List of Figures 2

List of Tables 3

Abstract 4

1. Introduction 5

1.1. Amyotrophic Lateral Sclerosis 6
1.1.1. Genetic causes of ALS 8
1.1.2. ALS Neuropathology 10
1.1.3. Therapies available for ALS 13

1.2. Cell autonomous and non-cell autonomous changes in ALS 14
1.2.1. Cell autonomous mechanisms in ALS 15
1.2.2. Non-cell autonomous mechanisms in ALS 19
Microglia 19
Astrocytes 23
Oligodendrocytes and oligodendrocyte progenitor cells (OPCs) 25
Interneurons and non-MN excitatory neurons 27

1.3. TAR DNA Binding Protein 43 29
1.3.1. Structure and physiological function of TDP-43 29
1.3.2. Pathophysiological Role of TDP-43 in ALS 31
Cytoplasmic Accumulation and Nuclear Depletion of TDP-43 32
pTDP-43: A key feature implicated in initiation and progression of cortical disease pathology in ALS 33

1.4. Transcriptomics and the era of single cell RNA sequencing 35
1.4.1. Single cell RNA sequencing 35
Challenges in single cell RNA sequencing 37

2. Aim of the study 39
Hypothesis 39
Research objectives 39

3. Material and Methods 40

3.1. Post- mortem human cortical specimen 40

3.2. RNA integrity determination 41

3.3. Isolation of nuclei from frozen post-mortem human specimen 42

3.4. Genomic library preparation & droplet-based snRNA-seq 42

3.5. Analysis of single nucleus RNA-seq data 44
3.5.1. Quality control (QC) and filtering 44
3.5.2. Annotation of global cell populations 44
3.5.3. Cell population specific subcluster analysis and annotation 44
3.5.4. Pseudotime trajectory inference 45
3.5.5. Gene expression analysis 45
3.5.6. Gene ontology (GO) enrichment analysis 46

3.5.7. Cell-cell interaction (Ligand-Receptor) analysis 46
3.6. Visualization 47
3.7. Immunohistochemistry 47
3.8. Quantitative histopathological assessment 48
3.9. Statistics 48
4. Results 49
4.1. pTDP-43 pathology 49
4.2. Alterations in all cell types in ALS 49
4.3. Cell type specific molecular alterations 54
4.3.1. Microglia 54
4.3.2. Astrocytes 63
4.3.3. Oligodendrocytes 66
4.3.4. Oligodendrocyte progenitor cells (OPCs) 69
4.3.5. Excitatory neurons 72
4.3.6. Interneurons 76
4.3.7. Cell-Cell interaction analysis 79
5. Discussion 84
5.1. Global alterations in the absence of pTDP-43 pathology 84
5.2. Microglia 86
5.3. Astrocytes 90
5.4. Oligodendrocytes & OPCs 92
5.5. Excitatory neurons 93
5.6. Interneurons 95
5.7. Cell-Cell Interaction Analysis Reveals Altered Communication Patterns in ALS 96
5.8. Differences in disease trajectory of sALS and fALS 98
5.9. Limitations of the study 99
6. Concluding Remarks 101
Bibliography 103
Declaration of Author Contributions 132
Acknowledgements 133

List of Abbreviations

AD	Alzheimer's disease
ALS	Amyotrophic lateral sclerosis
AQP4	Aquaporin 4
CNS	Central nervous system
CSF	Cerebrospinal fluid
C9ORF72	Chromosome 9 open reading frame 72
DNA	Deoxyribonucleic acid
DPR	Dipeptide Repeat
EAAT1	Excitatory amino acid transporter 1
EAAT2	Excitatory amino acid transporter 2
EMG	Electromyogram
ER	Endoplasmic reticulum
fALS	Familial amyotrophic lateral sclerosis
FC	Frontal cortex
fMRI	Functional magnetic resonance imaging
FTD	Frontotemporal dementia
FUS	Fused in sarcoma
GABA	Gamma-aminobutyric acid
GFAP	Glial fibrillary acidic protein
HRE	Hexanucleotide repeat expansion
IN	Interneuron
iPSC	Induced pluripotent stem cell
LMN	Lower motor neuron
MC	Motor cortex
MND	Motor neuron disease
MRI	Magnetic resonance imaging
mRNA	Messenger ribonucleic acid
NGS	Next generation sequencing
NMDAR	N-methyl-D-aspartate receptor
PD	Parkinson's disease
pTDP-43	Phosphorylated transactive response DNA-binding protein 43
SOD1	Superoxide dismutase 1
sALS	Sporadic amyotrophic lateral sclerosis
SST	Somatostatin
ROS	Reactive oxygen species
UMN	Upper motor neuron
TDP-43	Transactive response DNA-binding protein 43
Tg	Transgenic
Wt	Wild type

List of Figures

Figure 1. Distribution of genetic mutations in familial ALS (fALS) and sporadic ALS (sALS) in European and Asian populations. 7
Figure 2. Neuropathological features characteristic of classic ALS. 12
Figure 3. Cell autonomous changes involved in the neurodegeneration of motor neurons are partially explained by genetic alterations in ALS. 17
Figure 4. Altered non-cell autonomous mechanisms identified in ALS. 20
Figure 5. TDP-43 and its role in ALS pathophysiology. 30
Figure 6. Various inclusions observed in ALS neuropathology. 34
Figure 7. Schematic overview of methods and RIN of samples used for snRNA-seq. 41
Figure 8. pTDP-43 pathology in end-stage ALS patients included in this study. 49
Figure 9. Single nuclei RNA-seq analysis of global data. 51
Figure 10. Top 10 Gene Ontology (GO) terms enriched for differentially expressed genes (DEGs) identified in global data. 52
Figure 11. Top 10 Gene Ontology (GO) terms enriched for differentially expressed genes (DEGs) identified in pseudobulk global snRNA-seq data. 53
Figure 12. Principal Component Analysis (PCA) of main cell types in the frontal cortex (FC) and motor cortex (MC) across HC and ALS patients show microglia to be the most divergent population. 54
Figure 13. Single nuclei RNA-seq analysis of microglia. 56
Figure 14. Top 10 Gene Ontology (GO) terms enriched for differentially expressed genes (DEGs) identified in microglia. 57
Figure 15. Top enriched GO terms in microglia and corresponding differentially expressed genes (DEGs). 59
Figure 16. Microglial activation precedes pTDP-43 pathology in end-stage ALS patients. 61
Figure 17. Poly-GA inclusions are present in the absence of pTDP-43 pathology and poly-GA load partially correlates with pTDP-43 pathology in end-stage fALS patients. 62
Figure 18. Single nuclei RNA-seq analysis of astrocytes. 64
Figure 19. Top 10 Gene Ontology (GO) terms enriched for differentially expressed genes (DEGs) identified in astrocytes. 65
Figure 20. Single nuclei RNA-seq analysis of oligodendrocytes (OL) and oligodendrocyte progenitor cells (OPCs). 67
Figure 21. Top 10 Gene Ontology (GO) terms enriched for differentially expressed genes (DEGs) identified in oligodendrocytes. 68
Figure 22. Single nuclei RNA-seq analysis of oligodendrocyte progenitor cells (OPCs). 70
Figure 23. Top 10 Gene Ontology (GO) terms enriched for differentially expressed genes (DEGs) identified in oligodendrocyte progenitor cells (OPCs). 71
Figure 24. Single nuclei RNA-seq analysis of excitatory neurons. 74
Figure 25. Top 10 Gene Ontology (GO) terms enriched for differentially expressed genes (DEGs) identified in excitatory neurons. 75
Figure 26. Single nuclei RNA-seq analysis of interneurons. 77
Figure 27. Top 10 Gene Ontology (GO) terms enriched for differentially expressed genes (DEGs) identified in interneurons. 78
Figure 28. Cell-cell communications are altered in ALS compared to HC in frontal (FC) and motor cortex (MC). 80
Figure 29. Region and sample comparison of cell-cell interaction frequency heatmaps. 81
Figure 30.Cell-cell interactions involving microglia are altered early in ALS. 82
Figure 31. Summary of main findings. 101

List of Tables

Table 1. Details of post-mortem human specimens used in this study. 40

Abstract

Amyotrophic Lateral Sclerosis (ALS) is a devastating neurodegenerative disease characterized by the loss of upper and lower motor neurons (UMN and LMN). The presence of pathological phosphorylated TAR DNA-binding protein 43 (pTDP-43) inclusions is the hallmark of ALS pathology, yet the causal relationship between pTDP-43 aggregates and motor neuron (MN) loss is a subject of debate. Investigation of post-mortem brain specimen of ALS patients, hence reflecting end-stage ALS, poses a challenge in identifying early molecular alterations, preceding the onset of pTDP-43 pathology. I addressed this gap by exploiting the fact that pTDP-43 pathology is believed to first occur in motor cortex (MC) from where it spreads in a corticofugal manner to later affect anatomically connected brain regions. To identify early molecular events in ALS I identified ALS patient samples, which displayed clear pTDP-43 pathology in MC but lacked the same in the connected frontal cortex (FC), known to be affected subsequently in the disease and which I thus consider a pTDP-43 pathology 'pre-stage'. Single-nuclei RNA sequencing (snRNA-seq) of post-mortem patient and control tissue was employed to explore region- and disease stage-specific transcriptional alterations in ALS.

I observed various alterations in non-MN cells early in the disease. The key finding of this study is the presence of microglial activation in FC of ALS patients prior to pTDP-43 pathology. Moreover, I show that the cellular crosstalk amongst microglia is already enhanced in FC of ALS patients even in the absence of pTDP-43 aggregates and continues to increase in the affected MC. Concurrently, I observed an upregulation of pro-inflammatory genes in astrocytes, oligodendrocytes and oligodendrocyte precursor cells (OPCs) in both regions. Furthermore, I found transcriptional changes in oligodendrocytes related to synaptic function in FC and MC, arguing for an early impact on oligodendrocytes in ALS, highlighting their susceptibility to ALS disease processes. My results indicate that activation of glial cells is an early event in the disease pathogenesis that precedes the deposition of pTDP-43. Reactive glia cells could thus play a critical role already during the early stages of the disease. In addition, I report a new vulnerable excitatory neuron subtype in MC that appears to be lost in ALS patients as well as a reduced somatostatin expressing interneuron subtype. These findings strongly argue for a broader impact of disease processes, encompassing neurons other than the well-known degenerating motor neurons.

In summary, my investigation reveals early changes in gene transcription in cells other than upper motor neurons (UMNs), suggesting the involvement of non-cell autonomous mechanisms in ALS before the onset of pathological alterations related to pTDP-43.

1. Introduction

In the summer of 2014, millions bravely poured buckets of ice-cold water over their heads in the name of the "Ice Bucket Challenge" to create awareness for a devastating neurodegenerative disease, called amyotrophic lateral sclerosis (ALS). For many, this was the first time they had heard of it, despite that our knowledge of ALS has been growing since the first time it was diagnosed by Jean-Martin Charcot in 1869 (Duyckaerts et al., 2021). Charcot conducted studies on clinical cases and autopsy material to discern the lesions he observed in the central nervous system (CNS). He identified two main sites of lesions that differ in terms of the clinical phenotype of the patients. The lesions in the anterior horn of the spinal cord were present in patients with clinical paralysis with muscle atrophy, whereas the lesions in the lateral horn resulted in progressive paralysis without muscle atrophy (Kumar et al., 2011). Charcot's work has brought together the clinical signs of limb weakness and muscle wasting that were thought to be distinct diseases at the time. He thus deduced the relationship between the phenotypes of inflammation or *'sclerosis'* of the anterior and lateral horn columns together with the degeneration of nerve cells innervating the affected muscles i.e., 'amyotrophic'. Still internationally recognized as 'Charcot's disease', the term 'ALS' was not used until 1874 (Goetz, 2000).

Building on Charcot's discovery, we now know that not only lower motor neurons (LMN) located in the spinal cord but also upper motor neurons (UMN), forming the pyramidal tract of the spinal cord with their long axonal projections, are degenerating in ALS (Jin et al., 2019). Thus, rather referred to as 'Motor Neuron Disease' in the UK, ALS gathered more attention worldwide with the diagnoses of the famous American baseball player Lou Gehrig and the celebrated English theoretical physicist Stephen Hawking. Despite the progress made in understanding the pathomechanisms of ALS, there are no effective treatment options to prevent or halt the progression of the disease available to date, with the very recent exception for a rare genetic form.

In the pursuit of developing treatments for ALS, perhaps one of the key aspects, uncovered in last the decade by the scientific community, is the involvement of other neuronal and glial cells in the disease pathology. While mouse models of ALS present a consistent motor phenotype associated with LMN degeneration, the evaluation of the cortical pathology in ALS mouse models has either resulted in variable findings or has not been conducted in detail. Yet, the assessment of cortical pathology in ALS is vital for understanding the early mechanisms leading to both UMN and LMN degeneration. For instance, cortical hyperexcitability is one of the early signs of ALS and shown to have a potential causal relationship with UMN neurodegeneration. Its root cause has been initially attributed to the altered processes exclusively present in vulnerable UMNs (i.e., cell autonomous mechanisms), however, over

the years, ample evidence has proved that in fact, molecular and functional alterations in glial cells and interneurons (i.e., non-cell autonomous mechanisms) contribute to cortical hyperexcitability, amongst other mechanisms (Gunes et al., 2022). In my thesis, I have aimed to delineate the early molecular changes, occurring in cells other than the vulnerable UMNs and I strove to understand these distinct mechanisms on a transcriptional level. I have investigated these alterations by employing cutting-edge single nucleus RNA-sequencing (snRNA-seq) from post-mortem cortical specimens of ALS patients and controls, with a focus on region- and cell type-specific transcriptomic modifications preceding the occurrence of pTDP-43 pathology.

1.1. Amyotrophic Lateral Sclerosis

Amyotrophic lateral sclerosis (ALS) is a lethal neurodegenerative disease, primarily characterized by progressive paralysis as a result of the degeneration of upper motor neurons (UMN) in the cortex and lower motor neurons (LMN) in the spinal cord and brainstem (Kiernan et al., 2011). Although motor neuron disease (MND) and ALS are often used interchangeably, MND is an umbrella term for several types of diseases, affecting motor neurons, of which ALS accounts for 80-90% of all cases (Román, 1996). Despite being considered a rare disease, ALS is actually the third most common neurodegenerative disease after Alzheimer's (AD) and Parkinson's disease (PD) (Lamptey et al., 2022). With a higher incidence rate in populations of European ancestral origin; the incidence of ALS ranges from 0.6 to 3.8 per 100,000 people per year (Hardiman et al., 2017; Benjaminsen et al., 2018; Lian et al., 2019; Longinetti and Fang, 2019), and occurs with a prevalence of 4 to 8 per 100,000 people (Chiò et al., 2013; Hardiman et al., 2017; Longinetti et al., 2018; Longinetti and Fang, 2019; Turgut et al., 2019). In addition to the demographic differences, males are ~3 times more likely to be diagnosed with ALS (Longinetti and Fang, 2019; Luna et al., 2019). Interestingly, multiple studies report a potential link between lifestyle (Daneshvar et al., 2021), dietary (D'Amico et al., 2021; Goncharova et al., 2021); and environmental risk factors in the pathogenesis of ALS (Lian et al., 2019). For example, professional football players of the National Football League (NFL) have been reported to be ~4 times more likely to develop ALS compared to non-athletes (Daneshvar et al., 2021). Similarly, "blue-collar" workers, who are carrying out intense physically demanding work on a daily basis, also have a higher risk of developing ALS (Farrugia Wismayer et al., 2021).

Clinically, the symptoms patients present with, differ based on the site of onset of the initial neurodegeneration. About 25% of patients have a bulbar onset, which is presented with difficulty in speech and swallowing, and a worse prognosis than the spinal onset variant (Kiernan et al., 2011). The majority of patients present with a spinal onset and primarily exhibit muscle weakness and spasms in extremities. The heterogeneity of different forms of the

disease manifestation and inter-patient differences in LMN and/or UMN vulnerability makes ALS challenging to diagnose (Zhang et al., 2014).

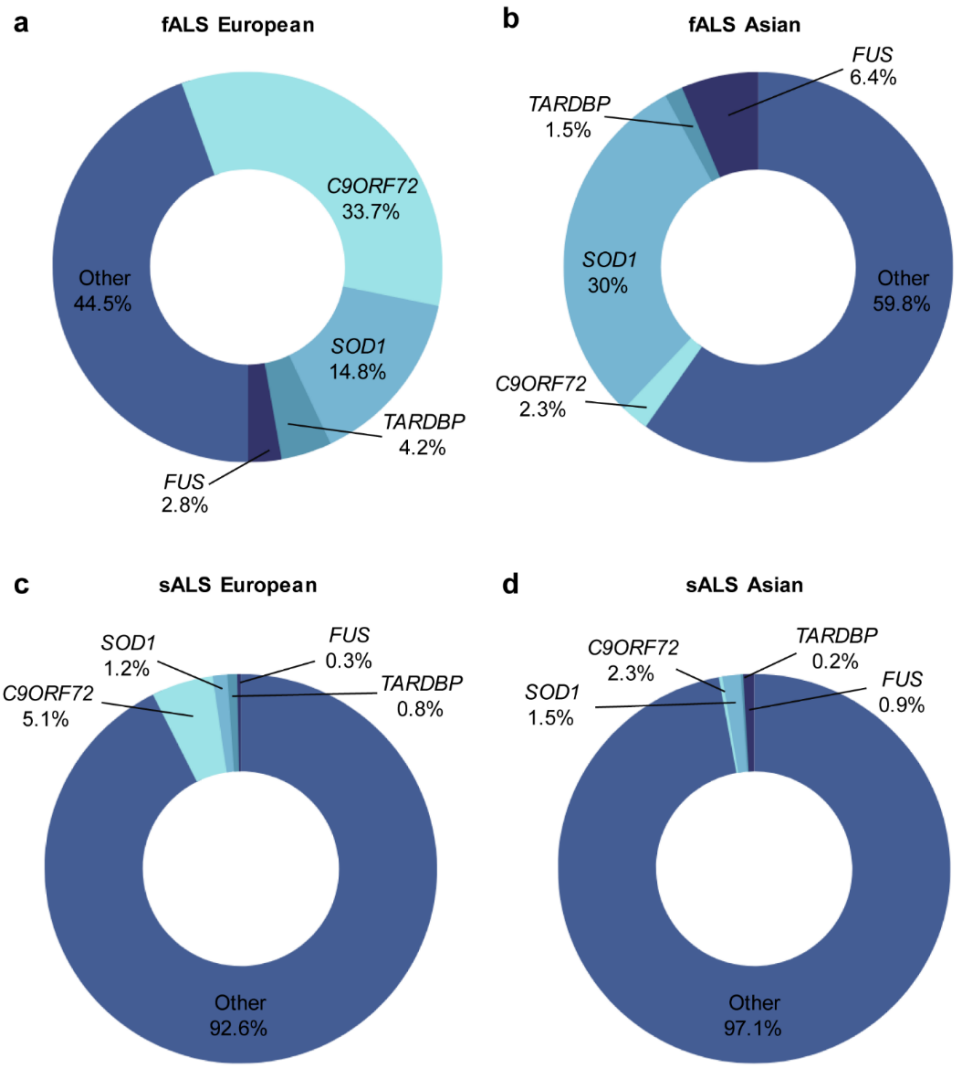

Figure 1. Distribution of genetic mutations in familial ALS (fALS) and sporadic ALS (sALS) in European and Asian populations.

The top four genetic causes of amyotrophic lateral sclerosis (ALS) in European (**a**) and Asian populations (**b**) involve mutations in chromosome 9 open reading frame 72 (*C9ORF72*), superoxide dismutase 1 (*SOD1*), transactive response DNA-binding protein (*TARDBP*) and fused in sarcoma (*FUS*). Note the difference between top leading genetic causes of fALS in European and Asian populations. These mutations and other genetic variants are absent in over 90% of sALS cases in Europe (**c**) and in Asia (**d**). Adapted from (Mejzini et al., 2019).

The cause of 90-95% of all ALS cases remains unexplained to date, classified as sporadic ALS (sALS), whereas the remaining 5-10% account for familial ALS (fALS), which are explained by genetic mutations (Chen et al., 2013b; Brown and Al-Chalabi, 2017; Mejzini et al., 2019). The mean age of disease onset is ~50-60 years with ~5 years earlier onset in fALS cases compared to sALS (Mehta et al., 2019). In addition to motor symptoms, 62% of fALS patients and 48% of sALS patients show signs of cognitive impairment (Wheaton et al., 2007).

As such, ALS often coexists with a condition called frontotemporal dementia (FTD), which is characterized by the neurodegeneration of the frontal and temporal lobes, resulting in cognitive deficits and behavioral changes in affected people. Despite being different diseases, due to the high comorbidity of ALS and FTD, "ALS-FTD spectrum disorders" is often used to describe this broad spectrum of neurodegenerative diseases (Ferrari et al., 2011). In fact, almost 50% of all ALS patients present symptoms of cognitive impairment similar to FTD, while 15% of them have a coexisting diagnosis of FTD (mostly behavioral variant FTD in which patients have early prominent behavioral changes) (Ringholz et al., 2005) and ~15% of FTD patients have ALS-like motor symptoms (Ling et al., 2013). Albeit the variety in the disease symptoms, all patients eventually succumb to the disease due to respiratory failure. Overall, the median survival time after onset of symptoms is 20-48 months, while in 10-20% of exceptional cases, patients survive longer than 10 years (Chiò et al., 2009).

1.1.1. Genetic causes of ALS

To date, over 50 genes and pathogenic gene variants have been linked to ALS (Taylor et al., 2016; Mejzini et al., 2019; Smukowski et al., 2022). The intronic hexanucleotide $(G_4C_2)_n$ repeat expansions (HRE) in the chromosome 9 open reading frame 72 *(C9ORF72)* is the leading genetic cause of fALS in Europe (**Figure 1a**) and is also detected in up to ~5% of sALS patients (**Figure 1c**) (Zou et al., 2017; Mejzini et al., 2019). In Asian populations, however, mutations in the superoxide dismutase 1 (*SOD1*) gene are the most common form of fALS accounting for 30% of the cases (**Figure 1b**), in addition to 1-2% of sALS cases (**Figure 1d**) (Zou et al., 2017; Mejzini et al., 2019). Furthermore, mutations in the transactive response DNA-binding protein 43 (*TARDBP*) and fused in sarcoma (*FUS*) make up to ~7% of fALS cases (Zou et al., 2017; Mejzini et al., 2019). To name a few, more rare ALS-associated mutations are reported in optineurin *(OPTN)*, TANK-binding kinase 1 *(TBK1)*, ataxin (*ATXN2*), heterogeneous ribonucleoprotein A1 (*hnRNPA1*) and alsin (*ALS2*) (Kim et al., 2013; Renton et al., 2014; Cirulli et al., 2015; Glass et al., 2022).

Identified in 1993, *SOD1 was* the first gene implicated in hereditary ALS (Rosen et al., 1993). More than 200 variants of *SOD1* mutations have been identified, the majority of them are missense mutations inherited in an autosomal dominant manner (e.g., D90A, A4V, G93A) (Ruffo et al., 2022). The SOD1 peptide functions as a scavenger of reactive oxygen species (ROS), therefore, it was initially postulated that loss of function in SOD1 could be causative to ALS. Later, this idea was abandoned as *SOD1* knockout mice do not develop an ALS-like phenotype despite increased ROS (Reaume et al., 1996). In the $SOD1^{G93A}$ mouse model of ALS, where mutant SOD1 is overexpressed in cytoplasm and wild type SOD1 is depleted in the nucleus, increased DNA damage was reported (Sau et al., 2007). Moreover, non-native forms of wild-type SOD1 are present in sALS patients in addition to non-native toxic oligomeric

conformations of mutant SOD1 in fALS patients, despite the lack of mutations in highly amyloidogenic sequence fragments that are known to cause fibril-like aggregation (also called “hot spot” mutations) (Khare et al., 2005; Boillée et al., 2006a; Pasinelli and Brown, 2006; Tzotzos and Doig, 2010). These findings indicate that while the loss of SOD1 enzymatic activity has a disease modifying role i.e., reduced protection from ROS, the main effect of *SOD1* mutations in ALS points to a toxic gain of function of mutant SOD1 i.e., protein misfolding and aggregation (Saccon et al., 2013).

An important breakthrough in the field came with the discovery of the mutations in the intronic region of *C9ORF72* gene in 2011. These mutations are based on HREs in the non-coding region of *C9ORF72* and could lead to the development of ALS (van der Zee et al., 2013; Gendron and Petrucelli, 2018). The number of $(G_4C_2)_n$ repeats differs between ALS patients, with some harboring hundreds or even thousands of these repeats, whereas less than 25 repeats are detected in healthy people and considered not pathogenic (Majounie et al., 2012; van der Zee et al., 2013). Under physiological conditions, the C9ORF72 transcript is involved in many cellular processes. It is localized in the nuclear membrane and regulates the nucleocytoplasmic import via Importin b1 and Ran-GTPase (Xiao et al., 2015). In addition, C9ORF72 is necessary for the recruitment and degradation of stress granules, and it regulates the expression of downstream genes involved in this process (e.g., *TIA-1*, *G3BP1*, *HuR*) (Maharjan et al., 2017). Moreover, C9ORF72 mediates the degradation of protein aggregates via interacting with cytosolic chaperones (Maharjan et al., 2017). Although there is still a lot to be uncovered about the physiological role of C9ORF72, accumulating evidence shows that C9ORF72 exerts its detrimental impact in ALS via a loss of function and haploinsufficiency, resulting in decreased functional protein and mRNA levels of the actual gene product as one consequence of HRE (Niblock et al., 2016; Barker et al., 2017; Smeyers et al., 2021). Both sense and anti-sense RNA transcripts of HRE are translated in an unconventional manner called repeat-associated non-AUG (RAN) translation, forming 5 toxic species of proteins, namely dipeptide repeat proteins (DPRs) (Ash et al., 2013; Mori et al., 2013a; Mori et al., 2013b). DPRs form aggregates, shown to be present in the neocortex, hippocampus and cerebellum of fALS patients harboring *C9ORF72* mutations, with the toxicity of the inclusions seemingly being dose dependent (Mori et al., 2013b).

Numerous mutations in genes encoding for RNA binding proteins (RBPs) are furthermore associated with ALS (Zhao et al., 2018). Under physiological conditions, RBPs regulate gene expression, RNA transport and local translation (Kim et al., 2021). In ALS, RBPs lose their physiological functions, disrupting regulation of RNA metabolism and structure, and resulting in formation of pathogenic cytoplasmic aggregations of certain proteins (Polymenidou et al., 2012; Tyzack et al., 2019; de Boer et al., 2021; Kim et al., 2021). Two extensively studied

RBPs are TDP-43 and FUS. TDP-43 is the translation product of *TARDBP,* predominantly located in the nucleus and it binds to both RNA and DNA to modulate gene expression in various ways (see section 1.3.1.). One striking consequence of *TARDBP* mutations is nuclear depletion and cytoplasmic mislocalization and aggregation of TDP-43 (Cykowski et al., 2014; Prasad et al., 2019; Benson et al., 2021). These inclusions are the pathological hallmark of ALS and are found in 97% of all ALS patients, even in the absence of *TARDBP* mutations (Neumann et al., 2006; Ling et al., 2013). Thus, loss of function of TDP-43 and toxicity of cytoplasmic aggregates are likely tightly linked to neurodegeneration. The possible pathologic mechanisms of TDP-43 in ALS are described later in detail (see section 1.3.2.).

Similar to TDP-43, mutations in FUS were shown to cause cytoplasmic accumulation of the protein as opposed to its nuclear localization (Zinszner et al., 1997), and are believed to enhance the propensity of FUS to aggregate in the cytoplasm. Nonetheless, mislocalization of FUS and aggregation of mutated FUS were demonstrated also in non-SOD1 fALS patients with no known FUS mutations (i.e., one patient with TDP43^{G298S} mutation and 10 with unknown genetic causes) and in sALS cases (Deng et al., 2010). Moreover, colocalized aggregates of FUS and TDP-43 in motor neurons are reported in a proportion of sALS and fALS (FUS mutation carriers) cases (Kwiatkowski et al., 2009; Deng et al., 2010).

Genetic variants of TDP-43 and FUS are not only involved in ALS pathogenesis but also in FTD. The presence of wild-type FUS inclusions is shown to be part of FUS - FTD pathology, and interestingly, overexpression of human wild-type FUS is sufficient to cause an ALS-like motor phenotype in a mouse model (Mitchell et al., 2013).

Overall, the plethora of genetic mutations only partially explains potential pathomechanisms in ALS, and many of the uncovered mechanisms point to a dysregulation in RNA metabolism, which seems to be not exclusive to ALS, but involved in many neurodegenerative diseases (Maziuk et al., 2017; Nussbacher et al., 2019).

1.1.2. ALS Neuropathology

Gross CNS changes (e.g., reduction of gray matter volume) in ALS vary from patient to patient. Post-mortem examination of ALS patients shows anterior horn atrophy and thinning of anterior roots of spinal cord (Duyckaerts et al., 2021). Although primary motor cortex is the most affected cortical region in ALS patients, magnetic resonance imaging (MRI) studies reports bilateral cortical thinning of not only primary motor cortex (MC) (i.e., at precentral gyrus) but also, prefrontal and ventral frontal cortices, cingulate gyrus, insula and other subcortical regions (Abrahams et al., 2005; Kassubek et al., 2005; Agosta et al., 2012). Surprisingly, ALS patients, that were also diagnosed with FTD at a later disease stage, already have pronounced frontal (FC) and temporal cortex gray matter atrophy even in the absence of clinical FTD

symptoms, when measured by voxel-based morphometry of MRI (Chang et al., 2005). In addition, reduced white matter density along the corticospinal tract and corpus callosum is also present in ALS patients (Kassubek et al., 2005).

Lacking early gross changes in CNS composition, the identification of disease pathology is dominated by microscopic observations. Degeneration of LMNs in spinal cord (**Figure 2a-b**) and UMNs, or Betz cells, located in layer 5 of motor cortex (**Figure 2c-d**) and demyelination of anterior and lateral horn axons are the hallmarks of the disease. Shrinkage of UMNs and LMNs in ALS (**Figure 2e-f**) is often accompanied by spongiosis (i.e., sponge like tissue morphology) and vacuolization (i.e., empty large spaces) around UMNs and LMNs are additional microscopic changes (**Figure 2g-h**) (Saberi et al., 2015).

One of the characteristic pathological features of ALS is the presence of Bunina bodies, which are eosinophilic cytoplasmic inclusions, found in degenerating neurons (**Figure 2i-j**). These small (3-6 µm) structures are composed of aggregated proteins, and their number can vary depending on the neuron. Bunina bodies are not often present in Betz cells but in LMNs (Okamoto et al., 2008). They are positive for proteins like cystatin c and transferrin (**Figure 2k-l**), while a small fraction also colocalizes with peripherin (Okamoto et al., 2008; Mizuno et al., 2011). Interestingly, these intracellular inclusions do not express proteins closely associated with neurodegeneration and neuroinflammation (e.g., tau, glial fibrillary acidic protein (GFAP), synaptophysin, p62) (Saberi et al., 2015), and it is unclear whether they express ubiquitin (Lowe et al., 1988; Murayama et al., 1990).

Another feature of ALS pathology is non-neuronal signs of neurodegeneration. Gliosis, or activation of adjacent glial cells as a response to affected neurons, is present in both sporadic and familial cases (McGeer and McGeer, 2002; Boillée et al., 2006b; Yamanaka et al., 2008). Post-mortem immunohistological analyses show that activation of microglia and astrocytes is a common feature in both the cortex and the spinal cord (Saberi et al., 2015) (**Figure 2m-n**). Promoting inflammation in the otherwise immune-privileged CNS, the activation of microglia and astrocytes is mainly a protective mechanism to fight off pathogenic molecular cues and to promote tissue repair (Ransohoff, 2016; Kwon and Koh, 2020). These processes result in an increase in the number of phagocytic glia as well as their hypertrophy (Konishi et al., 2022). In neurodegenerative diseases, however, an excessive or chronic inflammatory response can prove detrimental to the neurons causing “neuroinflammation” and damaging the tissue (Ransohoff, 2016; Kwon and Koh, 2020).

These various microscopic changes already point to the complexity of molecular and cellular changes occurring in both neuronal and non-neuronal cells in ALS. Since these findings are largely limited to post-mortem tissue analyses, the ALS field strives to understand how these processes (i.e., protein aggregation) and the sequence of events are linked to neurodegeneration (see section 1.2.).

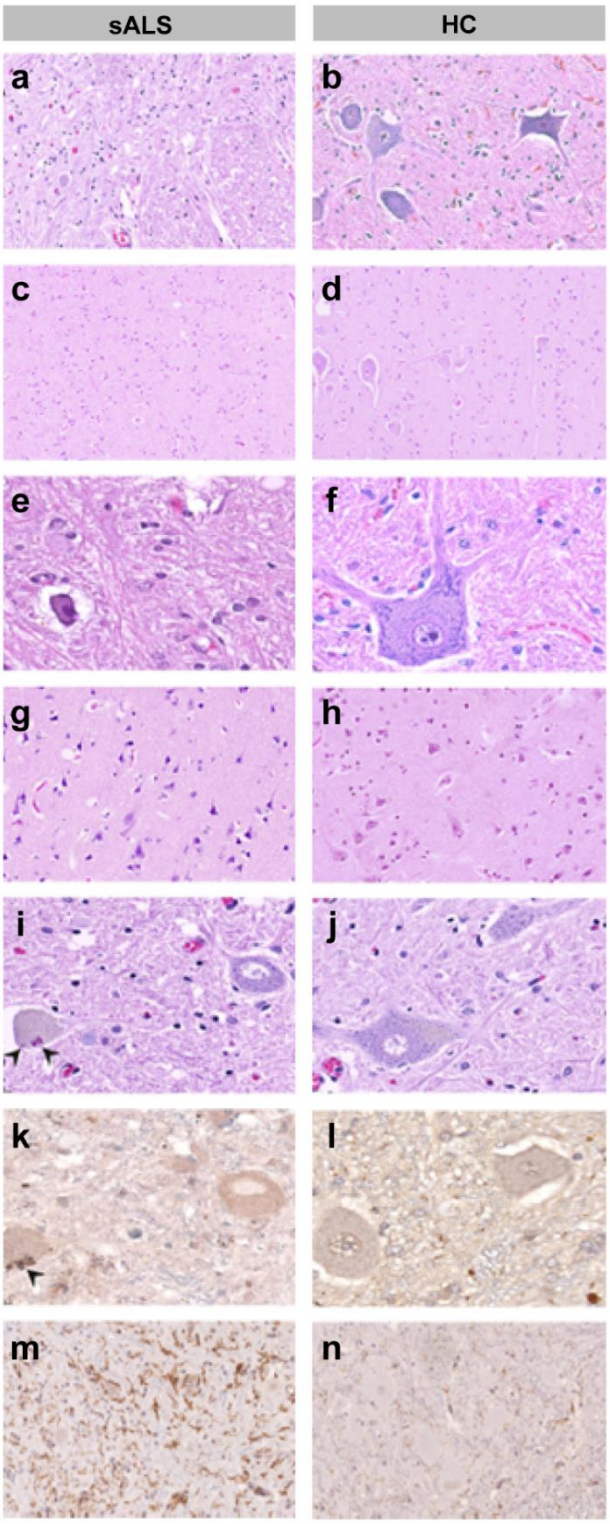

Figure 2. **Neuropathological features characteristic of classic ALS.**

Images illustrate the loss of motor neurons and the presence of astrogliosis in both the anterior horn of (**a**) the spinal cord (20x) and (**c**) the motor cortex (10x) of individuals with sporadic ALS (sALS), compared to respective regions from (**b, d**) control subjects (20x). (**e, f**) Shrinkage and contraction of motor neurons are present in ALS compared to control cases (40x). (**g**) Vacuolization and spongiosis in the motor cortex are evident in ALS (20x) as opposed to (**h**) control (20x). (**i**) Bunina bodies, marked by arrowheads, are visible in the cytoplasm of motor neurons in ALS (40x), contrasting with their absence in (**j**) control cases (40x). These Bunina bodies are found to be positive for cystatin c in (**k**) ALS (40x, arrowhead), whereas not present in the (**l**) control samples (40x). Lastly, microglial activation, as indicated by positive Iba1 staining, is observed in the anterior horn of the spinal cord in (**m**) ALS (20x), but not in (**n**) control samples (20x). (**a–j**) The tissue sections were stained with hematoxylin and eosin (H&E) for visualization. Taken and adapted from (Saberi et al., 2015).

1.1.3. Therapies available for ALS

Despite immense efforts to slow down or find a cure for ALS, there are only 4 Food and Drug Administration (FDA) approved treatment options available to combat ALS, namely riluzole, edaravone, relyvrio and tofersen. Upon diagnosis, riluzole is given as the first-line treatment to ALS patients since 1995. Being the first FDA-approved medication for ALS, riluzole works by blocking pre-synaptic release of glutamate and by acting as an antagonist to N-methyl-D-aspartate receptors (NMDARs) (Doble, 1996) on postsynaptic neurons. Initial clinical trials have shown an increase in survival for 2-3 months in riluzole-treated patients compared to placebo treated ALS patients (Bensimon et al., 1994). However, more than two decades after its initial clinical trial, real world data indicates that riluzole significantly extends patient survival by 6-21 months (Hinchcliffe and Smith, 2017; Andrews et al., 2020; Chen, 2020).

The second drug approved for ALS by the FDA in 2017 is edaravone, which was initially developed as a free radical scavenger for stroke (Rothstein, 2017; Cruz, 2018). It acts as an antioxidant, and potentially reduces oxidative stress in affected motor neurons. A combination therapy of riluzole and edaravone is often given to patients diagnosed in early stages (Dash et al., 2018; Samadhiya et al., 2022). While riluzole extends survival, the benefit of edaravone is only limited to slowing the progression of the disease by delaying muscle atrophy for a short time (Abe et al., 2017; Sawada, 2017; Samadhiya et al., 2022).

Developing treatments for ALS has been truly a challenging endeavor. Only from 2008 to 2019, 125 trials involving 76 drugs took place, with the majority being halted latest at the phase III stage (Wong et al., 2021). Very recently, in 2022, a new drug called relyvrio has been approved by FDA. Formerly called AMX0035, this small molecule drug is a coformulation of sodium phenylbutyrate-taurursodiol, providing a combination therapy. With its mechanism of action still to be worked out in detail, sodium phenylbutyrate is a chemical chaperone involved in protein folding believed to help reducing pathological protein aggregation (e.g., pTDP-43 aggregates) (Suaud et al., 2011), whereas taurursodiol negatively modulates mitochondria associated apoptosis by inhibiting release of cytochrome c and subsequent caspase-3 activation as well as translocation of Bax (Bcl-2 associated X-protein) into mitochondrial membrane, thus helping to ward off neuronal death (Rodrigues et al., 2003). In phase II clinical trials, relyvrio has shown to extend survival for 6.5 months (Paganoni et al., 2021). However, as a result of a bigger phase III clinical trial, relyvrio has been recently retracted from the market due to insufficient beneficial effects in slowing the disease progression (ClinicalTrials.gov Identifier: NCT03533257).

In addition, for fALS patients, gene-targeted therapies using antisense oligonucleotides (ASOs) are being tested. ASOs are short DNA-like molecules that bind to specific sequences

of mRNA and prevent them from being translated into proteins. Tofersen for *SOD1*, is the first ASO that has been approved by the FDA recently (ClinicalTrials.gov Identifier: NCT04972487). Patients with *SOD1* mutations treated with tofersen showed a reduction in plasma neurofilament light chain (NfL), whose increase in CSF is used as an indicator of CNS damage, and shown to slow down the disease progression in a 12-month treatment programme (Wiesenfarth et al., 2024). A clinical trial for ION363, an ASO developed for *FUS*, is still ongoing (ClinicalTrials.gov Identifier: NCT04768972). In contrast, a clinical trial for WVE-004, an ASO developed to target *C9ORF72* hexanucleotide repeat expansions was halted, as it did not show clinically meaningful improvement in patients, despite successfully reducing levels of a DPR subtype, poly(GP) (Wave Life Sciences, 2023). Similarly, another trial for BIIB078, an ASO for *C9ORF72* mRNA, was discontinued in the phase I trial due to no difference in clinical symptoms between the placebo and BIIB078 group at 60 mg (ClinicalTrials.gov Identifier NCT04288856). Interestingly, at 90 mg, BIIB078 treatment even caused a greater decline in patients compared to placebo group (ClinicalTrials.gov Identifier: NCT04288856).

Moreover, a cell-based therapy called NurOwn, which employs mesenchymal stem cells (MSCs) to reduce inflammation and modulate immune function, was shown to slow down the disease progression in less advanced patients in a phase III clinical trial and its FDA approval is pending (Cudkowicz et al., 2022). Another alternative medication called CNM-Au8, is a nanoparticle designed to target and destroy mutant SOD1, has been proved safe but did not show efficacy in disease progression and patient survival (Vucic et al., 2023).

Altogether, disappointing outcomes of above-mentioned drug trials have corroborated the complexity of ALS. Undoubtedly, finding an effective treatment to slow down the disease progression or even a cure for this debilitating disease, requires more insights into pathomechanisms of ALS.

1.2. Cell autonomous and non-cell autonomous changes in ALS

After numerous failed trials, the lack of effective treatments for ALS proved the complexity of the disease was underestimated. Initially, the identification of selectively vulnerable neurons in ALS, namely UMNs and LMNs, prompted an overall ‘motor neuron centered’ view of the disease. Over the last decades, ALS research thus focused on uncovering what was making motor neurons susceptible to neurodegeneration. Many altered molecular mechanisms in the affected motor neurons are implicated, which are collectively referred to as ‘cell autonomous mechanisms’ of ALS. However, how these changes (e.g., impaired Ca^{2+} buffering, RNA processing) are linked to neuronal death, remains incompletely understood. MNs are located within intricate circuitries, modulated and supported by other cell types. While MNs exhibit cell autonomous changes that can lead to neurodegeneration, neighboring cells and supporting

cells in the nervous system can directly or indirectly influence these changes by modulating the cellular environment, releasing signaling molecules, and providing essential factors for neuronal health and function. This interplay between neurons and surrounding cells is crucial for the proper functioning of the nervous system. In line with this notion, the research focus has shifted to also include 'non-cell autonomous changes' in ALS, a term referring to the alterations in any cell types except the affected motor neurons, typically used to refer to glia, but in a broader sense also including immune cells and non-affected neuronal populations. Indeed, accumulating evidence suggests that the motor neuron-centric view of ALS pathogenesis is incomplete and many molecular and functional changes in non-motor neuron populations are present in ALS.

In this chapter, I will describe cell autonomous changes reported in human patients, mouse models and human patient - derived induced pluripotent stem cell (hiPSC) models of ALS. Moreover, I will briefly summarize non-cell autonomous molecular changes in ALS, focusing on astrocytes, microglia, oligodendrocytes, oligodendrocyte progenitor cells (OPCs), non-MN excitatory neurons and interneurons.

1.2.1. Cell autonomous mechanisms in ALS

The pathophysiology of ALS encompasses the selective degeneration of both UMNs and LMNs. The initial hypothesis was that the neurodegeneration stemmed primarily from cell-autonomous mechanisms. Many studies have shown multiple mechanisms contributing to MN death within the cell, such as oxidative stress (Barber and Shaw, 2010), dysregulated protein homeostasis due to the endoplasmic reticulum (ER) stress (Nishitoh et al., 2008; Lautenschlaeger et al., 2012; Jara et al., 2015; Ruegsegger and Saxena, 2016), deficits in DNA damage repair (Higelin et al., 2018; Naumann et al., 2018; Sun et al., 2020), excitotoxicity (Van Den Bosch et al., 2006), impaired axonal transport (Xiao et al., 2006; Bilsland et al., 2010; Marinković et al., 2012), changes in intrinsic neuronal excitability (Pieri, 2003; Fogarty et al., 2015; Saba et al., 2016; Kim et al., 2017; Martínez-Silva et al., 2018), reduced Ca^{2+} buffering capacity (Grosskreutz et al., 2010; Kawamata and Manfredi, 2010) and defects in RNA metabolism (Polymenidou et al., 2012; Barker et al., 2017; Butti and Patten, 2018) (**Figure 3**).

One key mechanism hypothesized to contribute to MN vulnerability is the alteration of 'intrinsic excitability', which refers to the propensity of a neuron to respond to glutamatergic input by eliciting an action potential (Gunes et al., 2020). To explore changes in intrinsic motor neuron excitability and other cell-autonomous mechanisms, many mouse and cell models have been established. For instance, $SOD1^{G93A}$ transgenic (tg) mice show UMN hyperexcitability at the neonatal age and in the symptomatic stage, but not in the presymptomatic stage (Kim et al., 2017; Buskila et al., 2019). In another study, cortical slice cultures from $SOD1^{G93A}$ mice showed

enhanced UMN excitability (reduced rheobase) at the early presymptomatic stage (Fogarty et al., 2015; Fogarty et al., 2016a; Fogarty et al., 2016b; Saba et al., 2016). Moreover, $SOD1^{G93A}$ tg mice have an altered motor cortex transcriptome with over 300 genes being altered already at the early postnatal age, of which CACNB4 (voltage-dependent L-type calcium channel subunit beta-4) and GABRA4 [g-aminobutyric acid (GABA) receptor subunit alpha-4] are implicated in changes in intrinsic neuronal excitability (Kim et al., 2017). Overall, electrophysiological recordings from UMNs report hyperexcitability in different disease stages, while genetic makeup of the disease model play a role in the reported changes in intrinsic excitability (Gunes et al., 2020).

Of note, a proportion of UMNs in humans is connected monosynaptically to LMNs, whereas in mice the circuitry is wired differently. Due to this difference, early changes in UMNs in mouse models of ALS are difficult to interpret with regards to their impact on LMNs and also with respect to their human counterparts. This led to efforts of creating *in vitro* models to capture human-specific disease mechanisms, such as human fibroblast derived iPSCs. Remarkably, differentiation of stem cells derived from patients proved very useful for studying electrophysiological features of motor neurons. Furthermore, it allowed for investigating early and late-stage specific changes modelled by the age of cultures. In summary, 2-6 week old cultures of hiPSC-MNs (subtype unspecified), potentially corresponding to the presymptomatic stage of ALS, were shown to be hyperexcitable and hyperactive (increased firing rate-input (F-I) gain and spontaneous activity) (Wainger et al., 2014; Devlin et al., 2015), whereas neurons in more matured cultures (7-10 week old) became hypoexcitable and hypoactive (Sareen et al., 2013; Zhang et al., 2013b; Devlin et al., 2015; Naujock et al., 2016; Guo et al., 2017). These studies, however, represent a model system for studying LMNs, characterized by the expression of choline acetyltransferase (ChAT). Of note, the differentiation process of hiPSC-MNs yields a mixture of neuronal populations, of which about 50% can be classified as LMN (Devlin et al., 2015). Regarding the investigation of cell autonomous mechanisms of UMNs in a dish, the field still strives for a reliable UMN hiPSC model (Giacomelli et al., 2022). Existing UMN cultures include excitatory neurons and interneurons, together with UMNs, which are classified by cell diameter but not gene expression patterns. This methodological imperfection does not yet allow to study the cortical layer specific MN pathology seen in ALS. In one of the few studies involving cortical hiPSC cultures, cortical neurons with *C9ORF72* mutations showed enhanced network activity and increased firing rate in 4-6 week old cultures, corroborating the early cortical hyperexcitability seen in ALS patients (Perkins et al., 2021).

While the exact cause of the described alterations in intrinsic excitability of UMNs and LMNs is still debated, a plethora of altered molecular mechanisms were linked to altered neuronal excitability and activity. Neurons are critically dependent on spatially and temporally controlled Ca^{2+} dynamics for sustaining functions, ranging from neurotransmitter release to activity-dependent transcription. Mitochondria and ER are the main sources of Ca^{2+} in a cell and their interaction is vital for Ca^{2+} homeostasis within a cell. Multiple downstream effects of mitochondrial and ER dysfunction could result in altered intracellular Ca^{2+} content and consecutive generation of oxidative stress. In ALS, amongst other neurodegenerative diseases, the ER-mitochondria associations seem to be disrupted (Kawamata and Manfredi, 2010; Stoica et al., 2014). There is evidence that low cytosolic Ca^{2+} buffering together with a high Ca^{2+} influx during neurotransmission contribute to the vulnerability of MNs in ALS (Grosskreutz et al., 2010). Excessive Ca^{2+} influx during glutamatergic neurotransmission has previously been reported in both rodent models as well as iPSC-derived neurons as a result of increased Ca^{2+} permeability of AMPA receptors (AMPAR) (Rothstein et al., 1990; Rothstein et al., 1992; Couratier et al., 1993; Kawamata and Manfredi, 2010; Selvaraj et al., 2018). The increased expression of the AMPAR subunit GluA1 has been shown to enhance C9ORF72 hiPSC motor neuron vulnerability to excitotoxicity (Selvaraj et al., 2018). Later, this phenotype was reversed by CRISPR/Cas9-mediated correction of the *C9ORF72* gene (Selvaraj et al., 2018).

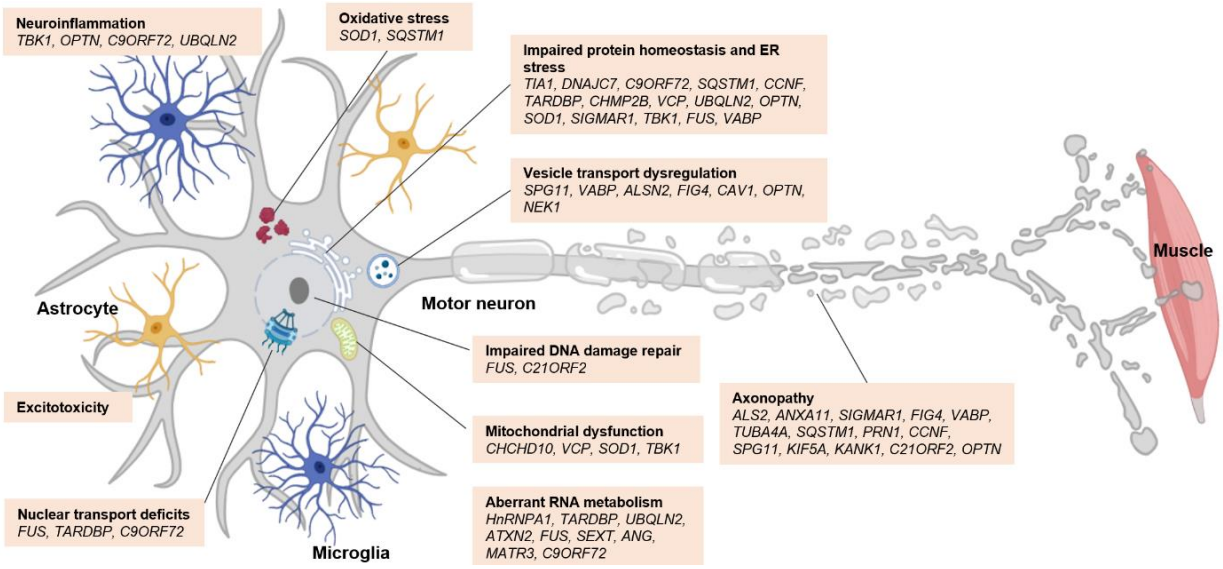

Figure 3. Cell autonomous changes involved in the neurodegeneration of motor neurons are partially explained by genetic alterations in ALS.

Numerous genetic alterations and risk factors are linked to disrupted cellular functions, such as RNA processing, nuclear and axonal transport deficits in vulnerable motor neurons. Increased neuroinflammation and protein dyshomeostasis, and downstream endoplasmic reticulum (ER) stress are also present in ALS MN. Adapted from (Mead et al., 2023). Figure was created with BioRender.com.

The regulation of Ca^{2+} homeostasis is therefore critical to the physiological function of neurons. One of the main Ca^{2+} buffers are mitochondria, which can take up significant amounts of Ca^{2+} from the cytosol (Pivovarova and Andrews, 2010). Dafinca et al. showed that in hiPSC derived LMN obtained from patients, harboring a *TARDBP* or *C9ORF72* mutation, a slower normalization of intracellular Ca^{2+} was observed upon glutamatergic stimulation as mitochondrial Ca^{2+} uptake was reduced but also Ca^{2+} release from the ER was compromised (Dafinca et al., 2020). The authors also demonstrated that the slow mitochondrial Ca^{2+} uptake leads to neuronal death as a result of ROS accumulation and subsequent cytochrome c-initiated apoptosis (Dafinca et al., 2020). Similarly, additional studies employing C9ORF72 hiPSC LMNs (Dafinca et al., 2016), $SOD1^{A4V}$ hiPSC LMNs (Kiskinis et al., 2014) and hiPSC LMNs generated from sporadic ALS patients (Alves et al., 2015) show evidence for mitochondrial dysfunction, enhanced oxidative and ER stress associated with Ca^{2+} dysregulation, and decreased cell survival. Moreover, also in a cortical hiPSC culture harboring C9ORF72 repeat expansions, increased ROS were detected in 3-month-old cortical neurons (Lopez-Gonzalez et al., 2016).

Findings made in cell culture experiments are in agreement with findings in human tissue, as for instance in a bulk RNA-seq study, an increased expression of oxidative stress markers in post-mortem frontal and motor cortex of ALS patients was reported, while the source of the oxidative stress was not clearly linked to a neuronal subpopulation (Tam et al., 2019). Although the detailed cascade of events is still incompletely understood, the current notion holds that increased neuronal excitability and excessive activation of glutamatergic receptors are upstream of the accumulation of ROS and intracellular Ca^{2+} overload, triggering excitotoxicity and ultimately neuronal death (Van Den Bosch et al., 2006; Vucic et al., 2009).

Building upon the finding of pathological aggregation of RNA binding proteins like TDP-43, FUS, DPRs in motor neurons, researchers studied the possible link between protein aggregation and motor neuron death. These mislocalized, misfolded and aggregated RNA binding proteins were shown to interfere not only with gene expression but also to impair intracellular trafficking via excessive cytoplasmic accumulation of their misfolded forms (Polymenidou et al., 2012). Such accumulation of proteins was shown to disrupt proteostasis in ALS, thus leading to a decreased availability of axonal transport proteins (e.g., dynein, microtubules) and impairing the axonal transport of organelles bidirectionally (e.g., endosomes, mitochondria, mRNA granules) (De Vos and Hafezparast, 2017). Since TDP-43 aggregates are present in the majority of ALS patients, even in the absence of *TARDBP* mutations, hiPSC models generated from *TARDBP*-associated ALS patients are employed often to study cell autonomous mechanisms of motor neuron degeneration, albeit being vastly restricted to modeling LMNs for now (Hawrot et al., 2020; Giacomelli et al., 2022). Bilican et

al. showed that TDP-43 hiPSCs harboring the M337V mutation displayed an accumulation of insoluble TDP-43, which was associated with a decreased survival of these neurons (Bilican et al., 2012). In another study employing TDP-43 hiPSCs (harbouring either G298S, A315T, M337V mutations), LMNs exhibited impaired transportation of neurofilament mRNA granules at 9 days in vitro (DIV), which worsened as the neurons reached 14-17 DIV (Alami et al., 2014). Intriguingly, Kreiter et al., showed that the presence of TDP-43 mutations was sufficient to cause axonal transport deficits in the absence of aberrant TDP-43 inclusions in TDP-43 hiPSC with S393L or G294V mutations (Kreiter et al., 2018). Moreover, mutant neurons had significant signs of neurodegeneration as they aged but did not display any TDP-43 mislocalization and/or aggregation (Kreiter et al., 2018). These findings implicate that mechanisms of neuronal vulnerability can be tied to early axonal transport deficits that occur before cytoplasmic protein aggregation.

Taken together, defects in Ca^{2+} buffering capacity (Grosskreutz et al., 2010; Kawamata and Manfredi, 2010), neuronal excitability changes and excitotoxicity (Van Den Bosch et al., 2006), impaired proteostasis (Ruegsegger and Saxena, 2016), RNA processing (Polymenidou et al., 2012), and axonal transport deficits (Marinković et al., 2012) are characteristic of ALS associated dyshomeostasis in vulnerable neurons (Boillée et al., 2006a). Undoubtedly, more research is required to unravel the exact mechanisms driving cell autonomous changes in ALS, in particular focusing on UMN vulnerability.

1.2.2. Non-cell autonomous mechanisms in ALS

There is growing evidence showing alterations in cell types other than affected motor neurons in ALS (Nagai et al., 2007; Hossaini et al., 2011; Zhang et al., 2016). Elucidating non-cell autonomous processes and their connection to motor neuron degeneration remains a challenging task. Bulk RNA-seq analysis of the whole transcriptome of CNS tissue from ALS patients highlighted the deregulation of over thousand genes in ALS patients, however, the cellular heterogeneity was poorly elucidated in this study (D'Erchia et al., 2017). In the following section, I will describe findings from non-MN cell types and report molecular and functional modifications that have been reported so far in the field (**Figure 4**).

Microglia

Microglia are considered the resident immune and phagocytosing cells in the CNS, which participate in various functions related to immune response, maintaining physiological state, the monitoring of neural activity and synaptic connections (Nimmerjahn et al., 2005; Schafer et al., 2013; Badimon et al., 2020). They are responsible for detecting and responding to pathogens, damaged cells, and debris (Liddelow et al., 2017). When there's inflammation or injury in the brain, microglia become (re)activated, characterized by the upregulation of pro-

and anti-inflammatory factors and the release of cytokines, such as interleukin 1 alpha (IL-1α), tumor necrosis factor alpha (TNFα), and complement component 1q (C1q) or immune molecules like ROS and nitric oxide (NO) to recruit other immune cells and initiate an immune response (Li and Barres, 2018).

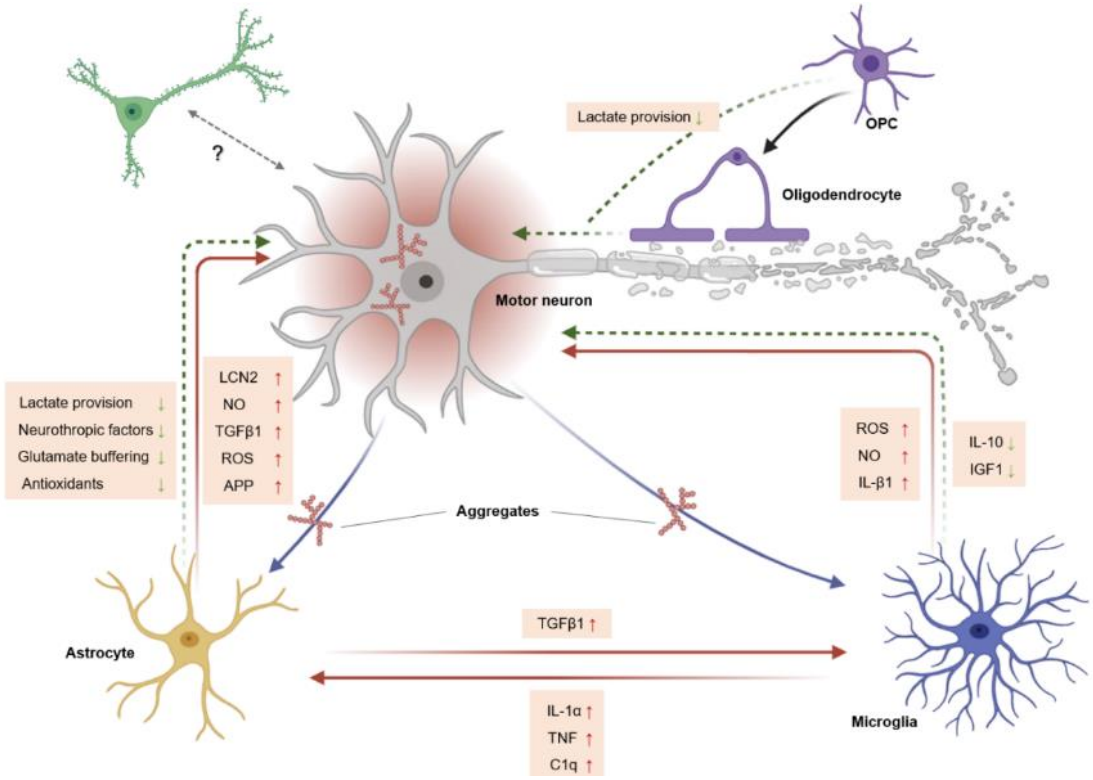

Figure 4. Altered non-cell autonomous mechanisms identified in ALS.

The pathophysiological roles of microglia, astrocytes, oligodendrocytes and interneurons in ALS involve a complex interplay of factors. The malfunctioning and aggregation of proteins such as superoxide dismutase 1 (SOD1), TAR DNA-binding protein 43 (TDP-43), and dipeptide repeat (DPR) protein are linked to the activation of astrocytes and microglia (blue arrows), a key mechanism to neuronal damage in ALS. These glial cells are thought to acquire harmful properties, involving both increased toxicity (red arrows), and a reduction in their supportive functions (green dashed arrows). These alterations are instigated by the presence of mutations associated with ALS in genes like *SOD1*, *TARDBP*, and *C9ORF72*, while they can also occur in the absence of these mutations. These interruptions in the complex intercellular communication between these cell types are thought to worsen the neurotoxicity and disease progression of vulnerable motor neurons. APP, amyloid precursor protein; IGF1, insulin-like growth factor 1; LCN2, lipocalin 2; NO, nitric oxide; ROS, reactive oxygen species; TGFβ1, transforming growth factor β1; TNF, tumor necrosis factor; IL-1α, interleukin 1 alpha; IL- β1, interleukin beta 1; IL-10, interleukin 10. Taken and adapted from (Vahsen et al., 2021). Figure was created with BioRender.com.

These microglia secreted factors are shown to lead to the activation of quiescent astrocytes and amplify the inflammatory response (Liddelow et al., 2017). Excessive or chronic activation can lead to neuroinflammation, a state of inflammation in the CNS driven by the activation of glia, including microglia and astrocytes. Activated glia secrete immune modulatory molecules (e.g., cytokines) and even excitatory amino acids, which together compromise neuronal function, leading to eventual neuronal damage (Liddelow et al., 2017). Mutant $SOD1^{G93A}$ activates microglia, which secrete interleukin 1 beta (IL-1β) to trigger neuroinflammation (Meissner et al., 2010). Yet, the role of IL-1β in neurotoxicity is unclear as IL-1β knockdown expands the lifespan in $SOD1^{G93A}$ tg mice (Meissner et al., 2010), whereas it does not alter the disease progression in $SOD1^{G37R}$ tg mice (Nguyen et al., 2001). In contrast, other studies show

that microglia could play a protective effect in the disease context. For example, in presymptomatic SOD1 ^{G93A} tg mice, interleukin 10 (IL-10), an anti-inflammatory cytokine, is increased ~16 times compared to wt mice (Gravel et al., 2016). Moreover, overexpression of IL-10 delayed disease onset, whereas IL-10 receptor blockage sped up disease progression, implicating a dual role of microglia in ALS (Gravel et al., 2016).

Neuroinflammation is implicated in various neurological disorders, including Alzheimer's disease, Parkinson's disease, multiple sclerosis (MS), and others (Ajami et al., 2018). In ALS patients, neuroinflammation in motor and temporal cortices has been reported, which was assessed by (positron emission tomography) PET imaging employing ligands specific for immune marker (e.g., translocator protein 18 (TSPO), peripheral benzodiazepine receptor (pBR) ligand PK11195). However, these ligands are not specific to microglia, and bind also to other immune cells, astrocytes or endothelial cells, making it difficult to draw a direct conclusion of how microglial activation in patients is presented in the course of the disease (Turner et al., 2004; Corcia et al., 2012; Alshikho et al., 2018)

Single cell RNA-seq studies reported high microglial heterogeneity in both mouse and human CNS under physiological conditions (Keren-Shaul et al., 2017; Mathys et al., 2017; Hammond et al., 2019; Gerrits et al., 2020; Masuda et al., 2020). In the disease context, morphological and functional changes of microglial subpopulations were already evidenced in mouse models of neurodegenerative diseases (Mathys et al., 2017; Ajami et al., 2018). The identification of a so called disease-associated microglia (DAM) subpopulation that detect damage within the CNS, and their reactivation often involves a triggering receptor expressed on myeloid cells 2 (TREM2) signaling pathway, was first reported in an AD mouse model and in human post-mortem AD brains (Keren-Shaul et al., 2017). A larger proportion of microglia displaying a DAM signature, defined by the downregulation of homeostatic genes (e.g., *P2ry12*, *Cx3cr1*) and upregulation of *Trem2*, *Tyrobp*, *Lpl*, *Cst7*, was further depicted in spinal cord and whole brain single cell RNA-seq of SOD1^{G93A} mice as the disease further progressed (Keren-Shaul et al., 2017). Similar alterations in microglia reactivity were shown in RNA-seq datasets obtained from post-mortem Alzheimer´s disease patients (Friedman et al., 2018; Grubman et al., 2019; Mathys et al., 2019). Using a machine learning algorithm, Tam et al. identified a subgroup of ALS patients that presented with a DAM signature in post-mortem motor and frontal cortex (Tam et al., 2019). In another study, bulk RNA-seq of post-mortem motor cortex from ALS patients confirmed microglia reactivity mainly driven by a subpopulation of microglia expressing markers overlapping with the mentioned DAM (Dols-Icardo et al., 2020). Activated microglia, as shown in a recent snRNA-seq study of ALS patients, differentially express genes involved in lipid metabolism compared to healthy controls, although the role of these

transcriptomic changes for microglia function and/or MN degeneration was not investigated further (Limone et al., 2023).

A number of molecules, suggestive for an activated immune system, have been identified in ALS patients (McCombe et al., 2020). Post-mortem immunohistochemistry (IHC) analysis of motor cortex samples from familial and sporadic ALS patients indicated that microglia in close proximity to Betz cells exhibit amongst others a higher expression of monocyte chemoattractant protein-1 (MCP1) and CC chemokine receptor 2 (CCR2), which are markers associated with an innate immune response (Jara et al., 2017). Moreover, cerebrospinal fluid (CSF) levels of chitinase proteins in ALS patients, a known marker for microglial activation, have been repeatedly shown to be increased compared to neurologically healthy individuals (Steinacker et al., 2018; Thompson et al., 2019).

Although microglia activation is a common feature in mouse models and patients, not all DAM features seen in humans are replicable in mouse models, as shown in AD studies (Friedman et al., 2018). The role of microglia reactivity in ALS is a much-debated topic, as some studies suggest also a neuroprotective role of DAMs rather than exerting a purely detrimental impact on neurons. For example, in the rNLS8 mouse model of ALS, which overexpresses doxycycline-inducible human TDP-43 lacking the nuclear localization sequence (hTDP-43 ΔNLS), microglia proliferation was even further increased and microglia-mediated effective clearance of neuronal hTDP-43 was observed, together with an increased survival of the neurons when hTDP-43 expression was suppressed in neurons (Walker et al., 2015; Spiller et al., 2018). Similarly, diminishing mutant SOD1 in microglia of $SOD1^{G37R}$ tg mice increased survival significantly (Boillée et al., 2006b). Furthermore, in another study with $SOD1^{G37R}$ tg mice, selective deletion of mutant SOD1 expression in astrocytes delayed the microglial activation, which resulted in slower disease progression, too (Yamanaka et al., 2008). In an elegant study, bone marrow transplants from $SOD1^{G93A-/-}$ (wt) mice into early symptomatic $SOD1^{G93A}$ tg mice resulted in the generation/differentiation of wt macrophages and surprisingly resulted in a neuroprotective microglial phenotype, compared to the proinflammatory microglia signature typical of $SOD1^{G93A}$ tg mice (Chiot et al., 2020). Strikingly, this set of neuroprotective microglial gene expression was preserved until end-stage. These data suggest a key role also of peripheral macrophages in the modulation of microglial activation in the CNS (Chiot et al., 2020). In another study, a monoculture of hiPSC derived microglia from C9ORF72 fALS patients was shown to undergo no significant alterations in the expression of microglial activation genes (i.e., chemokines) when compared to wt cells, supporting the notion that microglial function is tightly regulated by the surrounding environment and other cells, ultimately defining the fate of the affected neurons. Together, non-cell autonomous function of

microglia and the dual role of microglial activation in ALS, and overall in neurodegeneration is yet to be uncovered (Deczkowska et al., 2018).

Astrocytes

Astrocytes are the most abundant type of glial cells in the CNS and represent a vital component of the motor circuitry. Effective clearance of glutamate from the synaptic cleft by astrocytes is crucial for spatiotemporal confined synaptic transmission. This clearance is also necessary to protect neurons from overstimulation and a potentially resulting neuronal death, a phenomenon named 'glutamate mediated excitotoxicity'. Ineffective clearance of glutamate as a key mechanism of MN death in ALS was first hypothesized as elevated levels of glutamate in the CSF of ALS patients have been detected in some studies (Rothstein et al., 1990; Shaw et al., 1995). Others, however, have reported no change of glutamate levels in the CSF of ALS patients when compared to healthy controls (Perry et al., 1990). Moreover, astrocytic expression of the excitatory amino acid transporter 2 (EAAT2), the main transporter facilitating glutamate uptake, is decreased in post-mortem ALS tissue (Rothstein et al., 1995), as well as in animal models suggestive of glutamate mediated excitotoxicity. Additionally, a heterozygous knockout of EAAT2 in SOD1^{G93A} tg mice resulted in more aggressive disease progression and decreased survival (Pardo et al., 2006). However, the heterozygous knockout of EAAT2 interferes with the development of CNS, affecting synapses potentially already prenatally. Thus, it does not entirely clarify if downregulation of the EAAT2 pre-symptomatically is detrimental to the MNs. To this end, Li et al. delivered AAV9-Gfa2-GLT1 intraspinally (cervical) to SOD1^{G93A} tg mice to upregulate EAAT1 expression at symptom onset (Li et al., 2015). They found that restoring EAAT2 levels did neither prevent phrenic MN degeneration, nor slow down disease progression or prolong animal survival, indicating that a rescue of focal EAAT2 expression is likely not an effective therapy (Li et al., 2015). Yet, it remains still debated if EAAT2 downregulation is occurring both in motor cortex and spinal cord of ALS patients and what the impact is on synaptic glutamate and thus UMN/LMN health.

In addition to neurotransmitter (e.g., glutamate, GABA) clearance, astrocytes are also responsible for the maintenance of extracellular K^+ concentration. Although many other channels are involved in K^+ clearance, one main K^+ inward-rectifying channel (Kir), Kir4.1, which is selectively expressed on astrocytes, has been reported to be reduced in SOD1^{G93A} tg rats (Bataveljić et al., 2012). The accumulation of extracellular K^+ increases neuronal depolarization and excitability (Do-Ha et al., 2018). Astrocytes are not only responsible for presynaptic glutamate turnover and K^+ homeostasis but have been suggested to modulate neuronal activity by gliotransmission (Halassa and Haydon, 2010; de Ceglia et al., 2023). It has been proposed that astrocytes secrete several neurotransmitters, such as glutamate, d-serine, and ATP in response to an increase in intracellular Ca^{2+} (Halassa et al., 2007).

Alterations in gliotransmission could contribute to the pathogenesis of neurodegeneration in general (Halassa et al., 2007; de Ceglia et al., 2023). Interestingly, earlier studies have substantiated the notion that astrocytes contribute majorly to the degeneration of MNs, as the application of the supernatant of cultured astrocytes from ALS transgenic mice (Di Giorgio et al., 2007; Nagai et al., 2007; Marchetto et al., 2008) and astrocytes derived from post-mortem sALS and fALS patients (Haidet-Phillips et al., 2011; Qian et al., 2017) both were shown to be toxic to mouse MNs . Moreover, hiPSC derived astrocytes differentiated from sporadic and familial ALS patients further resulted in increased oxidative stress and neurotoxicity in co-cultured hiPSC derived human MNs (Meyer et al., 2014; Birger et al., 2019). The putative astrocyte-released toxic factor has been sought by numerous researchers (Di Giorgio et al., 2007; Nagai et al., 2007; Marchetto et al., 2008; Fritz et al., 2013). In a seminal study, Guttenplan et al., showed that astrocyte derived APOE and APOJ lipoparticles (saturated fatty acids), whose upregulation is often reported in CNS injuries, cause neuronal toxicity *in vitro* and *in vivo* (Guttenplan et al., 2021). Yet, neither the exact reason for the upregulation of lipids in reactive astrocytes nor the identity of other possible astrocyte-derived toxic factors has been clearly unveiled yet.

Astrocytes are typically identified by the presence of specific or highly concentrated astroglial proteins, including GFAP, aldehyde dehydrogenase 1 family member L1 (ALDH1L1), EAAT2, S100 calcium binding protein β (S100β), and aquaporin-4 (AQP4). When exposed to any biological threat in their vicinity, astrocytes initiate a reactive response, resulting in an increased expression of certain astrocytic markers like GFAP and ALDH1L1 - a phenomenon known as astrogliosis. Unlike microgliosis, the overall number of astrocytes does often not escalate during astrogliosis; instead, the number of reactive astrocytes are increased by the conversion of physiological astrocytes. Reactive astrocytes are responsible for the secretion of multiple proinflammatory factors such as S100β, chemokines, cytokines (interleukin-1β (IL-1β), interleukin 6 (IL-6), tumor necrosis factor-alpha (TNF-α)) (Diaz-Amarilla et al., 2011; Mishra et al., 2016; Tripathi et al., 2017; Kia et al., 2018; Nowicka et al., 2022). Astrocytes expressing mutated FUS^{R521G} protein were shown to induce motor neuron death in culture by releasing TNF-α (Kia et al., 2018). Moreover, S100β is elevated as well as its receptor for advanced glycation end products (RAGE) and High Mobility Group Box 1 (HMGB1) protein in $SOD1^{G93A}$ mouse model of ALS (Nowicka et al., 2022). In another study, activated astrocytes expressing S100β and connexin 43 (Cx43) decreased the survival of spinal motor neurons obtained from $SOD1^{G93A}$ tg rats in co-culture (Diaz-Amarilla et al., 2011). Reactive astrocytes carrying mutant SOD1 were shown to release amyloid precursor protein (APP) fragments in mice that were linked to MN toxicity (Mishra et al., 2020). Furthermore, activated astrocytes release elevated levels of transforming growth factor (TGF)-β1, dysregulating of autophagy and proteostasis in cultured human motor neurons (Tripathi et al., 2017).

Under physiological conditions, astrocytes also protect neurons from nitric oxide (NO) and ROS; whereas wt astrocyte cultures treated with CSF taken from ALS patients exhibit impaired NO and ROS metabolism of astrocytes, while anti-inflammatory (i.e., IL-10) and neurotropic factors (i.e., vascular endothelial growth factor (VEGF) and brain-derived neurotrophic factor (BDNF)) were down regulated (Mishra et al., 2016). Moreover, iPSC derived astrocytes obtained from C9ORF72-ALS patients exhibited elevated ROS levels (Birger et al., 2019). In addition, Lipocalin-2 (LCN2), belonging to the secreted lipocalin protein family, is an autocrine mediator of gliosis, mainly expressed by glial cells (Suk, 2016). In transgenic rats expressing ALS-linked mutant TDP-43 or FUS exclusively in neurons, LCN2 was upregulated in reactive astrocytes, potentially exerting a direct neurotoxic effect (Bi et al., 2013).

Intriguingly, the activation of astrocytes and microglia seems to be a shared phenomenon across neurodegenerative diseases. Multiple snRNA-seq studies of entorhinal and prefrontal cortex samples obtained from post-mortem Alzheimer's disease (AD) patients point to a disease-associated inflammatory gene expression pattern in astrocyte subpopulations (Mathys et al., 2019; Leng et al., 2021). While in ALS, reactive astrocytes (GFAP+) have been reported in post mortem spinal cord and motor cortex, determined by immunohistological analyses (Kawamata et al., 1992; Nagy et al., 1994; Schiffer et al., 1996).

In a bulk RNA-seq transcriptomics study of post mortem motor cortex of ALS patients, increased expression of *CD44* and *GFAP* was reported in ALS when compared to healthy controls (Tam et al., 2019). Furthermore, spatial snRNA-seq of the lumbar spinal cord of $SOD1^{G93A}$ tg mice show increased expression of reactive astrocytic markers (*Gfap* and *Aif1*) in the vicinity of vulnerable ventral horn neurons already early symptomatically (Maniatis et al., 2019). Taken together, disease- associated changes in astrocytic molecular make-up and function is strongly evidenced in ALS, and in other neurodegenerative diseases like AD and Huntington's disease (Habib et al., 2020; Khakh and Goldman, 2023).

Oligodendrocytes and oligodendrocyte progenitor cells (OPCs)

Oligodendrocytes are responsible for producing and maintaining myelin in the CNS. Each oligodendrocyte can extend its processes to wrap around multiple axons, forming myelin sheaths that cover segments of these axons, increasing the speed of neuronal signal transmission. Oligodendrocytes are formed via differentiation of OPCs, which are multipotent but mainly give rise to oligodendrocytes (Raffaele et al., 2021). Oligodendrocytes and OPCs due to their pivotal role in myelination are extensively studied in demyelinating diseases like multiple sclerosis (MS). In ALS, a reduction in cerebral white matter density, measured by diffusion tensor imaging (DTI), correlates with disease progression and severity, however the role of oligodendrocytes is not yet fully understood in ALS pathophysiology (Kalra et al., 2020).

Alterations of oligodendrocytes and OPCs have been implicated in ALS pathophysiology in rodent models of ALS as well as in patients (Raffaele et al., 2021). In SOD1^{G93A} mice loss of oligodendrocytes in the gray matter of the spinal cord occurs prior to LMN loss, suggesting early changes in ALS could originate from impairments in oligodendrocytes (Kang et al., 2013; Philips et al., 2013). Interestingly, at the very early developmental stages SOD1^{G93A} tg mice exhibit a loss of mature CC1^{+} oligodendrocytes in spinal cord while having increased expression of neural/glial antigen 2 (NG2) and G protein-coupled receptor 17 (GPR17), which are markers for immature oligodendrocytes (Bonfanti et al., 2020). In response to myelination defects and loss of oligodendrocyte function, increased NG2^{+} OPC proliferation was shown in the gray matter of the spinal cord of SOD1^{G93A} tg mice (Kang et al., 2013), yet the OPC regeneration mechanisms were shown to be defective, not resulting in a replacement of mature oligodendrocytes, further contributing to LMN loss (Kang et al., 2013; Philips et al., 2013).

Furthermore, oligodendrocytes provide lactate and other nutrients to MNs, which requires the expression of the monocarboxylate transporter (MCT1). Notably, a reduction of MCT1 protein levels in the motor and frontal cortex of sALS patients was shown (Lee et al., 2012). This finding was also replicated in SOD1^{G93A} mice spinal cord, suggesting a possible lack of oligodendrocyte support for both MNs and OPCs in the disease state (Lee et al., 2012; Philips et al., 2013). In a snRNA-seq study of post-mortem motor cortex specimen from ALS patients, a subgroup of oligodendrocytes were reported to have a downregulation of genes related to myelination (Limone et al., 2023). Interestingly, they reported an oligodendrocyte subcluster, which had higher expression of synaptic genes (i.e., *DLG1*, *DLG2*, *GRID2*), a finding which was interpreted as an enrichment of a ‘neuronally-engaged’ phenotype of oligodendrocytes in end-stage ALS (Limone et al., 2023).

Aforementioned TDP-43 pathology has been not only detected in neurons, but interestingly also in oligodendrocytes of sporadic and familial ALS patients, in both motor cortex and spinal cord (Arai et al., 2006; Mackenzie et al., 2007; Zhang et al., 2008). Similarly, cytoplasmic FUS inclusions in oligodendrocytes were reported in certain FUS mutation carriers (Mackenzie et al., 2011). While it still remains open how protein aggregation affects oligodendrocytes, physiological TDP-43 function is shown to be required for oligodendrocyte survival and myelination in mice as deletion of TDP-43 in oligodendrocytes results in decreased myelination (Wang et al., 2018). Despite their dysfunction, these oligodendrocytes were not toxic to LMNs (Wang et al., 2018). Strikingly, myelin basic protein (MBP) levels, assessed using immunoblotting, were shown to be reduced in the spinal cord of ALS patients with a high burden of TDP-43 inclusions in oligodendrocytes, reflecting oligodendrocyte involvement in ALS pathology (Lorente Pons et al., 2020).

These studies highlight that disease-associated modifications in oligodendrocytes and OPCs could play an important role in ALS pathophysiology. In order to discern changes in early disease stages that lead to MN death, maturation and differentiation of these cell types require a more detailed characterization.

Interneurons and non-MN excitatory neurons

As mentioned in section 1.2.1., increased cortical excitation and decreased inhibition is an early sign observed in ALS patients (Ziemann et al., 1997; Vucic et al., 2008; Menon et al., 2017; Van den Bos et al., 2018). The resulting imbalance of excitation-inhibition (E/I) was also evidenced in decreased GABA levels, measured by proton magnetic resonance spectroscopy (1^{H}-MRS). In addition, a functional hyperconnectivity between primary motor cortex and other brain areas, such as somatosensory networks and (pre)frontal areas, measured by functional magnetic resonance imaging (fMRI) was also observed in ALS patients (Foerster et al., 2012; Schulthess et al., 2016; Gunes et al., 2022). Interneurons, which in the cortex are inhibitory neurons, are crucial to maintaining the E/I balance, by regulating the activity of both excitatory and inhibitory neurons via GABAergic signaling. In neocortex, 20-30% of all neurons are inhibitory (Tamamaki et al., 2003; Markram et al., 2004; Sherwood et al., 2010; Wood et al., 2017), and can be divided coarsely into three largely non-overlapping populations, named according to the specific expression of proteins i.e., parvalbumin expressing interneurons (PV-INs), somatostatin expressing interneurons (SST-INs) and vasoactive intestinal polypeptide expressing (VIP-INs). These interneuron subtypes, making up almost all of the inhibitory neuron populations, modulate each other's activity and provide auto-feedback (Rudy et al., 2011; Prönneke et al., 2015; Nigro et al., 2018; Krabbe et al., 2019). The exact connectivity of different subtypes of INs and their functional differences in the human cortex remains elusive. Most of our knowledge of IN circuits comes from rodent models. In mice, PV-INs receive inhibitory input from SST-INs and also regulate their own activity with auto-inhibition (Pi et al., 2013; Fishell and Kepecs, 2020). While SST-INs provide inhibition to PV-INs and VIP-INs, VIP-INs inhibit SST-INs (Karnani et al., 2016; Fishell and Kepecs, 2020). Together, they fine tune the motor cortex microcircuit and balance cortical network activity (Bartos and Elgueta, 2012; Safari et al., 2017; Veres et al., 2017).

Post-mortem histological analysis of primary motor cortex from ALS patients revealed a reduction in the density of GABAergic interneurons in layer 5, however, no significant decrease in PV-INs (Maekawa et al., 2004). An earlier study on the other hand reported a significant reduction of PV expressing neurons in motor cortex of ALS patients in all three grades of ALS, namely mild, moderate and severe, determined by severity of Betz cell loss (Nihei et al., 1993). Immunohistochemical analysis of post-mortem ALS patient specimens showed a trend towards a reduction of neuropeptide Y (NPY) receptor type 1 (NPY- Y1) expression on the

somata of UMNs (classified as non-phosphorylated neurofilament marker SMI32+ neurons) compared to their apical dendrites localized at the cortical layer 2/3, implicating end-stage modifications between NPY+ INs and UMN communication (Clark et al., 2021). Another study demonstrated a reduction in $GABA_A$ receptor expression in post-mortem specimens, implicating impaired inhibition and GABAergic signaling (Petri et al., 2003). Moreover, a recent snRNA-seq study of the human cortex reported that transcriptomic changes in GABAergic neurons were correlating with high variance explained by polygenic risk factors in ALS, inferred from genome wide association studies (GWAS) (Saez-Atienzar et al., 2021).

So far in mouse models of ALS, changes in the density of interneuron subtypes in cortex have been variable. Number of PV-INs $SOD1^{G93A}$ tg mice are unchanged compared to wt, shown in multiple studies (Özdinler et al., 2011; Clark et al., 2017). Others, however, showed both early and late symptomatic $SOD1^{G93A}$ tg mice have an increased number of PV+ interneurons, selectively in motor and somatosensory areas (Minciacchi et al., 2009). In another model of ALS, the pre-symptomatic Wobbler mice, a decreased number of PV-INs and SST-INs in primary motor cortex was found (Nieto-Gonzalez et al., 2011). In the motor cortex of $SOD1^{G93A}$ tg mice, a notable decline in the density of NPY+ interneurons at symptom onset (8 weeks) was followed by a significant increase at the end stage (Clark et al., 2017). In contrast, the density of calretinin (CR) expressing interneurons gradually decrease starting at late symptomatic stages until the end-stage (Clark et al., 2017). In addition to density changes, subtype and disease stage specific changes in excitability of INs in motor cortex have been also found in many studies (Özdinler et al., 2011; Zhang et al., 2016b; Clark et al., 2017). Presymptomatic $SOD1^{G93A}$ tg mice possess hypoactive PV-IN (Khademullah et al., 2020), which become hyperexcitable during the early symptomatic stage (Kim et al., 2017). Hypoactive PV-INs were further recapitulated in TDP-43^{A315T} tg mice (3 weeks old), which could be due to hyperactive SST-INs that modulate their inhibition (Zhang et al., 2016b).

Regarding non-MN excitatory neurons, an interesting finding from a snRNA-seq study points to an additional layer 3/5 excitatory neuronal population in the motor cortex (expressing *SCN4B*) as being one of most transcriptionally affected excitatory populations, sharing signatures with vulnerable Betz (UMNs) cells in ALS and FTD patients (Pineda et al., 2024). Although it is not shown if this population is vulnerable in ALS. In another snRNA-seq study, Limone et al. reported that an upper layer excitatory neuron subpopulation (expressing CUX1) undergoes a significant upregulation of synaptic transcripts compared to healthy controls, arguing for a potential compensatory mechanism by this subtype (Limone et al., 2023).

Finally, neuromodulation is also compromised in ALS, evidenced by altered dopaminergic in the striatum (Takahashi et al., 1993; Borasio et al., 1998) and reduction of serotonergic neurons in the brainstem of ALS patients (Dentel et al., 2012).

In summary, alterations of non-MN neurons in ALS are evident and likely causing an excitation/inhibition imbalance in the network thus contributing to excitotoxicity. However, the exact cell type- and disease stage- specific changes of these circuit components remain to be studied in greater detail.

1.3. TAR DNA Binding Protein 43

Identified in 1995 as a suppressor of the human immunodeficiency virus 1 (HIV-1) gene expression (Ou et al., 1995), *TARDBP* is located on chromosome 1 and encodes for the highly conserved RNA and DNA binding protein TDP-43. TDP-43 belongs to heterogeneous nuclear ribonucleoprotein (hnRNP) family (Prasad et al., 2019) and is ubiquitously expressed in CNS as well as in peripheral organs (Zhang et al., 2007; Wang et al., 2008). Under physiological conditions, TDP-43 is primarily localized in the nucleus but also shuttles between the nucleus and cytoplasm. It serves numerous functions, including RNA processing (RNA transport, maturation, stability & translation) and stress granule formation (Ratti and Buratti, 2016). In the ALS-associated disease state, TDP-43 undergoes multiple posttranslational modifications and cytoplasmic mislocalization (i.e., loss of function) and aggregate formation (i.e., toxic gain of function) (Guo et al., 2011; Prasad et al., 2019) (see 1.3.2 for details). In this section, I will focus on the structure and function of TDP-43 in health and review its role in neurodegenerative diseases with a special focus on ALS.

1.3.1. Structure and physiological function of TDP-43

TDP-43 is composed of 414 amino acids and has a molecular weight of 43 kDa (Wang et al., 2008; Ayala et al., 2011). It has multiple functional domains, namely the N- terminus domain (NTD) with a nuclear localization signal (NLS), two RNA recognition motifs (RRM1/2) including the nuclear export signal (NES) in RRM2, the C-terminal domain (CTD) with a glutamine/asparagine-rich (Q/N) domain and a glycine-rich region (Prasad et al., 2019) (**Figure 5a**). The N-terminal domain (NTD) is critical for homodimerization of TDP-43 and the formation of high order oligomers both of which are present in healthy human brains (Zhang et al., 2013a; Afroz et al., 2017). The dimeric form of TDP-43 is predominantly found in neuronal nuclei (Shiina et al., 2010) and plays a role in its splicing activity (Jiang et al., 2017). The nuclear localization signal (NLS) is part of the NTD and mediates the nuclear import of TDP-43 (Prasad et al., 2019). NES and NLS together regulate the shuttling of TDP-43 between the cytoplasm and the nucleus and enable interactions within the hnRNP family (Buratti et al., 2005). For example, in the cytoplasm, TDP-43 was shown to regulate levels of mRNA transcripts implicated in neuronal viability such as the human low molecular weight neurofilament (hNFL) (Strong et al., 2007) and the histone deacetylase (HDAC6) (Fiesel et al., 2010). Moreover, TDP-43 mediates transportation of transcripts into axons and neurites thus modulating

neuronal activity (Wang et al., 2008). It is known to interact with the mitochondrial genome, playing a role in the mitochondrial electron transport chain pathway (Wang et al., 2016).

TDP-43 has multiple specialized regions through which it fine-tunes RNA metabolism (**Figure 5a**). The two RNA Recognition Motifs, RRM1 and RRM2, are required for binding targeted RNAs, acting as transcriptional enhancers or repressors (Buratti and Baralle, 2001; Ayala et al., 2005; Kuo et al., 2009). TDP-43 binds to more than 6000 pre-mRNA species and estimated to regulate transcription of 600 mRNAs (Polymenidou et al., 2011). It is involved in alternative splicing of 950 mRNAs, with its binding sites mostly localized to UG rich intronic sites, 3′ untranslated regions (UTRs) and non-coding RNAs (Polymenidou et al., 2011; Tollervey et al., 2011). RRM1 region of TDP-43 is shown to specifically bind to single stranded RNAs where more than 5 UG repeats are present, while the exact function of RRM2 regions is relatively vague, it seems to have less affinity to nucleic acids than RRM1 (Kuo et al., 2014).

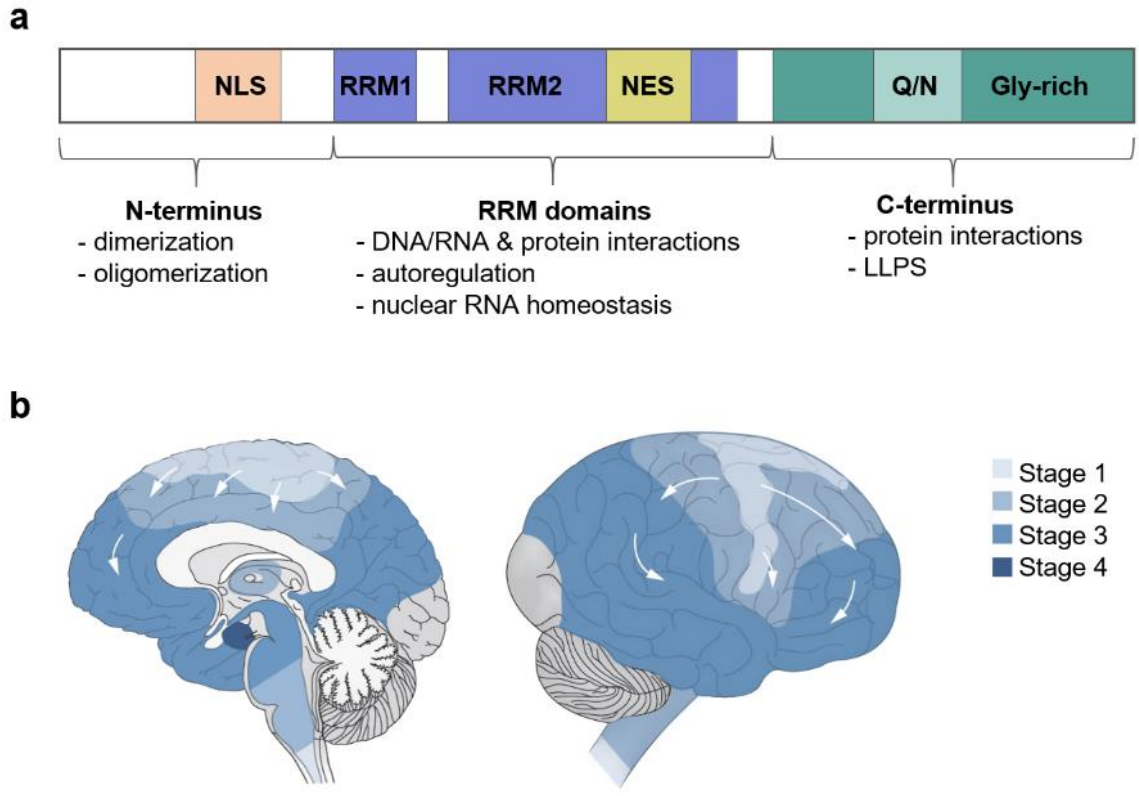

Figure 5. **TDP-43 and its role in ALS pathophysiology.**

(**a**) The diagram illustrates the functional domains of transactive response DNA-binding protein 43 kDa (TDP-43). TDP-43 consists of several key domains, including the N-terminal domain (N-terminus), which is implicated in TDP-43 dimerization and oligomerization; RNA recognition motifs (RRM1 and RRM2), essential for nucleic acid binding and nuclear RNA homeostasis; the nuclear localization signal (NLS), vital for nuclear import; the nuclear export signal (NES), facilitating nuclear export; and the C-terminal glycine-rich domain (C-terminus), associated with aggregation and pathogenic behavior. Adapted from (Versluys et al., 2022). (**b**) Propagation of phosphorylated TDP-43 (pTDP-43) aggregates in ALS. Stage 1: Onset of lesions in the agranular neocortex and bulbar (XII)/spinal somatomotor neurons. Stage 1: lesions develop in the primary motor cortex (also referred as agranular neocortex) and bulbar (XII)/spinal somatomotor neurons. Stage 2: The pTDP-43 pathology advances to affect the reticular formation, precerebellar nuclei, and specific parts of the thalamus. Aggregates form in the parvocellular segment of the red nucleus (RN) and the compact part of the substantia nigra (SN). Stage 3: Lesions extend to involve the postcentral neocortex (CN) and the putamen (PU). Stage 4: Further progression reaches the transentorhinal (TE) and entorhinal (EN) regions, as well as hippocampal areas (CA1–2) and the dentate fascia. Taken from (Braak et al., 2013)

TDP-43 autoregulates mRNA levels of *TARDBP* by binding its 3' UTR, too (Ayala et al., 2011; Polymenidou et al., 2011; Tollervey et al., 2011). This autoregulation is critical for self-oligomerization of TDP-43, which is implicated to be concentration-dependent (Chang et al., 2012). It is speculated that TDP-43 oligomerization could modulate its affinity to bind to nucleic acids and increase its RNA target specificity and perhaps recruit other RNA splicing factors, all contributing to the role of TDP-43 in RNA processing (Chang et al., 2012; Prasad et al., 2019). Besides mRNA, TDP-43 regulates the generation and the processing of micro-RNA (miRNAs) and long non-coding RNAs (lncRNAs). For example, nuclear TDP-43 is shown to control nucleases responsible for miRNA maturation (Freibaum et al., 2010; Kawahara and Mieda-Sato, 2012). Interestingly, TDP-43 also plays a role in nuclear paraspeckle and speckle formation (Shelkovnikova et al., 2018). Paraspeckles are regarded as subnuclear bodies found in the interchromatin space of mammalian cells that are formed by interaction between lnc-RNA species and members of drosophila behavior human splicing (DBHS) proteins (Fox and Lamond, 2010). As critical regulators of gene expression, they are responsible of the expression of potentially ALS-associated lncRNAs *NEAT1* and *MALAT1* (Tollervey et al., 2011; Liu et al., 2021).

On the other hand, the C- terminal domain (CTD) of TDP-43 has critical functions mostly in RNA splicing (Ayala et al., 2005). CTD has a rather unusual and disordered composition with prion-like low-complexity domains (PLCDS), consisting of a glycine-rich region and a glutamine-asparagine (Q/N) enriched segment (Kuo et al., 2009). These prion-resembling sequences regulate TDP-43's solubility and interactions between its hydrophilic and hydrophobic residues (Fuentealba et al., 2010). Under physiological conditions, these interactions promote the coalescence of TDP-43 molecules, leading to the formation of dynamic, membraneless compartments (i.e., stress granules) via a process called liquid-liquid phase separation (LLPS) (Shin and Brangwynne, 2017). However, in the presence of disease-associated mutations aberrant TDP-43 function could lead to irreversible stress granule formation, causing excessive aggregation, which is toxic to the cell (Johnson et al., 2009). Although there is accumulating evidence that PLCDs play a role in ALS-linked TDP-43 pathology, the exact contribution is still debated in the field (François-Moutal et al., 2019).

1.3.2. Pathophysiological Role of TDP-43 in ALS

While *TARDBP* mutations are only found in a small fraction of ALS patients, post-mortem examination reveal TDP-43 positive inclusions are present in the vast majority of patients (Ling et al., 2013). Aberrant forms of TDP-43 is also found in other neurodegenerative disorders, confirming its essential role in disease pathomechanisms (Meneses et al., 2021). TDP-43 pathology in ALS presents in many forms, both loss and excess TDP-43 is toxic to cells (Lee et al., 2011). Despite a lack of a clear consensus on how TDP-43 contributes to neurotoxicity,

aggregation of pTDP-43, nuclear depletion and cytoplasmic mislocalization are strongly linked to the initiation and/or progression of ALS (**Figure 5b**). In this section, evidence for a potential disease-causing role of TDP-43 will be discussed.

Cytoplasmic Accumulation and Nuclear Depletion of TDP-43

More than 50 pathogenic mutations in *TARDBP* are found in both sporadic and familial cases of ALS (de Boer et al., 2021). Nearly all of these mutations are missense mutations, encoding for the glycine rich part of C-terminal of TDP-43. It is suggested that these mutations contribute to ALS pathology through the generation of aberrant forms of misfolded TDP-43, altering protein-protein interactions and increasing its propensity to form aggregates. Multiple forms of TDP-43 aggregates have been linked to ALS via a toxic gain of function of the protein. For example, TDP-43 peptides with certain ALS-linked mutations (i.e., A315T and G335D) were shown to form amyloid-like aggregates with potential self- and cross- seeding properties (Guo et al., 2011; Jiang et al., 2016). In contrast to the transient TDP-43 inclusions formed under cellular stress, significantly larger stress granules and enhanced aggregation are observed in cell culture models expressing TDP-43 peptides with D169G, G348C and R361S mutations (Dewey et al., 2011; McDonald et al., 2011). Notably, in cell culture models, insoluble forms of TDP-43 were shown to have prion-like features (Furukawa et al., 2011; Nonaka et al., 2016). In one study, pathological forms of TDP-43 oligomers, obtained from ALS/FTD patient brains, were sufficient to induce insoluble TDP-43 inclusions in cultured neuroblastoma cells and were found to be transferred between cells. These aggregates shared the same pathological features like their parent aggregates and were heat/proteinase treatment resistant, implicating prion-like properties of TDP-43 (Nonaka et al., 2016).

On the contrary to mutations in CTD, mutations affecting the NTD and NLS regions (e.g., A90V) are more closely linked to its loss of function due to nuclear TDP-43 depletion (Winton et al., 2008; Barmada et al., 2010). Loss of normal nuclear TDP-43 is seen in both ALS patients and in disease models (Prasad et al., 2019). It is unclear if nuclear depletion is a result of impaired TDP-43 autoregulation in the nucleus under stress conditions, or due to uncontrolled export of normal TDP-43 to the cytoplasm for their sequestration into pathological TDP-43 assemblies (de Boer et al., 2021). Regardless of the exact mechanism, the loss of nuclear TDP-43 is detrimental to gene expression homeostasis. As such, nuclear TDP-43 depletion induced via ASO against TDP-43 in mice resulted in the downregulation of over 200 genes, which are important for synaptic function (Polymenidou et al., 2011). Moreover, the loss of nuclear TDP-43 function causes aberrant splicing patterns, which result in the incorporation of cryptic exons (CE) in multiple transcripts of genes that are linked to ALS/FTD (Ling et al., 2015). The expression of cryptic exons due to TDP-43 dysfunction was first shown in pre-mRNA of *STMN2* encoding for stathmin 2, a microtubule associated protein that has a major

role in axonal dynamics (Mehta et al., 2023). Strikingly, in the presence of CEs, reduced *STMN2* expression in both sporadic and familial ALS patients (except SOD1-fALS) was reported (Klim et al., 2019; Melamed et al., 2019). Soon later, a well-known ALS-linked GWAS hit *UNC13A* was reported to include CEs in its transcripts, again, shown to be dependent on TDP-43 malfunction (van Es et al., 2009; Ma et al., 2022). *UNC13A* has a vital role in synaptic function, especially in vesicle maturation during neurotransmitter release. Possibly owing to its involvement in neuronal functions, ALS patients with single nucleotide polymorphisms (SNPs) in *UNC13A* often have decreased survival compared to other ALS patients (Diekstra et al., 2012; Yang et al., 2019). Although there is a lot more to be uncovered about CEs and their functions in ALS, it would be safe to assume a potential role in ALS-FTD pathomechanisms (Mehta et al., 2023).

pTDP-43: A key feature implicated in initiation and progression of cortical disease pathology in ALS

Historically, ubiquitin positive inclusions were the first to be detected in both sALS and fALS patients, predominantly in LMNs (**Figure 6a-b**) and UMNs (**Figure 6c-d**) but also in glial cells (Lowe et al., 1988; Arai et al., 2003; Saberi et al., 2015). As ubiquitin has various functions in maintaining protein homeostasis, the presence of skein-like, dense cytoplasmic ubiquitin positive structures indicated that other proteins could be involved in their formation. Almost two decades later, it was shown that these inclusions were closely related to TDP-43 inclusions, and regulate TDP-43 function (Arai et al., 2006; Neumann et al., 2006). TDP-43 undergoes multiple post-translational modifications (PTMs) such as phosphorylation, ubiquitination, acetylation, cysteine oxidation and poly ADP-ribosylation, all reported to be present in ALS cases (Arai et al., 2006; Neumann et al., 2006; Kametani et al., 2016; Prasad et al., 2019). TDP-43 PTMs are shown to modulate the aggregation, condensation and solubility of TDP-43, although detailed characterization of the PTMs is still required to understand how they exactly contribute to the toxicity of TDP-43.

Different forms of TDP-43 inclusions are present in ALS patients. While coarse/fine skein-like inclusions (**Figure 6e-f**) are seen in similar frequency in UMNs and LMNs, round or dot-like ones (**Figure 6g-h**) are found more often in LMNs (Saberi et al., 2015). As mentioned before, the presence of hyper-phosphorylated TDP-43 inclusions is the most consistent finding in ALS pathology (**Figure 6i-j**), thus the C- terminal phosphorylation of TDP-43 has been the most profusely studied PTM (Ling et al., 2013; Prasad et al., 2019). The majority of findings attribute a toxic gain of function with regards to hyper-phosphorylation of TDP-43, arguing for an enhanced oligomerization and aggregation (Nonaka et al., 2009; Barmada et al., 2010). Whereas others report TDP-43 hyper-phosphorylation suppresses its condensation and

aggregation, which could be a protective mechanism (Gruijs da Silva et al., 2022), or a defense mechanism occurring only post-aggregation (Brady et al., 2011; Li et al., 2011).

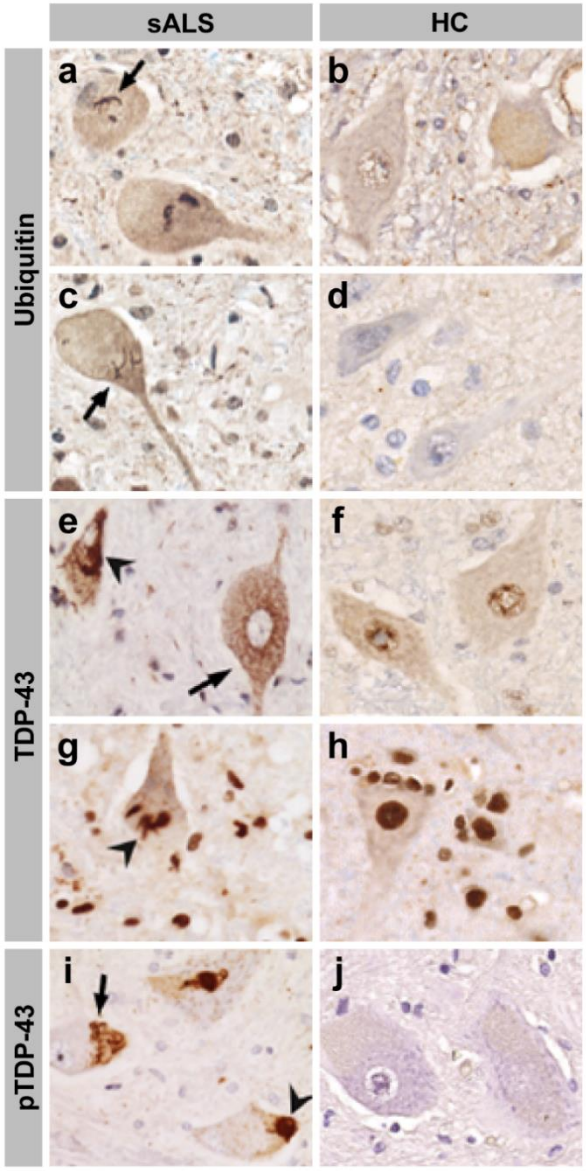

Figure 6. Various inclusions observed in ALS neuropathology.

The presence of ubiquitin positive skein-like inclusions (arrow) in spinal motor neurons of the lumbar anterior horn (**a**) and Betz cells of the motor cortex (**c**) in ALS cases, which are absent in healthy controls (HC) (**b, d**)**.** (**e**) TDP-43 inclusions, appearing both diffuse (arrow) and skein-like (arrowhead), along with nuclear clearing in ALS spinal motor neurons (**f**) while normal TDP-43 is localized in nucleus in control tissues. (**g**) Another type of TDP-43 inclusions appears dense and round in the motor cortex of individuals with ALS compared to (**h**) control cases. (**i**) Phosphorylated TDP-43 (pTDP-43) staining, showcasing skein-like inclusions (arrow) and dense round inclusions (arrowhead) in ALS lower motor neurons, (**j**) which are not evident in control specimens. All images are magnified at 40x. Taken and adapted from (Saberi et al., 2015).

pTDP-43 detection in CNS tissues is well-characterized and proven to be a useful tool for disease staging in ALS based on histological findings of brain regions. In fact, disease staging based on misfolded protein pathology was first proposed by Heiko Braak (Braak and Braak, 1991) for Alzheimer's and Parkinson's' diseases in 1991 (Braak and Braak, 1991). Many years after, Braak and colleagues also showed that the accumulation of hyper-phosphorylated TDP-43 inclusions was indicative of disease-stage in ALS-FTD (Braak et al., 2013). The initial site of pTDP-43 seeding and aggregation is the primary motor cortex, characterizing 'Braak stage 1', from where it spreads along anatomically connected regions (**Figure 5b**). The exact sequence of events such as nuclear depletion, aggregation or hyper-phosphorylation is not clear due to limitations with the post-mortem investigation of the brain. Yet, the mechanism by

which pTDP-43 aggregates affect neurons is suspected to be due to a toxic gain of function (Johnson et al., 2009). Although some studies have shown that the aggregation of the protein is not essential for cytotoxicity (Barmada et al., 2010; Sasaguri et al., 2016), other studies suggest a certain level of toxicity of TDP-43 aggregates (Igaz et al., 2011; Walker et al., 2015). Moreover, cytoplasmic TDP-43 aggregation induced by overexpressing TDP-43^{dNLS} results in reduced neurite growth (Winton et al., 2008). Surprisingly, the reversal of TDP-43^{dNLS} overexpression was shown to rescue neurons and reverse motor phenotypes in multiple models of ALS/FTD (Ke et al., 2015; Walker et al., 2015). In addition, TDP-43 aggregates have been shown to sequester nascent TDP-43, preventing it from functioning normally in the nucleus (Zhang et al., 2013a). These studies suggest that the cytoplasmic aggregation of TDP-43 could result in a toxic gain-of-function, yet the exact mechanisms are not completely understood.

Nevertheless, the accumulation of pTDP-43 inclusions in different brain regions is widely accepted as a sign of a progressed disease stage and valued as an additional resource for understanding the sequence of events in ALS pathology.

1.4. Transcriptomics and the era of single cell RNA sequencing

What is transcriptomics?

The term ‘transcriptome’ refers to the complete set of all RNA molecules transcribed from the DNA of a cell, tissue, or organism. In contrast to DNA, expression of RNA molecules is very dynamic and different forms of RNA interfere with gene expression. For example, mRNA encodes for proteins, while non-coding RNAs (microRNAs, long-non-coding RNAs & small nuclear RNAs) do not encode for proteins but regulate gene expression and cellular function, too. Hence, studying the transcriptome of an organism provides invaluable insights into how cells respond to disease states or environmental changes, and how these responses are orchestrated at the molecular level.

1.4.1. Single cell RNA sequencing

Transcriptome analysis has been typically carried out using techniques like micro-array and RNA- sequencing methods. Over the last decade, RNA sequencing methods have improved immensely, from bulk RNA-sequencing of the whole transcriptome (i.e., from pooled cells) to single cell resolution. The impressive breakthrough in the field came in 2009 when Tang et al. for the first time sequenced a single cell (i.e., a blastomere & an oocyte) and opened the necessary grounds for making single cell RNA sequencing (scRNA-seq) technology scalable and better compatible with high-throughput RNA sequencing (Tang et al., 2009). Since then, the field has evolved rapidly. A wide range of technologies from microfluidic-, microwell-, to

droplet-based systems have been developed by both academics and companies (Svensson et al., 2018). Now RNA sequencing of more than a million single cells with spatial resolution is possible at affordable costs, responsible for the steep increase in scientific publications in the 'single cell transcriptomics' field (Jovic et al., 2022). One commercially available platform used widely in the field due to its cost-effectiveness, which is also employed for my thesis, is called 10x Chromium Single Cell Expression platform (10x Genomics). This platform combines microfluidics and nucleotide barcoding (i.e., 3' unique molecular identifier (UMI) tagging) methods for droplet-based RNA-seq that were initially published in 2015, namely as inDrop and Drop-seq methods (Klein et al., 2015; Macosko et al., 2015).

Prior to a scRNA-seq experiment, the quality of the total transcripts is inferred by assessing the RNA integrity number (RIN), which assigns a number to the ratio of ribosomal units 28S and 18S of rRNA (Schroeder et al., 2006). In general, a RIN > 6 (10 being the best, 0 being the worst) is considered to indicate minimal degradation of transcripts from which a good quality cDNA library could be produced (Kukurba and Montgomery, 2015). However, the RIN is not directly informative about the integrity of all RNA species (like mRNA, miRNA, ncRNA etc.) and snap-frozen post-human samples with a lower RIN (e.g., RIN < 3) were shown to be viable for studying transcriptomics, too (Sonntag et al., 2016).

In short, the execution of a scRNA-seq experiment starts with the isolation of single cells from the tissue of interest, followed by cell lysis to isolate RNA from each cell, which is encapsulated in a droplet with a distinct UMI. Regardless of the platform, the initial step after obtaining RNA requires its conversion to cDNA via reverse transcription (RT). The next steps for preparing a cDNA library involve amplification of the cDNA e.g., via polymerase chain reaction (PCR), and later indexing samples with unique barcodes. In this way, multiplexed libraries (pooled from multiple samples) can be sequenced together in high-throughput technologies like Next Generation Sequencing (NGS), later to be de-multiplexed post sequencing.

Similar approaches have been also used for RNA-seq from single nuclei, since the isolation of viable cells from post-mortem samples is technically challenging. Snap-freezing of post-mortem tissue, however, preserves nuclear integrity, holding a great potential for studying transcriptomic changes in health and disease directly from human specimen (Krishnaswami et al., 2016). While single cell applications are crucial for investigating cytoplasmic RNA species (e.g., mature mRNA), RNA species isolated from nuclei are shown to be as informative as single cell transcriptomics (Lake et al., 2017). In fact, transcriptome coverage in single cell vs single nuclei experiments is very similar (Lake et al., 2017; Ding et al., 2020). Yet, snRNA-seq could be more informative for studying certain aspects of diseases as it is superior in capturing nuclear RNA species, such as non-coding and other regulatory of RNAs, whose emerging

roles have been implicated in many neurodegenerative diseases, including ALS (Salta and De Strooper, 2017; Laneve et al., 2021).

Challenges in single cell RNA sequencing

Taking advantage of utilizing human specimen together with the advancements in NGS and single cell RNA-seq technology, it is now possible to attain an unprecedented understanding of molecular changes in health and disease in a cell type -, disease stage - and region-specific manner. Though a very powerful tool, scRNA-seq, just like many other techniques generating large data requires rigorous biostatistical analysis and post-hoc validation to interpret the findings. Since the field is relatively young, researchers constantly strive to develop new tools and algorithms to maximize the access, harmonization and data analysis of these large RNA-seq datasets. Multiple pitfalls come with the technique and the analysis: high dimensionality, sample variability, and technical noise to name a few (Lähnemann et al., 2020; Squair et al., 2021).

The first task when analyzing a high-dimensional scRNA-seq data is to reconstruct the data in a low-dimensional way to make it more interpretable while conserving biologically relevant information (Kiselev et al., 2019; Jovic et al., 2022). The ‘smoothing out’ of unwanted variance in the dataset, be it from sampling bias or due to high sample-inherent variance (e.g., from human specimen), is being circumvented by taking expression levels of all cells in the data into account, regardless of cell type and condition (e.g., disease vs healthy). Moreover, to deal with ‘the curse of dimensionality’, unsupervised data clustering is performed for which multiple algorithms are available, such as Principle component analysis (PCA), t-distributed Stochastic Neighbor Embedding (t-SNE) and Uniform Manifold Approximation and Projection (UMAP) (Kiselev et al., 2019; Zhang et al., 2023). PCA is a linear reduction method, which allows for maintaining the variance between large pairwise distances, whereas t-SNE is a non-linear technique that takes into account similarities between small pairwise distances. UMAP is another non-linear dimensionality reduction method that enables the preservation of the global data structure in 2D space, which is not possible with t-SNE due to differences in the random initialization process (Kobak and Linderman, 2021). None of these is clearly superior in segregating cell types. Which dimensionality reduction methods to employ to process single-cell data is largely a researcher-dependent decision. Data-smoothing also still remains a challenge as it can compromise important information for downstream analyses (i.e., differentially expressed genes (DEGs) analysis) and thus no one-fits-it-all algorithm is available to date (Jovic et al., 2022).

Another source of unwanted variance is the data generation process. Single-cell cDNA libraries are produced from very small amounts of mRNA, which are further amplified for

adequate detection during sequencing. While requiring only minute amounts of mRNA is advantageous for working with precious samples, it has clear drawbacks. When a transcript expressed in one cell is not detected in another, it is assigned a zero-expression value: a phenomenon called 'dropout' (Lähnemann et al., 2020; Linderman et al., 2022). This results in many 'zeros' in data that could be explained either by 'technical' or 'biological' variance. A 'technical zero' could be the result of undersampling of transcripts from a sample, whereas a 'biological zero' could be assigned to a cell that was not captured with mRNA expression of a particular gene at that time (Lähnemann et al., 2020). In order to preserve biological 'dropouts' while avoiding technical zeros at the same time, many imputation algorithms are used before any dimensionality reduction is performed (Linderman et al., 2022). The imputation of 'dropouts' is a crucial step as the incorrectly assigned variance could be detrimental for downstream analyses (Jovic et al., 2022; Wang et al., 2022a). One way to tackle this problem is to convert single-cell data (i.e., by aggregating the gene expression values of a sample) into a bulk-seq data structure to create a 'pseudo-bulk' dataset (Murphy and Skene, 2022). Thus, comparing downstream analyses from both single cell and pseudo-bulk versions of a dataset adds an additional layer of control during data interpretation.

Here, I have only pointed out the most critical problems with single-cell data analysis (for more technical limitations, readers are referred to a detailed review (Lähnemann et al., 2020)). These drawbacks show that any biological conclusion drawn from single cell data warrants further scrutiny and validation (e.g., of candidate DEGs with IHC and/or via *in situ* hybridization (e.g., RNAscope™, Advanced Cell Diagnostics)).

2. Aim of the study

ALS is a lethal disease, which primarily affects motor areas of the central nervous system, resulting in UMN and LMN loss. The presence of pTDP-43 inclusions is often regarded as the culprit of the neurodegeneration and is accompanied by glial reactivity. It, however, is still a matter of debate whether pTDP-43 aggregates are causal to neuronal death or an indicator of a neurodegenerative process per se. As the availability of human CNS tissue samples is mainly restricted to the end-stage ALS, it remains challenging to identify early molecular alterations, preceding the occurrence of pTDP-43 pathology. In this thesis, I addressed this point by elucidating early molecular events in ALS. To this end, I included two neuropathologically distinguished regions 1) primary motor cortex (MC) with typical pTDP-43 inclusions (thus characterized as Braak stage 1), and 2) frontal cortex (FC) without pTDP-43 inclusions, which however would be classified as Braak stage 2 if pTDP-43 inclusions were already present, thus was considered as a 'pre-stage' with regards to TDP-43 pathology. I performed snRNA-seq of nuclei isolated from the post-mortem patient and control tissue and explored region - and disease stage - specific transcriptional alterations in ALS.

Hypothesis

I hypothesize that in ALS, a cascade of events in non-MN cells could be an early contributor to disease pathology. For instance, microglia could undergo an early phenotypic shift towards a pro-inflammatory state, initiating a neuroinflammatory response. Astrocytes may also undergo reactive changes, compromising their supportive functions and exacerbating the neurotoxic environment. Interneurons and other excitatory neurons could be early contributors to synaptic dysfunction, disrupting the delicate balance of excitatory and inhibitory signaling. Additionally, oligodendrocytes may display early dysfunction, leading to compromised neuronal support and axonal integrity. The interplay of these glial cells and neurons in the early disease stages may collectively contribute to the initiation and progression of ALS pathology prior to the occurrence of pTDP-43 aggregates, a classical hallmark of the disease. The sequence of transcriptomic changes can be unraveled through the regional comparison of MC and FC, which lies 'downstream' in the disease trajectory with respect to the presence of pTDP-43 aggregates.

Research objectives

I. What are early molecular changes in ALS pathophysiology in the absence of pTDP-43 aggregates?

II. Which cell types are primarily affected and what kind of early intercellular communication alterations are observed in ALS?

3. Material and Methods

3.1. Post- mortem human cortical specimen

Snap frozen post-mortem human brain samples were obtained from the Neurobiobank München. FC (Broadmann`s area 4) and MC (Broadmann`s area 8) of 5 ALS patients (median age 63 y) including sporadic (n = 2) and familial (n = 3) ALS cases, and neurologically healthy controls (HC, median age 42 y) were included in this work. Sporadic cases did not harbor any known genetic cause associated with ALS, while familial cases were carriers of $(G_4C_2)_n$ hexanucleotide repeat expansions in the *C9ORF72* locus. The inclusion criterion for this study was the absence of the classical pTDP-43 pathology in the FC of the patients, whereas MC of the same patients were identified as Braak stage 1, characterized by the presence of pTDP-43 inclusions. Any patients with FTD or any other form of dementia were excluded. The cause of death for ALS patients was due to complications from ALS who can be thus classified as 'end-stage' ALS and no cognitive impairment (e.g., dementia) was reported at the time of their death.

The experiments performed with human donor material have been approved by Ludwig Maximilians University (LMU) of Munich Ethics Committee. Detailed information about human cortical specimens can be found in **Table 1.**

Sample	diagnosis	sex	age (years)	PMI (hours)	region	RIN (FC/MC)
HC1	-	F	67	38	FC + MC	8.3/6.9
HC2	-	M	42	42	FC + MC	9.3/7.8
HC3	-	M	41	31	FC + MC	7.2/7.5
ALS1	sALS	F	70	39	FC + MC	8.1/8.1
ALS2	sALS	F	78	62	FC + MC	8.3/8.1
ALS3	fALS	F	63	3	FC + MC	8.5/6.6
ALS4	fALS	F	46	20	FC + MC	7.5/7.2
ALS5	fALS	M	49	25	FC + MC	6.6/7.3

Table 1. Details of post-mortem human specimens used in this study.

Abbreviations: ALS, amyotrophic lateral sclerosis; HC, healthy control; F, female; M, male; sALS, sporadic ALS; fALS, familial ALS; PMI, post-mortem interval; RIN, RNA integrity number; FC, frontal cortex; MC, motor cortex.

3.2. RNA integrity determination

To assess the quality of mRNA prior to snRNA-seq experiments, I measured the RNA integrity of the post-mortem human brain samples. To this end, ~2 mg of frozen human cortical tissue was cut with a scalpel (on dry ice) and total RNA isolation was done by using the RNeasy Micro Kit (Qiagen, Cat #74004). I determined the RNA integrity number (RIN) by running an automated RNA electrophoresis assay (Bioanalyzer RNA 6000 Nano assay, Cat #5067-1511) on an Agilent 2100 BioAnalzyer instrument. All post-mortem human brain samples included in this work had a RIN > 6.5 (**Figure 7a**).

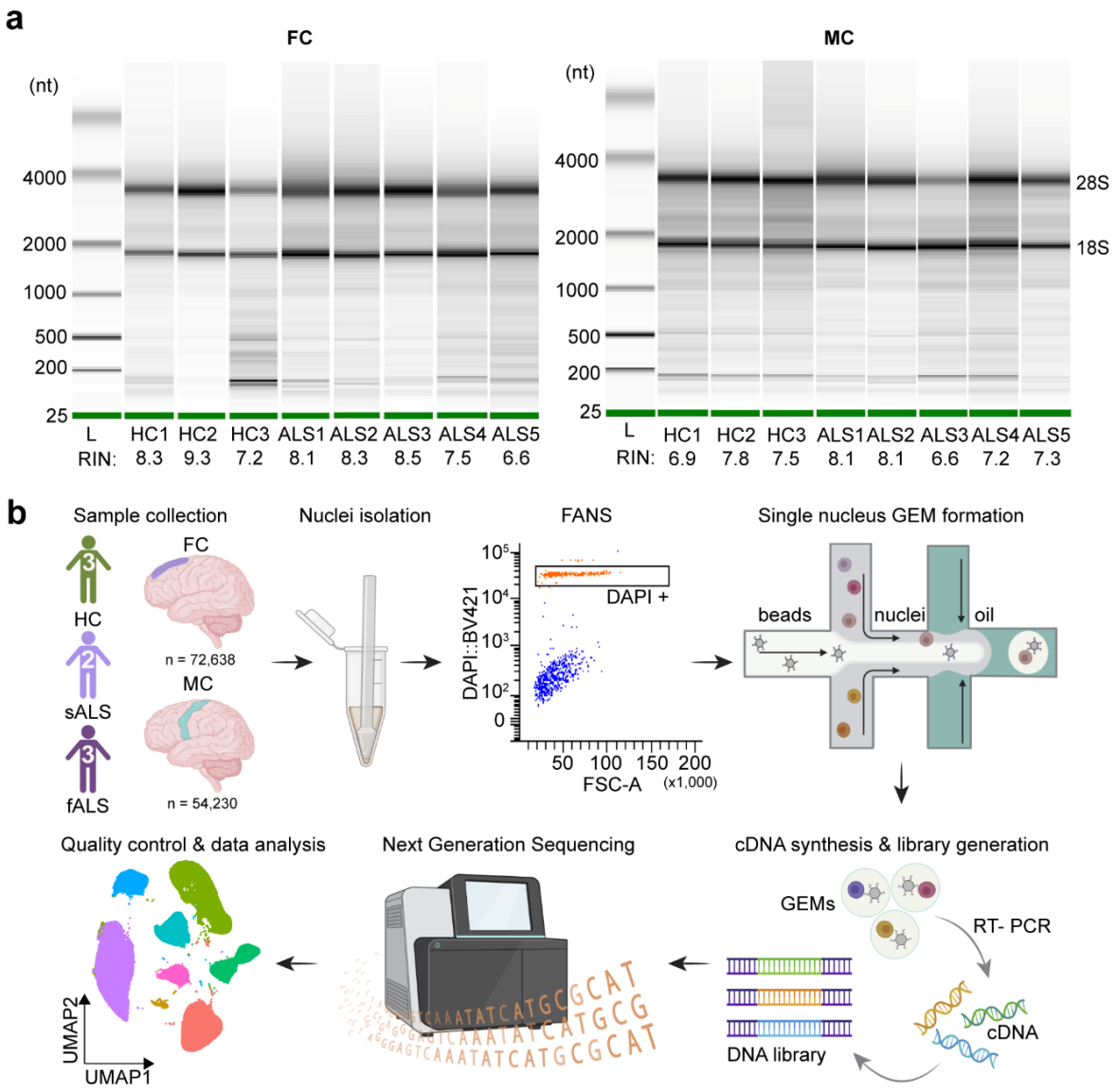

Figure 7. Schematic overview of methods and RIN of samples used for snRNA-seq.

(**a**) Gel electrophoresis profiles of total RNA isolated from respective samples. RNA integrity numbers (RIN) are derived from the ratio of the bands of the 28S and 18S rRNA subunit. (**b**) Experimental workflow for snRNA-seq. Frontal cortex (FC, n = 72, 638 nuclei) and motor cortex (MC, n = 54,230 nuclei in total of 8 tissue samples), were collected. Abbreviations: ALS, amyotrophic lateral sclerosis; HC, healthy control; FANS, fluorescence-activated nuclei sorting; GEM, Gel Bead-in-Emulsion; DAPI, 4′,6-diamidino-2-phenylindole; FSC-A, forward scatter area; RT-PCR, reverse transcription polymerase chain reaction; MC, motor cortex; FC, frontal cortex; L, ladder; nt, nucleotide. Figure was created with BioRender.com.

3.3. Isolation of nuclei from frozen post-mortem human specimen

For the isolation of nuclei an optimized version of the “Frankenstein protocol for nuclei isolation from fresh and frozen tissue” was used (Martelotto, 2020) (**Figure 7b**). For each sample, a gray matter section from snap frozen cortical tissue was collected with a scalpel while kept on dry ice to preserve the RNA integrity. As little as ~2 mg of tissue was then mechanically homogenized in Nuclei EZ Lysis Buffer (Sigma-Aldrich, Cat #NUC101) with the help of a pestle (Starlab, Cat #I1415-5390) in nuclease free tubes (Eppendorf, Cat #0030108078). The resulting homogenate was filtered using a 70 µm strainer (Miltenyi Biotec, Cat #130-098-462), and the filtered suspension was centrifuged at 500 xg for 5 min at 4 °C (Eppendorf, centrifuge 5417R, rotor: F-45-30-11). After removal of the supernatant, nuclei were resuspended in a buffer, described in aforementioned protocol as ‘Buffer 1’, whose final concentration is composed of 1x Dulbecco’s phosphate buffered saline (DPBS, Sigma-Aldrich, Cat #D8537), 1% bovine serum albumin (BSA, Sigma-Aldrich, Cat #A1595) and 0.2 U/µl RNAse inhibitor (Roche, Cat #3335399001). Followed by 5 minutes of incubation at 4 °C, the nuclei were further separated from impurities (e.g., myelin) by an additional centrifugation at 500 xg for 5 minutes at 4 °C and subsequent removal of supernatant. After resuspending the pelleted nuclei in Buffer 1, a small fraction (~5 µl) of the isolated nuclei was counterstained (1:1) with 0.4% Trypan Blue (Gibco, Cat #15250061) and visually checked for its integrity under a bright field microscope (Leica DMi1). Having determined nuclear integrity, the remaining nuclei solution was then stained with DAPI (Thermo Fisher, Cat #62248) for a final concentration of 10 µg/ml. Prior to fluorescence-activated nuclei sorting (FANS), the nuclei solution was once more filtered with a 30 µm strainer (Miltenyi Biotec, Cat #130-098-458). To achieve single nuclei with the least impurities possible, nuclei were sorted for the DAPI+ gate with a 70 µm nozzle at sorting precision ‘single cell’ in Aria III Cell Sorter (BD Biosciences). 20.000 nuclei/sample were sorted into a well of a 96-well cell culture plate (Corning Inc., Cat #3799) with a master mix solution (23.2 µL/well), for an estimated recovery of 10.000 nuclei post-sequencing. The master mix solution per sample (i.e., a total of 23.2 µL per well) is composed of RT Reagent B (18.8 µl), Template Switch Oligo (2.4 µl) and Reducing Agent (2.0 µl), which are part of the Chromium Next GEM Single Cell 3' Kit v3.1 (10x Genomics, Cat #1000121), used for generating droplet-based snRNA-seq libraries in this study. All steps of nuclei isolation (homogenization, centrifugation, incubation, FANS) were done at 4 °C and only pre-chilled (on ice) solutions and nuclease free plastic ware (e.g., tubes, pipette tips) were used unless otherwise mentioned.

3.4. Genomic library preparation & droplet-based snRNA-seq

The generation of cDNA libraries from the sorted nuclei was done with the commercial high-throughput single-cell RNA-seq platform 10x Chromium 3’ (v3.1) (10x Genomics). The

respective user guide for the Chromium Next GEM Single Cell 3' Reagent Kit v3.1 provided by the manufacturer was followed for each step of the library production (Doc #CG000204, Rev D). Below is the summary of steps followed for the generation of snRNA-seq libraries in this thesis.

Step 1: GEM generation and barcoding

Sorted nuclei in the master mix were partitioned into Gel Bead-in-Emulsion (GEMs), a process which facilitates the capturing of a single nucleus in one droplet together with a unique feature barcode from the 10x 3' v3.1 gel beads. Per sample, 23.2 µl of the nuclei-master mix suspension was added with 8.7 µl Reverse Transcription Enzyme C and an additional 23 µl of H_2O to reach a final volume of 75 µl prior to GEM formation. 70 µl of this cell-enzyme suspension was loaded onto Chip G for the automated single droplet formation on the microfluidic platform 10x Genomics Chromium Single Cell Controller. This system enables the capturing of one nucleus/cell per droplet, combined with the barcoded oligonucleotides. Right after the formation of the GEMs, the barcode containing gel bead is dissolved and co-partitioned nuclei are lysed, rendering their RNA accessible for reverse transcription via a primer containing an Illumina TruSeq Read 1 sequence, 16 nucleotide (nt) 10x barcode, 12 nt unique molecular identifier (UMI), 30 nt poly(dT) sequence and template switch oligo (TSO). Formed GEMs are incubated in a thermal cycler, resulting in uniquely barcoded full length cDNAs from poly-adenylated mRNAs from a single nucleus.

Step 2: Post GEM–RT cleanup & cDNA amplification

This step is required for the purification of the first-strand cDNA from the reaction mixture obtained after step 1. Using Dynabeads MyOne SILANE beads (Invitrogen, Cat #370-12D), cDNA is extracted via magnetic separation. Next, ensuring sufficient nucleic acid for library preparation, purified full-length cDNA is amplified with the recommended polymerase chain reaction (PCR) conditions for targeting > 6,000 nuclei recovery. Prior to the library preparation, amplified cDNA is purified with the SPRIselect reagent (Beckman Coulter, Cat #B23318).

Step 3: 3' Gene expression library construction

cDNA is processed further for the 3' gene expression library production. Shortly, enzymatic fragmentation is used to remove the TSO, opening the poly(dT) end of the cDNA. P5 and P7 primers (for Illumina NGS platform), a single sample index (Single Index Kit T Set A, 10x Genomics, Cat #1000213) and TruSeq read 2 primer are then added to the poly(dT) sequence via End Repair, A-tailing, Adaptor Ligation, and PCR steps. 2 step SPRI select is performed to obtain the targeted size of the final library (300-600 bp with a mean of 400 bp). The resulting cDNA libraries thus contain P5 and P7 primers for Illumina and a single sample index for identification of transcripts coming from individual samples.

Step 4: Next generation sequencing and data pre-processing

Pooled libraries were sequenced using the NovaSeq6000 system (Illumina) with S4 flow cell (500M reads/sample) with 2 x 150 bp paired-end read length. Data in this thesis is obtained via sequencing services provided by Institute of Clinical Molecular Biology (IKMB) of the University of Kiel, Germany. The Cell Ranger Single Cell Software Suite (cellranger-v5.0.1, 10x Genomics) was used to align reads to the human reference genome (GRCh38), sample de-multiplexing and gene expression quantification, returning a unique molecular identified (UMI) count matrix.

3.5. Analysis of single nucleus RNA-seq data

3.5.1. Quality control (QC) and filtering

The resulting gene expression count matrix is analyzed by the 'R' package 'Seurat' (v4.0.2) for single cell RNA sequencing, using the default 'RNA' assay (Hao et al., 2021). Nuclei with unique feature counts less than 500 and a number of UMIs less than 1000 were filtered out. In addition, to filter unhealthy/dying nuclei, nuclei with more than 1% mitochondrial gene expression were removed. The raw counts were then log-normalized and variable genes were detected with 'FindVariableFeatures', using the selection method 'mean.var.plot' for the top variable genes. Data was scaled using the 'ScaleData' function, while regressing out the variance introduced by the number of UMIs detected per nucleus, and a PCA was run to achieve linear dimensionality reduction.

3.5.2. Annotation of global cell populations

Clustering of the main cell types was done by executing the 'FindNeighbors' function (for top 5 PCAs) and 'FindClusters' function. The 'FindAllMarkers' function was used to determine markers for main cell populations (e.g., astrocytes, interneurons etc.). Top significant genes (Wilcoxon rank sum test, $p < 0.05$) expressed differentially between a cell type and the rest were used for annotating that cell population.

3.5.3. Cell population specific subcluster analysis and annotation

7 out of 8 main cell types (excluding endothelial cells due to low cell counts) were subset from the QC filtered data and separately subjected to further analysis. Raw counts from each cell type were log-normalized and top variable features were identified with the selection method 'mean.var.plot' and scaled by regressing out the number of UMIs per nucleus. Although my samples were all sequenced at the same time in order to avoid a sequencing bias, I yet observed a striking variability across individual samples, which I treated as a "batch effect". To

this end, datasets consisting of all cells of a given cell type only (e.g., all microglia) were integrated using the 'Harmony' package in 'R' which corrects for sample variation (e.g., from different batches) (Korsunsky et al., 2019). Harmonized data was used for clustering and downstream analysis. Cell-type subcluster specific markers were identified by using the 'FindAllMarkers' function with the following criteria: 1) genes detected in a minimum in 20% of cells (min.pct = 0.20) and 2) genes with a minimum relative average gene expression of log2 fold change (Log2FC) threshold of 0.2 when compared to the rest of the cells. If a subcluster-exclusive marker was not assigned at the former step, additional markers (e.g., to distinguish two closely related subclusters) were detected with 'FindMarkers' function. For this, genes expressed in a minimum of 25% of either subclusters with log2 fold change = 0.2 was set and their significance was probed using the Wilcoxon rank sum test ($p < 0.05$). These criteria were kept identical for all cell types. After subclusters were identified for each of the 7 main cell types, I assessed the relative abundancy (%) of those by dividing the number of nuclei in that subcluster by total number of nuclei in that cell type (e.g., # homeostatic (HOM) microglia / # all microglia) and multiplying by 100.

3.5.4. Pseudotime trajectory inference

Prior to further downstream analyses, pseudotime inference was performed on cell types (i.e., OPCs-oligodendrocytes, microglia and astrocytes), from which differentiation and/or maturation information could be inferred. The 'Monocle3' package in 'R' was used for this purpose and the starter subcluster was chosen, corresponding to the most 'physiological' or most 'naïve' subcluster (Trapnell et al., 2014; Qiu et al., 2017; McInnes and Healy, 2018; Cao et al., 2019). For example, for the microglia I opted for the cluster HOM as starting point, as it displays higher expression levels of homeostatic microglia markers (e.g., *P2RY12*, *P2RY13*, *CX3CR1*) compared to the other microglia subclusters and is thus considered to represent the more 'physiological' state. For astrocytes the same concept was applied, which led to the selection of cluster 0 (e.g., lower *GFAP* expression compared to other subclusters) as the 'starting' point. Lastly, for oligodendrocytes, I used OPCs as a starting cluster accounting for the notion that OPCs can further differentiate into oligodendrocytes and are thus considered a precursor state.

3.5.5. Gene expression analysis

Two types of comparisons for DEGs were made in my dataset: 1) genotype comparison per region (ALS vs HC); 2) region comparison per genotype (MC vs FC). For all DEGs analyses, I compared all cells of a population (e.g., all microglia) within a genotype or region. First, I compared the gene expression of ALS patients with HCs in FC and MC to identify disease related alterations, separately. Second, I explored if there was a difference between cortical

areas in ALS, for which I compared gene expression levels between FC and MC in ALS patients. Third and last, I checked whether there was a difference in the transcriptome of MC vs FC of HCs. For all comparisons, I defined DEGs as genes that are differentially expressed in at least 10% of a cell type compared to the other genotype/region with a $\log_2$FC threshold of 0 to detect minute changes that can arise from transcriptomic changes in small subclusters. Mitochondrial (*MT-*) and ribosomal genes (*RPS*, *RPL*) as well as sex-linked genes (*UTY*, *XIST*, *PCDH11Y*, *USP9Y*, *NLGN4Y*, *TTTY14*, *TTTY10*, and *XACT*) were filtered out due to slight sex imbalance in my dataset. Significance was determined using the Wilcoxon rank sum test and p-values were adjusted with the Benjamini-Hochberg method. Genes with false discovery rate (FDR) < 0.05 were kept for further analyses.

For the global data (that is all cell types included), in addition to snRNA-seq gene expression analysis as described above, data were converted to pseudobulk with the 'AggregateExpression' function, in which raw gene counts are aggregated (or summed). DEGs of pseudobulk data were identified with the 'DESeq2' package in 'R' (Love et al., 2014). The resulting p values were corrected for multiple comparisons via the Benjamini-Hochberg method. DEGs with FDR < 0.05 were considered significant.

3.5.6. Gene ontology (GO) enrichment analysis

Pathway enrichment analysis of differentially expressed genes (FDR < 0.05, |Log2FC| >0) was done using the 'EnrichR' tool (Chen et al., 2013a; Kuleshov et al., 2016; Xie et al., 2021). I subjected up- and downregulated genes together to get an overall impression of the pathways dysregulated in the disease state. The top 10 gene ontology (GO) terms (p < 0.05, computed from Fischer's exact test) were plotted for 3 databases, GO Biological Process 2023 (BP), GO Molecular Function 2023 (MF), GO Cellular Component 2023 (CC). Here, I used p values instead of adjusted p values, as the rank-based order of the most enriched pathways is conserved.

3.5.7. Cell-cell interaction (Ligand-Receptor) analysis

I used the 'Liana' package (0.1.10) (Türei et al., 2021; Dimitrov et al., 2022) to probe for changes in the cell-cell interaction in ALS compared to HCs in FC and MC. First, I ran the 'Liana' pipeline to infer interactions (i.e., ligand-receptor (LR) pairs) using the "Consensus" database (Dimitrov et al., 2022) and highly ranked interactions were filtered per criterion aggregate_rank ≤ 0.01. The specificity of these interactions, that is the specificity of an L-R pair in cell-cell pairs, was calculated by NATMI's edge specificity weights (Hou et al., 2020). The expression magnitude of genes, on the other hand, was computed by 'SignalCellSignalR' L-R score, which assigns a non-negative regularized score ranging from 0 to 1, making it possible to compare between different datasets (Cabello-Aguilar et al., 2020).

Since I do not have the same number of nuclei in my 4 conditions (that is HC-FC, HC-MC, ALS-FC and ALS-MC), I took the smallest number of cells available for each cell type and pseudorandomly selected this number of cells from the overall cell type population. This procedure was repeated 100 times for each 'condition' and cell type. The limiting number of nuclei were microglia, n = 1,729; astrocytes, n = 1,913; oligodendrocytes, n = 8,486; OPCs, n = 1,499; excitatory neurons, n = 3,707; interneurons CGE, n = 1,485; interneurons MGE, n = 1,528; endothelial cells = 108. Median values (calculated in R) of bootstrapped ligand-receptor frequencies were used for visualization of the frequency heatmaps. Note that endothelial cells were included only in this analysis.

3.6. Visualization

All plots were created in 'R' (v4.2.2). UMAPs and ViolinPlots were created with the 'Seurat' (v4.0.2) package. The 'EnhancedVolcano' package (v1.16.0) was used for Volcano plots of DEGs. Heatmap for DEGs (both snRNA-seq and pseudobulk) and dot plot were created with the 'DoHeatmap' and 'DotPlot' function in the 'Seurat' package, respectively. Prior, z-scored expression values were calculated from the mean average expression of genes per patient (for heatmaps) or per cluster (for dot plot) for each region via 'AverageExpression' function in the same package. Heatmaps for cell-cell interaction analysis were plotted via the inbuilt 'heatmap' function in 'R'.

3.7. Immunohistochemistry

Snap-frozen post-mortem FC and MC (defined by the presence of Betz cells) samples of approximately 1 cm^3 were thawed at room temperature (RT) for 10 minutes, fixed in 4% neutral-buffered formaldehyde for approximately 48 hours at RT and then paraffinized. Paraffin embedded tissue was then cut on a microtome (Thermo Scientific Microm HM 340E) at RT into 4 µm thick sections and mounted on Superfrost Plus adhesion slides (Epredia, Cat #J1800AMNZ) using Fluoromount-G mounting medium (Southern Biotech, Cat #0100-01). For the detection of pTDP-43 and poly-GA, brain sections were incubated 32 minutes at 37°C with the primary antibody anti-pTDP-43 (1:50 dilution, clone 1D3 monoclonal rat, in-house production Helmholtz Institute Munich, provided by Christian Haass; Sigma-Aldrich, formerly sold under Cat #MABN14) or anti-poly-GA antibody (1:50 dilution, clone 5E9, monoclonal mouse, Sigma-Aldrich, Cat #MABN889). For the detection of activated microglia, sections were incubated for 32 minutes at 37°C with the anti-HLA-DP+DQ+DR primary antibody (1:100 dilution, clone CR3/43, monoclonal mouse, DAKO, Cat #M0775). The secondary antibody against rat-IgG (1:2000 dilution, rabbit IgG(H+L) by P.A.R.I.S.) was used with an incubation time of 28 minutes at RT. For all stainings, HRP-conjugated secondary antibody detection with DAB (3, 3'- diaminobenzidine, brown) and hematoxylin counter staining (blue) steps were

performed on Ventana BenchMark ULTRA (Roche) system using ultraView Universal DAB Detection Kit (Roche, Cat #05269806001) according to the instructions of the manufacturer. After staining, sections were covered with Fluoromount-G mounting medium (Southern Biotech, Cat # 0100-01) and fixed with a coverslip (24x50 mm, Menzel, Cat #MZ-0029) to be scanned with Pannoramic Midi II Slide Scanner (3DHistech, software Panoramic Scanner version 2.0.5) at fluorescence mode (magnification 20x).

3.8. Quantitative histopathological assessment

For both stainings, I have included adjacent sections from each paraffinized tissue block. In this way, I was able to match the regions of interest (ROIs) in both sections per patient to match pTDP-43 load and microglia activation. The selection of ROIs was as follows: 1000 µm × 3000 µm sized ROIs were spread evenly around a single gyrus where the top edge was at the pial surface. 5 ROIs per brain section were selected using QuPath (v0.4.3) (Bankhead et al., 2017). For both the pTDP-43 and HLA-DP+DQ+DR signal, image processing was done in a similar manner using ImageJ (Fiji, v1.54f). First, the DAB RGB type images channels were split and the blue channel corresponding to the DAB signal was chosen for further analysis. Images were thresholded (method MaxEntropy) and binarized and the % area of the DAB positive signal was measured.

3.9. Statistics

The ‘stats’ package in ‘R’ (v4.2.2) was used for computing FDR (Benjamini-Hochberg method). For the beta-regression, the ‘betareg’ package (v3.1.4) in ‘R’ was utilized. Statistical analyses for immunohistochemistry (one-sided Wilcoxon rank sum test) were done in Prism 7 (Graphpad). P values for GO terms were computed by EnrichR tool (Fischer’s exact test). Cell-cell interaction frequency differences were tested via two-tailed t test using ‘R’.

4. Results

4.1. pTDP-43 pathology

Since my study aims to understand molecular changes occurring prior to pTDP-43 pathology in ALS, I first confirmed the absence of pTDP-43 in FC as well as its presence in MC in my ALS cohort (**Figure 8a-b**). The percentage of the area occupied by pTDP-43 was significantly higher in ALS patients MC and absent in ALS FC and HC (**Figure 8c**, HC FC vs ALS FC p = 0.3369, HC MC vs ALS MC p <0.0001, ALS FC vs ALS MC p <0.0001, one –sided Wilcoxon rank sum test).

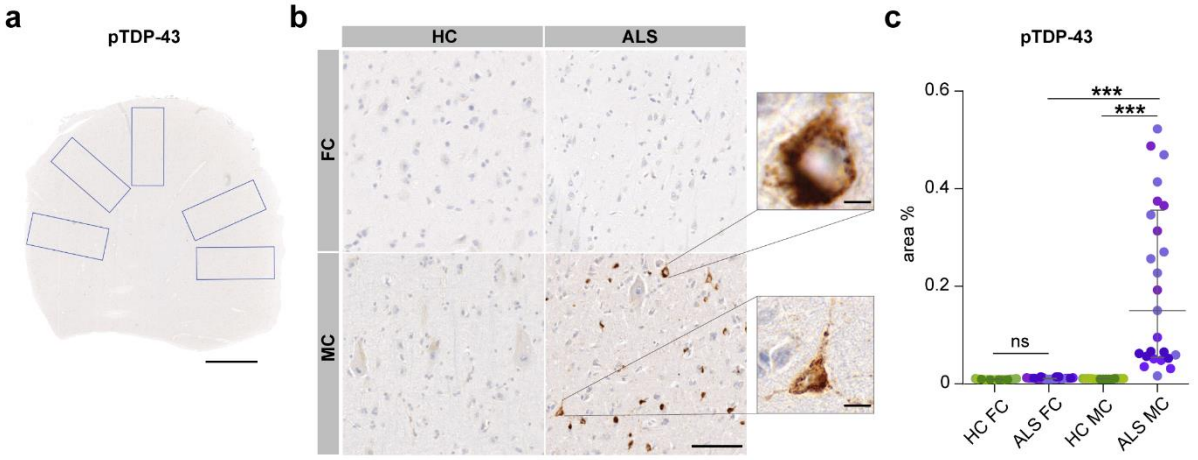

Figure 8. pTDP-43 pathology in end-stage ALS patients included in this study.

(**a**) An example overview of the randomized sampling of 5 equally sized regions of interest (ROIs) from a frontal cortex of an ALS patient for the quantification of pTDP-43 abundance. (**b**) Examples of DAB (3, 3'- diaminobenzidine) positive anti-pTDP-43 antibody signal in the gray matter of frontal (FC) and motor (MC) cortex of the same patient per group. Close ups show pTDP-43 in rounded cytoplasmic inclusion form (top) and in skein like neuronal inclusion (bottom). (**c**) Quantification of anti-pTDP-43 staining shows presence of pTDP-43 inclusions in motor cortex but not in frontal cortex of ALS patients (data points correspond to ROIs, color shade indicates patient identity, one –sided Wilcoxon rank sum test). Data in (c) represents median & IQR. Scale bar in (a) 2 mm and (b) 100 µm, insert (top) 10 µm and insert (bottom) 20 µm. *** p < 0.001.

4.2. Alterations in all cell types in ALS

I performed single nuclei RNA-seq of human post-mortem FC and MC samples from 5 ALS patients (fALS, n = 3; sALS, n = 2) and 3 healthy controls. A total of 126,868 nuclei were obtained: 72,638 from FC and 54,230 from MC. I identified 8 main cell types (**Figure 9a**). The key molecular marker genes used to differentiate cell types were: excitatory neurons (*SLC17A7*), interneurons caudal ganglionic eminence (CGE) (*GAD1*, *GAD2*, *ADARB2*), interneurons medial ganglionic eminence (MGE) (*GAD1*, *GAD2*, *LHX6*), microglia (*P2RY12*, *CX3R1*), astrocytes (*AQP4*, *GFAP*, *SLC1A2*), oligodendrocytes (*MBP, MOG*), OPCs (*OLIG1, MBP, PDGFRA*), and endothelial cells (*CLDN5*) (**Figure 9b**). For the global data (that is all cell types included), I investigated differences in DEGs of snRNA-seq and in the pseudobulk converted version of the same dataset to circumvent “drop-out” of lowly expressed genes. In the former dataset, I found in FC 1,806 genes which were downregulated (e.g*., CARNS1, SCD, GLDN*) and 2,027 that were upregulated (e.g., *HSP90AA1, FKPB5, BCL6, GFAP, NEAT1)* in

ALS patients compared to HC (**Figure 9c**). In MC, 1,933 genes were downregulated (e.g., *AC012494.1, KDM5D, PLP1*) and 1,527 upregulated DEGs were identified in ALS patients vs HCs (**Figure 9c**). In the pseudobulk version of the dataset, on the other hand, fewer DEGs were found (**Figure 9d**). Regarding the significant DEGs, there were 86 downregulated (e.g., *CIART, NR4A1, NPAS4*) and 238 upregulated (e.g., *SERPINA3, FKBP5, ANKRD22, RASD1, GPNMB*) genes in FC; and 152 downregulated (e.g., *AL136985.9, AC005972.3, ACY3*) and 240 upregulated (e.g., *SERPINA3, FKBP5, SLC26A7, ANKRD22, CHI3L1, CD163)* genes in MC in ALS patients compared to HCs (**Figure 9d**). The mean expression values of the top 25 down- and upregulated DEGs calculated and z-scored expression levels were plotted as a heatmap for both snRNA-seq and pseudobulk DEGs for MC and FC, comparing ALS patients to HCs. (**Figure 9e-f**). Next, GO terms enriched for identified DEGs in ALS vs HCs per region were identified. In FC, the GO analyses for snRNA-seq showed enrichment of terms related to neuronal function and adhesion like “GTPase regulator activity”, “axon guidance”, “nervous system development”, “cadherin binding” as well ubiquitin-mediated processes e.g., “ubiquitin dependent ER-associated protein degradation (ERAD) pathway” and “ubiquitin protein ligase binding” (**Figure 10a**). In MC, similar GO terms were enriched in addition to pathways related to neuronal signaling and neuron projection, such as “glutamate receptor signaling pathway”, “synaptic transmission, glutamatergic”, “neurotransmitter receptor activity involved in regulation of post synaptic membrane potential” and “neuron projection guidance” (**Figure 10b**).

For the pseudobulk DEGs, pathways enriched in FC were related to protein metabolism, e.g., “response to unfolded protein”, “ubiquitin/-like protein ligase binding” and pathways implicating inflammatory response such as “positive regulation of tumor necrosis factor production” and “macrophage activation” (**Figure 11a**). In MC, more pathways related to inflammation and intracellular signaling were enriched, such as, “positive-/regulation of chemokine production”, “regulation of phosphorylation”, “protein serine/threonine kinase inhibitor activity”, and cellular compartment of “secretory granule membrane” were highlighted (**Figure 11b**).

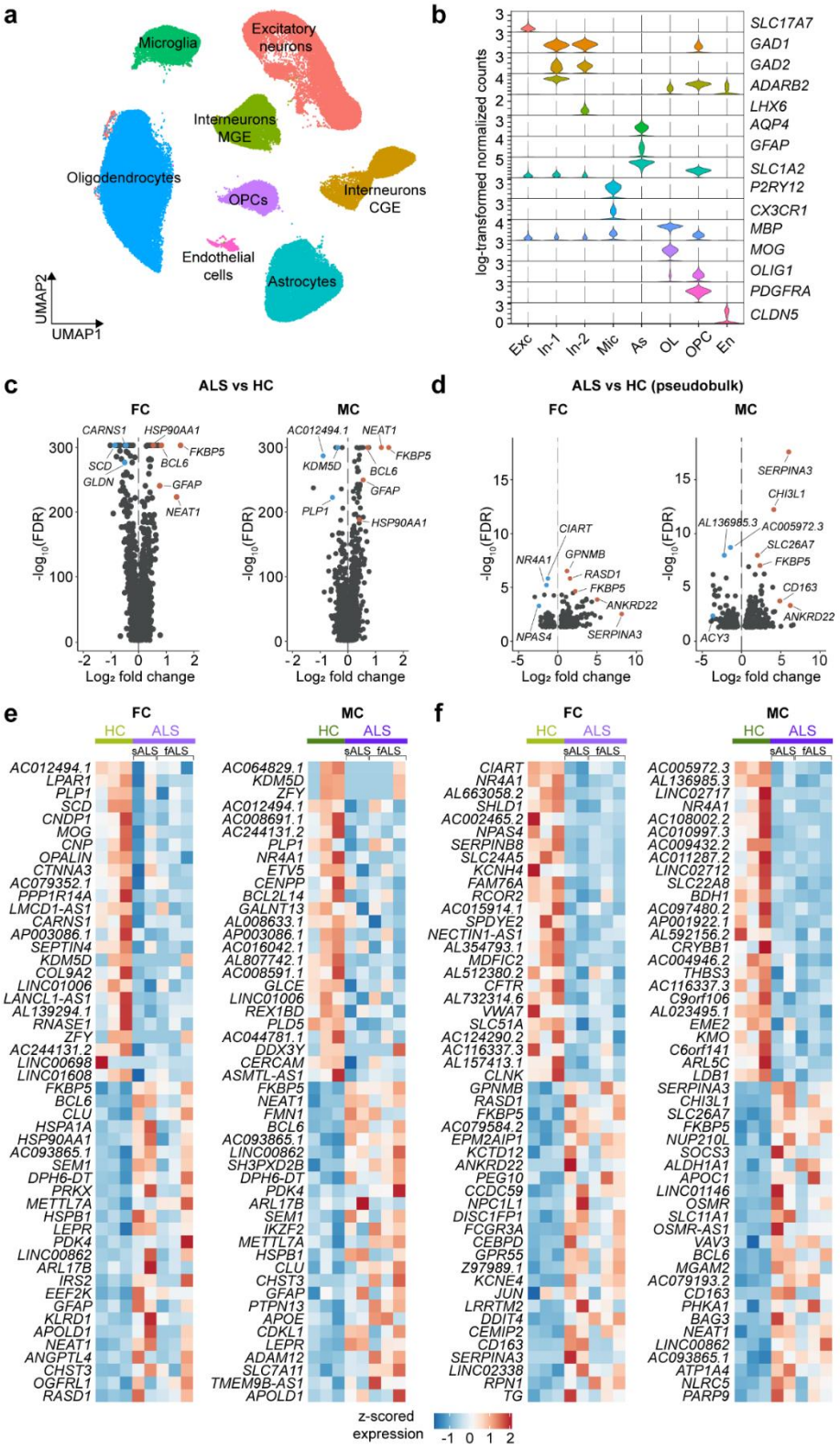

Figure 9. Single nuclei RNA-seq analysis of global data.

(**a**) Global UMAP depicting 8 main cell types identified in dataset. OPCs, oligodendrocyte precursor cells; MGE, medial ganglionic eminence; CGE, caudal ganglionic eminence. (**b**) Violin plot of cell type specific marker genes and their respective expression levels. Exc, excitatory neurons; In-1, interneurons CGE; In-2, interneurons MGE; Mic, microglia; As, astrocyte; OL, oligodendrocytes; OPC, oligodendrocyte precursor cells; En, endothelial cells. (**c**) Volcano plots of differentially expressed genes (DEGs) of all nuclei in frontal cortex (FC, n = 72,638) and in motor cortex (MC, n = 54,230) of amyotrophic lateral sclerosis (ALS) patients compared to healthy controls (HC). Significant DEGs of snRNA-seq data were determined with Wilcoxon Rank Sum test and false discovery rate (FDR) was inferred from p-values via Benjamini-Hochberg method. Only DEGs with FDR < 0.05 and $|\text{Log}_2$ fold change$| > 0$ are plotted. (**d**) Violin plots of DEGs of the pseudobulk version of snRNA-seq data including all nuclei in frontal cortex (FC, n = 72,638) and in motor cortex (MC, n = 54,230). Significant DEGs of pseudobulk-converted snRNA-seq data were determined with Wald test and false discovery rate (FDR) was inferred from p-values via Benjamini-Hochberg method. Only DEGs with FDR < 0.05 and $|\text{Log}_2$ fold change$| > 0$) are plotted. (**e**) Heatmaps of top 25 downregulated (blue) and 25 top upregulated (red) DEGs shown in (c). Z-scored gene expression values were calculated from mean gene expression of all cell types per patient per region. (**f**) Heatmaps of top 25 downregulated (blue) and 25 top upregulated (red) DEGs shown in (d). Z-scored gene expression values were calculated from mean gene expression of all cell types per patient per region. sALS, sporadic ALS; fALS, familial ALS.

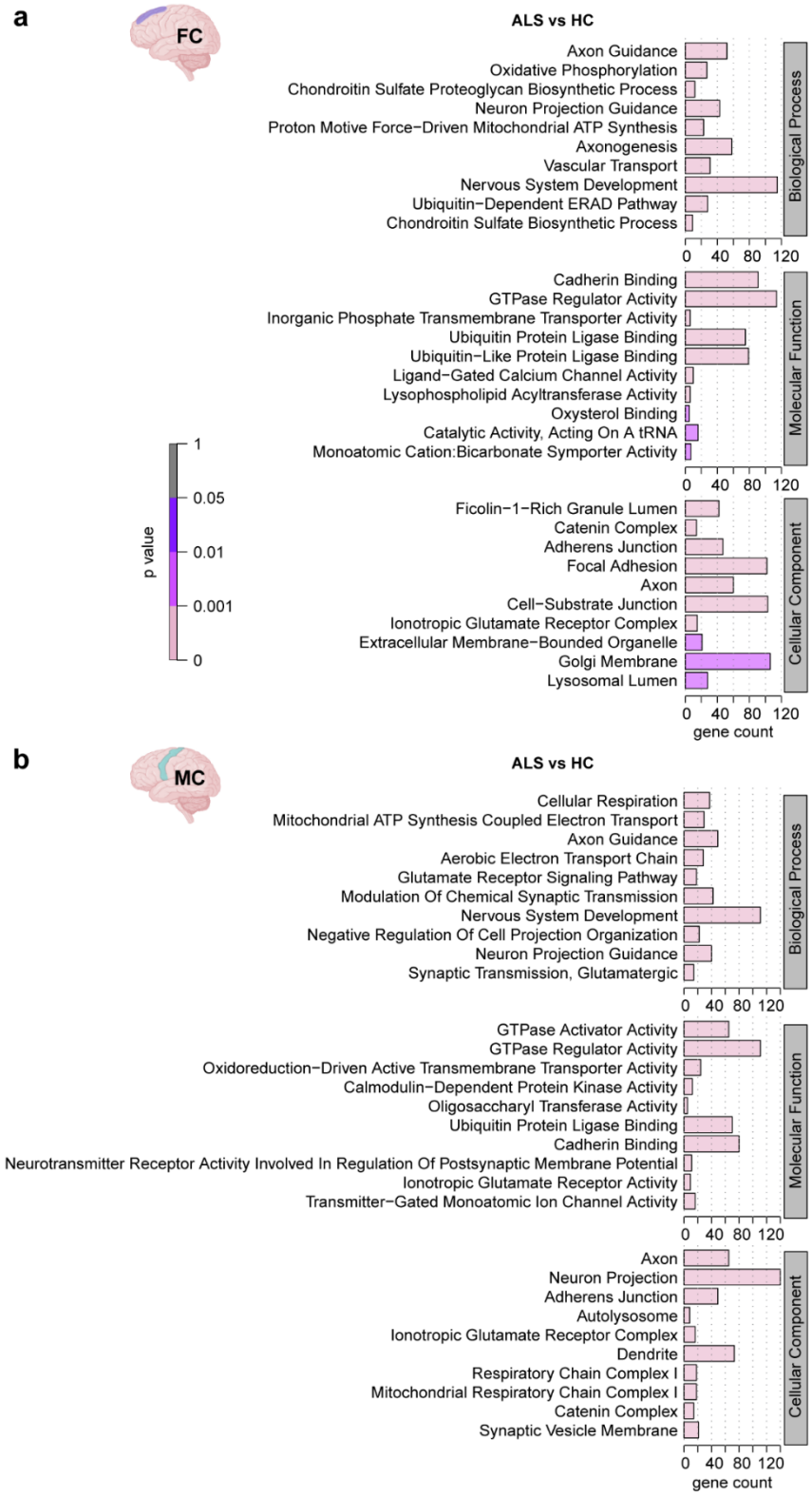

Figure 10. Top 10 Gene Ontology (GO) terms enriched for differentially expressed genes (DEGs) identified in global data.

(**a**) DEGs in frontal cortex (FC) of amyotrophic lateral sclerosis (ALS) compared to healthy controls (HC). (**b**) DEGs in motor cortex (FC) of amyotrophic lateral sclerosis (ALS) compared to healthy controls (HC). DEGs are identified as combination of up- and down- regulated genes (ALS vs HC) in respective cortical area for all cell types (i.e., global data). GOs are shown across three databases: Biological Process, Molecular Function, and Cellular Component. Significant GO terms were determined using Fischer's exact test with $p < 0.05$. Icons were created with BioRender.com.

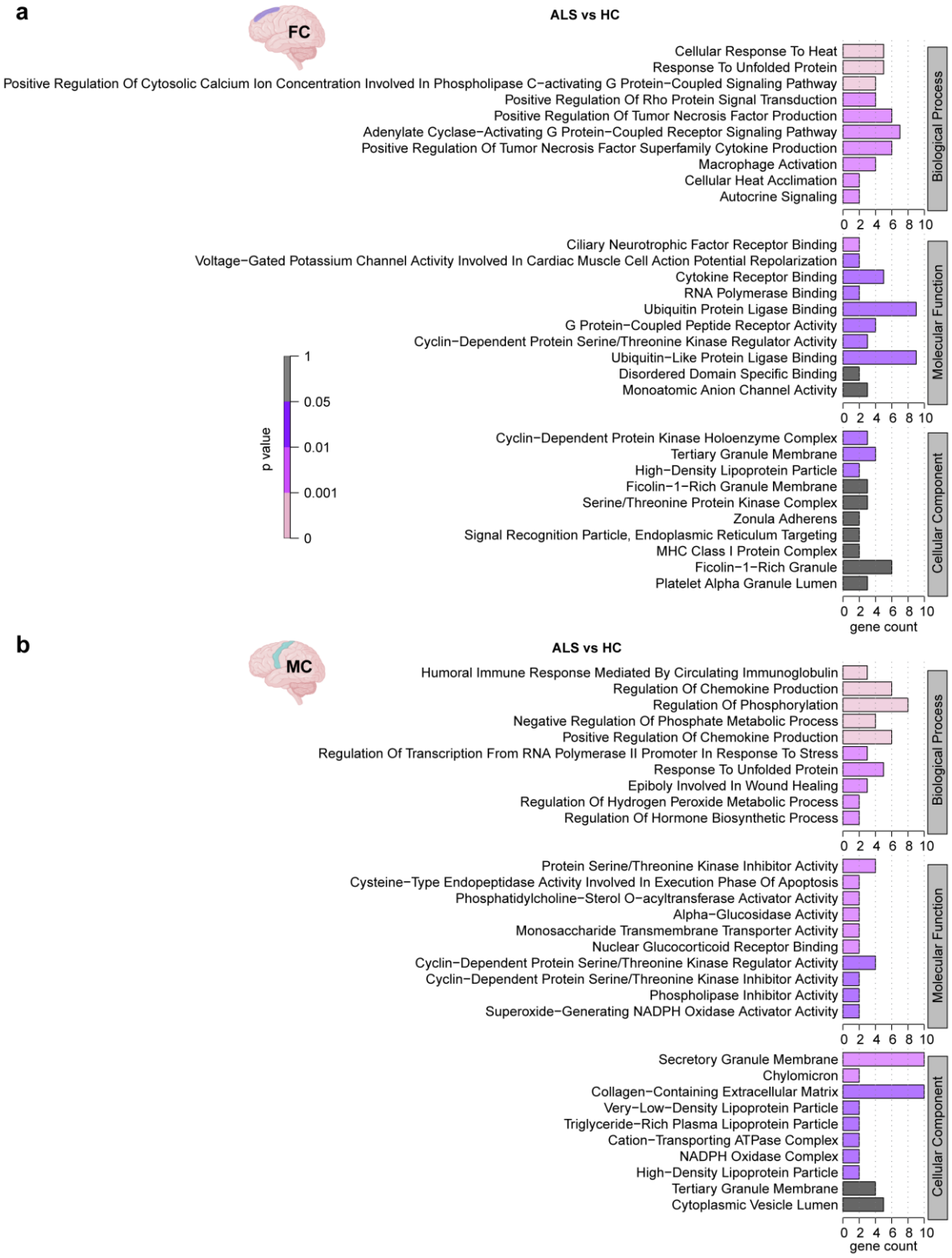

Figure 11. Top 10 Gene Ontology (GO) terms enriched for differentially expressed genes (DEGs) identified in pseudobulk global snRNA-seq data.

(**a**) DEGs in frontal cortex (FC) of ALS compared to HC. (**b**) DEGs in motor cortex (FC) of ALS compared to HC. DEGs are identified as combination of up- and down- regulated genes (ALS vs HC) in respective cortical area for all cell types (i.e., global data). GOs are shown across three databases: Biological Process, Molecular Function, and Cellular Component. Significant GO terms were determined using Fischer's exact test with $p < 0.05$. Icons were created with BioRender.com.

4.3. Cell type specific molecular alterations

In order to identify the main cell type(s) driving the transcriptomic variation between ALS and HC, I performed a Principal Component Analysis (PCA) of FC (**Figure 12a**) and MC (**Figure 12b**) snRNA-seq data. In FC, PCA analysis showed that microglial cells exhibit the most significant variance along PC1, which accounts for 39.0% of the total variance in the data set. Other glial cells, such as oligodendrocytes, astrocytes, and OPCs, as well as the neuronal subpopulations, however, showed lesser differences between disease cases and healthy controls.

In the MC, microglial cells again show the most significant variance along PC1, accounting for 42.7% of the total variance (**Figure 12b**). Interestingly, in MC, fALS cases have greater transcriptomic divergence from HCs than sALS cases, particularly in the microglia and other glial populations. Moreover, I also saw that transcriptomic changes in neuronal populations were slightly changed in MC between ALS and HCs, which seems to be a “later” event in the disease. Since I aimed to understand early molecular changes in the disease, as highlighted by its early divergence in FC in both fALS and sALS patients, I first focused on the analysis of microglia data and later dived into analyses of other cell types.

4.3.1. Microglia

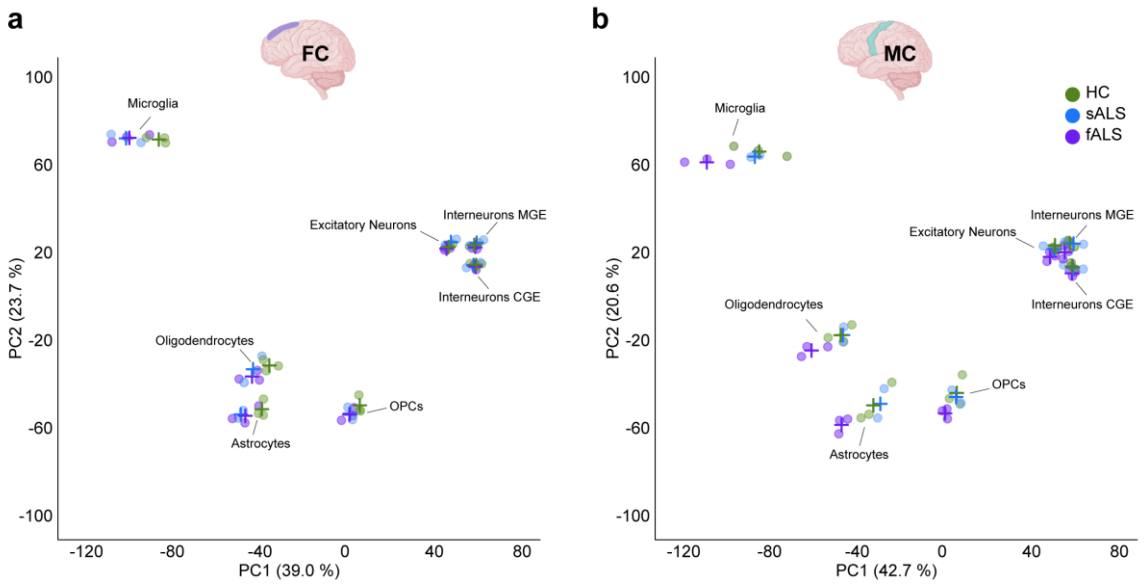

Figure 12. Principal Component Analysis (PCA) of main cell types in the frontal cortex (FC) and motor cortex (MC) across HC and ALS patients show microglia to be the most divergent population.

PC1 and PC2 (percentage of overall variance explained by these components added in brackets) depicting the contribution of each cell type to the overall variance of the snRNA-seq data of each sample (ALS and HC) of FC (**a**) and MC (**b**) superimposed by the centroid of cell-type specific clusters.

A total of 7,836 microglial nuclei were analyzed, 3,920 from FC and 3,916 from MC, respectively. Microglia were classified into 7 subclusters, namely HOM, homeostatic microglia; INT, intermediate; DAM1, disease associated microglia 1; DAM2, disease associated microglia 2; DAM3, disease associated microglia 3; AM, activated microglia; ProM, proliferating microglia (**Figure 13a, top**). The pseudotime trajectory of microglial subclusters (starter cluster HOM) exhibits the differentiation of DAMs and AM from HOM, potentially depicting sequence of microglial reactivation states (**Figure 13a, bottom**). Subcluster enriched markers were HOM (*P2RY12, P2RY13, CX3CR1*), DAM1 (*TMEM163, CD163, SPP1*, *HAMP, TYROBP*), DAM2 (*SPP1, XYLT1, TREM2, TYROBP*), DAM3 (*FTH1, TYROBP, SPP1*), AM (CD83), ProM (*BRIP1, CENPK*) (**Figure 13b**). Note the regional difference in DAM2 markers, e.g., *TREM2* and *TYROBP* expression is present in MC but not yet in FC (**Figure 13b**). The INT subcluster was identified as microglia that has lower *CX3CR1* compared to HOM and while having increased expression of *SPP1*, more than HOM but less than DAMs (**Figure 13b**) while seemingly emerging from HOM cluster and branching towards DAM clusters in pseudotime trajectory analysis (**Figure 13a, bottom**). Next, I determined the fraction of cells per subcluster in both conditions and regions (**Figure 13c**). In ALS, I observed a significant almost 4x decrease in the fractions of HOM in FC and MC compared to HCs (**Figure 13c,** HC FC vs ALS FC p = 0.012, HC MC vs ALS MC p = 0.00021). On the contrary, significantly larger fractions of INT microglia were detected in both regions in ALS (**Figure 13c,** HC FC vs ALS FC p = 0.0000736, HC MC vs ALS MC p = 0.0000559). Moreover, ALS patients had twice as many DAM1 in MC than HCs, while they also had significantly higher fractions of DAM1 in MC compared to FC (**Figure 13c**, HC MC vs ALS MC p = 0.000162, ALS FC vs ALS MC p = 0.000877). Additionally, the DAM2 abundance was significantly increased in ALS FC in comparison to HCs (HC FC vs ALS FC p = 0.00238), while a similar but not statistically significant trend was also present in MC (**Figure 13c**). Regarding significantly DEGs, I detected in FC 553 downregulated (e.g., *DLEU1, AC008691.1, NAV2, LINC02712, DLEU7*) and 358 upregulated genes (e.g., *NEAT1, FKBP5, SPP1, DENND3, SLC1A3, ACSL1*); and in MC 527 downregulated (e.g., *AC008691.1, LINC02712, ST6GALNAC3, P2RY12, CX3CR1*) and 948 upregulated genes (e.g., *SLC1A3, SPP1, NEAT1, DPYD, ACSL1, SLC11A1, APOE, CD163*) in ALS patients compared to HCs (**Figure 13d**). Heatmaps of z-scored expression values of top 25 down- and upregulated DEGs in (ALS vs HC) were calculated from mean expression values per patient and plotted for both regions (**Figure 13e**). In MC of ALS patients 257 downregulated (e.g., *MRC1, ITPR2, LINC02712*) and 760 upregulated genes (e.g., *APOE, CPM, MITF, ATG7*) were detected compared to FC (FDR < 0.05 and $|\text{Log}_2$ fold change$| > 0$, **Figure 13f**). Moreover, MC of HCs had 52 downregulated (e.g., *IFI44L, MERTK*) and 60 upregulated genes (e.g., *CD74, LINC02476, FGL1, SPP1*) when compared to FC (**Figure 13f**).

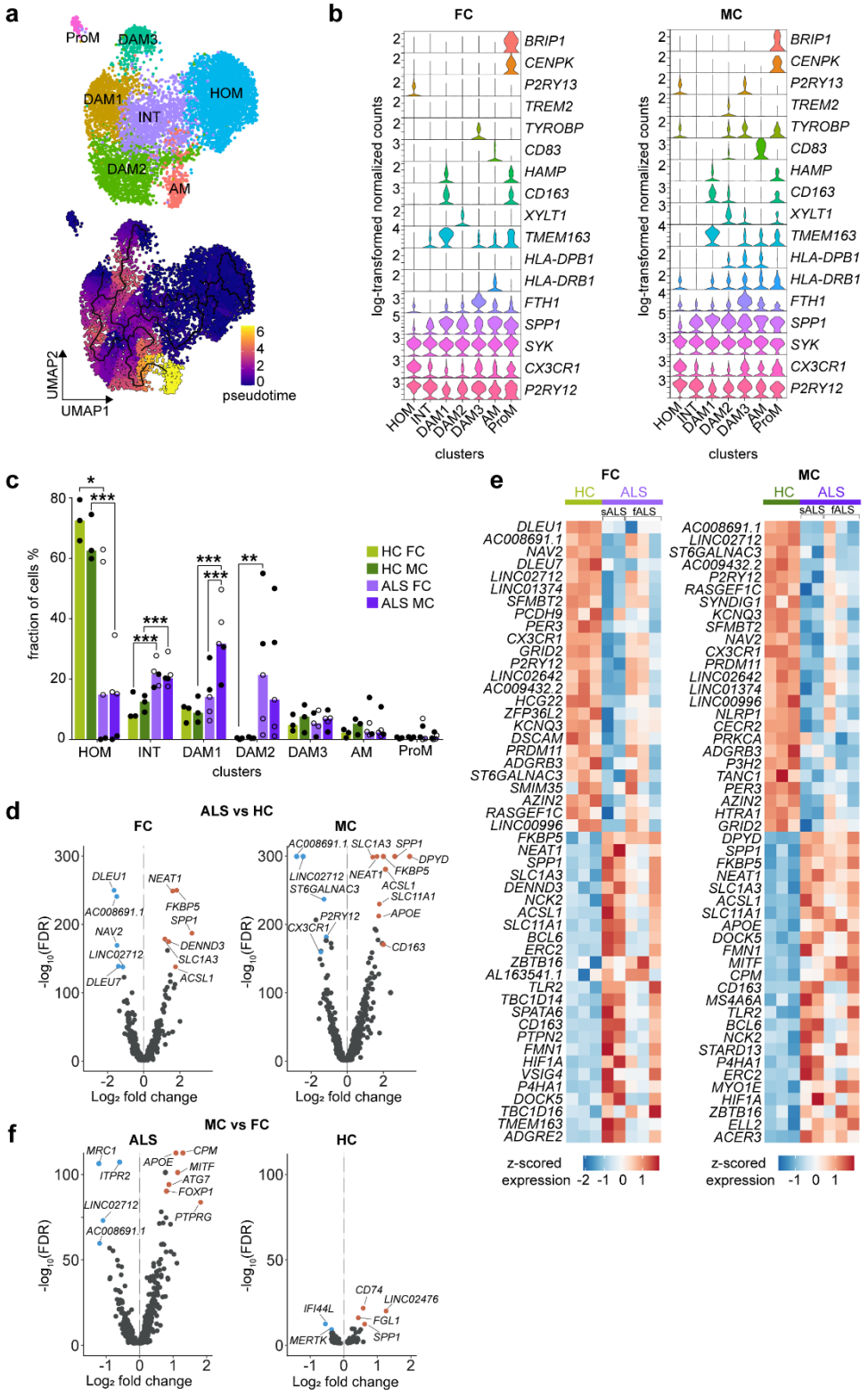

Figure 13. Single nuclei RNA-seq analysis of microglia.

(**a**) 7 subclusters of microglia (n = 7,836) were identified (top). Pseudotime trajectory analysis of microglia subclusters (bottom) in which HOM (homeostatic microglia) were assigned as the starter subcluster. (**b**) Violin plot of subcluster specific marker genes and their respective expression levels in frontal (FC) and motor (MC) cortex. (**c**) Fraction of nuclei per subcluster (beta-regression). Circles indicate fALS patients. (**d**) Volcano plots of differentially expressed genes (DEGs) of all microglia nuclei in frontal cortex (FC, n = 3,920) and in motor cortex (MC, n = 3,916) of ALS patients compared to healthy controls (HC). DEGs with FDR < 0.05 and |Log_2 fold change| > 0) are plotted. (**e**) Heatmaps of top 25 downregulated (blue) and 25 top upregulated (red) DEGs shown in (d). Z-scored gene expression values were calculated from mean gene expression of all microglia per patient per region. (**f**) Volcano plots of differentially expressed genes (DEGs) of all nuclei in ALS (n = 4,736) patients and HC (n = 3,100) of MC compared to FC. Significant DEGs of snRNA-seq data were determined with Wilcoxon rank sum test and false discovery rate (FDR) was inferred from p-values via Benjamini-Hochberg method. DEGs with FDR < 0.05 and |Log_2 fold change| > 0) are plotted. UMAP, Uniform Manifold Approximation and Projection; INT, intermediate; DAM, disease associated microglia; AM, activated microglia; ProM, proliferating microglia; sALS, sporadic ALS; fALS, familial ALS. Data in (c) represents median +/- 95% confidence interval (CI). * p < 0.05, ** p < 0.01, *** p < 0.001.

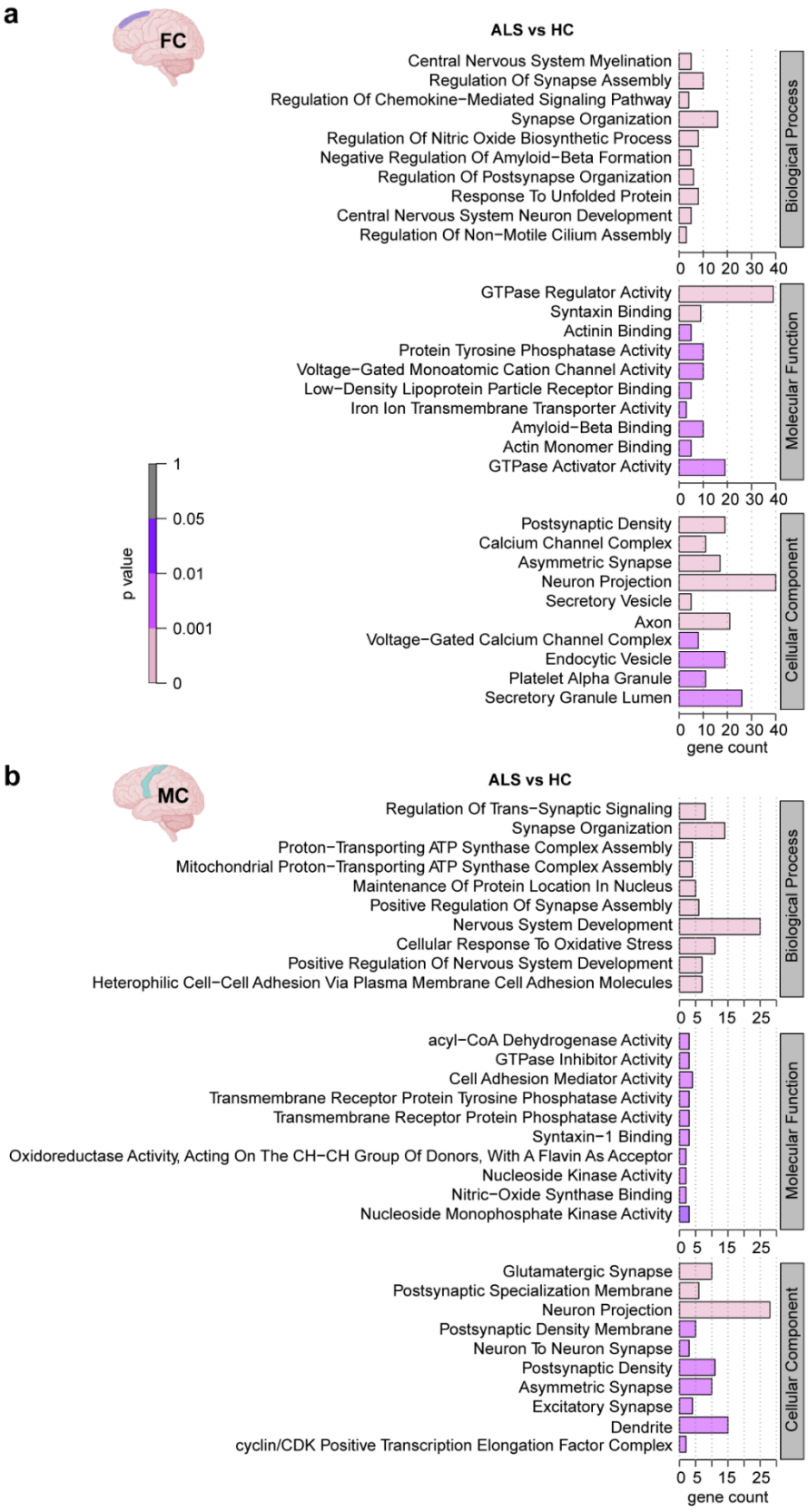

Figure 14. Top 10 Gene Ontology (GO) terms enriched for differentially expressed genes (DEGs) identified in microglia.

(**a**) DEGs in frontal cortex (FC) of ALS compared to HC. (**b**) DEGs in motor cortex (FC) ALS compared to HC. DEGs are identified as combination of up- and down- regulated genes (ALS vs HC) in respective cortical area for microglia. GOs are shown across three databases: Biological Process, Molecular Function, and Cellular Component. Significant GO terms were determined using Fischer's exact test with $p < 0.05$. Icons were created with BioRender.com.

In addition, I checked the GO terms enriched for the DEGs in MC and FC of ALS patients in comparison to HC. In FC, I found many GO terms regarding the modulation of neuronal functions, such as “central nervous system myelination”, “synapse organization”, “regulation of postsynapse organization” and processes involved in microgliosis and inflammation e.g., “regulation of chemokine-mediated signaling pathway”, “GTPase regulator activity” and “low-density lipoprotein particle receptor binding” (**Figure 14a**). Furthermore, in MC, I report more enrichment for GO terms involving neuronal signaling and health e.g., “regulation of trans-synaptic signaling”, “synapse organization”, and GO terms that are associated with microglial stress “cellular response to oxidative stress”, “maintenance of protein location in nucleus”, “mitochondrial/proton-transporting ATP synthase complex assembly” (**Figure 14b**). A subset of GOs were categorized into 3 processes, namely “synaptic function”, “inflammation & oxidative stress” and “proteostasis” (**Figure 15a**). DEGs that were enriched for synaptic function were shared in both regions, indicating microglial modulation of synapses to be an early process. Expression of DEGs of the selected GO terms was plotted in each microglial subcluster for ALS and HCs in FC and MC (**Figure 15b**). I report a downregulation of synapse related genes (*GRID2*, *SYNDIG1 and CX3CR1*) in both regions in ALS in all subclusters except for HOM. The most striking downregulation of these genes was observed in DAM1 cluster already in ALS FC in comparison to HC FC (**Figure 15b**). Moreover, genes shared between inflammation and proteostasis processes, such as HSP90AA1 and HSPA1A were upregulated specifically in the AM cluster in both regions in ALS patients (**Figure 15b**). Lastly, I report decreased *PRKN* expression in DAM1 and DAM2 clusters in FC and MC of ALS patients, implicating early modification of gene expression in the mentioned subclusters (**Figure 15b**).

a

Process	GO terms (BP)	Region	DEGs
Synaptic function	Regulation Of Synapse Assembly	FC	*PTPRD, GRID2, LRRTM3, NRXN1, IL1RAPL1, SYNDIG1, IL1RAP, PDLIM5, TLR2, SNCA*
		MC	*ROBO2, PTPRD, GRID2, NLGN1, NRXN1, IL1RAPL1, SYNDIG1*
	Regulation Of Trans-Synaptic Signaling	FC	*CX3CR1, GRIA2, SLC4A8, GRID2, CACNA1A, EIF4EBP2, GRIK2*
		MC	*CX3CR1, GRIA2, SLC4A8, NLGN1, GRID2, NRG3, GRIK2, LRRC4C*
Inflammation & oxidative stress	Regulation Of Chemokine-Mediated Signaling Pathway	FC	*PADI2, SLIT2, HIF1A, ROBO1*
	Regulation Of Nitric Oxide Biosynthetic Process	FC	*CX3CR1, HSP90AA1, HSP90AB1, SMAD3, INSR, NOS1AP, ATP2B4, CLU*
	Cellular Response to Oxidative Stress	MC	*CCS, ERMP1, NCF1, PYROXD1, ABL1, PEX2, MPV17, PTPRK, FOS, FOXO1, HSPA1B*
Proteostasis	Response To Unfolded Protein	FC	*PRKN, PTPN1, HSP90AA1, HSP90AB1, HSPH1, HSPB1, HSPA1A, RHBDD1*
	Maintenance Of Protein Location In Nucleus	MC	*SUN2, TAF8, CHCHD10, RANGAP1, SYNE1*

b

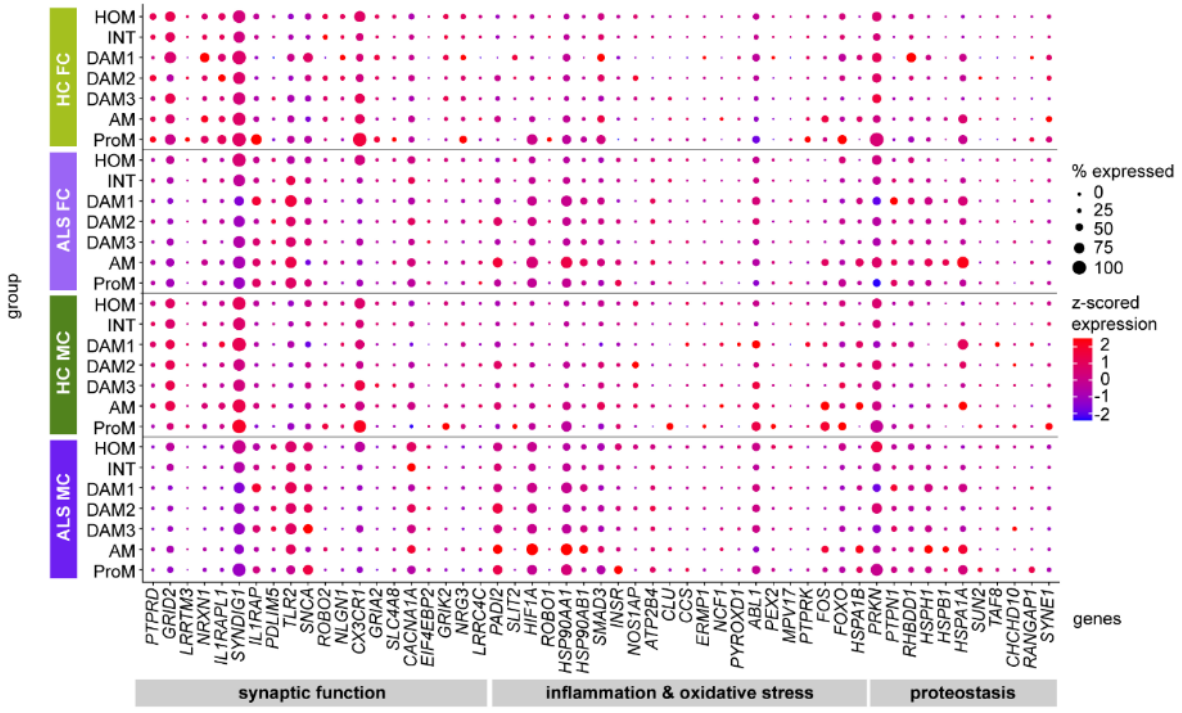

Figure 15. Top enriched GO terms in microglia and corresponding differentially expressed genes (DEGs).

GO terms enriched in ALS compared to HC were classified into 3 categories of cellular processes, namely “synaptic function”, “inflammation & oxidative stress” and “proteostasis” (**a**) Region-specific DEGs corresponding to enriched GO terms in ALS. (**b**) Z-scored expression of DEGs in microglia listed in the panel (a). FC, frontal cortex; MC, motor cortex; BP, biological processes, HOM, homeostatic microglia; INT, intermediate microglia; DAM, disease associated microglia; AM, activated microglia; ProM, proliferating microglia.

Given my observation of an enrichment of DEGs related to microglial activation in FC prior to or in the absence of pTDP-43 pathology, I next determined if microglial reactivity was present in FC and MC of ALS patients. To this end, I performed immunohistochemistry using an anti-human leukocyte antigen DR, DP and DQ (anti-HLA-DR+DP+DQ) antibody, the expression of which indicates microglial activation (**Figure 16a-b**). As expected, I found increased microglial activation in MC of ALS patients compared to MC in HC (**Figure 16c**, HC MC vs ALS MC p <0.0001). Importantly, I also found microglial reactivity in FC in ALS patients despite the absence of pTDP-43 pathology, which was more pronounced in MC (**Figure 16c**, HC FC vs ALS FC p = 0.0113, ALS FC vs ALS FC p <0.0001). Next, I checked if the pTDP-43 load correlates with microglial activation in FC (**Figure 16d, left**) and in MC (**Figure 16d, right**) of ALS patients. I saw that the microglial activation was partially explained by the increase of the pTDP-43 load in MC (**Figure 16d, right**, FC R^2 = 0.21, MC R^2 = 0.51).

Furthermore, as my cohort included 3 fALS (*C9ORF72* mutation carriers) cases, I also checked the presence of any DPRs. Since poly-GA inclusions are the most abundant DPR species in ALS, I have performed anti-poly-GA staining on a subsequent tissue section with the same 5 ROIs that were selected for anti-HLA-DR+DP+DQ and anti-pTDP-43 staining quantification (**Figure 17a**).

IHC confirmed that the fALS patients in my study had poly-GA inclusions in the absence of pTDP-43 in FC (**Figure 17b**), where microglial activation was shown to be present already (**Figure 16c**). The poly-GA load was not significantly different in FC than in MC (**Figure 17c,** p=0.13). I further checked if the poly-GA load was affected by pTDP-43 load in each cortical region. While FC did not show a strong correlation between the variation of pTDP-43 inclusions (17%) inclusions explained by the presence of poly-GA inclusions (**Figure 17d, left**), surprisingly, I saw that 65% of the variance in pTDP-43 load could be accounted for by the poly-GA load in the MC (**Figure 17d, right**). These results suggest the region-specific relationship between poly-GA pathology and pTDP-43 load.

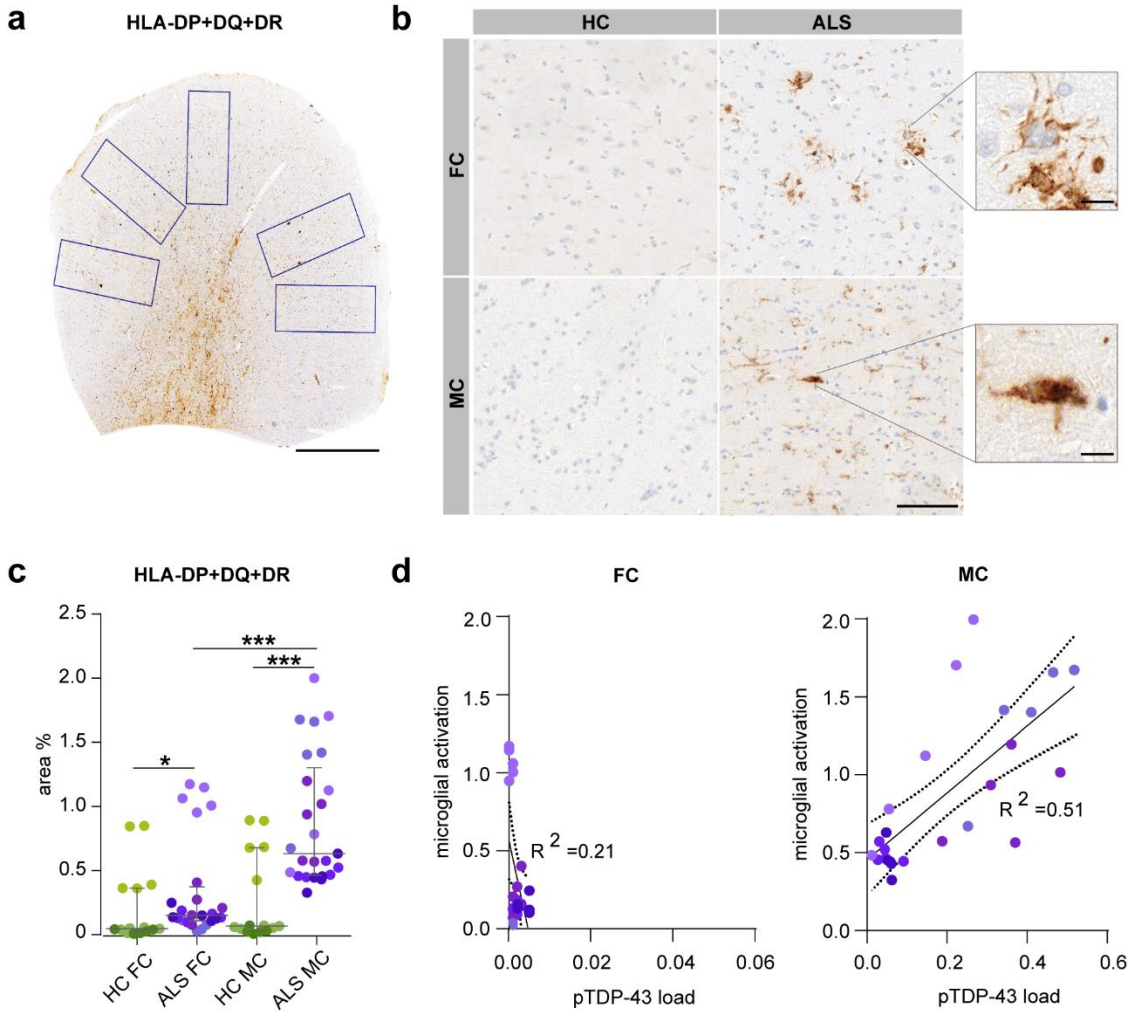

Figure 16. Microglial activation precedes pTDP-43 pathology in end-stage ALS patients.

(**a**) Overview of anti-HLA-DR+DP+DQ staining from the subsequent frontal cortex section of the same ALS patient shown in Figure 8a. (**b**) Examples of anti-HLA-DR+DP+DQ immunoreactivity (DAB, brown) in the gray matter of FC and MC of the same patient. Inserts demonstrate fine processes of activated microglia gathering around potentially damaged cells (top) and activated amoeboid microglia with high expression of HLA-DR+DP+DQ (bottom). (**c**) Quantification of anti- HLA-DR+DP+DQ staining (data points correspond to ROIs, color shade indicates patient identity, one –sided Wilcoxon rank sum test). (**d**) Microglial activation (calculated by area% of anti-HLA-DR+DP+DQ immunoreactivity) in ALS patients can be partially explained by the increased pTDP-43 load in MC, it is seemingly independent of pTDP-43 in FC (simple linear regression). DAB, 3, 3'- diaminobenzidine; ROI, region of interest; HLA-DR+DP+DQ, human leukocyte antigen DR, DP and DQ. Data in (c) represents median & IQR. Scale bar in (a) 2 mm and (b) 100 µm, insert (top) 20 µm and insert (bottom) 15 µm. * $p < 0.05$, *** $p < 0.001$.

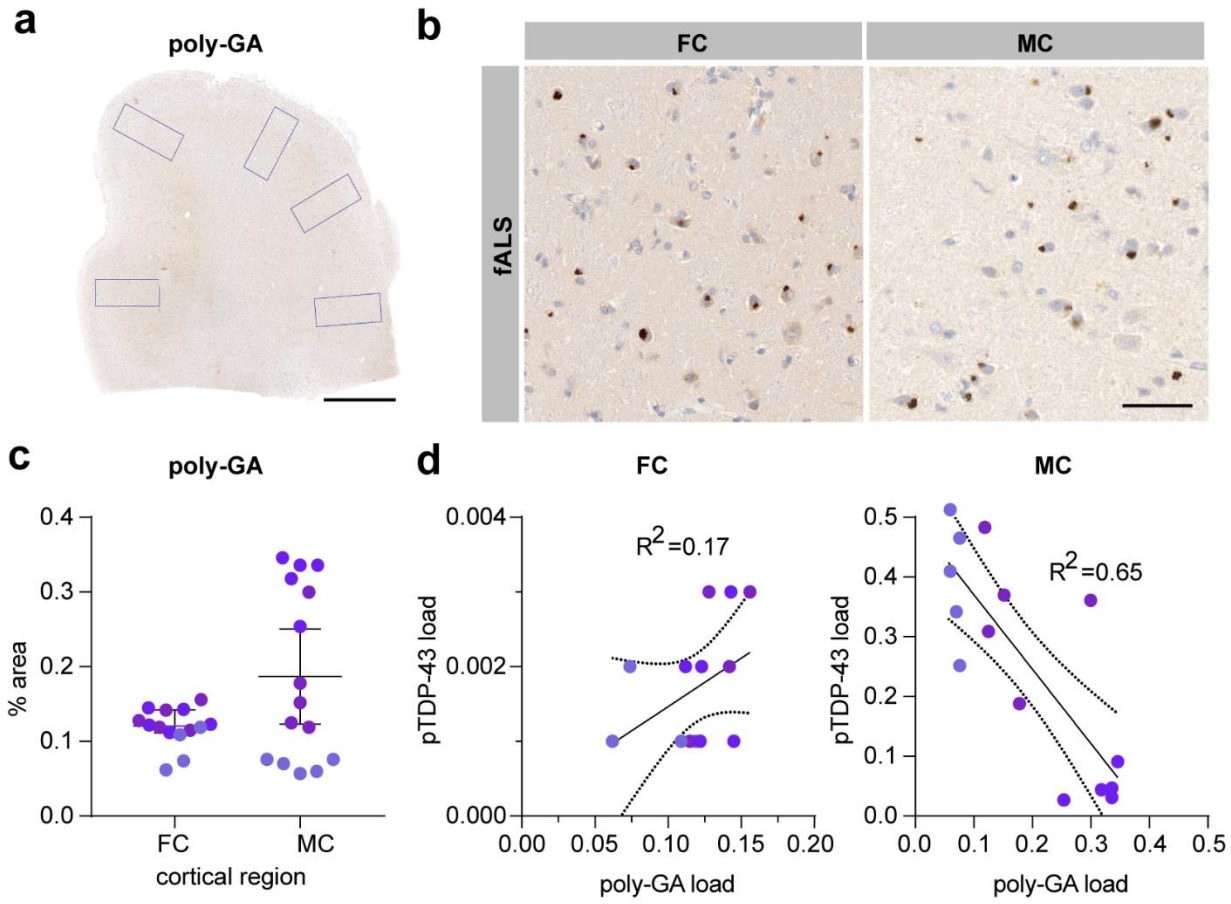

Figure 17. Poly-GA inclusions are present in the absence of pTDP-43 pathology and poly-GA load partially correlates with pTDP-43 pathology in end-stage fALS patients.

(**a**) Overview of anti-poly-GA staining from a fALS patient (C9ORF72). (**b**) Examples of cytoplasmic anti-poly-GA immunoreactivity (DAB, brown) in the gray matter of FC and MC of the same patient. (**c**) Quantification of anti-poly-GA staining in fALS patients shows no significance in poly-GA load per cortical region (data points correspond to ROIs, color shade indicates patient identity, one –sided Wilcoxon rank sum test). (**d**) Scatterplot of pTDP-43 load vs poly-GA load in FC (left) and MC (right) in fALS patients show pTDP-43 load is partially dependent on poly-GA load in MC (simple liner regression). DAB, 3, 3'- diaminobenzidine; ROI, region of interest. Data in (c) represents median & IQR. Scale bar in (a) 2 mm and (b) 100 µm. * $p < 0.05$, *** $p < 0.001$.

4.3.2. Astrocytes

I analyzed 19,138 astrocytic nuclei in this study, of which 12,950 were from FC and 6,188 nuclei from MC. I identified 4 subclusters, numbered as astrocyte clusters 0, 1, 2 and 3 (**Figure 18a, top**). In order to gain insight into differentiation and/or activation state of these clusters, I inferred pseudotime trajectories, starting from cluster 0, as it was the cluster with the highest expression of homeostatic astrocytic genes (e.g., low *GFAP, VCAN*; high *SLC1A2*) (**Figure 18a, bottom**). Cluster 0 was identified with higher expression of markers *SGCD*, *WIF1*; cluster 1 had higher *GFAP* expression than cluster 0 but lower expression of *DPP1*, *VCAN* and *S100B* compared to clusters 2 and 3 (**Figure 18b**). I saw that clusters 2 and 3, both expressing *TNC,* are the most distinct and potentially differing most in their gene expression patterns with respect to clusters 0 and 1. In ALS, I observed an increased fraction of cluster 1 astrocytes in MC (HC MC vs ALS MC p = 0.00552), while a decrease in the number of cluster 2 astrocytes in MC compared to HCs (**Figure 18c**, HC MC vs ALS MC p = 0.0132). Moreover, in FC of ALS patients, I identified significantly downregulated 1026 genes (e.g., *MMD2, HPSE2, AC00249.2, CD38*) and upregulated 1521 genes (e.g*., CLU, NEAT1, AQP4, IRS2, FKBP5, GJA1, GFAP, CHI3L1*) compared to HCs; whereas in MC, 1602 genes were significantly downregulated (e.g., *MMD2, C9ORF62, AC00249.2, JUN*) and 1369 genes were significantly upregulated (e.g., *TRPM3, NEAT1, FKBP5, SAMD4A, CHI3L1, CD44, SERPINA3*) (**Figure 18d**). A heatmap illustrating the z-scored expression values of the 25 most downregulated and upregulated DEGs in ALS vs HC was generated for these DEGs. The calculations were based on the mean expression values per patient and depicted for both specific regions (**Figure 18e**). Comparison of MC vs FC in different cohorts (that is ALS and HC) revealed 1065 downregulated (e.g., *PDE4D, ADGRV1. OBI-AS1, AC002429.2, FTH1*) and 1277 upregulated genes (e.g., TRPM3, AC012405.1, GFAP, AC073941.1, RGS6) in ALS; whereas HCs had 1087 downregulated (e.g., *HPSE2, ADGRV1, OBI-AS1, ME1*) and 717 upregulated genes (e.g., *PTGDS, CLU, NR4A1, JUN, JUNB, GFAP*) (**Figure 18f**). Next, I checked which GO terms these DEGs (**Figure 18d**) were enriched for in ALS, separated by region (FC and MC). GO terms associated with neuronal function such as “synapse organization”, “glutamatergic synapse”, and compartments and processes associated with secretion and adhesion (e.g., “transport across blood-brain barrier”, “intracellular organelle lumen”, “vascular transport”, “Golgi membrane”, “cell-substrate junction”); as well as GO terms related to protein metabolism, “response to unfolded protein”, “Hsp90 binding” were indicated (**Figure 19a**). Furthermore, in MC, most prominently enriched GO terms were proteostasis (e.g., “regulation of protein phosphorylation”, “response to unfolded protein”, “ubiquitin/ubiquitin-like protein ligase binding”, “protein homodimerization activity”) and neuronal activity modulation associated (e.g., “modulation of chemical synaptic transmission”) (**Figure 19b**).

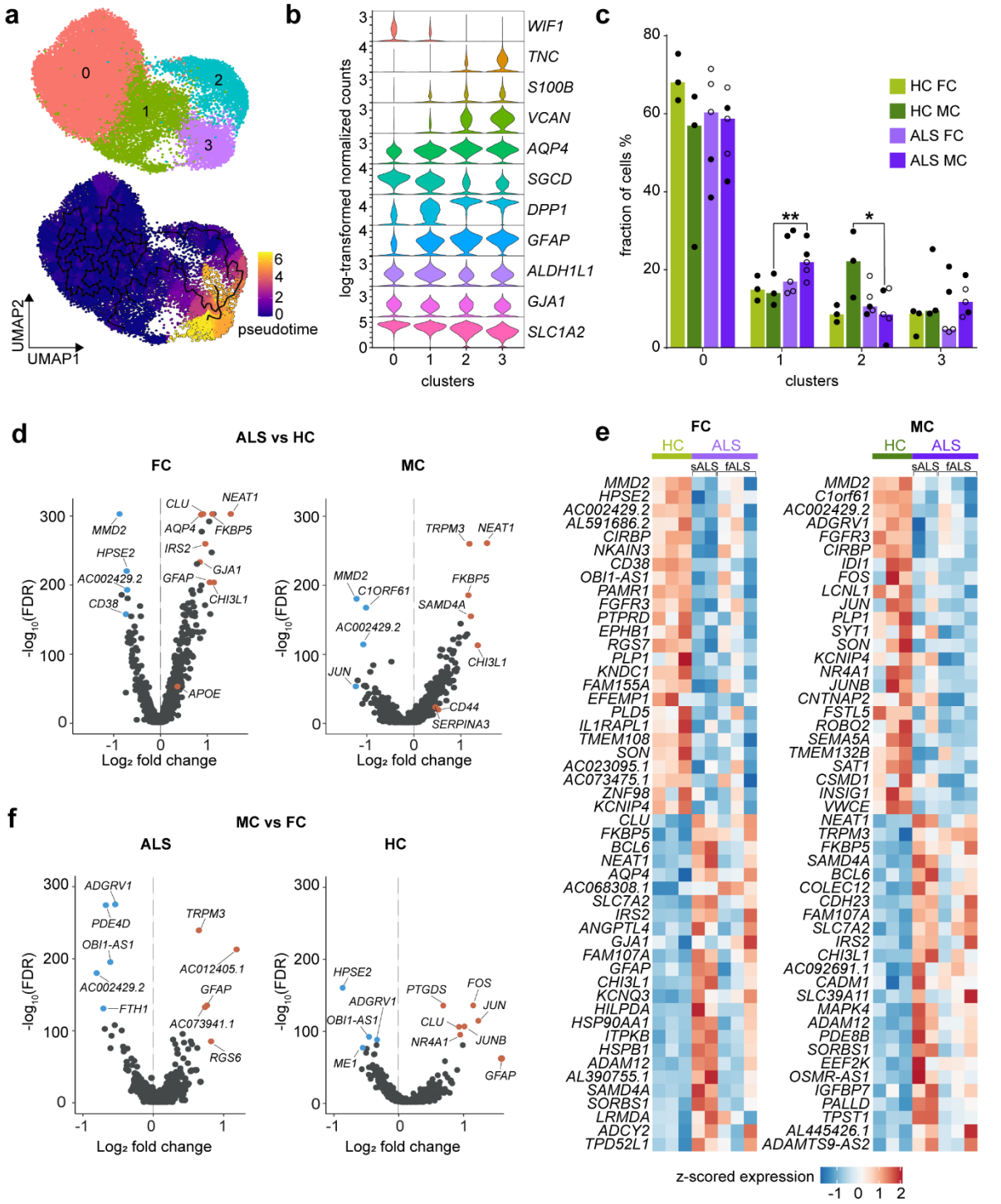

Figure 18. Single nuclei RNA-seq analysis of astrocytes.

(**a**) 4 subclusters of astrocytes (n = 19,138) were identified (top). Pseudotime trajectory analysis of astrocyte subclusters (bottom) with the starter subcluster 0. (**b**) Violin plot of subcluster specific marker genes and their respective expression levels in frontal (FC) and motor (MC) cortex. (**c**) The fraction of nuclei per subcluster (beta-regression). Circles indicate fALS patients. (**d**) Volcano plots of DEGs of all nuclei in FC (n = 12,950) and in MC (n = 6,188) ALS patients compared to HC (Wilcoxon rank sum test and false discovery rate (FDR) was inferred from p-values via Benjamini-Hochberg method, DEGs with FDR < 0.05 and $|Log_2$ fold change$|$ > 0) are plotted). (**e**) Heatmaps of top 25 downregulated (blue) and 25 top upregulated (red) DEGs shown at panel (d) Z-scored gene expression values were calculated from mean gene expression of all astrocytes per patient per region. (**f**) Volcano plots of DEGs of all nuclei in ALS (n = 12,872) patients and HC (n = 6,266) of MC compared to FC. DEGs with FDR < 0.05 and $|Log_2$ fold change$|$ > 0 are plotted. UMAP, Uniform Manifold Approximation and Projection; sALS, sporadic ALS; fALS, familial ALS. Data in (c) represents median & 95% confidence interval (CI). * p < 0.05, ** p < 0.01.

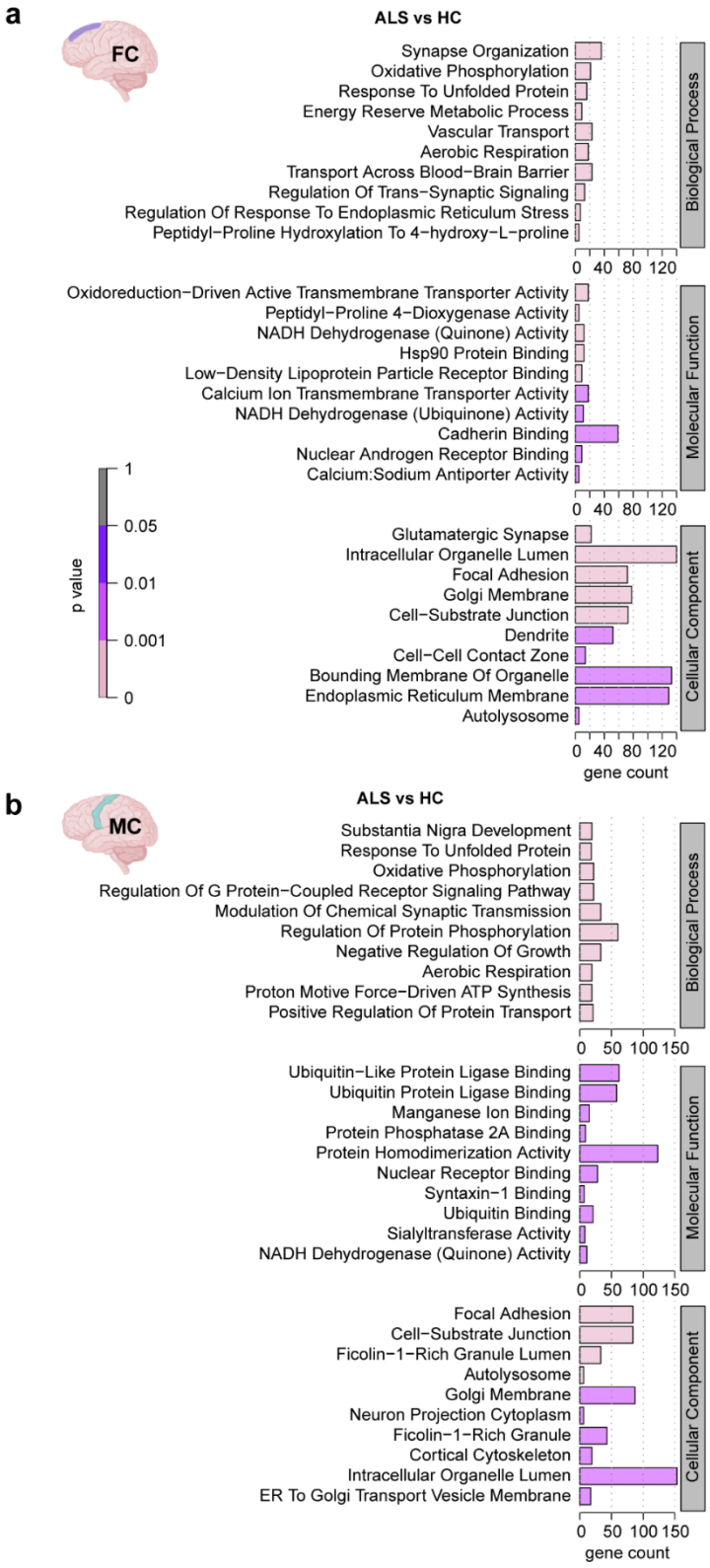

Figure 19. Top 10 Gene Ontology (GO) terms enriched for differentially expressed genes (DEGs) identified in astrocytes.

(**a**) DEGs in frontal cortex (FC) of ALS compared to HC. (**b**) DEGs in motor cortex (FC) of ALS compared to HC. DEGs are identified as combination of up- and down- regulated genes (ALS vs HC) in respective cortical area for all astrocytes. GOs are shown across three databases: Biological Process, Molecular Function, and Cellular Component. Significant GO terms were determined using Fischer's exact test with $p < 0.05$. Icons were created with BioRender.com.

4.3.3. Oligodendrocytes

I have obtained a total of 42,799 oligodendrocytes (20,724 from FC and 22,075 from MC), and classified them into 4 subclusters namely OL1, OL2, OL3 and OL4 (OL, oligodendrocyte) (**Figure 20a, top**). The pseudotime trajectory of oligodendrocyte subclusters were inferred using OPCs as starter cluster (**Fig 20a, bottom**). This trajectory exhibited similarities to OPALIN expression levels within subclusters, suggesting potential insights into their maturation and/or differentiation states (**Fig 20a, bottom**). Cluster specific markers for were OL1 (*OPALIN, ROR1*), OL2 (*RBFOX1*), OL3 (*OPALIN, FRY*) and OL4 (*FTH1, TXNRD1*) (**Figure 20b**). I have not found significant changes in the fraction of oligodendrocyte subclusters in between groups (ALS, HC) and regions (FC, MC) (**Figure 20c**). Yet, I identified numerous DEGs. In FC, I have identified a total of 1,190 genes that exhibited significant downregulation (e.g., *SCD, PLP1, SNDP1, SLC4A8*), while 689 genes (e.g., *PIEZO2, LRP2, FKBP5, NEAT1, ADAM12, HSP90AA1*) showed significant upregulation compared to HC (**Figure 20d**). In the MC, I observed significant downregulation of 971 genes (e.g., *PLD5, CSD, GALNT13, ABTB2*) and significant upregulation of 1,153 genes (e.g., *NCKAP5, LRP2, ADAM12, PIEZO2, LUCAT1*) in ALS compared to (**Figure 20d**). A heatmap depicting the z-scored expression values of the top 25 downregulated and upregulated DEGs in ALS vs HC was generated for these genes, with calculations based on the mean expression values per patient and representation in both regions (**Figure 20e**). When comparing different regions (MC vs FC) in different cohorts (ALS and HC), I found 991 genes that were downregulated in MC, including *FCHSD2, PLXDC2, KCNIP4, LRP4*; in contrast, there were 1,348 upregulated genes in MC such as *SPP1, CNP, FTL, SYT14* (**Figure 20f**). On the other hand, in the HC group, there were 838 downregulated genes (e.g., *FCHSD2, ANK3, CD55*) in MC when compared to FC, while 567 genes were upregulated, such as *CDK18, HAPLN2, GNG7* (**Figure 20f**). Next, enriched GO terms were inferred from the significant DEGs in ALS patients in comparison to HCs in MC and FC. In both regions, I saw an enrichment of GO terms such as “modulation of synaptic activity”, “plasma membrane bounded cell projection assembly”, “regulation of trans-synaptic signaling” and “glutamatergic synapse” (**Figure 21a-b**). In contrast, in FC I also observed GO terms often associated with glutamatergic signaling e.g., “glutamate receptor signaling pathway”, “(ionotropic) glutamate receptor activity” (**Figure 21a**). More terms related to protein metabolism were enriched in MC, including “ubiquitin/ubiquitin-like protein ligase binding” (**Figure 21b**). In addition, “GABAergic synapse” was implicated in MC (**Figure 21b**).

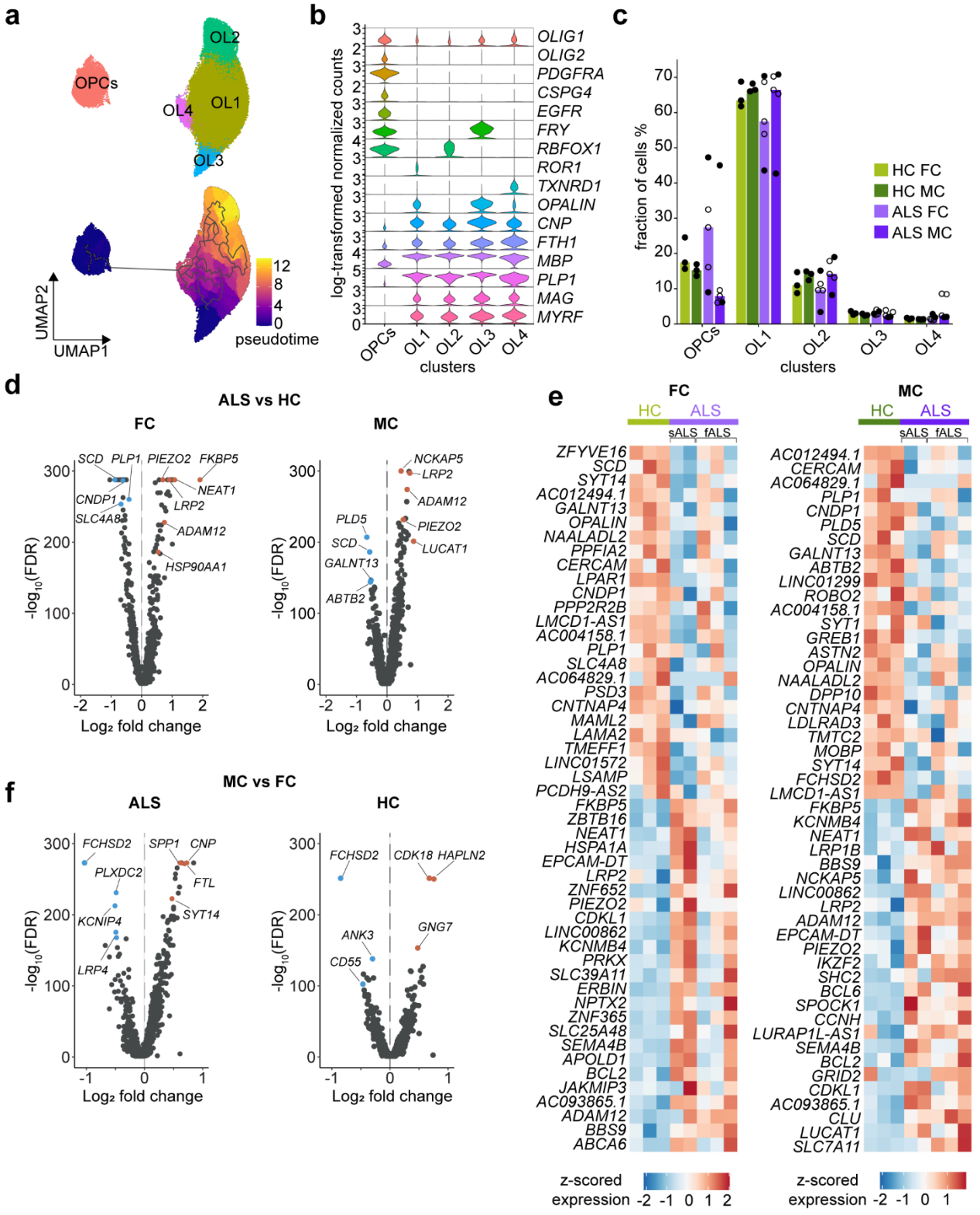

Figure 20. Single nuclei RNA-seq analysis of oligodendrocytes (OL) and oligodendrocyte progenitor cells (OPCs).

(**a**) 4 subclusters of oligodendrocytes (n = 42,799) and one cluster of OPCs (n = 8,400) were identified (top). Pseudotime trajectory analysis of OL and OPCs (bottom) with the assigned starter cluster of OPCs. (**b**) Violin plot of subcluster specific marker genes and their respective expression levels in FC and MC. (**c**) The fraction of nuclei per subcluster (beta-regression). Circles indicate fALS patients. (**d**) Volcano plots of DEGs of all OLs in frontal cortex (FC, n = 20,724) and in motor cortex (MC, n = 22,075) of ALS patients compared to HC (Wilcoxon rank sum test and false discovery rate (FDR) was inferred from p-values via Benjamini-Hochberg method, DEGs with FDR < 0.05 and |Log_2 fold change| > 0) are plotted). (**e**) Heatmaps of top 25 downregulated (blue) and 25 top upregulated (red) DEGs shown at panel (d). Z-scored gene expression values were calculated from mean gene expression of all OLs per patient per region. (**f**) Volcano plots of DEGs of all OLs in ALS (n = 25,375) patients and HC (n = 17,424) of MC compared to FC. UMAP, Uniform Manifold Approximation and Projection; sALS, sporadic ALS; fALS, familial ALS. Data in (c) represents median & 95% confidence interval (CI). * p < 0.05, ** p < 0.01, *** p < 0.001.

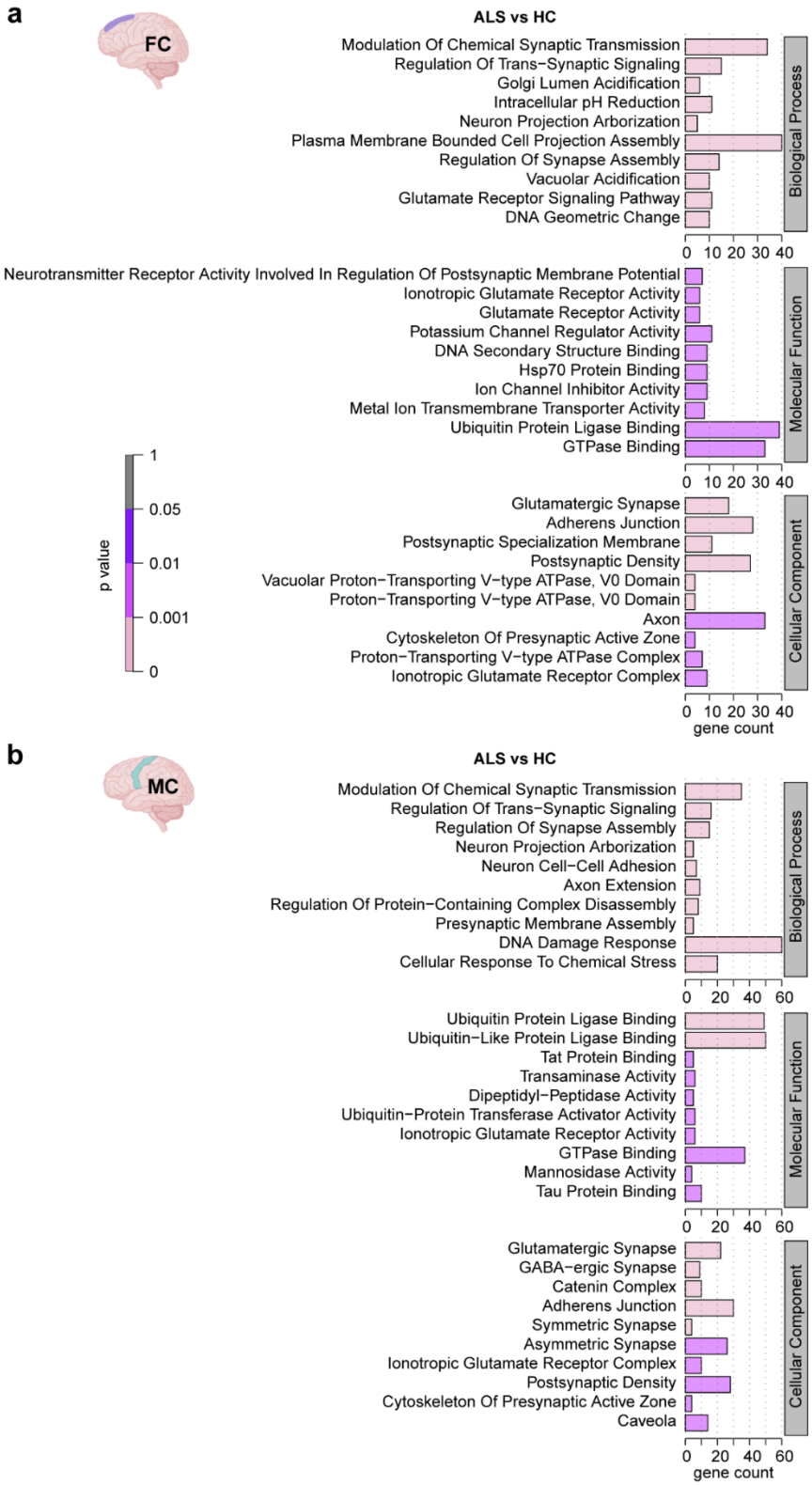

Figure 21. Top 10 Gene Ontology (GO) terms enriched for differentially expressed genes (DEGs) identified in oligodendrocytes.

(**a**) DEGs in frontal cortex (FC) of ALS compared to HC. (**b**) DEGs in motor cortex (FC) of ALS compared to HC. DEGs are identified as combination of up- and down- regulated genes (ALS vs HC) in respective cortical area for all oligodendrocytes. GOs are shown across three databases: Biological Process, Molecular Function, and Cellular Component. Significant GO terms were determined using Fischer's exact test with $p < 0.05$. Icons were created with BioRender.com.

4.3.4. Oligodendrocyte progenitor cells (OPCs)

I obtained a total of 8,400 OPCs, with 5,307 from FC and 3,093 from MC. I have identified one OPC cluster (**Figure 22a**), with expression of OPC specific markers such as *OLIG1, OLIG2, PDFRA, CSPG4* and *EGFR* (**Figure 22b**). Furthermore, no significant changes in the fraction of OPCs were observed between different groups, such as ALS and HC or between regions (FC and MC) (**Figure 22c**). Regarding DEGs, in ALS FC, 605 genes displayed significant downregulation (e.g., *SOX2-OT, NKAIN3, GPR158*), while 1,436 genes showed significant upregulation (e.g., *FKBP5, ZFPM2, EEF2K, PDZD2, SMOC1, ITGA8, GPC5*) when compared to HC (**Figure 22a**). In the ALS MC, 582 genes exhibited significant downregulation (e.g., *AC009041.2, C9ORF61, GINS3*), and 1,295 genes displayed significant upregulation (e.g*., FKBP5, ZFPM2, HIF3A, EEF2K, PDZD2, ITGA8*) in ALS compared to HC (**Figure 22a**). When comparing different regions (MC vs FC) in different cohorts (ALS and HC), I identified 1,248 genes that were downregulated in ALS MC (e.g., *GPC5, CNTN5, PTPRT, GPNMB*). In contrast, there were 225 upregulated genes in ALS MC, including *SEMA3E, CDH19, CACNA1A, CALN1, CST3* (**Figure 22b**). In the HC group, 1,511 genes were downregulated in MC (e.g., *GPC5, SLC4A4, CNTN5*) when compared to FC, while 256 genes were upregulated, such as *AC999041.2, SEMA3E, MYTL1, MT3* and *CST3* (**Figure 22b**). Furthermore, I conducted an enrichment analysis to infer enriched GO terms from significant DEGs in ALS patients compared to HC in both MC and FC. GO terms linked to neuronal function and signaling, such as “neuron development”, “modulation of chemical synaptic transmission”, “(voltage-gated) potassium channel signaling”, “ionotropic/AMPA glutamate receptor complex’ and lipid metabolism related pathways like “cholesterol binding”, “sterol binding”, “regulation of lipase activity” were enriched for OPCs in FC of ALS patients in comparison to HCs (**Figure 23a**). Whereas in MC, GO terms such as “neurotransmitter secretion”, “signal release from synapse”, “Golgi membrane”, “transition metal ion binding” and “zinc ion binding” (**Figure 23b**).

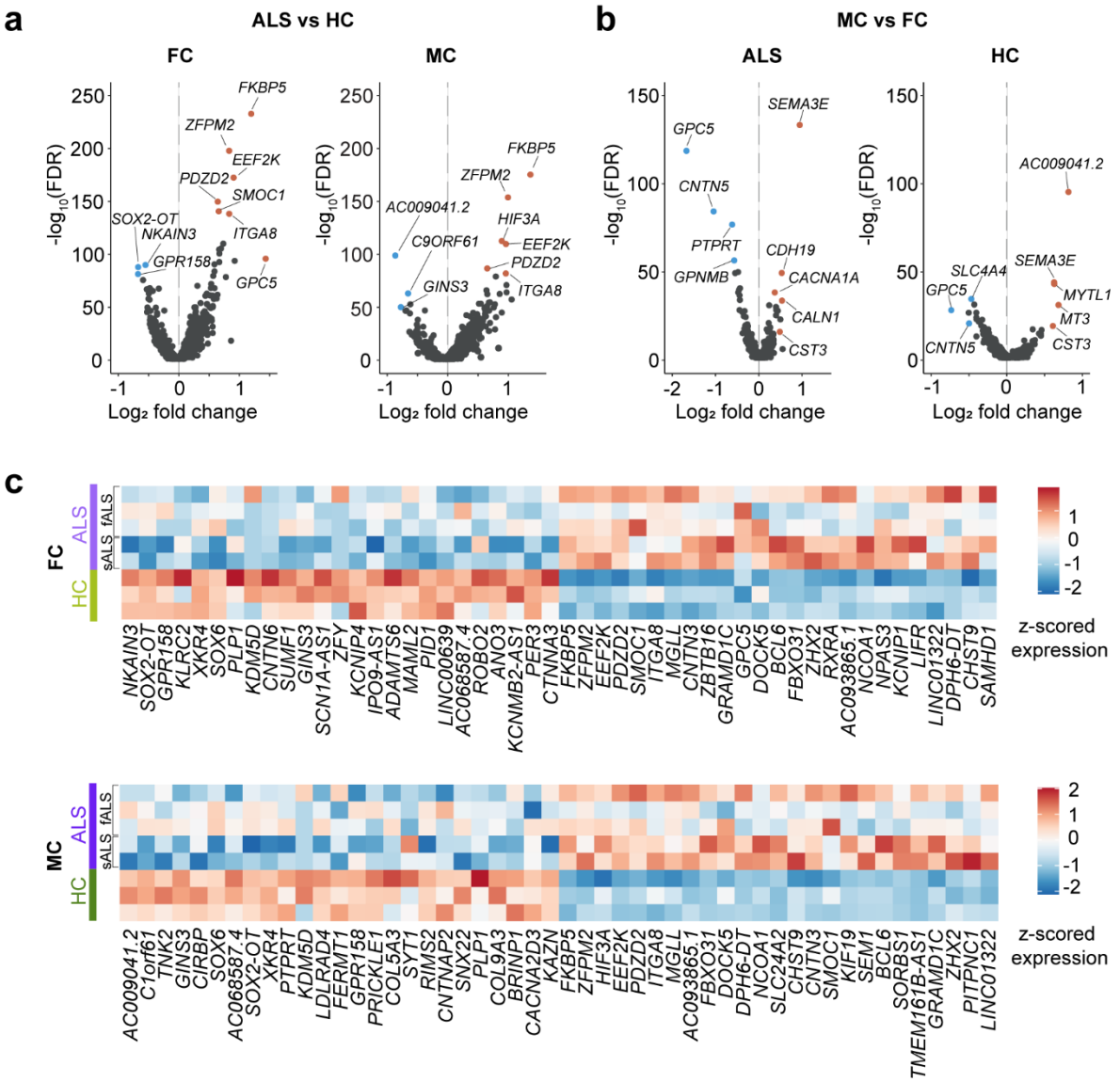

Figure 22. Single nuclei RNA-seq analysis of oligodendrocyte progenitor cells (OPCs).

(**a**) Volcano plots of DEGs of OPCs in frontal cortex (n = 5,307) and in motor cortex (n = 3,093) of ALS patients compared to HC (with Wilcoxon rank sum test and false discovery rate (FDR) was inferred from p-values via Benjamini-Hochberg method, DEGs with FDR < 0.05 and |Log_2 fold change| > 0) are plotted). (**b**) Volcano plots of DEGs of all OLs in ALS (n = 4,822) patients and HC (n = 3,578) of MC compared to FC. (**c**) Heatmaps of top 25 downregulated (blue) and 25 top upregulated (red) DEGs shown at panel (a). Z-scored gene expression values were calculated from mean gene expression of all OPCs per patient per region. UMAP, Uniform Manifold Approximation and Projection; sALS, sporadic ALS; fALS, familial ALS.

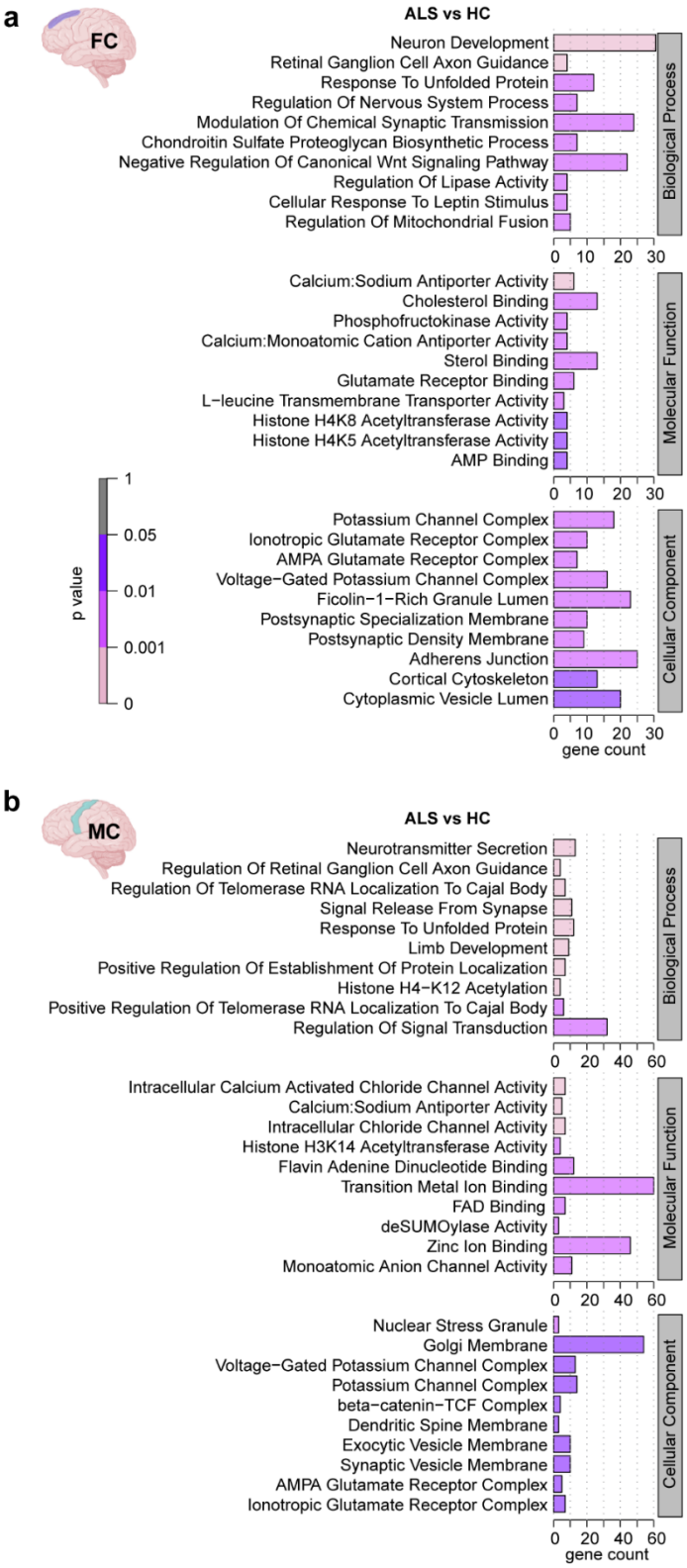

Figure 23. Top 10 Gene Ontology (GO) terms enriched for differentially expressed genes (DEGs) identified in oligodendrocyte progenitor cells (OPCs).

(**a**) DEGs in frontal cortex (FC) of ALS compared to HC. (**b**) DEGs in motor cortex (FC) of ALS compared to HC. DEGs are identified as combination of up- and down- regulated genes (ALS vs HC) in respective cortical area for all OPCs. GOs are shown across three databases: Biological Process, Molecular Function, and Cellular Component. Significant GO terms were determined using Fischer's exact test with $p < 0.05$. Icons were created with BioRender.com.

4.3.5. Excitatory neurons

I have collected a combined count of 20,403 excitatory neurons, with 12,253 originating from FC and 8,150 originating from MC. These cells were subsequently categorized into 13 distinct subclusters based on expression of 4 main genes, namely LINC00507 (2 clusters), RORB (5 clusters), THEMIS (2 clusters), FEZF2 (4 clusters) (**Figure 24a**). Combination of marker genes were assigned per subcluster, namely LINC00507-1 (*LINC00507*+, *ACVR1C+),* LINC00507-2 (*LINC00507*+ *LINC02055*+), RORB-1 (*RORB*+, *TLL1*+), RORB-2 (*RORB*+, *ALDH1A1*+), RORB-3 (*RORB*+, *ADGRL4*+), RORB-4 (*RORB*+, *PLCH1*+, *CUX2*-), RORB-5 (*RORB*+, *PLCH1*+, *CUX2*+), THEMIS-1 (*THEMIS*+, *CDH13*+), THEMIS-2 (*THEMIS*+, *NTNG2*+), FEZF2-1 (*FEZF2*+, *GNAL*+), FEZF2-2 (*FEZF2*+, *HTR2C*+), FEZF2-3 (*FEZF2*+, *LINC02232*+), FEZF2-4 (*FEZF2*+, *POU3F1*+, *ADRA1A*+) (**Figure 24b**). Intriguingly, in ALS MC, the fraction of cells in the LINC05007-2 cluster almost halved in comparison to HCs (HC MC vs ALS MC p = 0.0105), while two RORB clusters, RORB-3 (HC MC vs ALS MC p = 0.00992), and RORB-4 (HC MC vs ALS MC p = 0.024), were more enriched in ALS (**Figure 24c**). The fraction of cluster FEZF2-4 cells, which expresses UMN markers (e.g., *FEZF2 and POU3F1*) was decreased significantly in ALS MC in comparison to HC (**Figure 24c,** HC MC vs ALS MC p = 0.0037). Moreover, ALS patients had significant regional (MC vs FC) differences in the fraction of cells in clusters FEZF2-1 (ALS FC vs ALS MC p = 0.313), FEZF2-2 (ALS FC vs ALS MC p = 0.000000178) and FEZF2-4 (ALS FC vs ALS MC p = 0.00000856) (**Figure 24c**). In addition, I observed a reduced proportion of cluster RORB-1 in FC of ALS patients (**Figure 24c,** HC FC vs ALS FC p = 0.0469). In the FC, I identified a total of 2,009 genes that were significantly downregulated (e.g., *AL592156.2, PHACTR1, KCNH4, SVOP, ETV5, PRMT8*), while 1,278 genes (e.g., *SNX31, AP001347.1, AL592183.1, PRNP, KIF13A, SYN3*) exhibited significant upregulation compared to the HC (**Figure 24d**). In the MC, I observed significant downregulation in 2,412 genes (e.g., *AL008633.1, CIRBP, ETV5, SVOP*) and significant upregulation in 1,544 genes (e.g., *SNX31, AP001347.1, CCND3, AC006148.1, SNTG1, FKBP5, SYN3)* in ALS when compared to HC (**Figure 24d**). In the ALS group, there were 1,953 downregulated genes, including *SLC22A10, SHISA9, SASH1, MLIP* and *MAN1A1*; whereas in MC 1,737 genes, such as *GNAS, ACTB, FKBP5, GAPDH, CADPS2* and *CKB* (**Figure 24f**). On the other hand, in HC, there were 1,886 genes were significantly downregulated (e.g., *SLC22A10, KCNB2, CASC15*) in the MC when compared to the FC, while 1,553 genes were upregulated, including *NRGN, TMEM59L, CKB, ACTB, ATP6V0C* and *GAPDH* (**Figure 24f**). A heatmap displaying the z-scored expression levels of the 25 most downregulated and upregulated DEGs in ALS compared to the HC was generated by considering the average expression values for each patient and accounting for their presence in both brain regions (**Figure 24e**). Furthermore, I looked into the top enriched GO terms from significant DEGs in ALS patients compared to HC in both MC and FC. In FC, I saw an

enrichment of terms related to cell adhesion and synaptic organization e.g., “positive regulation of synapse assembly”, “cell-cell adhesion via plasma-membrane adhesion molecules”, “cell-cell adhesion mediated by cadherin”, “sprouting angiogenesis”, “homophilic cell adhesion via plasma membrane adhesion molecules” and “dendrites”; as well as terms associated with neuronal signaling such as “glutamate receptor signaling pathway”, “glutamate receptor activity”, “calcium:sodium antiporter activity’, “GABAergic synapse”, “glutamatergic synapse” and “potassium channel activity” (**Figure 25a**). Similarly, in MC, I observed enrichment of GO terms linked to cell adhesion and neuronal function such as “cell-cell adhesion mediated by cadherin”, “adherens junction”, “long-term synaptic depression”, “regulation of neuronal differentiation”, “neuron projection”, “dendrite”, and “3’,5’-cyclic-AMP binding phosphodiesterase activity” and “3’,5’-cyclic-nucleotide phosphodiesterase activity” (**Figure 25b**).

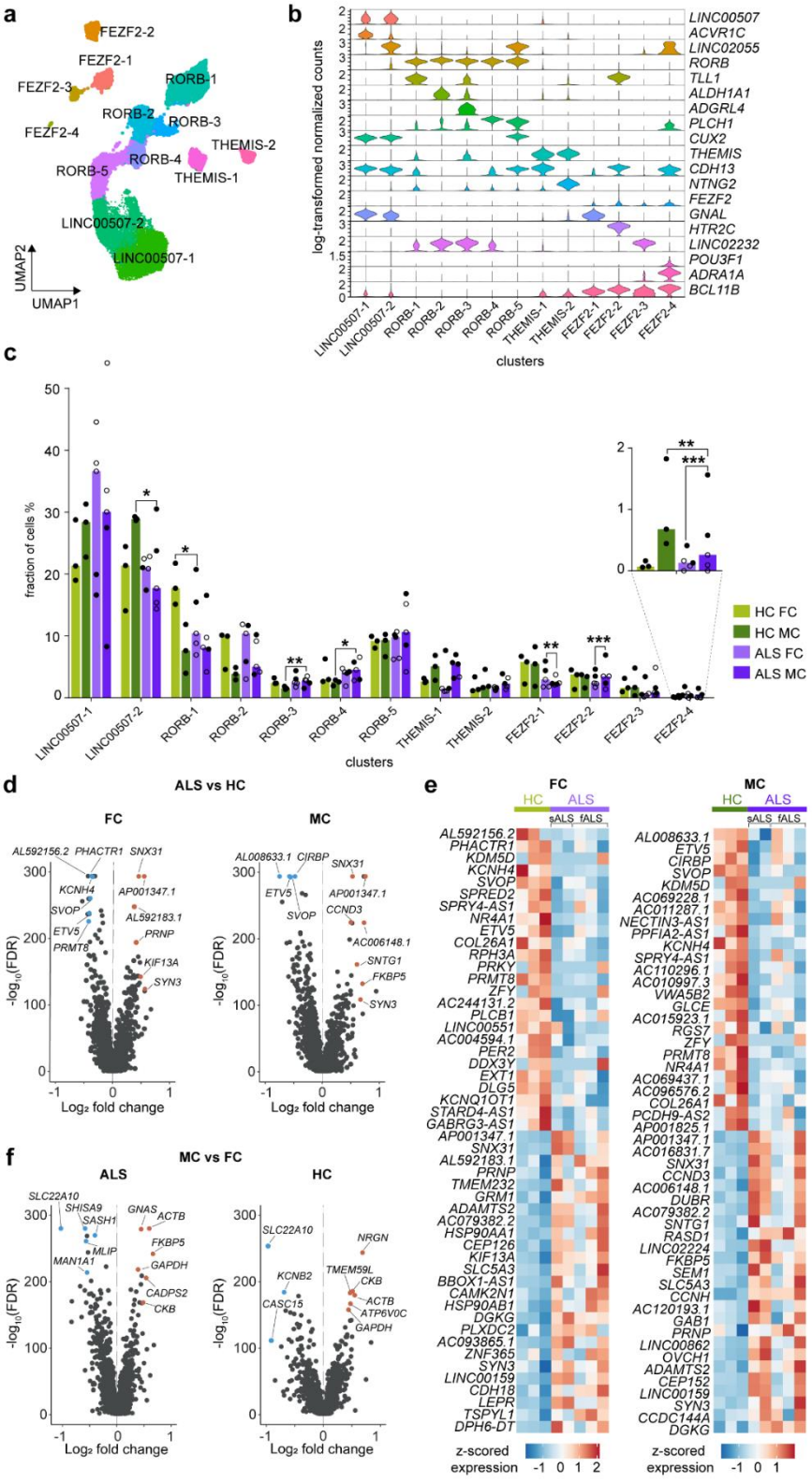

Figure 24. Single nuclei RNA-seq analysis of excitatory neurons.

(**a**) 13 subclusters of excitatory neurons (n = 20,403) have been identified. (**b**) Violin plot shows subcluster specific marker genes and their respective expression levels in frontal (FC) and motor (MC) cortex. (**c**) Fraction of nuclei per subcluster (beta-regression). Circles indicate fALS patients. (**d**) Volcano plots of differentially expressed genes (DEGs) of all excitatory neurons in frontal cortex (FC, n = 12,253) and in motor cortex (MC, n = 8,150) of ALS patients compared to HC (Wilcoxon rank sum test and false discovery rate (FDR) was inferred from p-values via Benjamini-Hochberg method, DEGs with FDR < 0.05 and $|\text{Log}_2$ fold change$| > 0$) are plotted). (**e**) Heatmaps of top 25 downregulated (blue) and 25 top upregulated (red) DEGs shown at panel (d). Z-scored gene expression values were calculated from mean gene expression of all OLs per patient per region. (**f**) Volcano plots of DEGs of all excitatory neurons in ALS (n = 12,695) patients and HC (n = 7,708) of MC compared to FC. UMAP, Uniform Manifold Approximation and Projection; sALS, sporadic ALS; fALS, familial ALS. Data in (c) represents median & 95% confidence interval (CI). * $p < 0.05$, ** $p < 0.01$, *** $p < 0.001$.

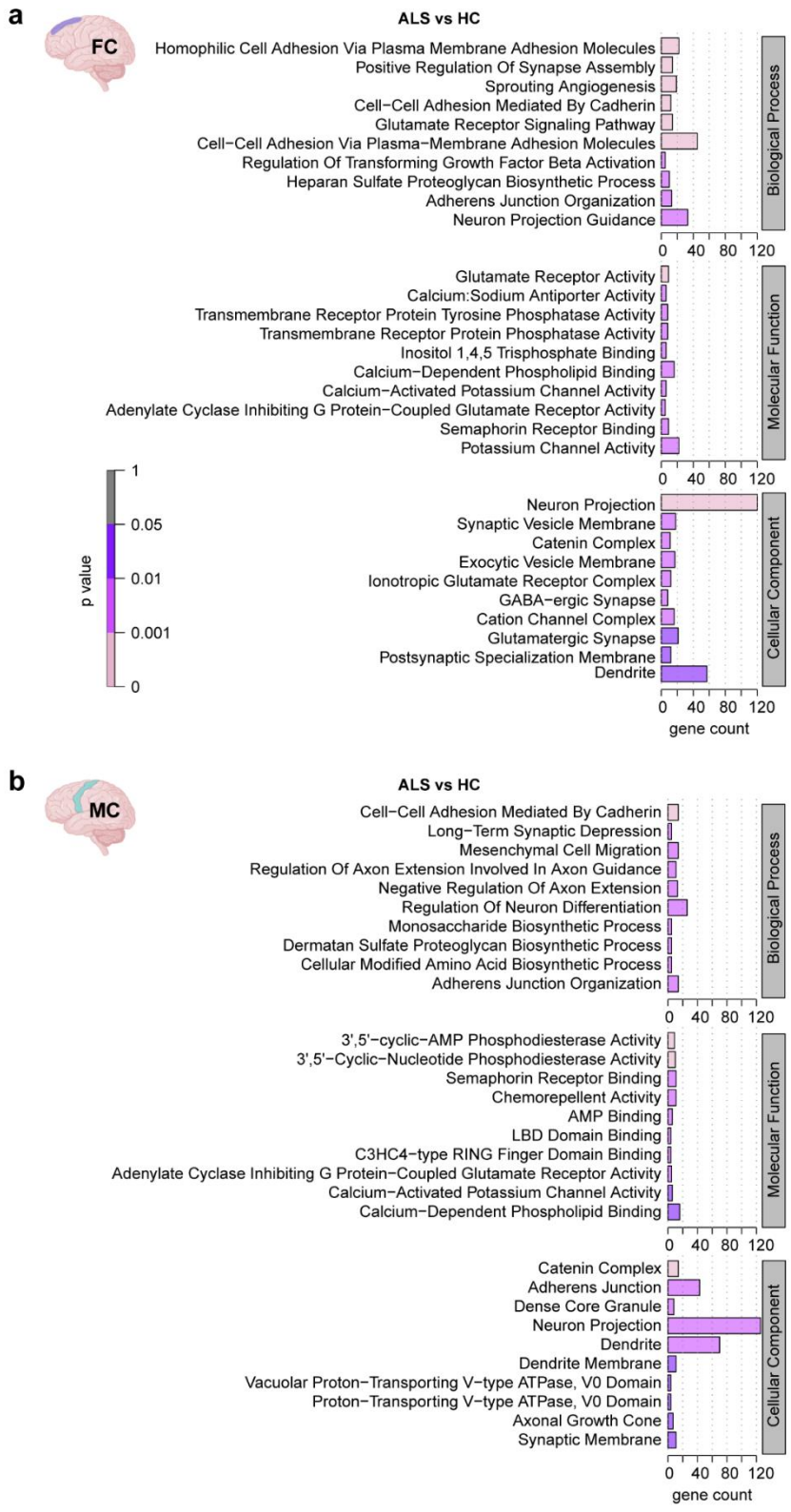

Figure 25. Top 10 Gene Ontology (GO) terms enriched for differentially expressed genes (DEGs) identified in excitatory neurons.

(**a**) DEGs in frontal cortex (FC) of ALS compared to HC. (**b**) DEGs in motor cortex (FC) of ALS compared to HC. DEGs are identified as combination of up- and down- regulated genes (ALS vs HC) in respective cortical area for all excitatory neurons. GOs are shown across three databases: Biological Process, Molecular Function, and Cellular Component. Significant GO terms were determined using Fischer's exact test with $p < 0.05$.

4.3.6. Interneurons

I have acquired a total of 21,254 interneurons, with 13,554 from FC and 7,700 from MC. These cells were categorized into 6 groups (11 subclusters) defined by positive expression of parvalbumin (PV, 2 clusters); somatostatin (SOM, 2 clusters); lysosomal associated membrane protein family member 5 (LAMP5, 3 clusters); vasoactive intestinal peptide (VIP, 2 clusters); calretinin (CR, 1 cluster) and cholecystokinin (CCK, 1 cluster) (**Figure 26a**). Subcluster specific marker genes were assigned as following: PV-1 (*PVALB*+, *MYO5B*+), PV-2 (*PVALB*+, *PTPRK*+), SOM-1 (*SST*+, *PCSK5*+), SOM-2 (*SST*+, *EPB41L4A*+), LAMP5-1 (*LAMP5*+, *IL1RAP*+), LAMP5-2 (*LAMP5*+, *COL5A2*+), LAMP5-3 (*LAMP5*+, *NOS1*+), VIP-1 (*VIP*+, *CCK*+), VIP-2 (*VIP*+, *BMPER*+), CR (*CALB2*+, *TAFA1*+) and CCK (*CCK*+, *PAX6*+) (**Figure 26b**). I observed a significant reduction of SOM-1 (HC FC vs ALS FC p = 0.0326) interneurons in FC and VIP-2 (ALS FC vs ALS MC p = 0.00726) interneurons in MC of ALS patients in comparison to HC (**Figure 26c**). In FC of ALS patients, PV-1 (ALS FC vs ALS MC p = 0.0356) and LAMP5-3 (ALS FC vs ALS MC p = 0.0000458) interneurons were less enriched compared to MC (**Figure 26c**). I saw a trend of reduction in the fraction of CR interneurons (ALS FC vs ALS MC p = 0.0509) and a significant decrease VIP-2 (ALS FC vs ALS MC p = 0.0142) and CCK (ALS FC vs ALS MC p = 0.0144) interneurons in MC of ALS patients compared to FC (**Figure 26c**). Next, in FC of ALS, I identified 2,406 downregulated (e.g*., KDM5D, SPRY4-AS1, KCNMB2-AS1, AC244131.2, SST*) and 1,128 upregulated (e.g., *AL592183.1, SNX31, HSP90AA1, SEM1, SYN3*) genes when compared to HC (**Figure 26d**). In MC of ALS, 2,876 genes (e.g., *KDM5D, SPRY4-AS1, GABRG3-AS1, CIRBP, SST*) were downregulated and 878 genes (e.g., *SNX31, AL592183.1, SEM1, IQCJ-SCHIP1, SYN3*) were upregulated (**Figure 26d**). In addition, regional comparison of MC and FC in ALS patients resulted in 1,877 downregulated genes such as *PLPPR1, GDA, GAS7* and *CNR1*; 1,188 upregulated genes (e.g., *AC005906.2, MIR34AHG, ACTB, GAPDH, LDLRAD4, AC120193.1, NEAT1*) (**Figure 26f**). Furthermore, in HC MC I identified 1,553 downregulated genes (e.g., *AC090579.1, GDA, KCNMB2-AS1, PLCH1*) and 779 upregulated genes (e.g., *ENO2, ATP6V0C, LDLRAD4, ACTB, SNCB, GAPDH, NEAT1*) (**Figure 26f**). A heatmap illustrating z-scored gene expression levels for the 25 most downregulated and upregulated DEGs in ALS compared to HC was generated, incorporating average expression values per patient and in both cortical regions (**Figure 26e**). Comparing ALS to HC, in FC I observed enrichment of GO terms such as “negative regulation of protein ubiquitination”, “cell-cell adhesion mediated by cadherin”, “adherens junction”, “synaptic transmission, glutamatergic”, “U4 snRNA binding”, “cholesterol binding” and “ionotropic/AMPA glutamate receptor complex” (**Figure 27a**). Enriched GO terms linked to cell adhesion (e.g., “cell-cell adhesion mediated by cadherin”, “adherens junction organization”, “adherens junction”) were also implicated in MC in addition to the pathways enriched for cellular trafficking and cellular clearance, namely “regulation of

lysosomal lumen pH", “synaptic/exocytic vesicle membrane”, “axon”, “trans-Golgi network membrane” (**Figure 27b**). Pathways linked to neuromodulation and energy metabolism such as “regulation of catecholamine secretion”, “pentose-phosphate shunt” and “amino sugar metabolic process” were also enriched in MC of ALS compared to HC (**Figure 27b**).

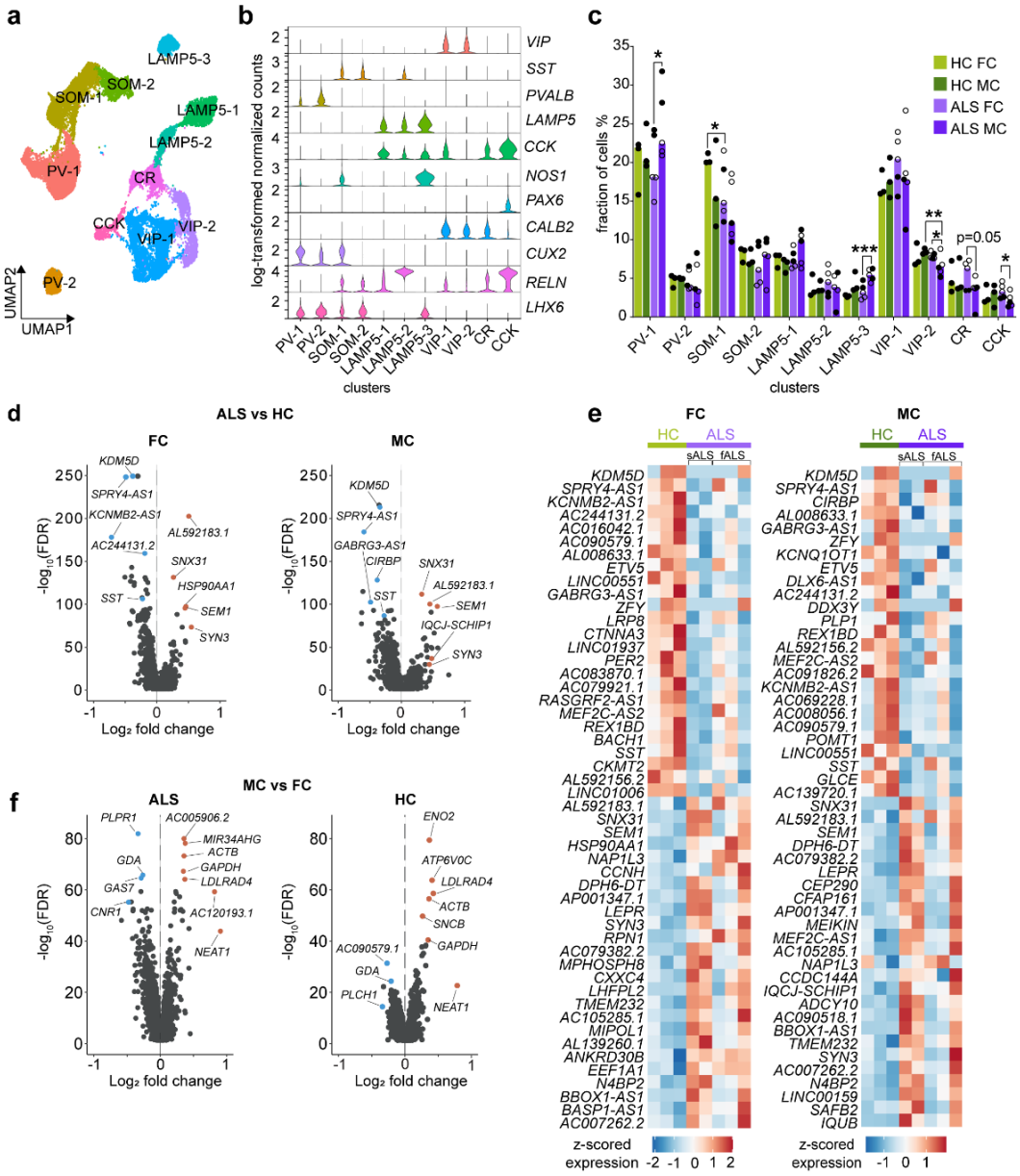

Figure 26. Single nuclei RNA-seq analysis of interneurons.

(**a**) 11 subclusters of interneurons (n = 21,254) have been identified. (**b**) Violin plot of subcluster specific marker genes and their respective expression levels in frontal (FC) and motor (MC) cortex. (**c**) The fraction of nuclei per subcluster (beta-regression). Circles indicate fALS patients. (**d**) Volcano plots of differentially expressed genes (DEGs) of all interneurons in frontal cortex (FC, n = 13,554) and in motor cortex (MC, n = 7,700) of ALS patients compared to HC (Wilcoxon rank sum test and false discovery rate (FDR) was inferred from p-values via Benjamini-Hochberg method, DEGs with FDR < 0.05 and |Log_2 fold change| > 0) are plotted). (**e**) Heatmaps of top 25 downregulated (blue) and 25 top upregulated (red) DEGs shown at panel (d). Z-scored gene expression values were calculated from mean gene expression of all interneurons per patient per region. (**f**) Volcano plots of differentially expressed genes (DEGs) of all interneurons in ALS (n = 13,847) patients and HC (n = 7,407) of MC compared to FC. DEGs with FDR < 0.05 and |Log_2 fold change| > 0 are plotted. Abbreviations: UMAP, Uniform Manifold Approximation and Projection; sALS, sporadic ALS; fALS, familial ALS; PV, parvalbumin; SOM, somatostatin; LAMP5, lysosomal associated membrane protein family member 5; VIP, vasoactive intestinal peptide; CR, calretinin; CCK, cholecystokinin. Data in (c) represents median & 95% confidence interval (CI). * p < 0.05, ** p < 0.01, *** p < 0.001.

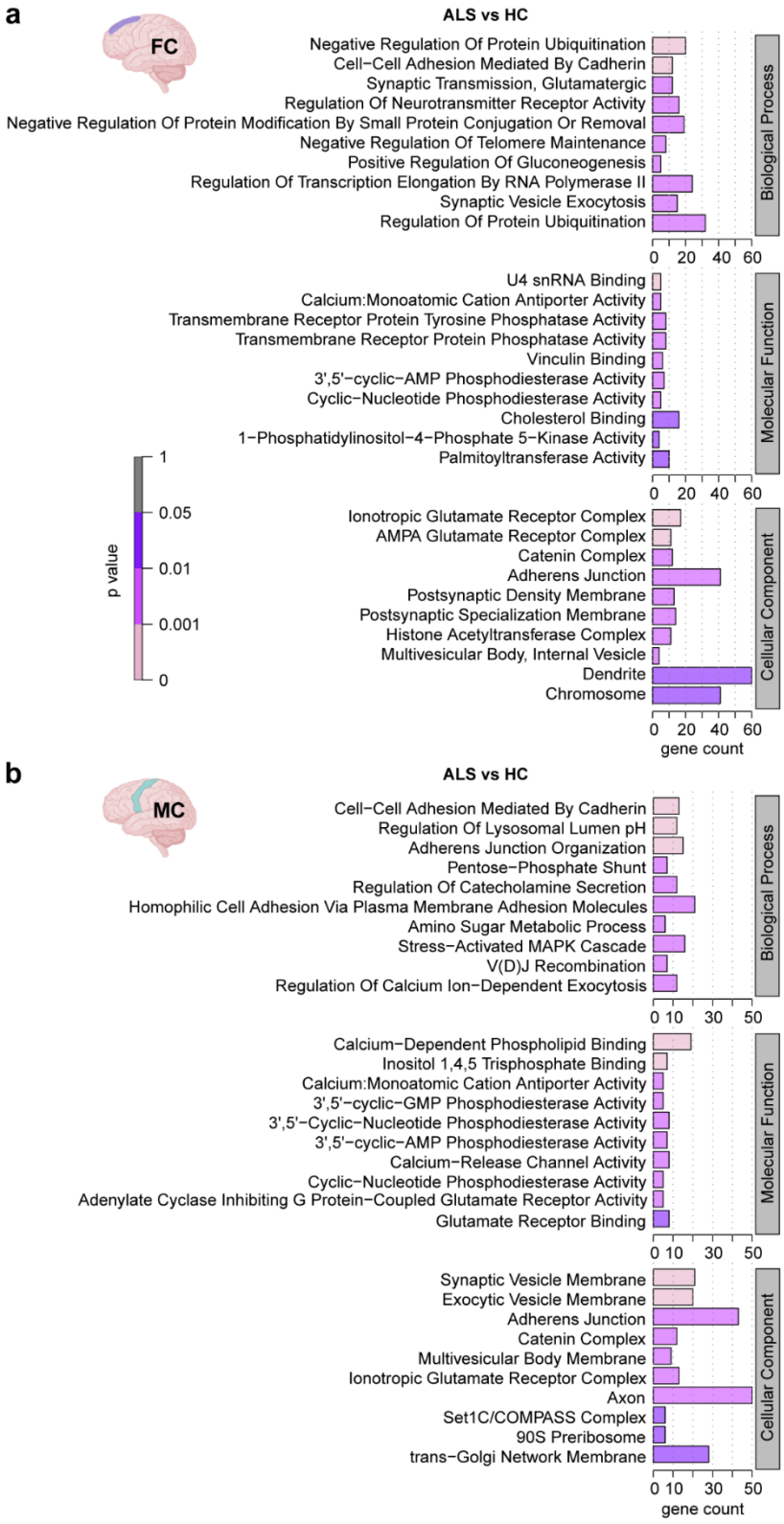

Figure 27. Top 10 Gene Ontology (GO) terms enriched for differentially expressed genes (DEGs) identified in interneurons.

(**a**) DEGs in frontal cortex (FC) of ALS compared to HC. (**b**) DEGs in motor cortex (FC) of ALS compared to HC. DEGs are identified as combination of up- and down- regulated genes (ALS vs HC) in respective cortical area for all interneurons. GOs are shown across three databases: Biological Process, Molecular Function, and Cellular Component.

4.3.7. Cell-Cell interaction analysis

I inquired about the early changes in communication between cell types. To this end, I checked the interaction of 8 cell types: microglia, astrocytes, oligodendrocytes, OPCs, endothelial cells, excitatory neurons, interneurons MGE and interneurons CGE. I performed cell-cell interaction or ligand (sender)-receptor (receiver) analysis in the following groups: HC FC (**Figure 28a**), HC MC (**Figure 28b**), ALS FC (**Figure 28c**), and ALS MC (**Figure 28d**); and visualized the inferred frequency of communication (or L-R pairings) with heatmaps. In ALS, microglia-microglia interaction is increased in both regions compared to HC, where the ALS MC has more enhanced compared to FC (**Figure 28a-d**). Similarly, astrocyte-astrocyte interactions are also increased in ALS compared to HC, in both regions. Furthermore, ALS FC has more pronounced astrocyte-astrocyte interaction compared to ALS MC, indicating an early disease mechanism (**Figure 28a-d**). Only in FC, but not in MC of ALS patients, excitatory neuron-astrocyte and microglia-astrocyte communication were decreased when compared to HC (**Figure 28a-d**). Moreover, in both FC and MC of ALS, astrocytes (as senders) have greater interaction with endothelial cells, excitatory neurons, microglia, OPCs and oligodendrocytes, but interestingly not with both interneuron populations as compared to HC (**Figure 28a-d**). A reduction of OPC-OPC interactions solely in MC of ALS patients in contrast to HC was also observed, implicating changes in later disease stage. In FC of ALS patients in comparison to HC, I saw a reduction of excitatory neuron-oligodendrocyte and interneuron CGE-oligodendrocyte communication. Strikingly, frequency of interneuron CGE-oligodendrocyte pairings was further reduced in MC of ALS while excitatory neuron-oligodendrocyte communication did not significantly change, implicating an early alteration in communication of the latter pair in the disease. Lastly, I saw increased communication within endothelial cells, as well as between endothelial cells-microglia and microglia-endothelial cells pairs in both FC and MC ALS when compared to HC (**Figure 28a-d**). Altered interactions were more pronounced in interneuron MGE population than changes in interneuron CGE in both regions (**Figure 28a-d**). To summarize early changes, that is changes already observed in FC, include interactions between astrocytes, microglia, endothelial cells as senders and astrocytes, microglia and excitatory neurons as receivers. Alterations in the later stage of the disease (that is present in MC), on the other hand, stems from interactions of astrocytes, microglia, endothelial cells and OPCs as senders; and astrocytes, microglia, endothelial cells, interneuron CGE and oligodendrocytes. Lastly, I compared the interaction frequency difference of cell-cell pairs between different regions in ALS vs HC and between regions (MC vs HC) in HC and ALS patients to visualize statistically significant changes (**Figure 29a-d**).

Next, I checked which ligand-receptor pairs could be responsible for the changes I see in altered cell-cell communication patterns in ALS. Since I saw a more pronounced change in microglia communication patterns, I plotted ligand-receptor pairs involving microglia as a sender (ligand) and a receiver (receptor) that are most specific to respective cell-cell pairs, together with their expression level (**Figure 30a-d**).

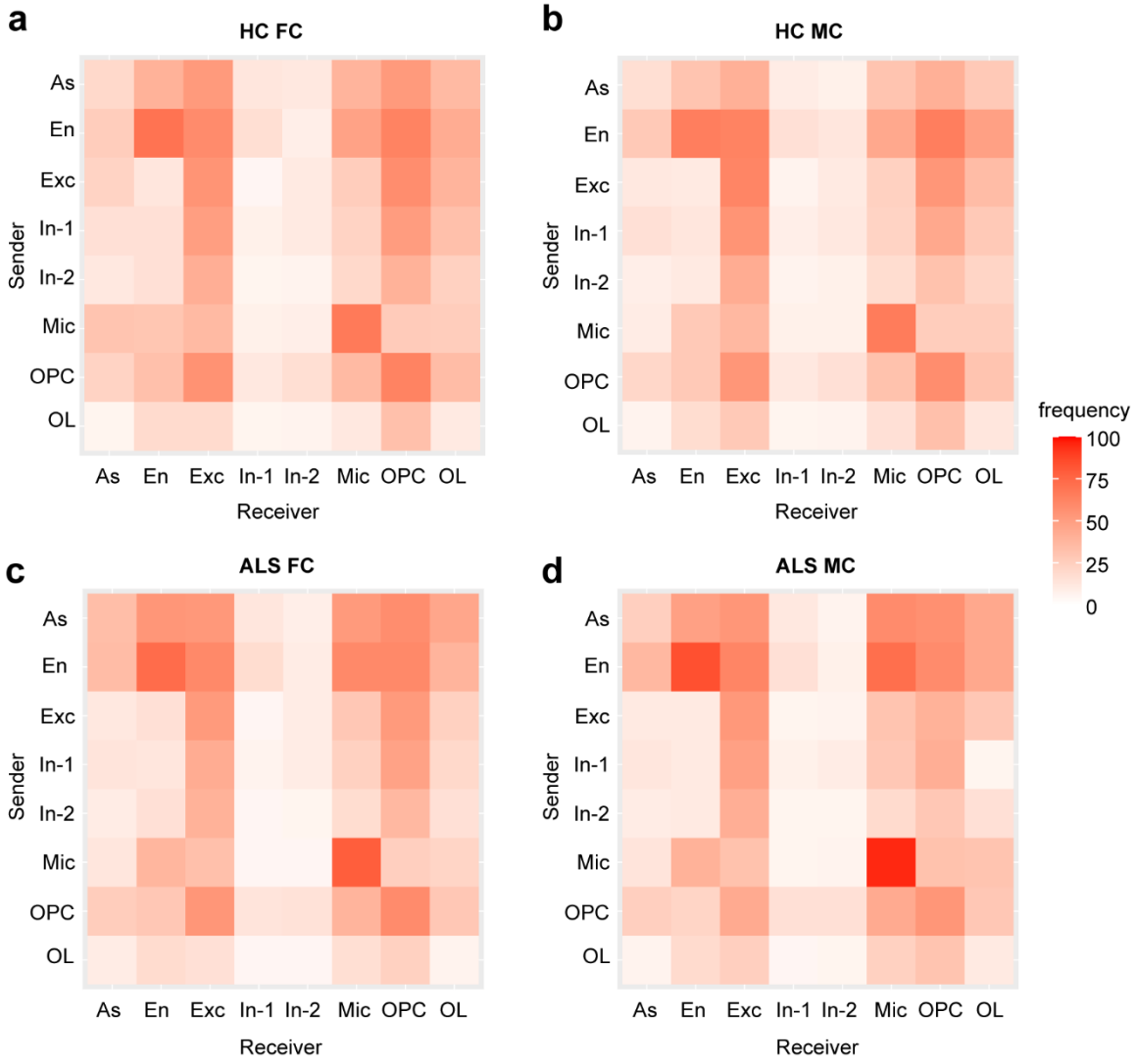

Figure 28. Cell-cell communications are altered in ALS compared to HC in frontal (FC) and motor cortex (MC).

Inferred cell-cell interaction frequency heatmaps for potentially communicating sender-receiver (ligand-receptor) pairs in (**a**) HC FC, (**b**) HC MC, (**c**) ALS FC and (**d**) ALS MC. As, astrocytes; En, endothelial cells; Exc, excitatory neurons; In-1, interneurons caudal ganglionic eminence (CGE); In-2, interneurons medial ganglionic eminence (MGE); Mic, microglia; OPC, oligodendrocyte precursor cells; OL, oligodendrocytes.

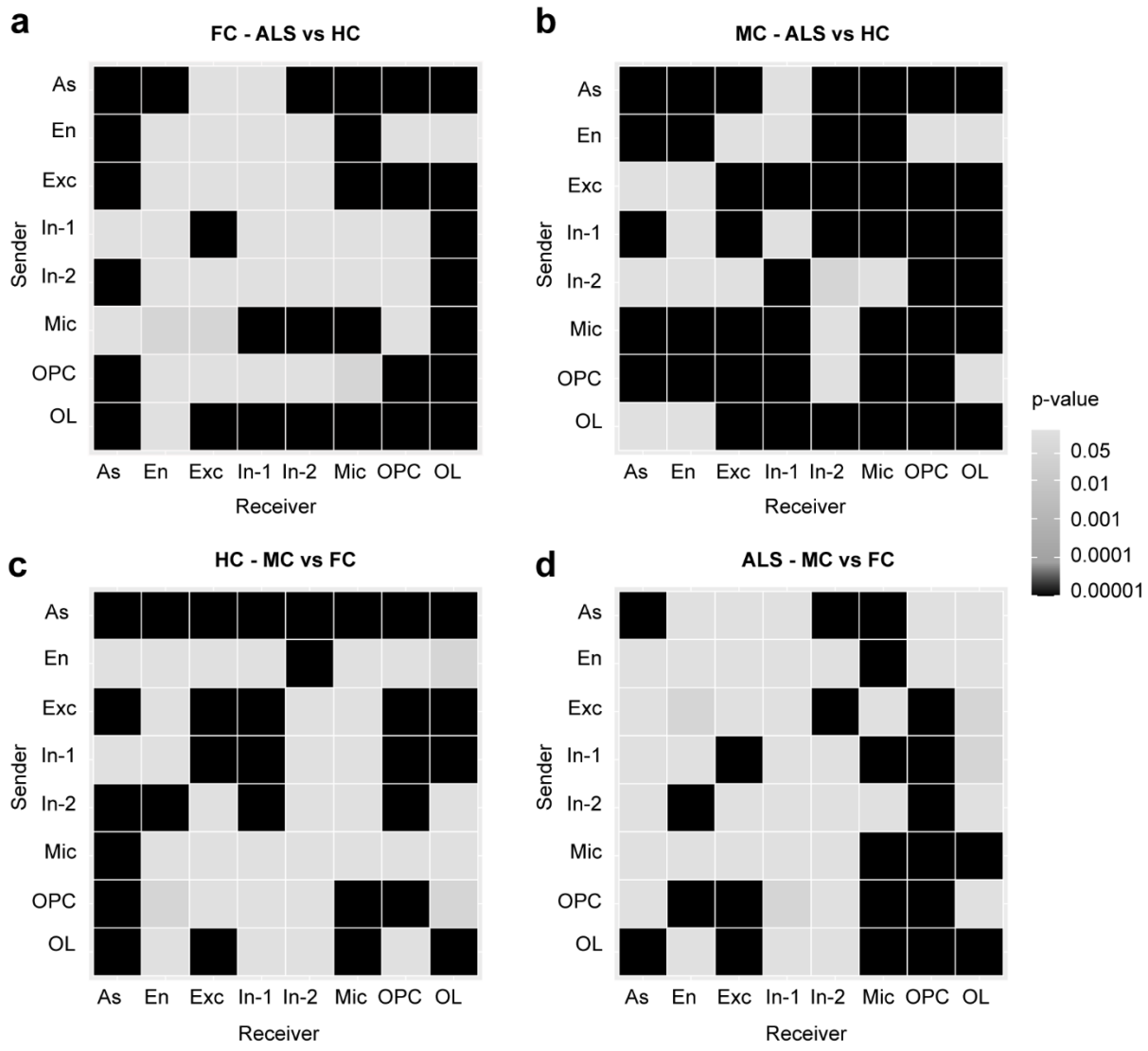

Figure 29. Region and sample comparison of cell-cell interaction frequency heatmaps.

Inferred cell-cell interaction frequencies were compared between samples ALS vs HC in (**a**) FC and in (**b**) MC and between regions MC vs FC of (**c**) HC and (**d**) ALS (two-tailed t test). As, astrocytes; En, endothelial cells; Exc, excitatory neurons; In-1, interneurons caudal ganglionic eminence (CGE); In-2, interneurons medial ganglionic eminence (MGE); Mic, microglia; OPC, oligodendrocyte precursor cells; OL, oligodendrocytes. * $p < 0.05$, ** $p < 0.01$, *** $p < 0.001$.

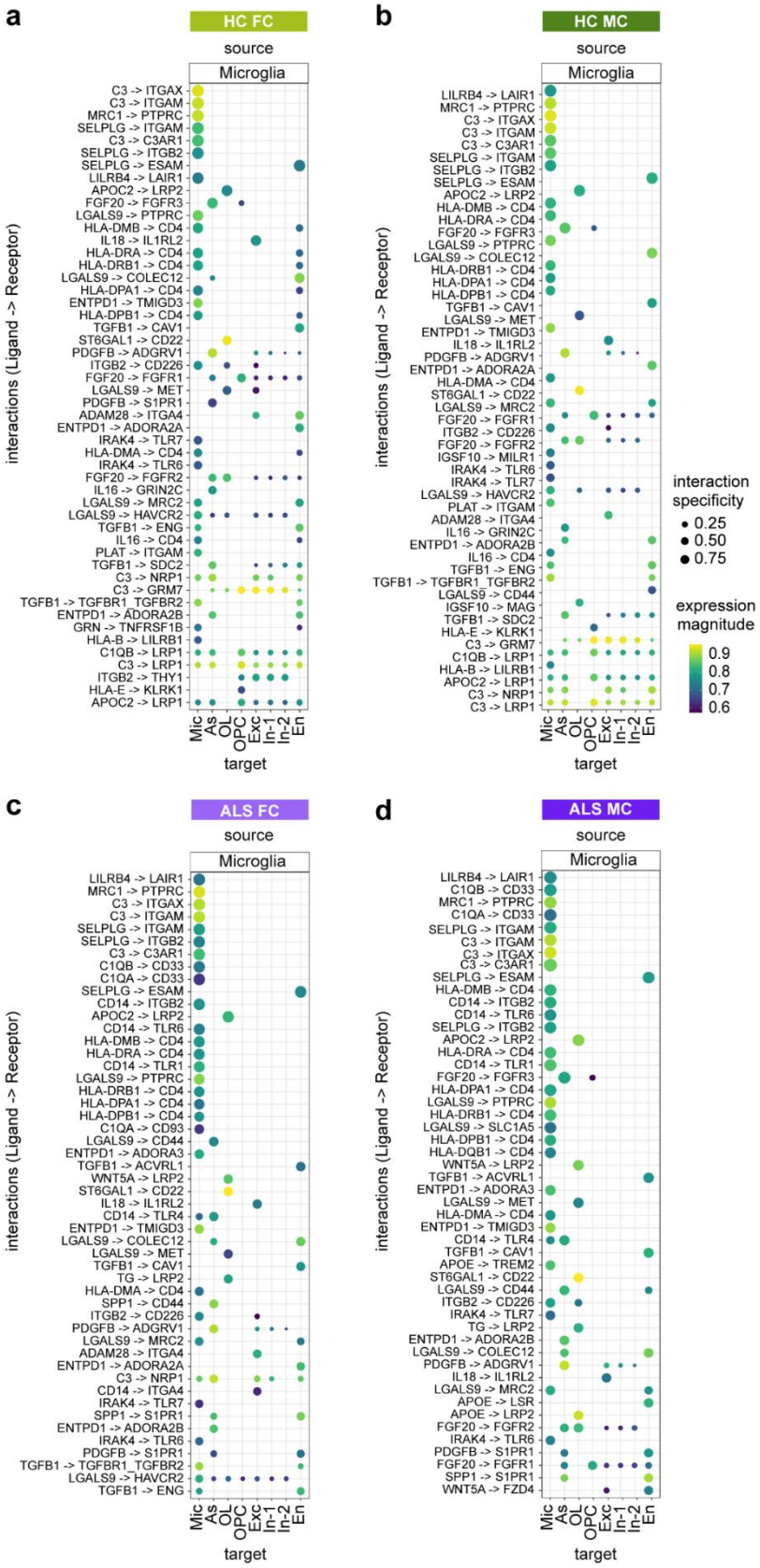

Figure 30.Cell-cell interactions involving microglia are altered early in ALS.

Dot plots of ligand-receptor pairs where microglia act as sender (ligand). Top 50 ligand-receptor pairs in decreasing cell-cell interaction specify is plotted for (**a**) HC FC, (**b**) HC MC, (**c**) ALS FC, (**d**) ALS MC. As, astrocytes; En, endothelial cells; Exc, excitatory neurons; In-1, interneurons caudal ganglionic eminence (CGE); In-2, interneurons medial ganglionic eminence (MGE); Mic, microglia; OPCs, oligodendrocyte precursor cells; OL, oligodendrocytes

My observation of altered cell-cell communication patterns involving microglia prompted me to look further into the top 50 most specific ligand-receptor pairs enriched in ALS microglia (**Figure 30a-d**). I also observed regional changes in ALS microglia-microglia communication such as reduction of MRC1-PTPRC signaling in MC when compared to FC. I saw a lower expression of microglia-microglia L-R pair, namely C1QA-CD33, in ALS FC in comparison to ALS MC, while this pair did not show up in HC (**Figure 30b & d**). Regarding other cell types, the most distinctive change is observed in microglia-astrocyte pair LGALS9-CD44 which was not detectable in HC but enriched in ALS FC and MC (**Figure 30c & d**). I report APOC2-LRP2 communication between microglia-oligodendrocytes to be enriched in ALS in comparison to HC in both regions (**Figure 30a-d**).

5. Discussion

In my thesis, I have investigated the "*early"* cortical molecular alterations in ALS patients by employing snRNA-seq in FC and MC of ALS patients and HCs. In this section, I discuss the findings of transcriptomic alterations regarding the 8 main cell types and their subtypes. I refer to "*early"* alterations as the changes in FC, which lacks the hallmark pTDP-43 inclusions. In contrast, *"late"* changes imply transcriptional modifications in MC, that is the initial site of pTDP-43 pathology and characterized by the loss of UMNs that are selectively vulnerable in ALS.

5.1. Global alterations in the absence of pTDP-43 pathology

In this study, I first looked for the transcriptomic changes stemming from all cell types combined. The snRNA-seq analysis of post-mortem FC and MC samples from the same ALS patients and HCs thus provided a comprehensive view of the molecular landscape in these regions. I identified 8 cell types, namely excitatory neurons, interneurons, microglia, astrocytes, oligodendrocytes, OPCs, and endothelial cells, providing a detailed portrait of cellular diversity in the context of ALS.

In terms of gene expression differences, the analysis revealed substantial alterations in the transcriptome of ALS patients compared to HCs. When considering all single nuclei across all cell-types together, a notable number of DEGs were identified in both regions. The downregulation of genes related to processes like lipid and carnosine metabolism (i.e., *CARNS1, CNDP1, SCD*) are apparent in ALS early on. *CARNS1* encodes for carnosine synthase 1, which is responsible for the biosynthesis of carnosine by oligodendrocytes and is both a precursor for GABA and acts as an antioxidant that is neuroprotective by limiting Zn^{2+} and Cu^{2+} mediated neurotoxicity (Schön et al., 2019), while carnosine dipeptidase 1 (*CNDP1*) is responsible for carnosine break down. Downregulation of *CARNS1* and *CNDP1* could indicate that both the catabolic and anabolic metabolism of carnosine is affected early in the disease. Moreover, stearoyl-CoA desaturase (SCD) is an enzyme crucial for the regulation of fatty acid desaturation, and its inhibition in AD mouse model was shown to be beneficial to dampen immune response and promote neuronal health (Hamilton et al., 2022). Additionally, in a cell culture model of PD SCD inhibition decreased α-synuclein (αSyn)-induced neurotoxicity in late cultures but was found to be toxic to early cultures (Nicholatos et al., 2021). Downregulation of *SCD* thus could be an early attempt to decrease a potential early immune response depicted by the upregulation of genes associated with cellular stress and inflammation (i.e., *HSP90AA1, FKBP5, BCL6, GFAP, NEAT1*). FK506-binding protein 51 (*FKBP5*) is an important epigenetic modulator of cellular stress and shown to be upregulated in ageing and other neurodegenerative diseases (Blair et al., 2013; Zannas et al., 2019). It acts

as a proinflammatory factor and activates nuclear factor-κ B (NFκB) signaling via IL-1β driven pathways (Kästle et al., 2018). *HSP90AA1*, encodes for heat shock protein 90 (Hsp90) whose impaired activity has been linked to increased sensitivity to TDP-43 induced toxicity in yeast and mammalian cell culture models (Lin et al., 2021). Moreover, long-non-coding RNA nuclear enriched abundant transcript 1 (*NEAT1*), a structural component of nuclear paraspeckle formation is increased in post/mortem spinal cord of sALS patients and was shown to be a regulator of TDP-43 function (Shelkovnikova et al., 2018). Although the exact mechanism by which NEAT1-TDP-43 interact is unknown, in yeast and *Drosophila* models, increased *NEAT1* expression was shown to alleviate TDP-43 induced cellular toxicity (Matsukawa et al., 2021). Together, upregulation of *NEAT1* suggests an early mechanism upstream of TDP-43 aggregation, likely to alleviate TDP-43 pathology, as it is hypothesized that the NEAT1 peptide could decrease TDP-43's interaction with other RBPs, and reduce its aggregation propensity (Matsukawa et al., 2021). Similarly, in the MC, the same inflammatory genes were further upregulated, concluding a global inflammatory signature is already present in the absence of pTDP-43 pathology.

I further compared if similar genes would appear when a pseudobulk version of the dataset was used for DEG analysis, in which case all transcriptomes of all cells are combined ignoring cell types and individual cells. This analysis identifies the genes which undergo the strongest change irrespective of cell-identity. Surprisingly, I did not detect an upregulation of *NEAT1* in FC, while it was consistently upregulated in MC of ALS patients as shown in the single nuclei version of the DEG analysis. This might be due to the pronounced upregulation of *NEAT1* in a subtype of cells, as it was indeed enriched in microglia of FC of ALS cases. Moreover, upregulation of *FKBP5* was further depicted in the pseudobulk data, suggesting a pronounced early transcriptomic regulation is a part of ALS pathophysiology preceding TDP-43 pathology. In addition, the upregulation of serpin family A member 3 (*SERPINA3*) was detected in ALS, in both regions in the pseudobulk analysis, while it was not identified as a DEG when considering single nuclei. This likely is, again, due to the fact that *SERPINA3* upregulation is very pronounced but primarily coming from an astrocyte subtype. *SERPINA3* modulates inflammatory responses, and acts upstream of NFκB signaling, that is believed to enhance neuroinflammation (Liu et al., 2023). In a meta-analysis of spinal cord transcriptomic data from post-mortem human samples and ALS mouse models, *GFAP* and *SERPINA3* have been reported as differentially expressed when compared to healthy controls and wt mice, validating my pseudo-bulk data DEG analysis (Saris et al., 2013).

I found that both the single nuclei and the pseudo-bulk version of my dataset show an upregulation of genes promoting inflammation in FC, thus before pTDP-43 pathology. Interestingly, the comparison of the single nuclei and pseudobulk datasets revealed

differences in the number of identified DEGs, emphasizing the importance of considering potential biases introduced by the analysis approach. The pseudobulk analysis, which aggregates data from individual nuclei, identified fewer DEGs, suggesting a potential impact of technical variability and cellular heterogeneity in the snRNA-seq dataset. When I performed a GO analysis for these genes, pathways enriched for FC and MC of ALS patients in comparison to HCs collectively indicate that ALS-associated gene expression changes involve a combination of neuronal, inflammatory, and protein metabolism-related processes. In both approaches, GO terms found in FC already involved “ubiquitin protein ligase binding”, indicating an early alteration in ubiquitination rate of misfolded/aggregated proteins by modifying the expression or activity of E1, E2 and E3 ligases, which could be causal to pTDP-43 aggregation or a compensatory mechanism to reestablish proteostasis. Although similar processes were identified in the GO analysis of both versions of the dataset, utilizing the increased resolution of snRNA-seq, I report an enrichment in “ubiquitin-dependent ERAD pathway” distinctively in FC. The ER is a crucial cellular component responsible for orchestrating protein folding. Initial phases of mutant TDP-43 misfolding could trigger the activation of the unfolded protein response (UPR) within the ER, aimed at reinstating a cellular equilibrium (Prasad et al., 2019). ERAD is critical for clearance of abnormal proteins, and altered/impaired ER function together with sustained UPR signaling can promote more ER stress (Jeon et al., 2023). Failure to resolve this stress can incite oxidative stress, ultimately leading to cellular death (Nishitoh et al., 2008; Jara et al., 2015). My data proposes that the ERAD pathway is likely differentially activated prior to pTDP-43 accumulation in ALS.

5.2. Microglia

To further delineate cell type specific alterations, leveraging my snRNA-seq dataset, I looked into cell type specific alterations in ALS. I observed the most pronounced molecular alterations in my ALS samples in microglia, in both cortical regions I investigated. Microglia serve as the innate immune - and phagocytic cells within the CNS, engaging in diverse functions related to immune response, modulating myelination, and the surveillance of neural activity and synaptic connections (Nimmerjahn et al., 2005; Schafer et al., 2013; Cserép et al., 2021; Gao et al., 2023). The function of microglia in neurodegeneration is commonly acknowledged to have dual aspects; protective, involving anti-inflammatory actions, and defensive, involving pro-inflammatory responses.

An extensive analysis using snRNA-seq in AD, ALS and aging has revealed the existence of a novel and rare subset of microglia termed Disease-Associated Microglia (DAM) (Keren-Shaul et al., 2017; Deczkowska et al., 2018). The discovery of DAMs was first reported in a mouse model expressing five human familial AD mutations (5XFAD), and has been consistently validated in various amyloid-β (Aβ) models of AD (Keren-Shaul et al., 2017; Deczkowska et

al., 2018). DAM are characterized by the expression of typical microglial genes such as *Iba1*, *Cst3*, and *Hexb*, coupled with the downregulation of "homeostatic" microglial genes like *P2ry12*, *P2ry13*, *Cx3cr1*, *CD33*, and *Tmem119*, while exhibiting increased expression of *Spp1, Tyrobp* and *Trem2* (Deczkowska et al., 2018). A widely investigated DAM related protein is TREM2, a receptor expressed on the surface of microglia, that is involved in various functions, including phagocytosis, the regulation of inflammatory responses, and the maintenance of tissue integrity. Mutations in the gene encoding TREM2 have been linked to an increased risk of several neurodegenerative diseases, including AD, FTD and PD (Kleinberger et al., 2014). While the exact role of TREM2 in neurodegenerative diseases remains elusive, it was shown to be a critical player of microglial differentiation (i.e., from homeostatic to reactive form). TREM2 is suggested to possess both a neuroprotective role through the phagocytosis of extracellular protein aggregates (such as Aβ plaques) and the clearance of cellular debris (Xiang et al., 2016), while activation of microglia via TREM2 was also shown to be pro-inflammatory (Deczkowska et al., 2018). Although the role of TREM2 in neurodegeneration seems to be much more complex than pro- or anti- inflammatory, a similar signature of microglia is present in ALS patients and in $SOD1^{G93A}$ mouse model (Maniatis et al., 2019), confirming its importance in disease.

The consistent presence of DAM markers (such as increased *TREM2, TYROBP* and decreased *P2RY12, CX3CR1* expression) in postmortem human AD brains further supports the idea that the DAM phenotype represents a distinct microglial response associated with the neurodegenerative process (Keren-Shaul et al., 2017). In my dataset, I identified 3 subclusters of DAMs; DAM1 and DAM2 express less purinergic receptor P2Y, G-protein coupled, 12 protein (*P2RY12*) and C-X3-C Motif Chemokine Receptor 1 (*CX3CR1*) compared to other microglia clusters, and DAM2 and DAM3 expresses TYROBP in comparison to other clusters. I did not find one DAM cluster has the combination of increased *TREM2, TYROBP* and decreased *P2RY12, CX3CR1* expression. However, thanks to the increased resolution of my dataset, I concluded these gene expression patterns are shared to an extent in all DAMs while I defined them with additional markers that separate these 3 DAM subtypes. DAM1 expresses combination of *TMEM163, CD163, SPP1*, *HAMP, TYROBP*; DAM2 expresses *SPP1, XYLT1, TREM2, TYROBP* and DAM3 expresses *SPP1*, *FTH1, TYROBP*. DAM1 and DAM3 are seemingly TREM2 independent microglia, while my DAM2 cluster could be corresponding to the classical DAM implicated in previous studies (Zhou et al., 2020; Wang et al., 2022b). Furthermore, I found that DAM1 microglia are enriched in Cluster of Differentiation 163 (*CD163*) a scavenger receptor whose soluble version is suggested to have an anti-inflammatory role in the aging brain (Han et al., 2022). Moreover, increased expression of *CD163* in DAM has been recently reported in a snRNA-seq study of post-mortem AD patients, but its immunoregulatory role in neurodegeneration is incompletely understood (Grubman et

al., 2019). In addition, I saw that DAM1 microglia express *HAMP,* which encodes for hepcidin, whose expression is increased in microglia in response to inflammation and cause iron accumulation in microglia (Urrutia et al., 2013). Since I saw a significant increase of DAM1-type microglia in the MC of ALS patients in comparison to ALS FC and HC MC, I can speculate that the DAM1 cluster serves a pro-inflammatory function, likely having a detrimental impact on neurons. Similarly, in the DAM3 cluster I detected an enhanced expression of ferritin heavy chain 1 (*FTH1*), indicating another cluster of microglia that could have an iron overload and/or potentially undergo iron-dependent cell death through the subsequent accumulation of lipid ROS, a process known as ferroptosis. While such specified iron-accumulating microglia are implicated in AD (Keren-Shaul et al., 2017; Ryan et al., 2023), in my data I did not see a significant change in abundance of the DAM3 microglia between ALS and HC in both regions. Yet, the significant increased expression of *ACSL1* in ALS microglia, a mediator for ferroptosis, suggested the DAM3 microglia are transcriptionally altered themselves or their function in disease state is modulated by other microglia.

In contrast, early changes observed in ALS are reflected in an almost 30% loss of HOM microglia in FC and MC of ALS patients. This reduced number of HOM might be due to increased demand of DAM differentiation, which would explain the increase in INT cluster abundance I observed in both regions. Combined with a significant increase in DAM2 cluster abundance in FC and with a similar trend in MC of ALS patients, I suggest that the differentiation of HOM microglia to INT and eventually to DAM2 could be an early mechanism in ALS. These processes are likely anti-inflammatory as the DAM2 cluster in my dataset is the only TREM2 expressing microglia subcluster. I can further hypothesize that less abundance of protective DAM2 and increase in DAM1 numbers could together drive disease progression.

A microglia subcluster, I termed AM, expresses high levels of cluster of differentiation 83 (*CD83)* compared to other clusters. *CD83* expression is crucial for activation of dendritic cells and macrophages, yet its role in microglia function is not clear. In the experimental autoimmune encephalomyelitis model (EAE) of neuroinflammation, *CD83* expression in microglia was shown to be associated with the activation of microglia but also plays a key role in the resolution of inflammation (Sinner et al., 2023). The authors also showed that *CD83*-deficient microglia express higher levels of chemokines, thus exacerbating the disease. In my dataset, I saw a downward trend of AM abundance (~5% of all microglia) in MC of ALS patients compared to HCs, which might indicate a compromised propensity of microglia to resolve inflammation later in the disease.

When I checked the enrichment of GO terms constituted by the DEGs in FC, the main processes affected were linked to neuronal functions, synapse organization, and processes related to microgliosis and inflammation. In MC, however, identified enriched GO terms were

associated with neuronal signaling, microglial stress, and mitochondrial function. More specifically, genes such as synapse differentiation-inducing gene protein 1 (*SYNDIG1*) and (glutamate ionotropic receptor delta type subunit 2 *GRID2*), which are important for excitatory synapse function, were significantly downregulated in ALS FC and MC, when compared to HC. Interestingly, *SYNDIG1* downregulation was most prominent in DAM and AM clusters, whereas *GRID2* expression was lowered in all microglia subtypes. Although the function of these genes in microglia are not yet known, they suggest that DAM and AM microglia could be more synaptically-engaged in disease state. I further report that the upregulation of genes, such as heat shock protein 90 alpha family class A member 1 (*HSP90AA1*) and *HSPA1A (*heat shock protein family A (Hsp70) member 1A), in both regions of ALS patients are present in most microglial subclusters, but most dominantly in the AM subcluster. These genes are responsible for regulating protein folding of specific target proteins, including TDP-43, while their overexpression can be involved in increased cellular stress (Lin et al., 2021). In combination with the enriched GO term 'unfolded protein response' in FC (but not in MC), I hypothesize that TDP-43 misfolding could occur in microglia, being the most transcriptionally affected cells type early in the disease. In addition, since AM express *CD83*, they can be engulfing nascent glia or neurons that are expressing misfolded TDP-43 early in the disease while eventually accumulating malfunctioning TDP-43. In theory, their increased heat shock protein expression could be a compensatory mechanism to prevent such TDP-43 accumulation. The AM has also increased hypoxia inducible factor 1 subunit alpha (*HIF1*) expression in FC of ALS patients, which is further enhanced in MC, indicative of an early increase of oxidative stress. Thus, I conclude that AM are possibly an early activated microglia subtype, involved in resolving the inflammation, yet their functions need to be explored further. These findings indicate that microglial activation and synapse remodeling could be preceding the pTDP-43 aggregation and appear early in the course of the disease. In line with my hypothesis, it has been shown that monocyte-derived microglia-like cells from sALS patients exhibit TDP-43 pathology and have abnormal phagocytosis patterns, which worsens as the disease progresses (Quek et al., 2022). Moreover, microglial activation prior to neuronal loss have been shown in mouse models of ALS, signifying the altered microglia state in early disease stages (Alexianu et al., 2001; Figueroa-Romero et al., 2019).

To validate early microglial reactivity, I performed immunostaining with an anti-HLA-DR+DP+DQ antibody on the sections obtained from the same cortical tissue used for snRNA-seq. Concordant with my snRNA-seq finding, I found that microglial activation, despite to a lower degree, was indeed present in FC already before pTDP-43 accumulation. Since I have not yet validated if any other pathological forms of TDP-43 (e.g., misfolding and/or cytoplasmically mislocalized TDP-43) are already present, I only conclude that pTDP-43 aggregate formation is downstream of microglial activation. As shown in previous studies,

TDP-43 could be a possible ligand to microglial TREM2 and serve a phagocytic, potentially neuroprotective, function in TDP-43 related neurodegeneration (Xie et al., 2022). In my data, I identified DAM2 type microglia (which I identified as early-stage enriched) that have detectable TREM2 expression only in MC. Although the nuclear expression of TREM2 is not a direct representation of its cellular protein expression, I found it surprising that only a small fraction of microglia showed TREM2 expression. This early-stage disease-engaged microglial subpopulation is already more abundant prior to pTDP-43 aggregation and seems to express TREM2 in MC where the TDP-43 pathology is worsened. I hypothesize that TREM2 expression in DAM2 is a late-stage event and potentially increasing TREM2-TDP-43 modulated phagocytic function of microglia. The presence of DAM2 microgliosis in FC but lack of TREM2 expression implicates that TREM2-TDP-43 interactions in microglia are likely not involved in early disease pathology.

5.3. Astrocytes

Another glial population, astrocytes, safeguards the delicate balance of inflammatory/supportive response to neuronal damage together with microglia. Astrocytes are the second most abundant cells after neurons within the CNS, covering a wide range of physiological functions. K^+ buffering, maintenance of blood brain barrier (BBB), providing neurotrophic support and neurotransmitter recycling are the few physiological functions of astrocytes. In ALS, these multifunctional cells lose their beneficial properties and become neurotoxic (Nagai et al., 2007; Liddelow et al., 2017; Guttenplan et al., 2021).

In my thesis, I identified 4 subclusters and analyzed their trajectories to identify their differentiation or activation process. Concordant with other studies, I observed a heterogeneous population of astrocytes with different gene expression patterns (Grubman et al., 2019; Pineda et al., 2024). Cluster 0 was enriched in markers such as sarcoglycan delta (*SGCD*) and WNT inhibitory factor (*WIF1*), whereas cluster 1 was assigned as a transition state due to its increased *GFAP* (and dipeptidyl peptidase I (*DPP1*) expression but the lack of reactive astrocytic markers such as tenascin (TNC) and versican (VCAN). CNS expression of SGCD is important for the formation of dystrophin-glycoprotein complex (DGC), in which dystrophin ensures stability and proper anchoring of ion channels and receptors, thus crucial for cellular function and calcium-mediated signaling of neurons and glia. Whereas, WIF1 is an inhibitor of Wnt-signaling pathway, a pathway known to be affected in ALS, and *WIF1* expressing astrocytes are reported to be only present in human but not in mice (Zhang et al., 2016c). My finding of enriched *WIF1* levels in cluster 0 indicates that this is non-reactive astrocyte population, whereas the high expression of *GFAP* in cluster 1 marks the differentiation and activation point of astrocytes and depicts the transition from non-reactive to reactive astrocytes. However, the lower expression of markers such as S100 calcium-binding

protein B (*S100B), VCAN* and *DPP1* compared to the clusters 2 and 3 indicate an early stage of activation and reactivity. I report clusters 2 and 3 to be reminiscent of disease associated astrocytes (DAA) shown in a mouse model of AD (Habib et al., 2020), with additional expression of genes *DPP1* and *VCAN* in my "DAA" clusters.

DPP1 encodes for dipeptidyl peptidase I (also known as cathepsin c), which is a lysosomal cysteine protease, crucial for triggering the activation of pro-inflammatory neutrophil serine proteases (NSPs). VCAN, on the other hand, is an extracellular proteoglycan, crucial for astrocytic functions, including cell adhesion, spreading, migration, proliferation, and differentiation. Increased *VCAN* expression is reported in chronic glial scars in the CNS (McKeon et al., 1999). In my data, I saw a significant reduction in the number of *VCAN* and *DPP1* expressing cluster 2 astrocytes, while an upward trend in other *VCAN* and *DPP1* expressing cluster 3 astrocytes was found. As depicted in the pseudotime analysis, an increase in non-reactive astrocytes in cluster 1 in MC can be a compensatory mechanism to replace cluster 2 astrocytes, which were recruited to differentiate further into a more reactive state, cluster 3. Cluster 3 astrocytes express tenascin (*TNC*), another extracellular matrix protein, which is also reported to be increased in glial scars, likely to have more healing properties in CNS insults, while promoting gliosis (Wiese et al., 2012). While I observed an increase in the number of reactive astrocytes (cluster 2) and a decrease in the transitional cluster (cluster 1) in MC, such changes in FC were not observed, pointing to astrogliosis to be a "late" disease modification.

Reversely, transcriptional changes were more pronounced in FC of ALS patients compared to HCs. I observed genes associated with reactive astrocytes to be upregulated (e.g., *CLU, NEAT1, AQP4, IRS2, FKBP5, GJA1, GFAP, CHI3L1)* already in FC, while their upregulation was less enhanced but present in MC. In addition to the known reactive astrocytic markers *GFAP,* FK506 binding protein 5 (*FKPB5*) and phagocytic glycoprotein-1 (*CD44*)*,* I saw that gap junction function was enhanced significantly early in the disease by elevated expression of *GJA1* (encoding for Cx43). Indeed, the elevated Cx43 expression is reported in iPSC-derived astrocytes obtained from ALS patients, and blocking Cx43 activity in $SOD1^{G93A}$ protects LMN degeneration and increases survival (Almad et al., 2022). Moreover, insulin receptor substrate 2 (*IRS2*), which is required for insulin/insulin-like growth factor (IGF)-1 receptor signaling to modulate glial cytokine secretion, is upregulated already in FC (Spielman et al., 2015).

As mentioned in section 1.2.2., ApoE secretion by astrocytes is reported to be upregulated and toxic to neurons (Guttenplan et al., 2021). Surprisingly, I saw an upregulation of ApoE in FC but not in MC, pointing to its secretion to be an early event in disease. Given that I only captured half as many astrocytes in MC compared to FC, it is also possible that certain effects are missed as they do not reach the significance cut-off. Another protein, chitinase-3-like-1

(*CHI3L1*), important for many inflammatory processes (e.g., inflammasome activation) as well as tissue repair and apoptosis is synthesized by activated astrocytes, and its expresion is significantly increased in both regions (Gaur et al., 2020). Regarding downregulated genes in ALS, I found monocyte to macrophage differentiation factor 2 (*MMD2*) in both FC and MC, which is shown to be a regulator of astrogliogenesis in development, yet its role in the aging brain is unknown (Kang et al., 2012). An interesting gene, cluster of differentiation 38 (*CD38*) also mostly expressed by the monocyte lineage, was downregulated in FC thus early in disease pathology. *CD38* is involved in Ca^{+2} signaling and it hydrolyzes extracellular ATP and NAD^{+} (Haag et al., 2007). Inhibition of *CD38* in a Duchenne muscular dystrophy (DMD) mouse model was shown to improve skeletal muscle function and slower disease progression (de Zélicourt et al., 2022). An *in vitro* study showed that glutamate release from neurons increases *CD38* expression in astrocytes, but the exact role of *CD38* in CNS is not well understood (Bruzzone et al., 2004).

Additionally, I found enriched GO terms linked to cellular compartments and processes associated with secretion and adhesion such as transport across BBB in FC and MC. Astrocytic processes are critical components of the BBB, an important barrier that prevents pathogens and other foreign substances from entering the CNS. In ALS, the BBB has been found to be disrupted, allowing an increased infiltration of immune cells and other substances that exacerbate neuroinflammation (Steinruecke et al., 2023). I thus reasoned that astrocytic dysfunction, compromising BBB integrity, might be an early event in ALS. On a similar note, signs of BBB impairment (e.g., pericyte degeneration) have been reported to be present in pre-symptomatic ALS patients (Winkler et al., 2013; Garbuzova-Davis and Sanberg, 2014), thus any impairments in astrocytic function could be part of this early mechanism and needs to be understood more in detail.

Moreover, I also identified other GO terms related to protein metabolism, prior to pTDP-43 aggregation, such as “response to unfolded protein”, “Hsp90 binding”. Thus, the unfolded protein response (UPR) in astrocytes, in response to TDP-43 dysfunction –but not to pTDP-43 accumulation- is an early pathophysiological event in ALS that could contributed to astrocytic activation and subsequent chemokine secretion, as implicated in AD (Licht-Murava et al., 2023).

5.4. Oligodendrocytes & OPCs

Oligodendrocytes and OPCs play critical roles in the development, maintenance, and function of the CNS. OPCs are a precursor cell type that gives rise to mature oligodendrocytes. In the human cortex, OPCs are abundant during development and persist into adulthood, and are characterized by their capacity for proliferation and differentiation into mature oligodendrocytes

in response to environmental cues. Oligodendrocytes are responsible for myelination and transfer of energy metabolites such as lactate to neurons.

In my data, I identified an OPC cluster and 4 oligodendrocyte clusters, where I saw no significant changes in their abundance in ALS patients when compared to HCs. Yet, I observed an upward trend in the number of OPCs in FC cortex of ALS patients in comparison to HCs. This could be due to a maturation deficit in OPCs, which is a finding previously reported in ALS mouse models (Kang et al., 2013). While oligodendrocyte and OPC involvement is known in ALS, their exact contribution is not yet clear (Raffaele et al., 2021). Recently, disease associated oligodendrocytes are reported in AD and multiple sclerosis (MS) in mouse models and in post-mortem human samples (Kenigsbuch et al., 2022; Pandey et al., 2022). Specifically, increased *C4b* and *Serpina3n* (human homolog of *SERPINA3*) expression of an oligodendrocyte subcluster were present in multiple mouse models (of AD and MS) presented in the study, yet these markers were not present in human samples (Pandey et al., 2022). While I identified similar subclusters with markers indicated in the previous studies, that is OL1 (*OPALIN*, *ROR1*), OL2 (*RBFOX1*), OL3 (*OPALIN*, *FRY*) and OL4 (*FTH1*, *TXNRD1*), the lack of characterization of oligodendrocyte populations in humans are posing a challenge.

I report upregulation of genes such as *FKBP5* and LDL Receptor Related Protein 2 (*LRP2*) in oligodendrocytes and OPCs that are potentially proinflammatory. LRP2 is a lipid receptor that plays a crucial role in endocytosis of ligands such as ApoE (Spuch et al., 2012). While I only detected an increased astrocytic ApoE expression in FC, I can infer that a potential increase of ApoE endocytosis by oligodendrocytes/OPCs could be a reason for elevated *LRP2* expression present in ALS.

Moreover, I saw an upregulation of Piezo type mechanosensitive ion channel component 2 (*PIEZO2*) in both regions in oligodendrocytes. The role of *PIEZO2* in the CNS is not well understood (Zong et al., 2023), yet as it facilitates migration of oligodendrocytes, together with the presence of GO terms related to the modulation of synaptic transmission, I interpret this finding as an enhanced oligodendrocyte-neuron contact early in the disease. As reported in another snRNA-seq study of the motor cortex of post-mortem ALS patients (Limone et al., 2023), a switch to neuron-supportive function in oligodendrocytes could be an early change in ALS.

5.5. Excitatory neurons

The vulnerable Betz cells (or UMN) in ALS only compose ~10% of all pyramidal neurons in layer Vb of the human primary motor cortex (Rivara et al., 2003). It is however conceivable that other glutamatergic cortical neurons are affected in ALS, too (Limone et al., 2023; Pineda et al., 2024). I identified 13 subclusters of excitatory neurons involving a small cluster

representing UMN (FEZF2-4), which was strongly reduced in ALS in accordance with the initial diagnosis. Surprisingly, I found that a population of excitatory neurons, characterized by the expression of LINC00507-2, composing 30% of all glutamatergic neurons in my dataset, are also likely vulnerable to ALS. More than 1/3 of this population seems to be lost in ALS patients in MC. In addition, I saw a reduction of RORB-1 expressing neurons in FC while this effect is not present in MC. The LINC00507-2 cluster also expresses the upper cortical layer marker, *CUX2*, whereas RORB-1 neurons express *FOXP2*, a cortical layer 6 marker (Kast et al., 2019; Miškić et al., 2021). My data thus points to a vulnerable layer 6 neuronal subcluster (RORB-1) that is affected selectively in FC, where this cluster is also more abundant than in MC HC. Moreover, other layer 5-6 clusters, namely FEZF2-1 and FEZF2-2, (characterized by *FEZF2* expression) are significantly different between FC and MC in ALS, which is likely due to the small fraction of neurons and sample variability. Thus, I conclude that excitatory neurons expressing LINC00507-2 (likely found in cortical layer 2/3 in MC) and neurons expressing RORB-1 (likely residing in layer 6 of FC) are 2 novel vulnerable neuronal subtypes in ALS. While the exact cell identity, location and synaptic connectivity of these subtypes are yet to be elucidated, loss of upper layer neurons (i.e., cluster LINC00507-2) which might provide synaptic input to UMNs could adversely affect UMN function.

In addition, excitatory neurons in FC had upregulation of genes such as sorting nexin 31 (*SNX31)*, prion protein (*PRNP),* synapsin III *(SYN3)* and kinesin family member 13A *(KIF13A),* while in MC I had more upregulated DEGs related to synaptic function syntrophin gamma 1 *(SNTG1), SYN3 and CCND3*. In both regions, I detected a significant upregulation of *SNX31*, which to my knowledge has not been reported to have differential expression in ALS. SNX31, although not studied in detail, has a function in the formation of early endosomes in a phosphatidylinositide 3 (PI3)-kinase-dependent manner, trafficking integrin to lysosomes for degradation (Tseng et al., 2014). Another endosome-related gene upregulated early in ALS is KIF13A, which ensures endosomal function by determining the positioning of the endosome in the cell. Supporting the notion of early changes in endosomal function, defects in endosomal trafficking in dendrites were reported pre-symptomatically in TDP-43^{M337V} tg mice (Sleigh et al., 2020). Hypothetically, early *SNX31* upregulation could be modulated by TDP-43, to decrease the availability of lysosomes and further induce its toxicity (Leibiger et al., 2018). Moreover, I saw an upregulation of *PRNP* in FC in ALS patients, but not in MC. Interestingly, *PRNP* is reported to be a disease onset modifier in C9ORF72 HRE carriers, however its exact role in ALS is not clear (van Blitterswijk et al., 2014). Lastly, I report an early alteration in cell-cell adhesion and modifications of synaptic connections in FC (due to increased SYN3 expression), shown by the most enriched GO terms. Moreover, terms related to glutamatergic signaling are surprisingly more strongly enriched in FC, which indicates altered glutamatergic

signaling in excitatory neurons, likely affecting the neuronal excitability and/or activity is an early mechanism in ALS patients.

5.6. Interneurons

Comprising 20-30% of all neocortical neurons, GABAergic interneurons are vital for maintaining E/I balance in the cortex and ensuring proper functioning of neural circuits in the brain. Cortical interneurons fine tune pUMNs activity as well as other excitatory neurons across cortical layers. Moreover, subtypes of INs are responsible for regulating each other's inhibition. This delicate equilibrium between excitatory and inhibitory signals is crucial for ensuring the precision and reliability of information processing. Since early cortical hyperexcitability is observed in ALS patients (Vucic et al., 2008; Vucic et al., 2021), it is hypothesized that interneurons could be affected and lead to dysregulation of network activity. As summarized in section 1.2.2., decreased cortical layer 5 GABAergic neuron density in post-mortem ALS patients is present at the end stage (Maekawa et al., 2004), while contradicting findings on change of PV-INs abundance in mouse models of ALS was reported (Özdinler et al., 2011; Clark et al., 2017). In this work, I looked into changes in interneurons in FC of ALS patients both in terms of their abundance and transcriptomic alterations.

Strikingly, I saw a significant loss of SST-INs (cluster SOM-1) in FC of ALS patients in comparison to HC. Followed by a similar trend in MC, yet it was not statistically significant. Considering these findings, SST-INs seemingly are affected early in the disease and could drive changes in PV (and other populations), which they have been shown to inhibit. Since hyperactivity of SST-INs has been shown early in the disease in the TDP-43^{A315T} tg model of ALS/FTD (Zhang et al., 2016a), this hyperactivity of SST-INs could be a compensatory mechanism in response to an early loss of SST-INs corresponding to our SOM-1 cluster in mice, which needs to be further assessed. The PV-1 subcluster of PV-INs seems to have a reduced number in FC of ALS when compared to HCs (not significant), yet I observed an increase of these neurons in MC of ALS in contrast to FC. As neurons in cortex are post-mitotic, this increase could be due to sampling bias (discussed in section 5.9). Nevertheless, the significant loss of SST-INs together with a possible increase of PV-1 later in the disease (ALS MC) implicate the SST-PV IN GABAergic signaling might be affected in the disease early on. The loss of SST inhibition could be a component of the reported early cortical hyperexcitability in ALS (Vucic et al., 2008; Van den Bos et al., 2018), which can be exacerbated in MC. Conversely, PV-INs lacking enough inhibition provided by SST-INs in FC, could dampen UMN signaling simultaneously. Since the connectivity of UMNs is complex, the subtype specific modulation of UMN activity and early-on affected interneuron subtypes need to be studied in more detail.

Interestingly, other subtypes of INs affected in ALS were more restricted to MC. I saw that the VIP-2 subcluster was decreased in MC of ALS patients. A decrease in VIP-INs inhibition could be an additional source of cortical hyperexcitability in MC. Furthermore, I report a reduction of CR and CCK interneurons in the late disease stage. LAMP5-INs connectivity is not clear in the human cortex, yet in AD frontal cortex samples synaptic LAMP5 expression was reduced and these neurons degenerated in mouse model of AD (Deng et al., 2022). In multiple mouse models of AD (either with Aβ or tau pathology), genetic reduction of LAMP5 expression in the cortex was tied to increased neural network excitation (Deng et al., 2022). Interestingly, I saw a potentially resistant subcluster of interneurons, which I named LAMP5-3. This subcluster corresponds to the recently identified layer 1 Rosehip neurons, which are not present in mouse cortex and are likely exclusively present in primates (Boldog et al., 2018).The role of a human-specific subcluster in ALS pathology thus requires further research, its role in human cortical hyperexcitability and thus of the neurodegenerative process is.

When I checked transcriptional changes in all INs, I observed that genes similar to excitatory neurons (such as *KDM5D, SNX31, HSP90AA1* and *SYN3)* were upregulated in both regions of ALS patients compared to HCs, whereas I saw a downregulation of *SST* and 26S proteasome subunit (*SEM1*). In addition, I report a downregulation of AC090579.1, AL008633.1, AC244131.2 and an upregulation of AL592183.1, AP001347.1, all of which are non-coding RNAs (ncRNAs), whose function in the CNS is not known. I also found a consistent downregulation of a transcriptional regulator Lysine Demethylase 5B (*KDM5D*) in both regions. Since ncRNAs regulate gene transcription in a broader context, I interpret that transcription of INs are affected early in the disease and likely affects SST-INs (SOM-1 cluster) more than others, making these neurons more vulnerable in ALS. When I look at the GO terms enriched in FC prior to MC of ALS patients, I see an enhancement of synaptic terms such as “positive regulation of synapse assembly” and “glutamate receptor signaling pathway”. Together with the loss of SST-INs and transcriptomic changes indicating the synaptic change (or remodeling) my data indicate INs are involved in early ALS pathology and their role needs to be studied in more detail.

5.7. Cell-Cell Interaction Analysis Reveals Altered Communication Patterns in ALS

My main observation in the cell-cell communication analysis was a clear alteration in microglia related interactions early in the disease. To this end, I assessed which Ligand-Receptor (L-R) pairs involving microglial interactions were expressed differently in ALS patients. Specifically, I found a reduction in MRC1-PTPRC signaling amongst microglia in MC when compared to FC in ALS. Mannose receptor 1 (MRC1) and protein tyrosine phosphatase receptor type C

(PTPRC) are both known to be involved in microglia activation and regulate the phagocytic activity of microglia (von Ehr et al., 2020; Al Barashdi et al., 2021). The reduction of this L-R pair within microglia points to an early disruption of microglial phagocytosis and possibly can cause a lack of pro-resolving type of microglia. Similarly, there was an increase in the expression of the microglia-microglia L-R pair C1QA-CD33 in ALS MC compared to ALS FC. Complement component C1q (C1QA) is a vital regulator of the inflammatory response initiated by microglia. CD33, on the other hand, is a receptor on microglia, which inhibits microglial phagocytosis. The upregulation of C1QA-CD33 signaling indicates compromised phagocytosis in the late stage, which is not yet severely affected early in the disease. The reduction of these L-R pairs in microglial communication indicates microglial communication and activation states are altered prior to any pTDP-43 pathology and could drive disease progression.

Extending my investigation to interactions with other cell types, a significant upregulation of microglia-astrocyte L-R pair LGALS9-CD44 was evident in both ALS FC and MC, while it was not present in HCs. Galectin 9 (LGALS9) is an immunoregulator molecule expressed on activated microglia and it was shown to promote proinflammatory responses when there is an insult to the CNS (Chen et al., 2019). The role of Galectin 9 is not clear in neurodegeneration, yet in PD it was shown to contribute to inflammation causal to dopaminergic neuron degeneration (Peng et al., 2022). On the other hand, CD44 is associated with an astrocyte-mediated inflammatory response and its expression is elevated in a subtype of astrocytes, namely astrocyte-restricted precursor cells (ARP), which are found to be promoting astrogliosis in both rodent and human tissue (Liu et al., 2004). Yet the exact mechanism of signaling between microglial LGALS9 and CD44 expressed on astrocytes is not clear, since I have shown microglial activation in early disease, I interpret enhanced signaling of this L-R pair to be promoting astrocytic activation. As I also observed a reduction of astrocyte cluster 2 (likely reactive) and increase in more homeostatic astrocyte cluster (cluster 1), I interpret LGALS9-CD44 pair to be promoting astrogliosis of cluster 1 and perhaps compensate for the decreased availability of cluster 2 astrocytes. As the subcluster abundance changes I reported are observed at MC of ALS patients, I can interpret the altered microglia-astrocyte communication in ALS to be an earlier component prior to the altered composition of astrocytic populations in the late disease stage.

Regarding the communication between microglia and oligodendrocytes, I found that the APOC2-LRP2 L-R pair expression was increased early in the disease in FC and continued to stay elevated in MC compared to HCs. Apolipoprotein C2 (APOC2) is one of many apolipoproteins that bind to low density lipoprotein receptor 2 (LRP2), whose activation results in endocytosis of APOC2 (Bruce et al., 2018; K et al., 2020). Expressed in mature oligodendrocytes, LRP2 (also called megalin) was shown to be involved in the formation and/or

maintenance of myelin on axons. The increased communication between microglial APOC2 and oligodendrocyte LRP2 implies that microglia could sense damage in axons of vulnerable neurons (e.g., UMNs) and could signal oligodendrocytes to increase their myelination. On the other hand, it could also be a compensatory mechanism as I saw an increase (albeit not significant) number of OPCs in the FC of ALS patients in comparison to HCs. As mentioned earlier, maturation problems of OPCs are mentioned in context of ALS. My observation of elevated OPC number in early stages of ALS combined with increased LRP2 activation on mature oligodendrocytes together indicate an early attempt to recover myelination related impairments.

In conclusion, this study unveils alterations in the cell-cell interactions involving microglia in ALS. I report that microglia-microglia and microglia-oligodendrocyte/astrocyte communication are to be altered prior to pTDP-43 aggregation. Further investigations of the identified ligand-receptor pairs between different cell types could contribute to a deeper understanding of the complex network underlying ALS pathophysiology.

5.8. Differences in disease trajectory of sALS and fALS

As mentioned above, one of the biggest challenges for understanding ALS pathophysiology comes from the vast disease complexity and heterogeneity of the patients. In my project, I have included sALS and fALS patients, between which I detected differences in my analysis. As a result of the PCA analysis, I found that the early transcriptomic changes in glial cells, and most importantly in microglia, are similar in both sALS and fALS cases. I concluded that microglial activation is present to a similar extent in FC, in the absence of TDP-43 pathology in all cases. Most strikingly, upon pTDP-43 pathology occurrence, these two subtypes of ALS patients differ in their transcriptome of all cell types and again most prominently in the microglia. To understand what might be setting fALS patients so apart from both sALS patients and HCs, I checked the presence of DPRs, which is a pathological hallmark of *C9ORF72* mutation carriers. As the most abundant DPR, I have detected poly-GA inclusions in FC and MC as expected, and their abundance did not differ between these regions. However, I have interestingly found that the TDP-43 aggregate load was correlating with the poly-GA load in MC where both pathologies are present. Comorbidity and putative interactions between DPRs and TDP-43 have been investigated before. To summarize, it has been shown that certain DPRs (i.e., poly-GA and poly-GR) can trigger TDP-43 pathology in mouse, drosophila and in vitro models by interfering with the nuclear import of TDP-43 (Chew et al., 2015; Khosravi et al., 2017; Nonaka et al., 2018; Solomon et al., 2018). I, therefore, hypothesize that poly-GA inclusions in MC could exacerbate the TDP-43 pathology and could lead to additional glial reactivity- which is most prominently seen in the altered transcriptome of microglia, followed by oligodendrocytes, astrocytes and OPCs. Although transcriptionally less striking than glial

cells, I also observe neuronal cells (excitatory and inhibitory) to be transcriptionally altered most in MC and specifically in fALS patients. In my thesis, I did not have the chance to investigate the “likely” DPR-induced changes specific to fALS patients and how/if DPR pathology could be involved in pre-TDP-43 pathology stage in ALS. Yet, I conclude that poly-GA-TDP-43 interactions in MC could be one of the key reasons why two ALS subtypes have different disease trajectories, and thus should be further studied.

5.9. Limitations of the study

SnRNA-seq of post-mortem human samples presents several challenges that impact the interpretation and reliability of transcriptomic data. Firstly, the quality of RNA extracted from post-mortem tissues is a significant concern. The post-mortem interval and conditions of tissue preservation can lead to RNA degradation, potentially introducing biases in the analysis and compromising the detection of low-abundance transcripts. The inherent cellular heterogeneity of post-mortem human samples poses a limitation to the resolution of snRNA-seq in particular for less abundant cell types. Variability in cell type composition among individuals potentially caused by slight variations in tissue sampling (e.g. alterations in the captured cortical layers) and tissues may obscure specific cell populations, complicating the identification of meaningful biological signals. Additionally, suboptimal nucleus isolation efficiency may introduce biases. For example, it is more difficult to isolate nuclei from more complex cells with extensive processes than cells with less complexity, which could affect the representation of certain cell types and influence the overall cellular resolution achievable with snRNA-seq.

The temporal dynamics of gene expression pose another limitation. Post-mortem samples capture a static snapshot of the transcriptome at the time of tissue collection, lacking the ability to capture dynamic changes over time. In addition, adult human brain is less dynamic than that of a developing brain, for which the pseudotime trajectory analysis tools are often developed. This limitation is particularly relevant for understanding processes with temporal dynamics such as glial activation, and requires comprehensive analysis and validation of findings in a model (e.g., iPSC models).

Integration of data from multiple post-mortem samples is complex due to inter-sample variability. Differences in post-mortem conditions, genetic backgrounds, and individual-specific factors can hinder achieving high reproducibility and reliability in cross-sample comparisons. In my study, I have a median age difference between sporadic and familial ALS due to onset age which introduces complexity. Since fALS patients develop and reach end stage at a much younger age, transcriptional changes related to aging might not be captured and hence could explain one aspect of data heterogeneity. Moreover, due to the scarcity of human specimens which do not have pTDP-43 pathology in FC, my dataset is relatively small and matching sex

between groups was difficult. Combined, these conditions contributed additional layers of complexity in my work.

In addition to technical difficulties and sample variability, my nuclei data possess profound information about ncRNAs. In all cell types analyzed in this thesis, I came across numerous ncRNAs as DEGs. Unfortunately, unlike protein-coding genes with well-defined roles, deciphering the functions of various ncRNAs remains a puzzle. The majority of ncRNAs function in human CNS are not known. Moreover, one of the foremost challenges in working with ncRNAs is their often-low abundance within cells. Traditional sequencing methods, optimized for protein-coding transcripts, may lack the sensitivity to capture these less prevalent molecules, further hindering my interpretation of these regulatory elements function in gene expression.

Another concern with interpreting human data is related to how a ‘healthy control’ defined. In my study, HCs are defined as neurologically healthy people at the time of death, yet detailed information on underlying health conditions is not available. Moreover, transcriptomic changes between the regions in HCs were detected in my study which signifies that other factors (e.g., aging) needs to be accounted for while interpreting data.

In summary, I address limitations in this thesis work while appreciating the abundance of information and high resolution in my data. SnRNA-seq technology is at the forefront of contemporary transcriptomics, offering unprecedented insights into cell specific alterations. I believe snRNA-seq of human specimens will create space for many discoveries in the pursuit of finding a cure for ALS and other disorders.

6. Concluding Remarks

In this thesis work, I highlighted many alterations in FC prior to pTDP-43 pathology in ALS brain samples. To summarize the main findings in my thesis, in early stages of ALS, I report a decreased number of homeostatic microglia with an increased abundance of disease-associated microglia, which is confirmed by immunohistological analyses. Moreover, I detected a subtype of layer 2/3 excitatory neuron subtype (LINC02306+ and LINC02055+) that is likely vulnerable to degeneration in ALS. In my ongoing work, I will validate my findings with RNAscope and IHC applications. I further plan to involve more samples in my dataset and include ALS/FTD patients that present pTDP-43 accumulation in FC, to address the time course of the events with respect to the appearance of pTDP-43 pathology. I have found that mechanisms regulating proteostasis, synaptic function neuronal signaling and cell-cell signaling are affected early in the disease prior to TDP-43 pathology and increasingly altered as the disease progresses (**Figure 31**). To confirm my findings, I will compare my data with publicly available datasets to address if the changes I report are present at a greater scale.

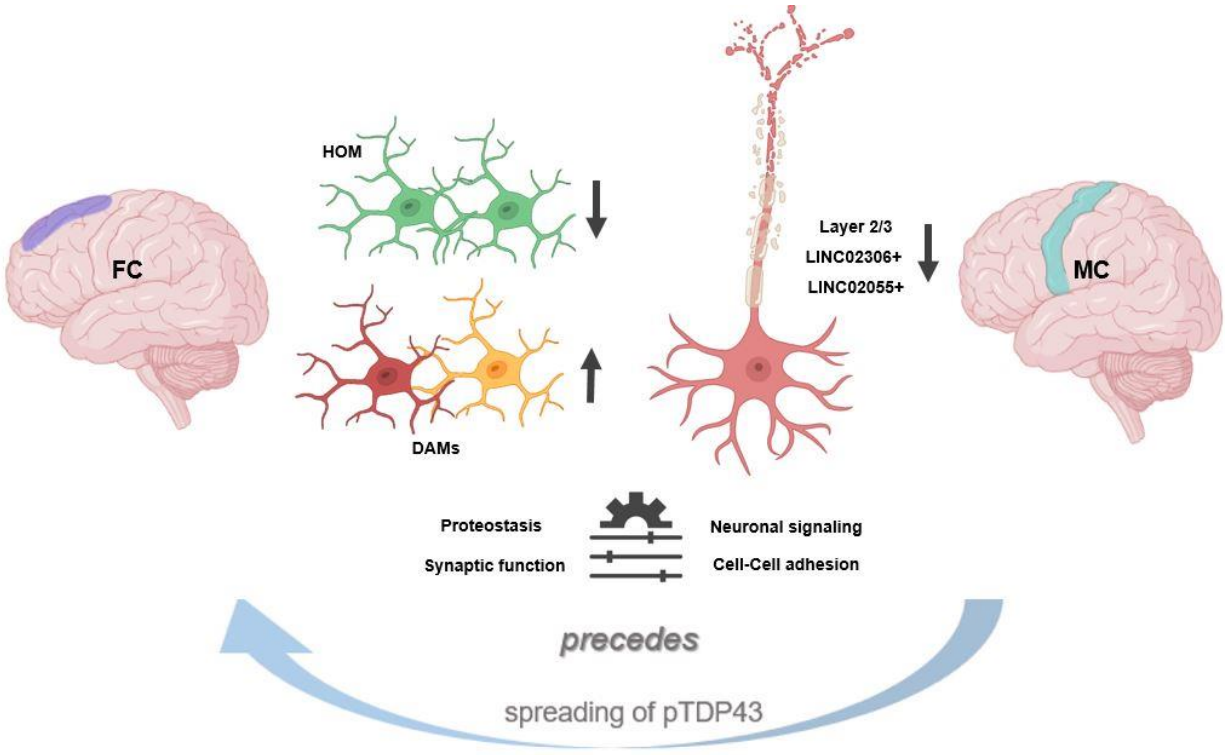

Figure 31. Summary of main findings.

Microglial activation and neuronal dysfunction are early key mechanisms in ALS and are present prior to pTDP-43 pathology. Created with Biorender.com.

My thesis work opens new avenues for research. Characterization of subclusters for each cell type in the human cortex is possibly the first step to uncover their transcriptomic changes. One question that remains open in my study is whether CEs are present early in the disease. As the sequencing depth for the detection of CEs needs to be much greater than what is required for snRNA-seq, I did not have the chance to address this question. Yet, I have not detected changes in neuronal *STMN2* and *UNC13A* expression in ALS patients in both regions (data not shown), indicating normal transcriptional levels in the nucleus of these genes early in the disease. Hence, it is necessary to address the presence and function of CEs in further studies that are designed for the detection of splice variants.

Moreover, I noted differences in the transcriptomic makeup of sporadic and familial ALS patients. I believe ALS subtype specific transcriptional changes could be a key player determining rate of disease progression in patients.

In conclusion, this thesis work adds to my understanding of cortical disease trajectory in ALS, while creating many questions to be answered with further research. Identifying early changes in ALS could lead to discovery of transcriptomic changes that can be corrected (e.g., via gene therapy) and potentially present a cure to this debilitating disease.

Bibliography

Abe, K., Aoki, M., Tsuji, S., Itoyama, Y., Sobue, G., Togo, M., et al. (2017). Safety and efficacy of edaravone in well defined patients with amyotrophic lateral sclerosis: a randomised, double-blind, placebo-controlled trial. *The Lancet Neurology* 16(7)**,** 505-512.

Abrahams, S., Goldstein, L.H., Suckling, J., Ng, V., Simmons, A., Chitnis, X., et al. (2005). Frontotemporal white matter changesin amyotrophic lateral sclerosis. *Journal of Neurology* 252(3)**,** 321-331. doi: 10.1007/s00415-005-0646-x.

Afroz, T., Hock, E.-M., Ernst, P., Foglieni, C., Jambeau, M., Gilhespy, L.A.B., et al. (2017). Functional and dynamic polymerization of the ALS-linked protein TDP-43 antagonizes its pathologic aggregation. *Nature Communications* 8(1)**,** 45. doi: 10.1038/s41467-017-00062-0.

Agosta, F., Valsasina, P., Riva, N., Copetti, M., Messina, M.J., Prelle, A., et al. (2012). The cortical signature of amyotrophic lateral sclerosis. *PLoS One* 7(8)**,** e42816. doi: 10.1371/journal.pone.0042816.

Ajami, B., Samusik, N., Wieghofer, P., Ho, P.P., Crotti, A., Bjornson, Z., et al. (2018). Single-cell mass cytometry reveals distinct populations of brain myeloid cells in mouse neuroinflammation and neurodegeneration models. *Nat Neurosci* 21(4)**,** 541-551. doi: 10.1038/s41593-018-0100-x.

Al Barashdi, M.A., Ali, A., McMullin, M.F., and Mills, K. (2021). Protein tyrosine phosphatase receptor type C (PTPRC or CD45). *J Clin Pathol* 74(9)**,** 548-552. doi: 10.1136/jclinpath-2020-206927.

Alami, N.H., Smith, R.B., Carrasco, M.A., Williams, L.A., Winborn, C.S., Han, S.S.W., et al. (2014). Axonal transport of TDP-43 mRNA granules is impaired by ALS-causing mutations. *Neuron* 81(3)**,** 536-543. doi: 10.1016/j.neuron.2013.12.018.

Alexianu, M.E., Kozovska, M., and Appel, S.H. (2001). Immune reactivity in a mouse model of familial ALS correlates with disease progression. (0028-3878 (Print)).

Almad, A.A., Taga, A., Joseph, J., Gross, S.K., Welsh, C., Patankar, A., et al. (2022). Cx43 hemichannels contribute to astrocyte-mediated toxicity in sporadic and familial ALS. *Proceedings of the National Academy of Sciences* 119(13)**,** e2107391119. doi: 10.1073/pnas.2107391119.

Alshikho, M.J., Zürcher, N.R., Loggia, M.L., Cernasov, P., Reynolds, B., Pijanowski, O., et al. (2018). Integrated magnetic resonance imaging and [(11) C]-PBR28 positron emission tomographic imaging in amyotrophic lateral sclerosis. *Ann Neurol* 83(6)**,** 1186-1197. doi: 10.1002/ana.25251.

Alves, C.J., Dariolli, R., Jorge, F.M., Monteiro, M.R., Maximino, J.R., Martins, R.S., et al. (2015). Gene expression profiling for human iPS-derived motor neurons from sporadic ALS patients reveals a strong association between mitochondrial functions and neurodegeneration. *Front Cell Neurosci* 9**,** 289. doi: 10.3389/fncel.2015.00289.

Andrews, J.A., Jackson, C.E., Heiman-Patterson, T.D., Bettica, P., Brooks, B.R., and Pioro, E.P. (2020). Real-world evidence of riluzole effectiveness in treating amyotrophic lateral sclerosis. *Amyotrophic Lateral Sclerosis and Frontotemporal Degeneration* 21(7-8)**,** 509-518.

Arai, T., Hasegawa, M., Akiyama, H., Ikeda, K., Nonaka, T., Mori, H., et al. (2006). TDP-43 is a component of ubiquitin-positive tau-negative inclusions in frontotemporal lobar degeneration and amyotrophic lateral sclerosis. *Biochemical and biophysical research communications* 351(3)**,** 602-611.

Ash, P.E., Bieniek, K.F., Gendron, T.F., Caulfield, T., Lin, W.L., Dejesus-Hernandez, M., et al. (2013). Unconventional translation of C9ORF72 GGGGCC expansion generates

insoluble polypeptides specific to c9FTD/ALS. *Neuron* 77(4)**,** 639-646. doi: 10.1016/j.neuron.2013.02.004.

Ayala, Y.M., De Conti, L., Avendaño-Vázquez, S.E., Dhir, A., Romano, M., D'Ambrogio, A., et al. (2011). TDP-43 regulates its mRNA levels through a negative feedback loop. *Embo j* 30(2)**,** 277-288. doi: 10.1038/emboj.2010.310.

Ayala, Y.M., Pantano, S., D'Ambrogio, A., Buratti, E., Brindisi, A., Marchetti, C., et al. (2005). Human, Drosophila, and C.elegans TDP43: nucleic acid binding properties and splicing regulatory function. *J Mol Biol* 348(3)**,** 575-588. doi: 10.1016/j.jmb.2005.02.038.

Badimon, A., Strasburger, H.J., Ayata, P., Chen, X., Nair, A., Ikegami, A., et al. (2020). Negative feedback control of neuronal activity by microglia. *Nature* 586(7829)**,** 417-423. doi: 10.1038/s41586-020-2777-8.

Bankhead, P., Loughrey, M.B., Fernández, J.A., Dombrowski, Y., McArt, D.G., Dunne, P.D., et al. (2017). QuPath: Open source software for digital pathology image analysis. *Sci Rep* 7(1)**,** 16878. doi: 10.1038/s41598-017-17204-5.

Barber, S.C., and Shaw, P.J. (2010). Oxidative stress in ALS: Key role in motor neuron injury and therapeutic target. *Free Radical Biology and Medicine* 48(5)**,** 629-641. doi: https://doi.org/10.1016/j.freeradbiomed.2009.11.018.

Barker, H.V., Niblock, M., Lee, Y.-B., Shaw, C.E., and Gallo, J.-M. (2017). RNA misprocessing in C9orf72-linked neurodegeneration. *Frontiers in cellular neuroscience* 11**,** 195.

Barmada, S.J., Skibinski, G., Korb, E., Rao, E.J., Wu, J.Y., and Finkbeiner, S. (2010). Cytoplasmic mislocalization of TDP-43 is toxic to neurons and enhanced by a mutation associated with familial amyotrophic lateral sclerosis. *J Neurosci* 30(2)**,** 639-649. doi: 10.1523/jneurosci.4988-09.2010.

Bartos, M., and Elgueta, C. (2012). Functional characteristics of parvalbumin- and cholecystokinin-expressing basket cells. *The Journal of physiology* 590(4)**,** 669-681. doi: 10.1113/jphysiol.2011.226175.

Benjaminsen, E., Alstadhaug, K.B., Gulsvik, M., Baloch, F.K., and Odeh, F. (2018). Amyotrophic lateral sclerosis in Nordland county, Norway, 2000–2015: Prevalence, incidence, and clinical features. *Amyotrophic Lateral Sclerosis and Frontotemporal Degeneration* 19(7-8)**,** 522-527.

Bensimon, G., Lacomblez, L., and Meininger, V. (1994). A Controlled Trial of Riluzole in Amyotrophic Lateral Sclerosis. *New England Journal of Medicine* 330(9)**,** 585-591. doi: 10.1056/NEJM199403033300901.

Benson, B.C., Shaw, P.J., Azzouz, M., Highley, J.R., and Hautbergue, G.M. (2021). Proteinopathies as Hallmarks of Impaired Gene Expression, Proteostasis and Mitochondrial Function in Amyotrophic Lateral Sclerosis. *Frontiers in Neuroscience* 15(1738). doi: 10.3389/fnins.2021.783624.

Bi, F., Huang, C., Tong, J., Qiu, G., Huang, B., Wu, Q., et al. (2013). Reactive astrocytes secrete lcn2 to promote neuron death. *Proc Natl Acad Sci U S A* 110(10)**,** 4069-4074. doi: 10.1073/pnas.1218497110.

Bilican, B., Serio, A., Barmada, S.J., Nishimura, A.L., Sullivan, G.J., Carrasco, M., et al. (2012). Mutant induced pluripotent stem cell lines recapitulate aspects of TDP-43 proteinopathies and reveal cell-specific vulnerability. *Proc Natl Acad Sci U S A* 109(15)**,** 5803-5808. doi: 10.1073/pnas.1202922109.

Bilsland, L.G., Sahai, E., Kelly, G., Golding, M., Greensmith, L., and Schiavo, G. (2010). Deficits in axonal transport precede ALS symptoms in vivo. *Proceedings of the National Academy of Sciences* 107(47)**,** 20523-20528. doi: 10.1073/pnas.1006869107.

Birger, A., Ben-Dor, I., Ottolenghi, M., Turetsky, T., Gil, Y., Sweetat, S., et al. (2019). Human iPSC-derived astrocytes from ALS patients with mutated C9ORF72 show increased oxidative stress and neurotoxicity. *EBioMedicine* 50**,** 274-289. doi: https://doi.org/10.1016/j.ebiom.2019.11.026.

Blair, L.J., Nordhues, B.A., Hill, S.E., Scaglione, K.M., O'Leary, J.C., 3rd, Fontaine, S.N., et al. (2013). Accelerated neurodegeneration through chaperone-mediated oligomerization of tau. *J Clin Invest* 123(10)**,** 4158-4169. doi: 10.1172/jci69003.

Boillée, S., Vande Velde, C., and Cleveland, D.W. (2006a). ALS: A disease of motor neurons and their nonneuronal neighbors. *Neuron* 52(1)**,** 39–59. doi: 10.1016/j.neuron.2006.09.018.

Boillée, S., Yamanaka, K., Lobsiger, C.S., Copeland, N.G., Jenkins, N.A., Kassiotis, G., et al. (2006b). Onset and Progression in Inherited ALS Determined by Motor Neurons and Microglia. *Science* 312(5778)**,** 1389-1392. doi: 10.1126/science.1123511.

Boldog, E., Bakken, T.E., Hodge, R.D., Novotny, M., Aevermann, B.D., Baka, J., et al. (2018). Transcriptomic and morphophysiological evidence for a specialized human cortical GABAergic cell type. *Nat Neurosci* 21(9)**,** 1185-1195. doi: 10.1038/s41593-018-0205-2.

Bonfanti, E., Bonifacino, T., Raffaele, S., Milanese, M., Morgante, E., Bonanno, G., et al. 2020. Abnormal Upregulation of GPR17 Receptor Contributes to Oligodendrocyte Dysfunction in SOD1 G93A Mice. *International Journal of Molecular Sciences* [Online], 21(7).

Borasio, G., Linke, R., Schwarz, J., Schlamp, V., Abel, A., Mozley, P., et al. (1998). Dopaminergic deficit in amyotrophic lateral sclerosis assessed with [I-123] IPT single photon emission computed tomography. *Journal of Neurology, Neurosurgery & Psychiatry* 65(2)**,** 263-265.

Braak, H., and Braak, E. (1991). Neuropathological stageing of Alzheimer-related changes. *Acta Neuropathologica* 82(4)**,** 239-259. doi: 10.1007/BF00308809.

Braak, H., Brettschneider, J., Ludolph, A.C., Lee, V.M., Trojanowski, J.Q., and Del Tredici, K. (2013). Amyotrophic lateral sclerosis--a model of corticofugal axonal spread. *Nat Rev Neurol* 9(12)**,** 708-714. doi: 10.1038/nrneurol.2013.221.

Brady, O.A., Meng, P., Zheng, Y., Mao, Y., and Hu, F. (2011). Regulation of TDP-43 aggregation by phosphorylation and p62/SQSTM1. *J Neurochem* 116(2)**,** 248-259. doi: 10.1111/j.1471-4159.2010.07098.x.

Brown, R.H., and Al-Chalabi, A. (2017). Amyotrophic Lateral Sclerosis. *New England Journal of Medicine* 377(2)**,** 162-172. doi: 10.1056/NEJMra1603471.

Bruce, K.D., Gorkhali, S., Given, K., Coates, A.M., Boyle, K.E., Macklin, W.B., et al. (2018). Lipoprotein Lipase Is a Feature of Alternatively-Activated Microglia and May Facilitate Lipid Uptake in the CNS During Demyelination. *Front Mol Neurosci* 11**,** 57. doi: 10.3389/fnmol.2018.00057.

Bruzzone, S., Verderio, C., Schenk, U., Fedele, E., Zocchi, E., Matteoli, M., et al. (2004). Glutamate-mediated overexpression of CD38 in astrocytes cultured with neurones. *J Neurochem* 89(1)**,** 264-272. doi: 10.1111/j.1471-4159.2003.02326.x.

Buratti, E., and Baralle, F.E. (2001). Characterization and functional implications of the RNA binding properties of nuclear factor TDP-43, a novel splicing regulator of CFTR exon 9. *J Biol Chem* 276(39)**,** 36337-36343. doi: 10.1074/jbc.M104236200.

Buratti, E., Brindisi, A., Giombi, M., Tisminetzky, S., Ayala, Y.M., and Baralle, F.E. (2005). TDP-43 binds heterogeneous nuclear ribonucleoprotein A/B through its C-terminal tail: an important region for the inhibition of cystic fibrosis transmembrane conductance

regulator exon 9 splicing. *J Biol Chem* 280(45)**,** 37572-37584. doi: 10.1074/jbc.M505557200.

Buskila, Y., Kékesi, O., Bellot-Saez, A., Seah, W., Berg, T., Trpceski, M., et al. (2019). Dynamic interplay between H-current and M-current controls motoneuron hyperexcitability in amyotrophic lateral sclerosis. *Cell death & disease* 10(4)**,** 310. doi: 10.1038/s41419-019-1538-9.

Butti, Z., and Patten, S.A. (2018). RNA Dysregulation in Amyotrophic Lateral Sclerosis. *Front Genet* 9**,** 712. doi: 10.3389/fgene.2018.00712.

Cabello-Aguilar, S., Alame, M., Kon-Sun-Tack, F., Fau, C., Lacroix, M., and Colinge, J. (2020). SingleCellSignalR: inference of intercellular networks from single-cell transcriptomics. *Nucleic Acids Res* 48(10)**,** e55. doi: 10.1093/nar/gkaa183.

Cao, J., Spielmann, M., Qiu, X., Huang, X., Ibrahim, D.M., Hill, A.J., et al. (2019). The single-cell transcriptional landscape of mammalian organogenesis. *Nature* 566(7745)**,** 496-502. doi: 10.1038/s41586-019-0969-x.

Chang, C.K., Wu, T.H., Wu, C.Y., Chiang, M.H., Toh, E.K., Hsu, Y.C., et al. (2012). The N-terminus of TDP-43 promotes its oligomerization and enhances DNA binding affinity. *Biochem Biophys Res Commun* 425(2)**,** 219-224. doi: 10.1016/j.bbrc.2012.07.071.

Chang, J.L., Lomen-Hoerth, C., Murphy, J., Henry, R.G., Kramer, J.H., Miller, B.L., et al. (2005). A voxel-based morphometry study of patterns of brain atrophy in ALS and ALS/FTLD. *Neurology* 65(1)**,** 75. doi: 10.1212/01.wnl.0000167602.38643.29.

Chen, E.Y., Tan, C.M., Kou, Y., Duan, Q., Wang, Z., Meirelles, G.V., et al. (2013a). Enrichr: interactive and collaborative HTML5 gene list enrichment analysis tool. *BMC Bioinformatics* 14**,** 128. doi: 10.1186/1471-2105-14-128.

Chen, J.J. (2020). Overview of current and emerging therapies for amytrophic lateral sclerosis. *The American Journal of Managed Care* 26(9 Suppl)**,** S191-S197.

Chen, S., Sayana, P., Zhang, X., and Le, W. (2013b). Genetics of amyotrophic lateral sclerosis: an update. *Mol Neurodegener* 8**,** 28. doi: 10.1186/1750-1326-8-28.

Chen, Z.Q., Yu, H., Li, H.Y., Shen, H.T., Li, X., Zhang, J.Y., et al. (2019). Negative regulation of glial Tim-3 inhibits the secretion of inflammatory factors and modulates microglia to antiinflammatory phenotype after experimental intracerebral hemorrhage in rats. *CNS Neurosci Ther* 25(6)**,** 674-684. doi: 10.1111/cns.13100.

Chiò, A., Logroscino, G., Hardiman, O., Swingler, R., Mitchell, D., Beghi, E., et al. (2009). Prognostic factors in ALS: A critical review. *Amyotroph Lateral Scler* 10(5-6)**,** 310-323. doi: 10.3109/17482960802566824.

Chiò, A., Logroscino, G., Traynor, B.J., Collins, J., Simeone, J.C., Goldstein, L.A., et al. (2013). Global Epidemiology of Amyotrophic Lateral Sclerosis: A Systematic Review of the Published Literature. *Neuroepidemiology* 41(2)**,** 118-130. doi: 10.1159/000351153.

Chiot, A., Zaïdi, S., Iltis, C., Ribon, M., Berriat, F., Schiaffino, L., et al. (2020). Modifying macrophages at the periphery has the capacity to change microglial reactivity and to extend ALS survival. *Nature Neuroscience* 23(11)**,** 1339-1351. doi: 10.1038/s41593-020-00718-z.

Cirulli, E.T., Lasseigne, B.N., Petrovski, S., Sapp, P.C., Dion, P.A., Leblond, C.S., et al. (2015). Exome sequencing in amyotrophic lateral sclerosis identifies risk genes and pathways. *Science* 347(6229)**,** 1436-1441. doi: 10.1126/science.aaa3650.

Clark, C.M., Clark, R.M., Hoyle, J.A., Chuckowree, J.A., McLean, C.A., and Dickson, T.C. (2021). Differential NPY-Y1 Receptor Density in the Motor Cortex of ALS Patients and Familial Model of ALS. *Brain Sciences* 11(8)**,** 969.

Clark, R.M., Blizzard, C.A., Young, K.M., King, A.E., and Dickson, T.C. (2017). Calretinin and neuropeptide y interneurons are differentially altered in the motor cortex of the SOD1 G93A mouse model of ALS. *Scientific reports* 7**,** 44461.

ClinicalTrials.gov Identifier: NCT04768972. Available: https://classic.clinicaltrials.gov/ct2/show/NCT04768972 [Accessed].

Corcia, P., Tauber, C., Vercoullie, J., Arlicot, N., Prunier, C., Praline, J., et al. (2012). Molecular imaging of microglial activation in amyotrophic lateral sclerosis. *PLoS One* 7(12)**,** e52941. doi: 10.1371/journal.pone.0052941.

Couratier, P., Sindou, P., Hugon, J., Couratier, P., Hugon, J., Vallat, J.M., et al. (1993). Cell culture evidence for neuronal degeneration in amyotrophic lateral sclerosis being linked to glutamate AMPA/kainate receptors. *The Lancet* 341(8840)**,** 265-268. doi: https://doi.org/10.1016/0140-6736(93)92615-Z.

Cruz, M.P. (2018). Edaravone (Radicava): A Novel Neuroprotective Agent for the Treatment of Amyotrophic Lateral Sclerosis. *P t* 43(1)**,** 25-28.

Cserép, C., Pósfai, B., and Dénes, Á. (2021). Shaping neuronal fate: functional heterogeneity of direct microglia-neuron interactions. *Neuron* 109(2)**,** 222-240.

Cudkowicz, M.E., Lindborg, S.R., Goyal, N.A., Miller, R.G., Burford, M.J., Berry, J.D., et al. (2022). A randomized placebo-controlled phase 3 study of mesenchymal stem cells induced to secrete high levels of neurotrophic factors in amyotrophic lateral sclerosis. *Muscle & Nerve* 65(3)**,** 291-302. doi: https://doi.org/10.1002/mus.27472.

Cykowski, M.D., Takei, H., Schulz, P.E., Appel, S.H., and Powell, S.Z. (2014). TDP-43 pathology in the basal forebrain and hypothalamus of patients with amyotrophic lateral sclerosis. *Acta neuropathologica communications* 2(1)**,** 1-11.

D'Amico, E., Grosso, G., Nieves, J.W., Zanghì, A., Factor-Litvak, P., and Mitsumoto, H. (2021). Metabolic Abnormalities, Dietary Risk Factors and Nutritional Management in Amyotrophic Lateral Sclerosis. *Nutrients* 13(7). doi: 10.3390/nu13072273.

Dafinca, R., Barbagallo, P., Farrimond, L., Candalija, A., Scaber, J., Ababneh, N.a.A., et al. (2020). Impairment of Mitochondrial Calcium Buffering Links Mutations in C9ORF72 and TARDBP in iPS-Derived Motor Neurons from Patients with ALS/FTD. *Stem Cell Reports* 14(5)**,** 892-908. doi: https://doi.org/10.1016/j.stemcr.2020.03.023.

Dafinca, R., Scaber, J., Ababneh, N.a., Lalic, T., Weir, G., Christian, H., et al. (2016). C9orf72 Hexanucleotide Expansions Are Associated with Altered Endoplasmic Reticulum Calcium Homeostasis and Stress Granule Formation in Induced Pluripotent Stem Cell-Derived Neurons from Patients with Amyotrophic Lateral Sclerosis and Frontotemporal Dementia. *Stem Cells* 34(8)**,** 2063-2078. doi: 10.1002/stem.2388.

Daneshvar, D.H., Mez, J., Alosco, M.L., Baucom, Z.H., Mahar, I., Baugh, C.M., et al. (2021). Incidence of and Mortality From Amyotrophic Lateral Sclerosis in National Football League Athletes. *JAMA Network Open* 4(12)**,** e2138801-e2138801. doi: 10.1001/jamanetworkopen.2021.38801.

Dash, R.P., Babu, R.J., and Srinivas, N.R. (2018). Two decades-long journey from riluzole to edaravone: revisiting the clinical pharmacokinetics of the only two amyotrophic lateral sclerosis therapeutics. *Clinical pharmacokinetics* 57(11)**,** 1385-1398.

de Boer, E.M.J., Orie, V.K., Williams, T., Baker, M.R., De Oliveira, H.M., Polvikoski, T., et al. (2021). TDP-43 proteinopathies: a new wave of neurodegenerative diseases. *Journal of Neurology, Neurosurgery & Psychiatry* 92(1)**,** 86. doi: 10.1136/jnnp-2020-322983.

de Ceglia, R., Ledonne, A., Litvin, D.G., Lind, B.L., Carriero, G., Latagliata, E.C., et al. (2023). Specialized astrocytes mediate glutamatergic gliotransmission in the CNS. *Nature* 622(7981)**,** 120-129. doi: 10.1038/s41586-023-06502-w.

De Vos, K.J., and Hafezparast, M. (2017). Neurobiology of axonal transport defects in motor neuron diseases: Opportunities for translational research? *Neurobiol Dis* 105**,** 283-299. doi: 10.1016/j.nbd.2017.02.004.

de Zélicourt, A., Fayssoil, A., Dakouane-Giudicelli, M., De Jesus, I., Karoui, A., Zarrouki, F., et al. (2022). CD38-NADase is a new major contributor to Duchenne muscular dystrophic phenotype. *EMBO Mol Med* 14(5)**,** e12860. doi: 10.15252/emmm.202012860.

Deczkowska, A., Keren-Shaul, H., Weiner, A., Colonna, M., Schwartz, M., and Amit, I. (2018). Disease-Associated Microglia: A Universal Immune Sensor of Neurodegeneration. *Cell* 173(5)**,** 1073-1081. doi: https://doi.org/10.1016/j.cell.2018.05.003.

Deng, H.-X., Zhai, H., Bigio, E.H., Yan, J., Fecto, F., Ajroud, K., et al. (2010). FUS-immunoreactive inclusions are a common feature in sporadic and non-SOD1 familial amyotrophic lateral sclerosis. *Annals of neurology* 67(6)**,** 739-748. doi: 10.1002/ana.22051.

Deng, Y., Bi, M., Delerue, F., Forrest, S.L., Chan, G., van der Hoven, J., et al. (2022). Loss of LAMP5 interneurons drives neuronal network dysfunction in Alzheimer's disease. *Acta Neuropathol* 144(4)**,** 637-650. doi: 10.1007/s00401-022-02457-w.

Dentel, C., Palamiuc, L., Henriques, A., Lannes, B., Spreux-Varoquaux, O., Gutknecht, L., et al. (2012). Degeneration of serotonergic neurons in amyotrophic lateral sclerosis: a link to spasticity. *Brain* 136(2)**,** 483-493. doi: 10.1093/brain/aws274.

Devlin, A.-C., Burr, K., Borooah, S., Foster, J.D., Cleary, E.M., Geti, I., et al. (2015). Human iPSC-derived motoneurons harbouring TARDBP or C9ORF72 ALS mutations are dysfunctional despite maintaining viability. *Nature Communications* 6(1)**,** 5999. doi: 10.1038/ncomms6999.

Dewey, C.M., Cenik, B., Sephton, C.F., Dries, D.R., Mayer, P., Good, S.K., et al. (2011). TDP-43 Is Directed to Stress Granules by Sorbitol, a Novel Physiological Osmotic and Oxidative Stressor. *Molecular and Cellular Biology* 31(5)**,** 1098-1108. doi: 10.1128/MCB.01279-10.

Di Giorgio, F.P., Carrasco, M.A., Siao, M.C., Maniatis, T., and Eggan, K. (2007). Non-cell autonomous effect of glia on motor neurons in an embryonic stem cell-based ALS model. *Nature neuroscience* 10(5)**,** 608-614. doi: 10.1038/nn1885.

Diaz-Amarilla, P., Olivera-Bravo, S., Trias, E., Cragnolini, A., Martinez-Palma, L., Cassina, P., et al. (2011). Phenotypically aberrant astrocytes that promote motoneuron damage in a model of inherited amyotrophic lateral sclerosis. *Proc Natl Acad Sci U S A* 108(44)**,** 18126-18131. doi: 10.1073/pnas.1110689108.

Diekstra, F.P., van Vught, P.W., van Rheenen, W., Koppers, M., Pasterkamp, R.J., van Es, M.A., et al. (2012). UNC13A is a modifier of survival in amyotrophic lateral sclerosis. *Neurobiol Aging* 33(3)**,** 630.e633-638. doi: 10.1016/j.neurobiolaging.2011.10.029.

Dimitrov, D., Türei, D., Garrido-Rodriguez, M., Burmedi, P.L., Nagai, J.S., Boys, C., et al. (2022). Comparison of methods and resources for cell-cell communication inference from single-cell RNA-Seq data. *Nat Commun* 13(1)**,** 3224. doi: 10.1038/s41467-022-30755-0.

Ding, J., Adiconis, X., Simmons, S.K., Kowalczyk, M.S., Hession, C.C., Marjanovic, N.D., et al. (2020). Systematic comparison of single-cell and single-nucleus RNA-sequencing methods. *Nature Biotechnology* 38(6)**,** 737-746. doi: 10.1038/s41587-020-0465-8.

Do-Ha, D., Buskila, Y., and Ooi, L. (2018). Impairments in Motor Neurons, Interneurons and Astrocytes Contribute to Hyperexcitability in ALS: Underlying Mechanisms and Paths to Therapy. *Molecular neurobiology* 55(2)**,** 1410–1418. doi: 10.1007/s12035-017-0392-y.

Doble, A. (1996). The pharmacology and mechanism of action of riluzole. *Neurology* 47(6 Suppl 4)**,** S233-241. doi: 10.1212/wnl.47.6_suppl_4.233s.

Dols-Icardo, O., Montal, V., Sirisi, S., López-Pernas, G., Cervera-Carles, L., Querol-Vilaseca, M., et al. (2020). Motor cortex transcriptome reveals microglial key events in amyotrophic lateral sclerosis. *Neurology-Neuroimmunology Neuroinflammation* 7(5).

Duyckaerts, C., Maisonobe, T., Hauw, J.J., and Seilhean, D. (2021). Charcot identifies and illustrates amyotrophic lateral sclerosis. *Free Neuropathol* 2. doi: 10.17879/freeneuropathology-2021-3323.

Farrugia Wismayer, M., Borg, R., Farrugia Wismayer, A., Bonavia, K., Vella, M., Pace, A., et al. (2021). Occupation and amyotrophic lateral sclerosis risk: a case-control study in the isolated island population of Malta. *Amyotrophic Lateral Sclerosis and Frontotemporal Degeneration* 22(7-8)**,** 528-534.

Ferrari, R., Kapogiannis, D., D Huey, E., and Momeni, P. (2011). FTD and ALS: a tale of two diseases. *Current Alzheimer Research* 8(3)**,** 273-294.

Fiesel, F.C., Voigt, A., Weber, S.S., Van den Haute, C., Waldenmaier, A., Görner, K., et al. (2010). Knockdown of transactive response DNA-binding protein (TDP-43) downregulates histone deacetylase 6. *Embo j* 29(1)**,** 209-221. doi: 10.1038/emboj.2009.324.

Figueroa-Romero, C., Guo, K., Murdock, B.J., Paez-Colasante, X., Bassis, C.M., Mikhail, K.A., et al. (2019). Temporal evolution of the microbiome, immune system and epigenome with disease progression in ALS mice. *Disease Models & Mechanisms* 13(2)**,** dmm041947. doi: 10.1242/dmm.041947.

Fishell, G., and Kepecs, A. (2020). Interneuron Types as Attractors and Controllers. *Annu Rev Neurosci* 43**,** 1-30. doi: 10.1146/annurev-neuro-070918-050421.

Foerster, B.R., Callaghan, B.C., Petrou, M., Edden, R.A., Chenevert, T.L., and Feldman, E.L. (2012). Decreased motor cortex gamma-aminobutyric acid in amyotrophic lateral sclerosis. *Neurology* 78(20)**,** 1596-1600. doi: 10.1212/WNL.0b013e3182563b57.

Fogarty, M.J., Klenowski, P.M., Lee, J.D., Drieberg-Thompson, J.R., Bartlett, S.E., Ngo, S.T., et al. (2016a). Cortical synaptic and dendritic spine abnormalities in a presymptomatic TDP-43 model of amyotrophic lateral sclerosis. *Scientific reports* 6**,** 37968. doi: 10.1038/srep37968.

Fogarty, M.J., Mu, E.W., Noakes, P.G., Lavidis, N.A., and Bellingham, M.C. (2016b). Marked changes in dendritic structure and spine density precede significant neuronal death in vulnerable cortical pyramidal neuron populations in the SOD1(G93A) mouse model of amyotrophic lateral sclerosis. *Acta Neuropathol Commun* 4(1)**,** 77. doi: 10.1186/s40478-016-0347-y.

Fogarty, M.J., Noakes, P.G., and Bellingham, M.C. (2015). Motor cortex layer V pyramidal neurons exhibit dendritic regression, spine loss, and increased synaptic excitation in the presymptomatic hSOD1(G93A) mouse model of amyotrophic lateral sclerosis. *J Neurosci* 35(2)**,** 643-647. doi: 10.1523/jneurosci.3483-14.2015.

Fox, A.H., and Lamond, A.I. (2010). Paraspeckles. *Cold Spring Harb Perspect Biol* 2(7)**,** a000687. doi: 10.1101/cshperspect.a000687.

François-Moutal, L., Perez-Miller, S., Scott, D.D., Miranda, V.G., Mollasalehi, N., and Khanna, M. (2019). Structural Insights Into TDP-43 and Effects of Post-translational Modifications. *Frontiers in Molecular Neuroscience* 12.

Freibaum, B.D., Chitta, R.K., High, A.A., and Taylor, J.P. (2010). Global analysis of TDP-43 interacting proteins reveals strong association with RNA splicing and translation machinery. *J Proteome Res* 9(2)**,** 1104-1120. doi: 10.1021/pr901076y.

Friedman, B.A., Srinivasan, K., Ayalon, G., Meilandt, W.J., Lin, H., Huntley, M.A., et al. (2018). Diverse Brain Myeloid Expression Profiles Reveal Distinct Microglial Activation States and Aspects of Alzheimer's Disease Not Evident in Mouse Models. *Cell Reports* 22(3)**,** 832-847. doi: https://doi.org/10.1016/j.celrep.2017.12.066.

Fritz, E., Izaurieta, P., Weiss, A., Mir, F.R., Rojas, P., Gonzalez, D., et al. (2013). Mutant SOD1-expressing astrocytes release toxic factors that trigger motoneuron death by inducing hyperexcitability. *J Neurophysiol* 109(11)**,** 2803-2814. doi: 10.1152/jn.00500.2012.

Fuentealba, R.A., Udan, M., Bell, S., Wegorzewska, I., Shao, J., Diamond, M.I., et al. (2010). Interaction with polyglutamine aggregates reveals a Q/N-rich domain in TDP-43. *J Biol Chem* 285(34)**,** 26304-26314. doi: 10.1074/jbc.M110.125039.

Furukawa, Y., Kaneko, K., Watanabe, S., Yamanaka, K., and Nukina, N. (2011). A Seeding Reaction Recapitulates Intracellular Formation of Sarkosyl-insoluble Transactivation Response Element (TAR) DNA-binding Protein-43 Inclusions. *Journal of Biological Chemistry* 286(21)**,** 18664-18672. doi: 10.1074/jbc.M111.231209.

Gao, C., Jiang, J., Tan, Y., and Chen, S. (2023). Microglia in neurodegenerative diseases: mechanism and potential therapeutic targets. *Signal Transduction and Targeted Therapy* 8(1)**,** 359. doi: 10.1038/s41392-023-01588-0.

Garbuzova-Davis, S., and Sanberg, P.R. (2014). Blood-CNS Barrier Impairment in ALS patients versus an animal model. (1662-5102 (Print)).

Gaur, N., Perner, C., Witte, O.W., and Grosskreutz, J. (2020). The Chitinases as Biomarkers for Amyotrophic Lateral Sclerosis: Signals From the CNS and Beyond. *Front Neurol* 11**,** 377. doi: 10.3389/fneur.2020.00377.

Gendron, T.F., and Petrucelli, L. (2018). Disease Mechanisms of C9ORF72 Repeat Expansions. *Cold Spring Harb Perspect Med* 8(4). doi: 10.1101/cshperspect.a024224.

Gerrits, E., Heng, Y., Boddeke, E., and Eggen, B.A.-O. (2020). Transcriptional profiling of microglia; current state of the art and future perspectives. (1098-1136 (Electronic)).

Giacomelli, E., Vahsen, B.F., Calder, E.L., Xu, Y., Scaber, J., Gray, E., et al. (2022). Human stem cell models of neurodegeneration: From basic science of amyotrophic lateral sclerosis to clinical translation. *Cell Stem Cell* 29(1)**,** 11-35. doi: 10.1016/j.stem.2021.12.008.

Glass, J.D., Dewan, R., Ding, J., Gibbs, J.R., Dalgard, C., Keagle, P.J., et al. (2022). ATXN2 intermediate expansions in amyotrophic lateral sclerosis. *Brain* 145(8)**,** 2671-2676. doi: 10.1093/brain/awac167.

Goetz, C.G. (2000). Amyotrophic lateral sclerosis: Early contributions of Jean-Martin Charcot. *Muscle & Nerve* 23(3)**,** 336-343. doi: https://doi.org/10.1002/(SICI)1097-4598(200003)23:3<336::AID-MUS4>3.0.CO;2-L.

Goncharova, P.S., Davydova, T.K., Popova, T.E., Novitsky, M.A., Petrova, M.M., Gavrilyuk, O.A., et al. 2021. Nutrient Effects on Motor Neurons and the Risk of Amyotrophic Lateral Sclerosis. *Nutrients* [Online], 13(11).

Gravel, M., Béland, L.C., Soucy, G., Abdelhamid, E., Rahimian, R., Gravel, C., et al. (2016). IL-10 Controls Early Microglial Phenotypes and Disease Onset in ALS Caused by

Misfolded Superoxide Dismutase 1. *J Neurosci* 36(3)**,** 1031-1048. doi: 10.1523/jneurosci.0854-15.2016.

Grosskreutz, J., Van Den Bosch, L., and Keller, B.U. (2010). Calcium dysregulation in amyotrophic lateral sclerosis. *Cell Calcium* 47(2)**,** 165-174. doi: https://doi.org/10.1016/j.ceca.2009.12.002.

Grubman, A., Chew, G., Ouyang, J.F., Sun, G., Choo, X.Y., McLean, C., et al. (2019). A single-cell atlas of entorhinal cortex from individuals with Alzheimer's disease reveals cell-type-specific gene expression regulation. *Nature Neuroscience* 22(12)**,** 2087-2097. doi: 10.1038/s41593-019-0539-4.

Gruijs da Silva, L.A., Simonetti, F., Hutten, S., Riemenschneider, H., Sternburg, E.L., Pietrek, L.M., et al. (2022). Disease-linked TDP-43 hyperphosphorylation suppresses TDP-43 condensation and aggregation. *Embo j* 41(8)**,** e108443. doi: 10.15252/embj.2021108443.

Gunes, Z.I., Kan, V.W., Jiang, S., Logunov, E., Ye, X., and Liebscher, S. (2022). Cortical Hyperexcitability in the Driver's Seat in ALS. *Clinical and Translational Neuroscience* 6(1)**,** 5.

Gunes, Z.I., Kan, V.W.Y., Ye, X., and Liebscher, S. (2020). Exciting Complexity: The Role of Motor Circuit Elements in ALS Pathophysiology. *Front Neurosci* 14**,** 573. doi: 10.3389/fnins.2020.00573.

Guo, W., Chen, Y., Zhou, X., Kar, A., Ray, P., Chen, X., et al. (2011). An ALS-associated mutation affecting TDP-43 enhances protein aggregation, fibril formation and neurotoxicity. *Nature Structural & Molecular Biology* 18(7)**,** 822-830. doi: 10.1038/nsmb.2053.

Guo, W., Naujock, M., Fumagalli, L., Vandoorne, T., Baatsen, P., Boon, R., et al. (2017). HDAC6 inhibition reverses axonal transport defects in motor neurons derived from FUS-ALS patients. *Nat Commun* 8(1)**,** 861. doi: 10.1038/s41467-017-00911-y.

Guttenplan, K.A., Weigel, M.K., Prakash, P., Wijewardhane, P.R., Hasel, P., Rufen-Blanchette, U., et al. (2021). Neurotoxic reactive astrocytes induce cell death via saturated lipids. *Nature* 599(7883)**,** 102-107. doi: 10.1038/s41586-021-03960-y.

Haag, F., Adriouch, S., Braß, A., Jung, C., Möller, S., Scheuplein, F., et al. (2007). Extracellular NAD and ATP: Partners in immune cell modulation. *Purinergic Signal* 3(1-2)**,** 71-81. doi: 10.1007/s11302-006-9038-7.

Habib, N., McCabe, C., Medina, S., Varshavsky, M., Kitsberg, D., Dvir-Szternfeld, R., et al. (2020). Disease-associated astrocytes in Alzheimer's disease and aging. *Nature Neuroscience* 23(6)**,** 701-706. doi: 10.1038/s41593-020-0624-8.

Haidet-Phillips, A.M., Hester, M.E., Miranda, C.J., Meyer, K., Braun, L., Frakes, A., et al. (2011). Astrocytes from familial and sporadic ALS patients are toxic to motor neurons. *Nat Biotechnol* 29(9)**,** 824-828. doi: 10.1038/nbt.1957.

Halassa, M.M., Fellin, T., and Haydon, P.G. (2007). The tripartite synapse: roles for gliotransmission in health and disease. *Trends Mol Med* 13(2)**,** 54-63. doi: 10.1016/j.molmed.2006.12.005.

Halassa, M.M., and Haydon, P.G. (2010). Integrated brain circuits: astrocytic networks modulate neuronal activity and behavior. *Annual review of physiology* 72**,** 335-355.

Hamilton, L.K., Moquin-Beaudry, G., Mangahas, C.L., Pratesi, F., Aubin, M., Aumont, A., et al. (2022). Stearoyl-CoA Desaturase inhibition reverses immune, synaptic and cognitive impairments in an Alzheimer's disease mouse model. *Nat Commun* 13(1)**,** 2061. doi: 10.1038/s41467-022-29506-y.

Hammond, T.R., Dufort, C., Dissing-Olesen, L., Giera, S., Young, A., Wysoker, A., et al. (2019). Single-Cell RNA Sequencing of Microglia throughout the Mouse Lifespan and in the Injured Brain Reveals Complex Cell-State Changes. *Immunity* 50(1)**,** 253-271.e256. doi: 10.1016/j.immuni.2018.11.004.

Han, X., Liu, Y.J., Liu, B.W., Ma, Z.L., Xia, T.J., and Gu, X.P. (2022). TREM2 and CD163 Ameliorate Microglia-Mediated Inflammatory Environment in the Aging Brain. *J Mol Neurosci* 72(5)**,** 1075-1084. doi: 10.1007/s12031-022-01965-4.

Hao, Y., Hao, S., Andersen-Nissen, E., Mauck, W.M., III, Zheng, S., Butler, A., et al. (2021). Integrated analysis of multimodal single-cell data. *Cell* 184(13)**,** 3573-3587.e3529. doi: 10.1016/j.cell.2021.04.048.

Hardiman, O., Al-Chalabi, A., Chio, A., Corr, E.M., Logroscino, G., Robberecht, W., et al. (2017). Amyotrophic lateral sclerosis. *Nature Reviews Disease Primers* 3(1)**,** 17071. doi: 10.1038/nrdp.2017.71.

Hawrot, J., Imhof, S., and Wainger, B.J. (2020). Modeling cell-autonomous motor neuron phenotypes in ALS using iPSCs. *Neurobiology of Disease* 134**,** 104680. doi: https://doi.org/10.1016/j.nbd.2019.104680.

Higelin, J., Catanese, A., Semelink-Sedlacek, L.L., Oeztuerk, S., Lutz, A.K., Bausinger, J., et al. (2018). NEK1 loss-of-function mutation induces DNA damage accumulation in ALS patient-derived motoneurons. *Stem Cell Res* 30**,** 150-162. doi: 10.1016/j.scr.2018.06.005.

Hinchcliffe, M., and Smith, A. (2017). Riluzole: real-world evidence supports significant extension of median survival times in patients with amyotrophic lateral sclerosis. *Degenerative Neurological and Neuromuscular Disease* 7**,** 61.

Hou, R., Denisenko, E., Ong, H.T., Ramilowski, J.A., and Forrest, A.R.R. (2020). Predicting cell-to-cell communication networks using NATMI. *Nat Commun* 11(1)**,** 5011. doi: 10.1038/s41467-020-18873-z.

Igaz, L.M., Kwong, L.K., Lee, E.B., Chen-Plotkin, A., Swanson, E., Unger, T., et al. (2011). Dysregulation of the ALS-associated gene TDP-43 leads to neuronal death and degeneration in mice. *J Clin Invest* 121(2)**,** 726-738. doi: 10.1172/jci44867.

Jara, J.H., Genç, B., Cox, G.A., Bohn, M.C., Roos, R.P., Macklis, J.D., et al. (2015). Corticospinal motor neurons are susceptible to increased ER stress and display profound degeneration in the absence of UCHL1 function. *Cerebral cortex* 25(11)**,** 4259-4272.

Jara, J.H., Genç, B., Stanford, M.J., Pytel, P., Roos, R.P., Weintraub, S., et al. (2017). Evidence for an early innate immune response in the motor cortex of ALS. *Journal of Neuroinflammation* 14(1)**,** 129. doi: 10.1186/s12974-017-0896-4.

Jeon, Y.M., Kwon, Y., Lee, S., and Kim, H.J. (2023). Potential roles of the endoplasmic reticulum stress pathway in amyotrophic lateral sclerosis. (1663-4365 (Print)).

Jiang, L.-L., Xue, W., Hong, J.-Y., Zhang, J.-T., Li, M.-J., Yu, S.-N., et al. (2017). The N-terminal dimerization is required for TDP-43 splicing activity. *Scientific Reports* 7(1)**,** 6196. doi: 10.1038/s41598-017-06263-3.

Jiang, L.-L., Zhao, J., Yin, X.-F., He, W.-T., Yang, H., Che, M.-X., et al. (2016). Two mutations G335D and Q343R within the amyloidogenic core region of TDP-43 influence its aggregation and inclusion formation. *Scientific Reports* 6(1)**,** 23928. doi: 10.1038/srep23928.

Jin, J., Hu, F., Zhang, Q., Chen, Q., Li, H., Qin, X., et al. (2019). Dominant Heterogeneity of Upper and Lower Motor Neuron Degeneration to Motor Manifestation of Involved

Region in Amyotrophic Lateral Sclerosis. *Sci Rep* 9(1)**,** 20059. doi: 10.1038/s41598-019-56665-8.

Johnson, B.S., Snead, D., Lee, J.J., McCaffery, J.M., Shorter, J., and Gitler, A.D. (2009). TDP-43 is intrinsically aggregation-prone, and amyotrophic lateral sclerosis-linked mutations accelerate aggregation and increase toxicity. *J Biol Chem* 284(30)**,** 20329-20339. doi: 10.1074/jbc.M109.010264.

Jovic, D., Liang, X., Zeng, H., Lin, L., Xu, F., and Luo, Y. (2022). Single-cell RNA sequencing technologies and applications: A brief overview. *Clinical and Translational Medicine* 12(3)**,** e694. doi: https://doi.org/10.1002/ctm2.694.

K, D.B., Tang, M., Reigan, P., and R, H.E. (2020). Genetic Variants of Lipoprotein Lipase and Regulatory Factors Associated with Alzheimer's Disease Risk. *Int J Mol Sci* 21(21). doi: 10.3390/ijms21218338.

Kalra, S., Müller, H.-P., Ishaque, A., Zinman, L., Korngut, L., Genge, A., et al. (2020). A prospective harmonized multicenter DTI study of cerebral white matter degeneration in ALS. *Neurology* 95(8)**,** e943. doi: 10.1212/WNL.0000000000010235.

Kametani, F., Obi, T., Shishido, T., Akatsu, H., Murayama, S., Saito, Y., et al. (2016). Mass spectrometric analysis of accumulated TDP-43 in amyotrophic lateral sclerosis brains. *Scientific Reports* 6(1)**,** 23281. doi: 10.1038/srep23281.

Kang, P., Lee, H.K., Glasgow, S.M., Finley, M., Donti, T., Gaber, Z.B., et al. (2012). Sox9 and NFIA coordinate a transcriptional regulatory cascade during the initiation of gliogenesis. *Neuron* 74(1)**,** 79-94. doi: 10.1016/j.neuron.2012.01.024.

Kang, S.H., Li, Y., Fukaya, M., Lorenzini, I., Cleveland, D.W., Ostrow, L.W., et al. (2013). Degeneration and impaired regeneration of gray matter oligodendrocytes in amyotrophic lateral sclerosis. *Nature Neuroscience* 16(5)**,** 571-579. doi: 10.1038/nn.3357.

Karnani, M.M., Jackson, J., Ayzenshtat, I., Hamzehei Sichani, A., Manoocheri, K., Kim, S., et al. (2016). Opening Holes in the Blanket of Inhibition: Localized Lateral Disinhibition by VIP Interneurons. *J Neurosci* 36(12)**,** 3471-3480. doi: 10.1523/jneurosci.3646-15.2016.

Kassubek, J., Unrath, A., Huppertz, H.J., Lulé, D., Ethofer, T., Sperfeld, A.D., et al. (2005). Global brain atrophy and corticospinal tract alterations in ALS, as investigated by voxel-based morphometry of 3-D MRI. *Amyotrophic Lateral Sclerosis* 6(4)**,** 213-220. doi: 10.1080/14660820510038538.

Kast, R.J., Lanjewar, A.L., Smith, C.D., and Levitt, P. (2019). FOXP2 exhibits projection neuron class specific expression, but is not required for multiple aspects of cortical histogenesis. *Elife* 8. doi: 10.7554/eLife.42012.

Kästle, M., Kistler, B., Lamla, T., Bretschneider, T., Lamb, D., Nicklin, P., et al. (2018). FKBP51 modulates steroid sensitivity and NFκB signalling: A novel anti-inflammatory drug target. *Eur J Immunol* 48(11)**,** 1904-1914. doi: 10.1002/eji.201847699.

Kawahara, Y., and Mieda-Sato, A. (2012). TDP-43 promotes microRNA biogenesis as a component of the Drosha and Dicer complexes. *Proc Natl Acad Sci U S A* 109(9)**,** 3347-3352. doi: 10.1073/pnas.1112427109.

Kawamata, H., and Manfredi, G. (2010). Mitochondrial dysfunction and intracellular calcium dysregulation in ALS. *Mech Ageing Dev* 131(7-8)**,** 517-526. doi: 10.1016/j.mad.2010.05.003.

Kawamata, T., Akiyama, H., Yamada, T., and McGeer, P.L. (1992). Immunologic reactions in amyotrophic lateral sclerosis brain and spinal cord tissue. *Am J Pathol* 140(3)**,** 691-707.

Ke, Y.D., van Hummel, A., Stevens, C.H., Gladbach, A., Ippati, S., Bi, M., et al. (2015). Short-term suppression of A315T mutant human TDP-43 expression improves functional deficits in a novel inducible transgenic mouse model of FTLD-TDP and ALS. *Acta Neuropathol* 130(5)**,** 661-678. doi: 10.1007/s00401-015-1486-0.

Kenigsbuch, M., Bost, P., Halevi, S., Chang, Y., Chen, S., Ma, Q., et al. (2022). A shared disease-associated oligodendrocyte signature among multiple CNS pathologies. *Nat Neurosci* 25(7)**,** 876-886. doi: 10.1038/s41593-022-01104-7.

Keren-Shaul, H., Spinrad, A., Weiner, A., Matcovitch-Natan, O., Dvir-Szternfeld, R., Ulland, T.K., et al. (2017). A Unique Microglia Type Associated with Restricting Development of Alzheimer's Disease. *Cell* 169(7)**,** 1276-1290.e1217. doi: 10.1016/j.cell.2017.05.018.

Khademullah, C.S., Aqrabawi, A.J., Place, K.M., Dargaei, Z., Liang, X., Pressey, J.C., et al. (2020). Cortical interneuron-mediated inhibition delays the onset of amyotrophic lateral sclerosis. *Brain* 143(3)**,** 800-810.

Khakh, B.S., and Goldman, S.A. (2023). Astrocytic contributions to Huntington's disease pathophysiology. *Annals of the New York Academy of Sciences* 1522(1)**,** 42-59. doi: https://doi.org/10.1111/nyas.14977.

Khare, S.D., Wilcox, K.C., Gong, P., and Dokholyan, N.V. (2005). Sequence and structural determinants of Cu, Zn superoxide dismutase aggregation. *Proteins: Structure, Function, and Bioinformatics* 61(3)**,** 617-632. doi: https://doi.org/10.1002/prot.20629.

Kia, A., McAvoy, K., Krishnamurthy, K., Trotti, D., and Pasinelli, P. (2018). Astrocytes expressing ALS-linked mutant FUS induce motor neuron death through release of tumor necrosis factor-alpha. *Glia* 66(5)**,** 1016-1033. doi: 10.1002/glia.23298.

Kiernan, M.C., Vucic, S., Cheah, B.C., Turner, M.R., Eisen, A., Hardiman, O., et al. (2011). Amyotrophic lateral sclerosis. *The Lancet* 377(9769)**,** 942-955. doi: 10.1016/S0140-6736(10)61156-7.

Kim, H.J., Kim, N.C., Wang, Y.-D., Scarborough, E.A., Moore, J., Diaz, Z., et al. (2013). Mutations in prion-like domains in hnRNPA2B1 and hnRNPA1 cause multisystem proteinopathy and ALS. *Nature* 495(7442)**,** 467-473. doi: 10.1038/nature11922.

Kim, J., Hughes, E.G., Shetty, A.S., Arlotta, P., Goff, L.A., Bergles, D.E., et al. (2017). Changes in the Excitability of Neocortical Neurons in a Mouse Model of Amyotrophic Lateral Sclerosis Are Not Specific to Corticospinal Neurons and Are Modulated by Advancing Disease. *J Neurosci* 37(37)**,** 9037-9053. doi: 10.1523/jneurosci.0811-17.2017.

Kim, W., Kim, D.Y., and Lee, K.H. (2021). RNA-Binding Proteins and the Complex Pathophysiology of ALS. *Int J Mol Sci* 22(5). doi: 10.3390/ijms22052598.

Kiselev, V.Y., Andrews, T.S., and Hemberg, M. (2019). Challenges in unsupervised clustering of single-cell RNA-seq data. *Nature Reviews Genetics* 20(5)**,** 273-282. doi: 10.1038/s41576-018-0088-9.

Kiskinis, E., Sandoe, J., Williams, Luis A., Boulting, Gabriella L., Moccia, R., Wainger, Brian J., et al. (2014). Pathways Disrupted in Human ALS Motor Neurons Identified through Genetic Correction of Mutant SOD1. *Cell Stem Cell* 14(6)**,** 781-795. doi: https://doi.org/10.1016/j.stem.2014.03.004.

Klein, A.M., Mazutis, L., Akartuna, I., Tallapragada, N., Veres, A., Li, V., et al. (2015). Droplet barcoding for single-cell transcriptomics applied to embryonic stem cells. *Cell* 161(5)**,** 1187-1201. doi: 10.1016/j.cell.2015.04.044.

Kleinberger, G., Yamanishi, Y., Suárez-Calvet, M., Czirr, E., Lohmann, E., Cuyvers, E., et al. (2014). TREM2 mutations implicated in neurodegeneration impair cell surface transport and phagocytosis. *Science Translational Medicine* 6(243)**,** 243ra286-243ra286. doi: 10.1126/scitranslmed.3009093.

Klim, J.R., Williams, L.A., Limone, F., Guerra San Juan, I., Davis-Dusenbery, B.N., Mordes, D.A., et al. (2019). ALS-implicated protein TDP-43 sustains levels of STMN2, a mediator of motor neuron growth and repair. *Nat Neurosci* 22(2)**,** 167-179. doi: 10.1038/s41593-018-0300-4.

Kobak, D., and Linderman, G.C. (2021). Initialization is critical for preserving global data structure in both t-SNE and UMAP. *Nat Biotechnol* 39(2)**,** 156-157. doi: 10.1038/s41587-020-00809-z.

Konishi, H., Koizumi, S., and Kiyama, H. (2022). Phagocytic astrocytes: Emerging from the shadows of microglia. *Glia* 70(6)**,** 1009-1026. doi: 10.1002/glia.24145.

Korsunsky, I., Millard, N., Fan, J., Slowikowski, K., Zhang, F., Wei, K., et al. (2019). Fast, sensitive and accurate integration of single-cell data with Harmony. *Nat Methods* 16(12)**,** 1289-1296. doi: 10.1038/s41592-019-0619-0.

Krabbe, S., Paradiso, E., d'Aquin, S., Bitterman, Y., Courtin, J., Xu, C., et al. (2019). Adaptive disinhibitory gating by VIP interneurons permits associative learning. *Nature neuroscience* 22(11)**,** 1834-1843.

Kreiter, N., Pal, A., Lojewski, X., Corcia, P., Naujock, M., Reinhardt, P., et al. (2018). Age-dependent neurodegeneration and organelle transport deficiencies in mutant TDP43 patient-derived neurons are independent of TDP43 aggregation. *Neurobiol Dis* 115**,** 167-181. doi: 10.1016/j.nbd.2018.03.010.

Krishnaswami, S.R., Grindberg, R.V., Novotny, M., Venepally, P., Lacar, B., Bhutani, K., et al. (2016). Using single nuclei for RNA-seq to capture the transcriptome of postmortem neurons. *Nat Protoc* 11(3)**,** 499-524. doi: 10.1038/nprot.2016.015.

Kukurba, K.R., and Montgomery, S.B. (2015). RNA Sequencing and Analysis. *Cold Spring Harb Protoc* 2015(11)**,** 951-969. doi: 10.1101/pdb.top084970.

Kuleshov, M.V., Jones, M.R., Rouillard, A.D., Fernandez, N.F., Duan, Q., Wang, Z., et al. (2016). Enrichr: a comprehensive gene set enrichment analysis web server 2016 update. *Nucleic Acids Res* 44(W1)**,** W90-97. doi: 10.1093/nar/gkw377.

Kumar, D.R., Aslinia, F., Yale, S.H., and Mazza, J.J. (2011). Jean-Martin Charcot: the father of neurology. *Clinical medicine & research* 9(1)**,** 46-49.

Kuo, P.-H., Doudeva, L.G., Wang, Y.-T., Shen, C.-K.J., and Yuan, H.S. (2009). Structural insights into TDP-43 in nucleic-acid binding and domain interactions. *Nucleic acids research* 37(6)**,** 1799-1808.

Kuo, P.H., Chiang, C.H., Wang, Y.T., Doudeva, L.G., and Yuan, H.S. (2014). The crystal structure of TDP-43 RRM1-DNA complex reveals the specific recognition for UG- and TG-rich nucleic acids. *Nucleic Acids Res* 42(7)**,** 4712-4722. doi: 10.1093/nar/gkt1407.

Kwiatkowski, T.J., Bosco, D.A., LeClerc, A.L., Tamrazian, E., Vanderburg, C.R., Russ, C., et al. (2009). Mutations in the FUS/TLS Gene on Chromosome 16 Cause Familial Amyotrophic Lateral Sclerosis. *Science* 323(5918)**,** 1205-1208. doi: 10.1126/science.1166066.

Kwon, H.S., and Koh, S.H. (2020). Neuroinflammation in neurodegenerative disorders: the roles of microglia and astrocytes. *Transl Neurodegener* 9(1)**,** 42. doi: 10.1186/s40035-020-00221-2.

Lähnemann, D., Köster, J., Szczurek, E., McCarthy, D.J., Hicks, S.C., Robinson, M.D., et al. (2020). Eleven grand challenges in single-cell data science. *Genome Biology* 21(1)**,** 31. doi: 10.1186/s13059-020-1926-6.

Lake, B.B., Codeluppi, S., Yung, Y.C., Gao, D., Chun, J., Kharchenko, P.V., et al. (2017). A comparative strategy for single-nucleus and single-cell transcriptomes confirms

accuracy in predicted cell-type expression from nuclear RNA. *Scientific Reports* 7(1)**,** 6031. doi: 10.1038/s41598-017-04426-w.

Lamptey, R.N.L., Chaulagain, B., Trivedi, R., Gothwal, A., Layek, B., and Singh, J. (2022). A Review of the Common Neurodegenerative Disorders: Current Therapeutic Approaches and the Potential Role of Nanotherapeutics. *Int J Mol Sci* 23(3). doi: 10.3390/ijms23031851.

Laneve, P., Tollis, P., and Caffarelli, E. (2021). RNA Deregulation in Amyotrophic Lateral Sclerosis: The Noncoding Perspective. *Int J Mol Sci* 22(19). doi: 10.3390/ijms221910285.

Lautenschlaeger, J., Prell, T., and Grosskreutz, J. (2012). Endoplasmic reticulum stress and the ER mitochondrial calcium cycle in amyotrophic lateral sclerosis. *Amyotroph Lateral Scler* 13(2)**,** 166-177. doi: 10.3109/17482968.2011.641569.

Lee, E.B., Lee, V.M., and Trojanowski, J.Q. (2011). Gains or losses: molecular mechanisms of TDP43-mediated neurodegeneration. *Nat Rev Neurosci* 13(1)**,** 38-50. doi: 10.1038/nrn3121.

Lee, Y., Morrison, B.M., Li, Y., Lengacher, S., Farah, M.H., Hoffman, P.N., et al. (2012). Oligodendroglia metabolically support axons and contribute to neurodegeneration. *Nature* 487(7408)**,** 443-448. doi: 10.1038/nature11314.

Leibiger, C., Deisel, J., Aufschnaiter, A., Ambros, S., Tereshchenko, M., Verheijen, B.M., et al. (2018). TDP-43 controls lysosomal pathways thereby determining its own clearance and cytotoxicity. *Hum Mol Genet* 27(9)**,** 1593-1607. doi: 10.1093/hmg/ddy066.

Li, H.Y., Yeh, P.A., Chiu, H.C., Tang, C.Y., and Tu, B.P. (2011). Hyperphosphorylation as a defense mechanism to reduce TDP-43 aggregation. *PLoS One* 6(8)**,** e23075. doi: 10.1371/journal.pone.0023075.

Li, K., Hala, T.J., Seetharam, S., Poulsen, D.J., Wright, M.C., and Lepore, A.C. (2015). GLT1 overexpression in SOD1(G93A) mouse cervical spinal cord does not preserve diaphragm function or extend disease. *Neurobiol Dis* 78**,** 12-23. doi: 10.1016/j.nbd.2015.03.010.

Li, Q., and Barres, B.A. (2018). Microglia and macrophages in brain homeostasis and disease. *Nat Rev Immunol* 18(4)**,** 225-242. doi: 10.1038/nri.2017.125.

Lian, L., Liu, M., Cui, L., Guan, Y., Liu, T., Cui, B., et al. (2019). Environmental risk factors and amyotrophic lateral sclerosis (ALS): a case-control study of ALS in China. *Journal of Clinical Neuroscience* 66**,** 12-18.

Licht-Murava, A., Meadows, S.M., Palaguachi, F., Song, S.C., Jackvony, S., Bram, Y., et al. (2023). Astrocytic TDP-43 dysregulation impairs memory by modulating antiviral pathways and interferon-inducible chemokines. *Sci Adv* 9(16)**,** eade1282. doi: 10.1126/sciadv.ade1282.

Liddelow, S.A., Guttenplan, K.A., Clarke, L.E., Bennett, F.C., Bohlen, C.J., Schirmer, L., et al. (2017). Neurotoxic reactive astrocytes are induced by activated microglia. *Nature* 541(7638)**,** 481-487. doi: 10.1038/nature21029.

Limone, F., A. Mordes, D., Couto, A., J. Joseph, B., M. Mitchell, J., Therrien, M., et al. (2023). Single-nucleus sequencing reveals enriched expression of genetic risk factors in Extratelencephalic Neurons sensitive to degeneration in ALS. *bioRxiv***,** 2021.2007.2012.452054. doi: 10.1101/2021.07.12.452054.

Lin, L.T., Razzaq, A., Di Gregorio, S.E., Hong, S., Charles, B., Lopes, M.H., et al. (2021). Hsp90 and its co-chaperone Sti1 control TDP-43 misfolding and toxicity. *Faseb j* 35(5)**,** e21594. doi: 10.1096/fj.202002645R.

Linderman, G.C., Zhao, J., Roulis, M., Bielecki, P., Flavell, R.A., Nadler, B., et al. (2022). Zero-preserving imputation of single-cell RNA-seq data. *Nature Communications* 13(1)**,** 192. doi: 10.1038/s41467-021-27729-z.

Ling, J.P., Pletnikova, O., Troncoso, J.C., and Wong, P.C. (2015). TDP-43 repression of nonconserved cryptic exons is compromised in ALS-FTD. *Science* 349(6248)**,** 650-655. doi: 10.1126/science.aab0983.

Ling, S.C., Polymenidou, M., and Cleveland, D.W. (2013). Converging mechanisms in ALS and FTD: disrupted RNA and protein homeostasis. *Neuron* 79(3)**,** 416-438. doi: 10.1016/j.neuron.2013.07.033.

Liu, C., Zhao, X.M., Wang, Q., Du, T.T., Zhang, M.X., Wang, H.Z., et al. (2023). Astrocyte-derived SerpinA3N promotes neuroinflammation and epileptic seizures by activating the NF-κB signaling pathway in mice with temporal lobe epilepsy. *J Neuroinflammation* 20(1)**,** 161. doi: 10.1186/s12974-023-02840-8.

Liu, D., Zuo, X., Zhang, P., Zhao, R., Lai, D., Chen, K., et al. (2021). The Novel Regulatory Role of lncRNA-miRNA-mRNA Axis in Amyotrophic Lateral Sclerosis: An Integrated Bioinformatics Analysis. *Comput Math Methods Med* 2021**,** 5526179. doi: 10.1155/2021/5526179.

Liu, Y., Han, S.S., Wu, Y., Tuohy, T.M., Xue, H., Cai, J., et al. (2004). CD44 expression identifies astrocyte-restricted precursor cells. *Dev Biol* 276(1)**,** 31-46. doi: 10.1016/j.ydbio.2004.08.018.

Longinetti, E., and Fang, F. (2019). Epidemiology of amyotrophic lateral sclerosis: an update of recent literature. *Current opinion in neurology* 32(5)**,** 771.

Longinetti, E., Regodón Wallin, A., Samuelsson, K., Press, R., Zachau, A., Ronnevi, L.-O., et al. (2018). The Swedish motor neuron disease quality registry. *Amyotrophic Lateral Sclerosis and Frontotemporal Degeneration* 19(7-8)**,** 528-537.

Lopez-Gonzalez, R., Lu, Y., Gendron, Tania F., Karydas, A., Tran, H., Yang, D., et al. (2016). Poly(GR) in C9ORF72-Related ALS/FTD Compromises Mitochondrial Function and Increases Oxidative Stress and DNA Damage in iPSC-Derived Motor Neurons. *Neuron* 92(2)**,** 383-391. doi: https://doi.org/10.1016/j.neuron.2016.09.015.

Lorente Pons, A., Higginbottom, A., Cooper-Knock, J., Alrafiah, A., Alofi, E., Kirby, J., et al. (2020). Oligodendrocyte pathology exceeds axonal pathology in white matter in human amyotrophic lateral sclerosis. *The Journal of Pathology* 251(3)**,** 262-271. doi: https://doi.org/10.1002/path.5455.

Love, M.I., Huber, W., and Anders, S. (2014). Moderated estimation of fold change and dispersion for RNA-seq data with DESeq2. *Genome Biol* 15(12)**,** 550. doi: 10.1186/s13059-014-0550-8.

Lowe, J., Lennox, G., Jefferson, D., Morrell, K., McQuire, D., Gray, T., et al. (1988). A filamentous inclusion body within anterior horn neurones in motor neurone disease defined by immunocytochemical localisation of ubiquitin. *Neuroscience Letters* 94(1)**,** 203-210. doi: https://doi.org/10.1016/0304-3940(88)90296-0.

Luna, J., Diagana, M., Aissa, L.A., Tazir, M., Pacha, L.A., Kacem, I., et al. (2019). Clinical features and prognosis of amyotrophic lateral sclerosis in Africa: the TROPALS study. *Journal of Neurology, Neurosurgery & Psychiatry* 90(1)**,** 20-29.

Ma, X.R., Prudencio, M., Koike, Y., Vatsavayai, S.C., Kim, G., Harbinski, F., et al. (2022). TDP-43 represses cryptic exon inclusion in the FTD–ALS gene UNC13A. *Nature* 603(7899)**,** 124-130. doi: 10.1038/s41586-022-04424-7.

Mackenzie, I.R.A., Ansorge, O., Strong, M., Bilbao, J., Zinman, L., Ang, L.-C., et al. (2011). Pathological heterogeneity in amyotrophic lateral sclerosis with FUS mutations: two

distinct patterns correlating with disease severity and mutation. *Acta Neuropathologica* 122(1)**,** 87-98. doi: 10.1007/s00401-011-0838-7.

Mackenzie, I.R.A., Bigio, E.H., Ince, P.G., Geser, F., Neumann, M., Cairns, N.J., et al. (2007). Pathological TDP-43 distinguishes sporadic amyotrophic lateral sclerosis from amyotrophic lateral sclerosis with SOD1 mutations. *Annals of Neurology* 61(5)**,** 427-434. doi: https://doi.org/10.1002/ana.21147.

Macosko, E.Z., Basu, A., Satija, R., Nemesh, J., Shekhar, K., Goldman, M., et al. (2015). Highly Parallel Genome-wide Expression Profiling of Individual Cells Using Nanoliter Droplets. *Cell* 161(5)**,** 1202-1214. doi: 10.1016/j.cell.2015.05.002.

Maekawa, S., Al-Sarraj, S., Kibble, M., Landau, S., Parnavelas, J., Cotter, D., et al. (2004). Cortical selective vulnerability in motor neuron disease: a morphometric study. *Brain* 127(6)**,** 1237-1251. doi: 10.1093/brain/awh132.

Maharjan, N., Künzli, C., Buthey, K., and Saxena, S. (2017). C9ORF72 Regulates Stress Granule Formation and Its Deficiency Impairs Stress Granule Assembly, Hypersensitizing Cells to Stress. *Mol Neurobiol* 54(4)**,** 3062-3077. doi: 10.1007/s12035-016-9850-1.

Majounie, E., Renton, A.E., Mok, K., Dopper, E.G., Waite, A., Rollinson, S., et al. (2012). Frequency of the C9orf72 hexanucleotide repeat expansion in patients with amyotrophic lateral sclerosis and frontotemporal dementia: a cross-sectional study. *Lancet Neurol* 11(4)**,** 323-330. doi: 10.1016/s1474-4422(12)70043-1.

Maniatis, S., Äijö, T., Vickovic, S., Braine, C., Kang, K., Mollbrink, A., et al. (2019). Spatiotemporal dynamics of molecular pathology in amyotrophic lateral sclerosis. *Science* 364(6435)**,** 89. doi: 10.1126/science.aav9776.

Marchetto, M.C., Muotri, A.R., Mu, Y., Smith, A.M., Cezar, G.G., and Gage, F.H. (2008). Non-cell-autonomous effect of human SOD1 G37R astrocytes on motor neurons derived from human embryonic stem cells. *Cell Stem Cell* 3(6)**,** 649-657. doi: 10.1016/j.stem.2008.10.001.

Marinković, P., Reuter, M.S., Brill, M.S., Godinho, L., Kerschensteiner, M., and Misgeld, T. (2012). Axonal transport deficits and degeneration can evolve independently in mouse models of amyotrophic lateral sclerosis. *Proceedings of the National Academy of Sciences* 109(11)**,** 4296-4301. doi: 10.1073/pnas.1200658109.

Markram, H., Toledo-Rodriguez, M., Wang, Y., Gupta, A., Silberberg, G., and Wu, C. (2004). Interneurons of the neocortical inhibitory system. *Nat Rev Neurosci* 5(10)**,** 793-807. doi: 10.1038/nrn1519.

Martelotto, L.G. (2020). *'Frankenstein' protocol for nuclei isolation from fresh and frozen tissue for snRNA-seq.* [Online]. Protocolsio. . [Accessed].

Martínez-Silva, M.d.L., Imhoff-Manuel, R.D., Sharma, A., Heckman, C.J., Shneider, N.A., Roselli, F., et al. (2018). Hypoexcitability precedes denervation in the large fast-contracting motor units in two unrelated mouse models of ALS. *eLife* 7. doi: 10.7554/eLife.30955.

Masuda, T., Sankowski, R., Staszewski, O., and Prinz, M. (2020). Microglia Heterogeneity in the Single-Cell Era. *Cell Reports* 30(5)**,** 1271-1281. doi: 10.1016/j.celrep.2020.01.010.

Mathys, H., Adaikkan, C., Gao, F., Young, J.Z., Manet, E., Hemberg, M., et al. (2017). Temporal Tracking of Microglia Activation in Neurodegeneration at Single-Cell Resolution. *Cell Rep* 21(2)**,** 366-380. doi: 10.1016/j.celrep.2017.09.039.

Mathys, H., Davila-Velderrain, J., Peng, Z., Gao, F., Mohammadi, S., Young, J.Z., et al. (2019). Single-cell transcriptomic analysis of Alzheimer's disease. *Nature* 570(7761)**,** 332-337. doi: 10.1038/s41586-019-1195-2.

Matsukawa, K., Kukharsky, M.S., Park, S.K., Park, S., Watanabe, N., Iwatsubo, T., et al. (2021). Long non-coding RNA NEAT1_1 ameliorates TDP-43 toxicity in in vivo models of TDP-43 proteinopathy. *RNA Biol* 18(11)**,** 1546-1554. doi: 10.1080/15476286.2020.1860580.

Maziuk, B., Ballance, H.I., and Wolozin, B. (2017). Dysregulation of RNA Binding Protein Aggregation in Neurodegenerative Disorders. *Frontiers in Molecular Neuroscience* 10.

McCombe, P.A., Lee, J.D., Woodruff, T.M., and Henderson, R.D. (2020). The Peripheral Immune System and Amyotrophic Lateral Sclerosis. *Front Neurol* 11**,** 279. doi: 10.3389/fneur.2020.00279.

McDonald, K.K., Aulas, A., Destroismaisons, L., Pickles, S., Beleac, E., Camu, W., et al. (2011). TAR DNA-binding protein 43 (TDP-43) regulates stress granule dynamics via differential regulation of G3BP and TIA-1. *Human Molecular Genetics* 20(7)**,** 1400-1410. doi: 10.1093/hmg/ddr021.

McGeer, P.L., and McGeer, E.G. (2002). Inflammatory processes in amyotrophic lateral sclerosis. *Muscle & Nerve* 26(4)**,** 459-470. doi: https://doi.org/10.1002/mus.10191.

McInnes, L., and Healy, J. (2018). UMAP: Uniform Manifold Approximation and Projection for Dimension Reduction. *ArXiv* abs/1802.03426.

McKeon, R.J., Jurynec, M.J., and Buck, C.R. (1999). The chondroitin sulfate proteoglycans neurocan and phosphacan are expressed by reactive astrocytes in the chronic CNS glial scar. *J Neurosci* 19(24)**,** 10778-10788. doi: 10.1523/jneurosci.19-24-10778.1999.

Mead, R.J., Shan, N., Reiser, H.J., Marshall, F., and Shaw, P.J. (2023). Amyotrophic lateral sclerosis: a neurodegenerative disorder poised for successful therapeutic translation. *Nature Reviews Drug Discovery* 22(3)**,** 185-212. doi: 10.1038/s41573-022-00612-2.

Mehta, P.R., Brown, A.-L., Ward, M.E., and Fratta, P. (2023). The era of cryptic exons: implications for ALS-FTD. *Molecular Neurodegeneration* 18(1)**,** 16. doi: 10.1186/s13024-023-00608-5.

Mehta, P.R., Jones, A.R., Opie-Martin, S., Shatunov, A., Iacoangeli, A., Al Khleifat, A., et al. (2019). Younger age of onset in familial amyotrophic lateral sclerosis is a result of pathogenic gene variants, rather than ascertainment bias. *Journal of Neurology, Neurosurgery & Psychiatry* 90(3)**,** 268. doi: 10.1136/jnnp-2018-319089.

Meissner, F., Molawi, K., and Zychlinsky, A. (2010). Mutant superoxide dismutase 1-induced IL-1beta accelerates ALS pathogenesis. *Proc Natl Acad Sci U S A* 107(29)**,** 13046-13050. doi: 10.1073/pnas.1002396107.

Mejzini, R., Flynn, L.L., Pitout, I.L., Fletcher, S., Wilton, S.D., and Akkari, P.A. (2019). ALS Genetics, Mechanisms, and Therapeutics: Where Are We Now? *Front Neurosci* 13**,** 1310. doi: 10.3389/fnins.2019.01310.

Melamed, Z., López-Erauskin, J., Baughn, M.W., Zhang, O., Drenner, K., Sun, Y., et al. (2019). Premature polyadenylation-mediated loss of stathmin-2 is a hallmark of TDP-43-dependent neurodegeneration. *Nat Neurosci* 22(2)**,** 180-190. doi: 10.1038/s41593-018-0293-z.

Meneses, A., Koga, S., O'Leary, J., Dickson, D.W., Bu, G., and Zhao, N. (2021). TDP-43 Pathology in Alzheimer's Disease. *Molecular Neurodegeneration* 16(1)**,** 84. doi: 10.1186/s13024-021-00503-x.

Menon, P., Geevasinga, N., van den Bos, M., Yiannikas, C., Kiernan, M.C., and Vucic, S. (2017). Cortical hyperexcitability and disease spread in amyotrophic lateral sclerosis. *Eur J Neurol* 24(6)**,** 816-824. doi: 10.1111/ene.13295.

Meyer, K., Ferraiuolo, L., Miranda, C.J., Likhite, S., McElroy, S., Renusch, S., et al. (2014). Direct conversion of patient fibroblasts demonstrates non-cell autonomous toxicity of

astrocytes to motor neurons in familial and sporadic ALS. *Proceedings of the National Academy of Sciences* 111(2)**,** 829-832. doi: 10.1073/pnas.1314085111.

Minciacchi, D., Kassa, R.M., Del Tongo, C., Mariotti, R., and Bentivoglio, M. (2009). Voronoi-based spatial analysis reveals selective interneuron changes in the cortex of FALS mice. *Exp Neurol* 215(1)**,** 77-86. doi: 10.1016/j.expneurol.2008.09.005.

Mishra, P.-S., Dhull, D.K., Nalini, A., Vijayalakshmi, K., Sathyaprabha, T.N., Alladi, P.A., et al. (2016). Astroglia acquires a toxic neuroinflammatory role in response to the cerebrospinal fluid from amyotrophic lateral sclerosis patients. *Journal of Neuroinflammation* 13(1)**,** 212. doi: 10.1186/s12974-016-0698-0.

Mishra, V., Re, D.B., Le Verche, V., Alvarez, M.J., Vasciaveo, A., Jacquier, A., et al. (2020). Systematic elucidation of neuron-astrocyte interaction in models of amyotrophic lateral sclerosis using multi-modal integrated bioinformatics workflow. *Nat Commun* 11(1)**,** 5579. doi: 10.1038/s41467-020-19177-y.

Miškić, T., Kostović, I., Rašin, M.R., and Krsnik, Ž. (2021). Adult Upper Cortical Layer Specific Transcription Factor CUX2 Is Expressed in Transient Subplate and Marginal Zone Neurons of the Developing Human Brain. *Cells* 10(2). doi: 10.3390/cells10020415.

Mitchell, J.C., McGoldrick, P., Vance, C., Hortobagyi, T., Sreedharan, J., Rogelj, B., et al. (2013). Overexpression of human wild-type FUS causes progressive motor neuron degeneration in an age- and dose-dependent fashion. *Acta Neuropathologica* 125(2)**,** 273-288. doi: 10.1007/s00401-012-1043-z.

Mizuno, Y., Fujita, Y., Takatama, M., and Okamoto, K. (2011). Peripherin partially localizes in Bunina bodies in amyotrophic lateral sclerosis. *J Neurol Sci* 302(1-2)**,** 14-18. doi: 10.1016/j.jns.2010.12.023.

Mori, K., Arzberger, T., Grässer, F.A., Gijselinck, I., May, S., Rentzsch, K., et al. (2013a). Bidirectional transcripts of the expanded C9orf72 hexanucleotide repeat are translated into aggregating dipeptide repeat proteins. *Acta Neuropathol* 126(6)**,** 881-893. doi: 10.1007/s00401-013-1189-3.

Mori, K., Weng, S.-M., Arzberger, T., May, S., Rentzsch, K., Kremmer, E., et al. (2013b). The C9orf72 GGGGCC Repeat Is Translated into Aggregating Dipeptide-Repeat Proteins in FTLD/ALS. *Science* 339(6125)**,** 1335-1338. doi: 10.1126/science.1232927.

Murayama, S., Mori, H., Ihara, Y., Bouldin, T.W., Suzuki, K., and Tomonaga, M. (1990). Immunocytochemical and ultrastructural studies of lower motor neurons in amyotrophic lateral sclerosis. *Annals of Neurology* 27(2)**,** 137-148. doi: https://doi.org/10.1002/ana.410270208.

Murphy, A.E., and Skene, N.G. (2022). A balanced measure shows superior performance of pseudobulk methods in single-cell RNA-sequencing analysis. *Nature Communications* 13(1)**,** 7851. doi: 10.1038/s41467-022-35519-4.

Nagai, M., Re, D.B., Nagata, T., Chalazonitis, A., Jessell, T.M., Wichterle, H., et al. (2007). Astrocytes expressing ALS-linked mutated SOD1 release factors selectively toxic to motor neurons. *Nat Neurosci* 10(5)**,** 615-622. doi: 10.1038/nn1876.

Nagy, D., Kato, T., and Kushner, P.D. (1994). Reactive astrocytes are widespread in the cortical gray matter of amyotrophic lateral sclerosis. *J Neurosci Res* 38(3)**,** 336-347. doi: 10.1002/jnr.490380312.

Naujock, M., Stanslowsky, N., Bufler, S., Naumann, M., Reinhardt, P., Sterneckert, J., et al. (2016). 4-Aminopyridine Induced Activity Rescues Hypoexcitable Motor Neurons from Amyotrophic Lateral Sclerosis Patient-Derived Induced Pluripotent Stem Cells. *STEM CELLS* 34(6)**,** 1563-1575. doi: 10.1002/stem.2354.

Naumann, M., Pal, A., Goswami, A., Lojewski, X., Japtok, J., Vehlow, A., et al. (2018). Impaired DNA damage response signaling by FUS-NLS mutations leads to neurodegeneration and FUS aggregate formation. *Nat Commun* 9(1)**,** 335. doi: 10.1038/s41467-017-02299-1.

Neumann, M., Sampathu Deepak, M., Kwong Linda, K., Truax Adam, C., Micsenyi Matthew, C., Chou Thomas, T., et al. (2006). Ubiquitinated TDP-43 in Frontotemporal Lobar Degeneration and Amyotrophic Lateral Sclerosis. *Science* 314(5796)**,** 130-133. doi: 10.1126/science.1134108.

Nguyen, M.D., Julien, J.P., and Rivest, S. (2001). Induction of proinflammatory molecules in mice with amyotrophic lateral sclerosis: no requirement for proapoptotic interleukin-1beta in neurodegeneration. *Ann Neurol* 50(5)**,** 630-639. doi: 10.1002/ana.1256.

Niblock, M., Smith, B.N., Lee, Y.-B., Sardone, V., Topp, S., Troakes, C., et al. (2016). Retention of hexanucleotide repeat-containing intron in C9orf72 mRNA: implications for the pathogenesis of ALS/FTD. *Acta neuropathologica communications* 4(1)**,** 1-12.

Nicholatos, J.W., Groot, J., Dhokai, S., Tran, D., Hrdlicka, L., Carlile, T.M., et al. (2021). SCD Inhibition Protects from α-Synuclein-Induced Neurotoxicity But Is Toxic to Early Neuron Cultures. *eNeuro* 8(4). doi: 10.1523/eneuro.0166-21.2021.

Nieto-Gonzalez, J.L., Moser, J., Lauritzen, M., Schmitt-John, T., and Jensen, K. (2011). Reduced GABAergic inhibition explains cortical hyperexcitability in the wobbler mouse model of ALS. *Cerebral Cortex* 21(3)**,** 625-635.

Nigro, M.J., Hashikawa-Yamasaki, Y., and Rudy, B. (2018). Diversity and Connectivity of Layer 5 Somatostatin-Expressing Interneurons in the Mouse Barrel Cortex. *The Journal of neuroscience : the official journal of the Society for Neuroscience* 38(7)**,** 1622-1633. doi: 10.1523/JNEUROSCI.2415-17.2017.

Nihei, K., McKee, A.C., and Kowall, N.W. (1993). Patterns of neuronal degeneration in the motor cortex of amyotrophic lateral sclerosis patients. *Acta Neuropathol* 86(1)**,** 55-64. doi: 10.1007/bf00454899.

Nimmerjahn, A., Kirchhoff, F., and Helmchen, F. (2005). Resting microglial cells are highly dynamic surveillants of brain parenchyma in vivo. *Science* 308(5726)**,** 1314-1318. doi: 10.1126/science.1110647.

Nishitoh, H., Kadowaki, H., Nagai, A., Maruyama, T., Yokota, T., Fukutomi, H., et al. (2008). ALS-linked mutant SOD1 induces ER stress-and ASK1-dependent motor neuron death by targeting Derlin-1. *Genes & development* 22(11)**,** 1451-1464.

Nonaka, T., Arai, T., Buratti, E., Baralle, F.E., Akiyama, H., and Hasegawa, M. (2009). Phosphorylated and ubiquitinated TDP-43 pathological inclusions in ALS and FTLD-U are recapitulated in SH-SY5Y cells. *FEBS Lett* 583(2)**,** 394-400. doi: 10.1016/j.febslet.2008.12.031.

Nonaka, T., Suzuki, G., Tanaka, Y., Kametani, F., Hirai, S., Okado, H., et al. (2016). Phosphorylation of TAR DNA-binding Protein of 43 kDa (TDP-43) by Truncated Casein Kinase 1δ Triggers Mislocalization and Accumulation of TDP-43 *. *Journal of Biological Chemistry* 291(11)**,** 5473-5483. doi: 10.1074/jbc.M115.695379.

Nowicka, N., Szymańska, K., Juranek, J., Zglejc-Waszak, K., Korytko, A., Załęcki, M., et al. (2022). The Involvement of RAGE and Its Ligands during Progression of ALS in SOD1 G93A Transgenic Mice. *Int J Mol Sci* 23(4). doi: 10.3390/ijms23042184.

Nussbacher, J.K., Tabet, R., Yeo, G.W., and Lagier-Tourenne, C. (2019). Disruption of RNA Metabolism in Neurological Diseases and Emerging Therapeutic Interventions. *Neuron* 102(2)**,** 294-320. doi: https://doi.org/10.1016/j.neuron.2019.03.014.

Okamoto, K., Mizuno, Y., and Fujita, Y. (2008). Bunina bodies in amyotrophic lateral sclerosis. *Neuropathology* 28(2)**,** 109-115. doi: 10.1111/j.1440-1789.2007.00873.x.

Ou, S.H., Wu, F., Harrich, D., García-Martínez, L.F., and Gaynor, R.B. (1995). Cloning and characterization of a novel cellular protein, TDP-43, that binds to human immunodeficiency virus type 1 TAR DNA sequence motifs. *J Virol* 69(6)**,** 3584-3596. doi: 10.1128/jvi.69.6.3584-3596.1995.

Özdinler, P.H., Benn, S., Yamamoto, T.H., Güzel, M., Brown, R.H., and Macklis, J.D. (2011). Corticospinal motor neurons and related subcerebral projection neurons undergo early and specific neurodegeneration in hSOD1G^{93}A transgenic ALS mice. *The Journal of neuroscience : the official journal of the Society for Neuroscience* 31(11)**,** 4166–4177. doi: 10.1523/jneurosci.4184-10.2011.

Paganoni, S., Hendrix, S., Dickson, S.P., Knowlton, N., Macklin, E.A., Berry, J.D., et al. (2021). Long-term survival of participants in the CENTAUR trial of sodium phenylbutyrate-taurursodiol in amyotrophic lateral sclerosis. *Muscle Nerve* 63(1)**,** 31-39. doi: 10.1002/mus.27091.

Pandey, S., Shen, K., Lee, S.H., Shen, Y.A., Wang, Y., Otero-García, M., et al. (2022). Disease-associated oligodendrocyte responses across neurodegenerative diseases. *Cell Rep* 40(8)**,** 111189. doi: 10.1016/j.celrep.2022.111189.

Pardo, A.C., Wong, V., Benson, L.M., Dykes, M., Tanaka, K., Rothstein, J.D., et al. (2006). Loss of the astrocyte glutamate transporter GLT1 modifies disease in SOD1(G93A) mice. *Exp Neurol* 201(1)**,** 120-130. doi: 10.1016/j.expneurol.2006.03.028.

Pasinelli, P., and Brown, R.H. (2006). Molecular biology of amyotrophic lateral sclerosis: insights from genetics. *Nat Rev Neurosci* 7(9)**,** 710-723. doi: 10.1038/nrn1971.

Peng, Q., Zhang, G., Guo, X., Dai, L., Xiong, M., Zhang, Z., et al. (2022). Galectin-9/Tim-3 pathway mediates dopaminergic neurodegeneration in MPTP-induced mouse model of Parkinson's disease. *Front Mol Neurosci* 15**,** 1046992. doi: 10.3389/fnmol.2022.1046992.

Perkins, E.M., Burr, K., Banerjee, P., Mehta, A.R., Dando, O., Selvaraj, B.T., et al. (2021). Altered network properties in C9ORF72 repeat expansion cortical neurons are due to synaptic dysfunction. *Molecular neurodegeneration* 16(1)**,** 13-13. doi: 10.1186/s13024-021-00433-8.

Perry, T.L., Krieger, C., Hansen, S., and Eisen, A. (1990). Amyotrophic lateral sclerosis: amino acid levels in plasma and cerebrospinal fluid. *Ann Neurol* 28(1)**,** 12-17. doi: 10.1002/ana.410280105.

Petri, S., Krampfl, K., Hashemi, F., Grothe, C., Hori, A., Dengler, R., et al. (2003). Distribution of GABAA receptor mRNA in the motor cortex of ALS patients. *J Neuropathol Exp Neurol* 62(10)**,** 1041-1051. doi: 10.1093/jnen/62.10.1041.

Philips, T., Bento-Abreu, A., Nonneman, A., Haeck, W., Staats, K., Geelen, V., et al. (2013). Oligodendrocyte dysfunction in the pathogenesis of amyotrophic lateral sclerosis. *Brain* 136(2)**,** 471-482. doi: 10.1093/brain/aws339.

Pi, H.J., Hangya, B., Kvitsiani, D., Sanders, J.I., Huang, Z.J., and Kepecs, A. (2013). Cortical interneurons that specialize in disinhibitory control. *Nature* 503(7477)**,** 521-524. doi: 10.1038/nature12676.

Pieri, M. (2003). Altered excitability of motor neurons in a transgenic mouse model of familial amyotrophic lateral sclerosis. *Neuroscience Letters*. doi: 10.1016/s0304-3940(03)00945-5.

Pineda, S.S., Lee, H., Ulloa-Navas, M.J., Linville, R.M., Garcia, F.J., Galani, K., et al. (2024). Single-cell dissection of the human motor and prefrontal cortices in ALS and FTLD. *Cell* 187(8)**,** 1971-1989.e1916. doi: 10.1016/j.cell.2024.02.031.

Pivovarova, N.B., and Andrews, S.B. (2010). Calcium-dependent mitochondrial function and dysfunction in neurons. *Febs j* 277(18)**,** 3622-3636. doi: 10.1111/j.1742-4658.2010.07754.x.

Polymenidou, M., Lagier-Tourenne, C., Hutt, K.R., Bennett, C.F., Cleveland, D.W., and Yeo, G.W. (2012). Misregulated RNA processing in amyotrophic lateral sclerosis. *Brain Research* 1462**,** 3-15. doi: https://doi.org/10.1016/j.brainres.2012.02.059.

Polymenidou, M., Lagier-Tourenne, C., Hutt, K.R., Huelga, S.C., Moran, J., Liang, T.Y., et al. (2011). Long pre-mRNA depletion and RNA missplicing contribute to neuronal vulnerability from loss of TDP-43. *Nat Neurosci* 14(4)**,** 459-468. doi: 10.1038/nn.2779.

Prasad, A., Bharathi, V., Sivalingam, V., Girdhar, A., and Patel, B.K. (2019). Molecular Mechanisms of TDP-43 Misfolding and Pathology in Amyotrophic Lateral Sclerosis. *Front Mol Neurosci* 12**,** 25. doi: 10.3389/fnmol.2019.00025.

Prönneke, A., Scheuer, B., Wagener, R.J., Möck, M., Witte, M., and Staiger, J.F. (2015). Characterizing VIP neurons in the barrel cortex of VIPcre/tdTomato mice reveals layer-specific differences. *Cerebral cortex* 25(12)**,** 4854-4868.

Qian, K., Huang, H., Peterson, A., Hu, B., Maragakis, N.J., Ming, G.-L., et al. (2017). Sporadic ALS Astrocytes Induce Neuronal Degeneration In Vivo. *Stem cell reports* 8(4)**,** 843–855. doi: 10.1016/j.stemcr.2017.03.003.

Qiu, X., Mao, Q., Tang, Y., Wang, L., Chawla, R., Pliner, H.A., et al. (2017). Reversed graph embedding resolves complex single-cell trajectories. *Nat Methods* 14(10)**,** 979-982. doi: 10.1038/nmeth.4402.

Quek, H., Cuní-López, C., Stewart, R., Colletti, T., Notaro, A., Nguyen, T.H., et al. (2022). ALS monocyte-derived microglia-like cells reveal cytoplasmic TDP-43 accumulation, DNA damage, and cell-specific impairment of phagocytosis associated with disease progression. *Journal of Neuroinflammation* 19(1)**,** 58. doi: 10.1186/s12974-022-02421-1.

Raffaele, S., Boccazzi, M., and Fumagalli, M. (2021). Oligodendrocyte Dysfunction in Amyotrophic Lateral Sclerosis: Mechanisms and Therapeutic Perspectives. *Cells* 10(3). doi: 10.3390/cells10030565.

Ransohoff, R.M. (2016). How neuroinflammation contributes to neurodegeneration. *Science* 353(6301)**,** 777-783. doi: 10.1126/science.aag2590.

Ratti, A., and Buratti, E. (2016). Physiological functions and pathobiology of TDP-43 and FUS/TLS proteins. *J Neurochem* 138 Suppl 1**,** 95-111. doi: 10.1111/jnc.13625.

Reaume, A.G., Elliott, J.L., Hoffman, E.K., Kowall, N.W., Ferrante, R.J., Siwek, D.F., et al. (1996). Motor neurons in Cu/Zn superoxide dismutase-deficient mice develop normally but exhibit enhanced cell death after axonal injury. *Nat Genet* 13(1)**,** 43-47. doi: 10.1038/ng0596-43.

Renton, A.E., Chiò, A., and Traynor, B.J. (2014). State of play in amyotrophic lateral sclerosis genetics. *Nature neuroscience* 17(1)**,** 17–23. doi: 10.1038/nn.3584.

Ringholz, G.M., Appel, S.H., Bradshaw, M., Cooke, N.A., Mosnik, D.M., and Schulz, P.E. (2005). Prevalence and patterns of cognitive impairment in sporadic ALS. *Neurology* 65(4)**,** 586-590. doi: 10.1212/01.wnl.0000172911.39167.b6.

Rivara, C.B., Sherwood, C.C., Bouras, C., and Hof, P.R. (2003). Stereologic characterization and spatial distribution patterns of Betz cells in the human primary motor cortex. *Anat Rec A Discov Mol Cell Evol Biol* 270(2)**,** 137-151. doi: 10.1002/ar.a.10015.

Rodrigues, C.M., Solá, S., Sharpe, J.C., Moura, J.J., and Steer, C.J. (2003). Tauroursodeoxycholic acid prevents Bax-induced membrane perturbation and cytochrome C release in isolated mitochondria. *Biochemistry* 42(10)**,** 3070-3080. doi: 10.1021/bi026979d.

Román, G.C. (1996). Neuroepidemiology of amyotrophic lateral sclerosis: clues to aetiology and pathogenesis. *J Neurol Neurosurg Psychiatry* 61(2)**,** 131-137. doi: 10.1136/jnnp.61.2.131.

Rosen, D.R., Siddique, T., Patterson, D., Figlewicz, D.A., Sapp, P., Hentati, A., et al. (1993). Mutations in Cu/Zn superoxide dismutase gene are associated with familial amyotrophic lateral sclerosis. *Nature* 362(6415)**,** 59-62. doi: 10.1038/362059a0.

Rothstein, J.D. (2017). Edaravone: A new drug approved for ALS. *Cell* 171(4)**,** 725. doi: 10.1016/j.cell.2017.10.011.

Rothstein, J.D., Martin, L.J., and Kuncl, R.W. (1992). Decreased glutamate transport by the brain and spinal cord in amyotrophic lateral sclerosis. *N Engl J Med* 326(22)**,** 1464-1468. doi: 10.1056/nejm199205283262204.

Rothstein, J.D., Tsai, G., Kuncl, R.W., Clawson, L., Cornblath, D.R., Drachman, D.B., et al. (1990). Abnormal excitatory amino acid metabolism in amyotrophic lateral sclerosis. *Ann Neurol* 28(1)**,** 18-25. doi: 10.1002/ana.410280106.

Rothstein, J.D., Van Kammen, M., Levey, A.I., Martin, L.J., and Kuncl, R.W. (1995). Selective loss of glial glutamate transporter GLT-1 in amyotrophic lateral sclerosis. *Ann Neurol* 38(1)**,** 73-84. doi: 10.1002/ana.410380114.

Rudy, B., Fishell, G., Lee, S., and Hjerling-Leffler, J. (2011). Three groups of interneurons account for nearly 100% of neocortical GABAergic neurons. *Developmental Neurobiology* 71(1)**,** 45-61. doi: 10.1002/dneu.20853.

Ruegsegger, C., and Saxena, S. (2016). Proteostasis impairment in ALS. *Brain Res* 1648(Pt B)**,** 571-579. doi: 10.1016/j.brainres.2016.03.032.

Ruffo, P., Perrone, B., and Conforti, F.L. (2022). SOD-1 Variants in Amyotrophic Lateral Sclerosis: Systematic Re-Evaluation According to ACMG-AMP Guidelines. *Genes (Basel)* 13(3). doi: 10.3390/genes13030537.

Ryan, S.K., Zelic, M., Han, Y., Teeple, E., Chen, L., Sadeghi, M., et al. (2023). Microglia ferroptosis is regulated by SEC24B and contributes to neurodegeneration. *Nature Neuroscience* 26(1)**,** 12-26. doi: 10.1038/s41593-022-01221-3.

Saba, L., Viscomi, M., Caioli, S., Pignataro, A., Bisicchia, E., Pieri, M., et al. (2016). Altered functionality, morphology, and vesicular glutamate transporter expression of cortical motor neurons from a presymptomatic mouse model of amyotrophic lateral sclerosis. *Cerebral cortex* 26(4)**,** 1512-1528.

Saberi, S., Stauffer, J.E., Schulte, D.J., and Ravits, J. (2015). Neuropathology of Amyotrophic Lateral Sclerosis and Its Variants. *Neurol Clin* 33(4)**,** 855-876. doi: 10.1016/j.ncl.2015.07.012.

Saccon, R.A., Bunton-Stasyshyn, R.K., Fisher, E.M., and Fratta, P. (2013). Is SOD1 loss of function involved in amyotrophic lateral sclerosis? *Brain* 136(Pt 8)**,** 2342-2358. doi: 10.1093/brain/awt097.

Saez-Atienzar, S., Bandres-Ciga, S., Langston, R.G., Kim, J.J., Choi, S.W., Reynolds, R.H., et al. (2021). Genetic analysis of amyotrophic lateral sclerosis identifies contributing pathways and cell types. *Sci Adv* 7(3). doi: 10.1126/sciadv.abd9036.

Safari, M.-S., Mirnajafi-Zadeh, J., Hioki, H., and Tsumoto, T. (2017). Parvalbumin-expressing interneurons can act solo while somatostatin-expressing interneurons act in chorus in

most cases on cortical pyramidal cells. *Scientific Reports* 7(1)**,** 12764. doi: 10.1038/s41598-017-12958-4.

Salta, E., and De Strooper, B. (2017). Noncoding RNAs in neurodegeneration. *Nat Rev Neurosci* 18(10)**,** 627-640. doi: 10.1038/nrn.2017.90.

Samadhiya, S., Sardana, V., Bhushan, B., Maheshwari, D., Goyal, R., and Pankaj (2022). Assessment of Therapeutic Response of Edaravone and Riluzole Combination Therapy in Amyotrophic Lateral Sclerosis Patients. *Ann Indian Acad Neurol* 25(4)**,** 692-697. doi: 10.4103/aian.aian_1083_21.

Sareen, D., O'Rourke, J.G., Meera, P., Muhammad, A.K.M.G., Grant, S., Simpkinson, M., et al. (2013). Targeting RNA foci in iPSC-derived motor neurons from ALS patients with a C9ORF72 repeat expansion. *Science translational medicine* 5(208)**,** 208ra149-208ra149. doi: 10.1126/scitranslmed.3007529.

Saris, C.G., Groen, E.J., Koekkoek, J.A., Veldink, J.H., and van den Berg, L.H. (2013). Meta-analysis of gene expression profiling in amyotrophic lateral sclerosis: a comparison between transgenic mouse models and human patients. *Amyotroph Lateral Scler Frontotemporal Degener* 14(3)**,** 177-189. doi: 10.3109/21678421.2012.729842.

Sasaguri, H., Chew, J., Xu, Y.F., Gendron, T.F., Garrett, A., Lee, C.W., et al. (2016). The extreme N-terminus of TDP-43 mediates the cytoplasmic aggregation of TDP-43 and associated toxicity in vivo. *Brain Res* 1647**,** 57-64. doi: 10.1016/j.brainres.2016.04.069.

Sau, D., De Biasi, S., Vitellaro-Zuccarello, L., Riso, P., Guarnieri, S., Porrini, M., et al. (2007). Mutation of SOD1 in ALS: a gain of a loss of function. *Human molecular genetics* 16(13)**,** 1604-1618.

Sawada, H. (2017). Clinical efficacy of edaravone for the treatment of amyotrophic lateral sclerosis. *Expert Opinion on Pharmacotherapy* 18(7)**,** 735-738.

Schafer, D.P., Lehrman, E.K., and Stevens, B. (2013). The "quad-partite" synapse: microglia-synapse interactions in the developing and mature CNS. *Glia* 61(1)**,** 24-36. doi: 10.1002/glia.22389.

Schiffer, D., Cordera, S., Cavalla, P., and Migheli, A. (1996). Reactive astrogliosis of the spinal cord in amyotrophic lateral sclerosis. *J Neurol Sci* 139 Suppl**,** 27-33. doi: 10.1016/0022-510x(96)00073-1.

Schön, M., Mousa, A., Berk, M., Chia, W.L., Ukropec, J., Majid, A., et al. (2019). The Potential of Carnosine in Brain-Related Disorders: A Comprehensive Review of Current Evidence. *Nutrients* 11(6). doi: 10.3390/nu11061196.

Schroeder, A., Mueller, O., Stocker, S., Salowsky, R., Leiber, M., Gassmann, M., et al. (2006). The RIN: an RNA integrity number for assigning integrity values to RNA measurements. *BMC Molecular Biology* 7(1)**,** 3. doi: 10.1186/1471-2199-7-3.

Schulthess, I., Gorges, M., Müller, H., Lulé, D., Del Tredici, K., Ludolph, A., et al. (2016). Functional connectivity changes resemble patterns of pTDP-43 pathology in amyotrophic lateral sclerosis. *Scientific reports* 6(1). doi: 10.1038/srep38391.

Selvaraj, B.T., Livesey, M.R., Zhao, C., Gregory, J.M., James, O.T., Cleary, E.M., et al. (2018). C9ORF72 repeat expansion causes vulnerability of motor neurons to Ca2+-permeable AMPA receptor-mediated excitotoxicity. *Nature Communications* 9(1)**,** 347. doi: 10.1038/s41467-017-02729-0.

Shaw, P.J., Forrest, V., Ince, P.G., Richardson, J.P., and Wastell, H.J. (1995). CSF and Plasma Amino Acid Levels in Motor Neuron Disease: Elevation of CSF Glutamate in a Subset of Patients. *Neurodegeneration* 4(2)**,** 209-216. doi: https://doi.org/10.1006/neur.1995.0026.

Shelkovnikova, T.A., Kukharsky, M.S., An, H., Dimasi, P., Alexeeva, S., Shabir, O., et al. (2018). Protective paraspeckle hyper-assembly downstream of TDP-43 loss of function in amyotrophic lateral sclerosis. *Mol Neurodegener* 13(1)**,** 30. doi: 10.1186/s13024-018-0263-7.

Sherwood, C.C., Raghanti, M.A., Stimpson, C.D., Spocter, M.A., Uddin, M., Boddy, A.M., et al. (2010). Inhibitory interneurons of the human prefrontal cortex display conserved evolution of the phenotype and related genes. *Proc Biol Sci* 277(1684)**,** 1011-1020. doi: 10.1098/rspb.2009.1831.

Shiina, Y., Arima, K., Tabunoki, H., and Satoh, J. (2010). TDP-43 dimerizes in human cells in culture. *Cell Mol Neurobiol* 30(4)**,** 641-652. doi: 10.1007/s10571-009-9489-9.

Shin, Y., and Brangwynne, C.P. (2017). Liquid phase condensation in cell physiology and disease. *Science* 357(6357). doi: 10.1126/science.aaf4382.

Sinner, P., Peckert-Maier, K., Mohammadian, H., Kuhnt, C., Draßner, C., Panagiotakopoulou, V., et al. (2023). Microglial expression of CD83 governs cellular activation and restrains neuroinflammation in experimental autoimmune encephalomyelitis. *Nat Commun* 14(1)**,** 4601. doi: 10.1038/s41467-023-40370-2.

Sleigh, J.N., Tosolini, A.P., Gordon, D., Devoy, A., Fratta, P., Fisher, E.M.C., et al. (2020). Mice Carrying ALS Mutant TDP-43, but Not Mutant FUS, Display In Vivo Defects in Axonal Transport of Signaling Endosomes. *Cell Rep* 30(11)**,** 3655-3662.e3652. doi: 10.1016/j.celrep.2020.02.078.

Smeyers, J., Banchi, E.-G., and Latouche, M. (2021). C9ORF72: What it is, what it does, and why it matters. *Frontiers in Cellular Neuroscience* 15.

Smukowski, S., Maioli, H., Latimer, C.S., Bird, T.D., Jayadev, S., and Valdmanis, P.N. (2022). Progress in Amyotrophic Lateral Sclerosis Gene Discovery. *Neurology Genetics* 8(3)**,** e669. doi: 10.1212/NXG.0000000000000669.

Sonntag, K.C., Tejada, G., Subburaju, S., Berretta, S., Benes, F.M., and Woo, T.U. (2016). Limited predictability of postmortem human brain tissue quality by RNA integrity numbers. *J Neurochem* 138(1)**,** 53-59. doi: 10.1111/jnc.13637.

Spielman, L.J., Bahniwal, M., Little, J.P., Walker, D.G., and Klegeris, A. (2015). Insulin Modulates In Vitro Secretion of Cytokines and Cytotoxins by Human Glial Cells. *Curr Alzheimer Res* 12(7)**,** 684-693. doi: 10.2174/1567205012666150710104428.

Spiller, K.J., Restrepo, C.R., Khan, T., Dominique, M.A., Fang, T.C., Canter, R.G., et al. (2018). Microglia-mediated recovery from ALS-relevant motor neuron degeneration in a mouse model of TDP-43 proteinopathy. *Nature Neuroscience* 21(3)**,** 329-340. doi: 10.1038/s41593-018-0083-7.

Spuch, C., Ortolano, S., and Navarro, C. (2012). LRP-1 and LRP-2 receptors function in the membrane neuron. Trafficking mechanisms and proteolytic processing in Alzheimer's disease. *Front Physiol* 3**,** 269. doi: 10.3389/fphys.2012.00269.

Squair, J.W., Gautier, M., Kathe, C., Anderson, M.A., James, N.D., Hutson, T.H., et al. (2021). Confronting false discoveries in single-cell differential expression. *Nature Communications* 12(1)**,** 5692. doi: 10.1038/s41467-021-25960-2.

Steinacker, P., Verde, F., Fang, L., Feneberg, E., Oeckl, P., Roeber, S., et al. (2018). Chitotriosidase (CHIT1) is increased in microglia and macrophages in spinal cord of amyotrophic lateral sclerosis and cerebrospinal fluid levels correlate with disease severity and progression. *J Neurol Neurosurg Psychiatry* 89(3)**,** 239-247. doi: 10.1136/jnnp-2017-317138.

Steinruecke, M., Lonergan, R.M., Selvaraj, B.T., Chandran, S., Diaz-Castro, B., and Stavrou, M. (2023). Blood-CNS barrier dysfunction in amyotrophic lateral sclerosis: Proposed

mechanisms and clinical implications. *J Cereb Blood Flow Metab* 43(5)**,** 642-654. doi: 10.1177/0271678x231153281.

Stoica, R., De Vos, K.J., Paillusson, S., Mueller, S., Sancho, R.M., Lau, K.-F., et al. (2014). ER–mitochondria associations are regulated by the VAPB–PTPIP51 interaction and are disrupted by ALS/FTD-associated TDP-43. *Nature Communications* 5(1)**,** 3996. doi: 10.1038/ncomms4996.

Strong, M.J., Volkening, K., Hammond, R., Yang, W., Strong, W., Leystra-Lantz, C., et al. (2007). TDP43 is a human low molecular weight neurofilament (hNFL) mRNA-binding protein. *Mol Cell Neurosci* 35(2)**,** 320-327. doi: 10.1016/j.mcn.2007.03.007.

Suaud, L., Miller, K., Panichelli, A.E., Randell, R.L., Marando, C.M., and Rubenstein, R.C. (2011). 4-Phenylbutyrate stimulates Hsp70 expression through the Elp2 component of elongator and STAT-3 in cystic fibrosis epithelial cells. *J Biol Chem* 286(52)**,** 45083-45092. doi: 10.1074/jbc.M111.293282.

Suk, K. (2016). Lipocalin-2 as a therapeutic target for brain injury: An astrocentric perspective. *Prog Neurobiol* 144**,** 158-172. doi: 10.1016/j.pneurobio.2016.08.001.

Sun, Y., Curle, A.J., Haider, A.M., and Balmus, G. (2020). The role of DNA damage response in amyotrophic lateral sclerosis. *Essays Biochem* 64(5)**,** 847-861. doi: 10.1042/ebc20200002.

Svensson, V., Vento-Tormo, R., and Teichmann, S.A. (2018). Exponential scaling of single-cell RNA-seq in the past decade. *Nature Protocols* 13(4)**,** 599-604. doi: 10.1038/nprot.2017.149.

Takahashi, H., Snow, B., Bhatt, M.H., Peppard, R., Eisen, A., and Calne, D.B. (1993). Evidence for a dopaminergic deficit in sporadic amyotrophic lateral sclerosis on positron emission scanning. *The Lancet* 342(8878)**,** 1016-1018.

Tam, O.H., Rozhkov, N.V., Shaw, R., Kim, D., Hubbard, I., Fennessey, S., et al. (2019). Postmortem Cortex Samples Identify Distinct Molecular Subtypes of ALS: Retrotransposon Activation, Oxidative Stress, and Activated Glia. *Cell Rep* 29(5)**,** 1164-1177 e1165. doi: 10.1016/j.celrep.2019.09.066.

Tamamaki, N., Yanagawa, Y., Tomioka, R., Miyazaki, J.I., Obata, K., and Kaneko, T. (2003). Green fluorescent protein expression and colocalization with calretinin, parvalbumin, and somatostatin in the GAD67-GFP knock-in mouse. *Journal of Comparative Neurology* 467(1)**,** 60-79.

Tang, F., Barbacioru, C., Wang, Y., Nordman, E., Lee, C., Xu, N., et al. (2009). mRNA-Seq whole-transcriptome analysis of a single cell. *Nat Methods* 6(5)**,** 377-382. doi: 10.1038/nmeth.1315.

Taylor, J.P., Brown, R.H., Jr., and Cleveland, D.W. (2016). Decoding ALS: from genes to mechanism. *Nature* 539(7628)**,** 197-206. doi: 10.1038/nature20413.

Thompson, A.G., Gray, E., Bampton, A., Raciborska, D., Talbot, K., and Turner, M.R. (2019). CSF chitinase proteins in amyotrophic lateral sclerosis. *J Neurol Neurosurg Psychiatry* 90(11)**,** 1215-1220. doi: 10.1136/jnnp-2019-320442.

Tollervey, J.R., Curk, T., Rogelj, B., Briese, M., Cereda, M., Kayikci, M., et al. (2011). Characterizing the RNA targets and position-dependent splicing regulation by TDP-43. *Nature neuroscience* 14(4)**,** 452-458.

Trapnell, C., Cacchiarelli, D., Grimsby, J., Pokharel, P., Li, S., Morse, M., et al. (2014). The dynamics and regulators of cell fate decisions are revealed by pseudotemporal ordering of single cells. *Nat Biotechnol* 32(4)**,** 381-386. doi: 10.1038/nbt.2859.

Tripathi, P., Rodriguez-Muela, N., Klim, J.R., de Boer, A.S., Agrawal, S., Sandoe, J., et al. (2017). Reactive Astrocytes Promote ALS-like Degeneration and Intracellular Protein

Aggregation in Human Motor Neurons by Disrupting Autophagy through TGF-β1. *Stem Cell Reports* 9(2)**,** 667-680. doi: 10.1016/j.stemcr.2017.06.008.

Tseng, H.Y., Thorausch, N., Ziegler, T., Meves, A., Fässler, R., and Böttcher, R.T. (2014). Sorting nexin 31 binds multiple β integrin cytoplasmic domains and regulates β1 integrin surface levels and stability. *J Mol Biol* 426(18)**,** 3180-3194. doi: 10.1016/j.jmb.2014.07.003.

Türei, D., Valdeolivas, A., Gul, L., Palacio-Escat, N., Klein, M., Ivanova, O., et al. (2021). Integrated intra- and intercellular signaling knowledge for multicellular omics analysis. *Mol Syst Biol* 17(3)**,** e9923. doi: 10.15252/msb.20209923.

Turgut, N., Varol SaraÇoglu, G., Kat, S., Balci, K., GÜldiken, B., Birgili, O., et al. (2019). An epidemiologic investigation of amyotrophic lateral sclerosis in Thrace, Turkey, 2006–2010. *Amyotrophic Lateral Sclerosis and Frontotemporal Degeneration* 20(1-2)**,** 100-106.

Turner, M.R., Cagnin, A., Turkheimer, F.E., Miller, C.C., Shaw, C.E., Brooks, D.J., et al. (2004). Evidence of widespread cerebral microglial activation in amyotrophic lateral sclerosis: an [11C](R)-PK11195 positron emission tomography study. *Neurobiol Dis* 15(3)**,** 601-609. doi: 10.1016/j.nbd.2003.12.012.

Tyzack, G.E., Luisier, R., Taha, D.M., Neeves, J., Modic, M., Mitchell, J.S., et al. (2019). Widespread FUS mislocalization is a molecular hallmark of amyotrophic lateral sclerosis. *Brain* 142(9)**,** 2572-2580. doi: 10.1093/brain/awz217.

Tzotzos, S., and Doig, A.J. (2010). Amyloidogenic sequences in native protein structures. *Protein Sci* 19(2)**,** 327-348. doi: 10.1002/pro.314.

Urrutia, P., Aguirre, P., Esparza, A., Tapia, V., Mena, N.P., Arredondo, M., et al. (2013). Inflammation alters the expression of DMT1, FPN1 and hepcidin, and it causes iron accumulation in central nervous system cells. *J Neurochem* 126(4)**,** 541-549. doi: 10.1111/jnc.12244.

Vahsen, B.F., Gray, E., Thompson, A.G., Ansorge, O., Anthony, D.C., Cowley, S.A., et al. (2021). Non-neuronal cells in amyotrophic lateral sclerosis - from pathogenesis to biomarkers. *Nat Rev Neurol* 17(6)**,** 333-348. doi: 10.1038/s41582-021-00487-8.

van Blitterswijk, M., Mullen, B., Wojtas, A., Heckman, M.G., Diehl, N.N., Baker, M.C., et al. (2014). Genetic modifiers in carriers of repeat expansions in the C9ORF72 gene. *Mol Neurodegener* 9**,** 38. doi: 10.1186/1750-1326-9-38.

Van den Bos, M.A., Higashihara, M., Geevasinga, N., Menon, P., Kiernan, M.C., and Vucic, S. (2018). Imbalance of cortical facilitatory and inhibitory circuits underlies hyperexcitability in ALS. *Neurology* 91(18)**,** e1669-e1676.

Van Den Bosch, L., Van Damme, P., Bogaert, E., and Robberecht, W. (2006). The role of excitotoxicity in the pathogenesis of amyotrophic lateral sclerosis. *Biochim Biophys Acta* 1762(11-12)**,** 1068-1082. doi: 10.1016/j.bbadis.2006.05.002.

van der Zee, J., Gijselinck, I., Dillen, L., Van Langenhove, T., Theuns, J., Engelborghs, S., et al. (2013). A pan-European study of the C9orf72 repeat associated with FTLD: geographic prevalence, genomic instability, and intermediate repeats. *Hum Mutat* 34(2)**,** 363-373. doi: 10.1002/humu.22244.

van Es, M.A., Veldink, J.H., Saris, C.G., Blauw, H.M., van Vught, P.W., Birve, A., et al. (2009). Genome-wide association study identifies 19p13.3 (UNC13A) and 9p21.2 as susceptibility loci for sporadic amyotrophic lateral sclerosis. *Nat Genet* 41(10)**,** 1083-1087. doi: 10.1038/ng.442.

Veres, J.M., Nagy, G.A., and Hájos, N. (2017). Perisomatic GABAergic synapses of basket cells effectively control principal neuron activity in amygdala networks. *eLife* 6**,** e20721. doi: 10.7554/eLife.20721.

Versluys, L., Ervilha Pereira, P., Schuermans, N., De Paepe, B., De Bleecker, J.L., Bogaert, E., et al. (2022). Expanding the TDP-43 Proteinopathy Pathway From Neurons to Muscle: Physiological and Pathophysiological Functions. *Frontiers in Neuroscience* 16.

von Ehr, A., Attaai, A., Neidert, N., Potru, P.S., Ruß, T., Zöller, T., et al. (2020). Inhibition of Microglial TGFβ Signaling Increases Expression of Mrc1. *Front Cell Neurosci* 14**,** 66. doi: 10.3389/fncel.2020.00066.

Vucic, S., Cheah, B.C., and Kiernan, M.C. (2009). Defining the mechanisms that underlie cortical hyperexcitability in amyotrophic lateral sclerosis. *Experimental neurology* 220(1)**,** 177-182.

Vucic, S., Menon, P., Huynh, W., Mahoney, C., Ho, K.S., Hartford, A., et al. (2023). Efficacy and safety of CNM-Au8 in amyotrophic lateral sclerosis (RESCUE-ALS study): a phase 2, randomised, double-blind, placebo-controlled trial and open label extension. *eClinicalMedicine* 60. doi: 10.1016/j.eclinm.2023.102036.

Vucic, S., Nicholson, G.A., and Kiernan, M.C. (2008). Cortical hyperexcitability may precede the onset of familial amyotrophic lateral sclerosis. *Brain* 131(Pt 6)**,** 1540-1550. doi: 10.1093/brain/awn071.

Vucic, S., Pavey, N., Haidar, M., Turner, B., and Kiernan, M. (2021). Cortical hyperexcitability: Diagnostic and pathogenic biomarker of ALS. *Neuroscience Letters* 759**,** 136039. doi: 10.1016/j.neulet.2021.136039.

Wainger, B.J., Kiskinis, E., Mellin, C., Wiskow, O., Han, S.S.W., Sandoe, J., et al. (2014). Intrinsic membrane hyperexcitability of amyotrophic lateral sclerosis patient-derived motor neurons. *Cell reports* 7(1)**,** 1–11. doi: 10.1016/j.celrep.2014.03.019.

Walker, A.K., Spiller, K.J., Ge, G., Zheng, A., Xu, Y., Zhou, M., et al. (2015). Functional recovery in new mouse models of ALS/FTLD after clearance of pathological cytoplasmic TDP-43. *Acta Neuropathol* 130(5)**,** 643-660. doi: 10.1007/s00401-015-1460-x.

Wang, I.F., Wu, L.S., Chang, H.Y., and Shen, C.K. (2008). TDP-43, the signature protein of FTLD-U, is a neuronal activity-responsive factor. *J Neurochem* 105(3)**,** 797-806. doi: 10.1111/j.1471-4159.2007.05190.x.

Wang, J., Ho, W.Y., Lim, K., Feng, J., Tucker-Kellogg, G., Nave, K.A., et al. (2018). Cell-autonomous requirement of TDP-43, an ALS/FTD signature protein, for oligodendrocyte survival and myelination. *Proc Natl Acad Sci U S A* 115(46)**,** E10941-e10950. doi: 10.1073/pnas.1809821115.

Wang, M., Gan, J., Han, C., Guo, Y., Chen, K., Shi, Y.-z., et al. 2022a. Imputation Methods for scRNA Sequencing Data. *Applied Sciences* [Online], 12(20).

Wang, S., Sudan, R., Peng, V., Zhou, Y., Du, S., Yuede, C.M., et al. (2022b). TREM2 drives microglia response to amyloid-β via SYK-dependent and -independent pathways. *Cell* 185(22)**,** 4153-4169.e4119. doi: 10.1016/j.cell.2022.09.033.

Wang, W., Wang, L., Lu, J., Siedlak, S.L., Fujioka, H., Liang, J., et al. (2016). The inhibition of TDP-43 mitochondrial localization blocks its neuronal toxicity. *Nat Med* 22(8)**,** 869-878. doi: 10.1038/nm.4130.

Wave Life Sciences (2023). "Wave Life Sciences Announces Topline Results from Phase 1b/2a FOCUS-C9 Study of WVE-004 for C9orf72-associated Amyotrophic Lateral Sclerosis and Frontotemporal Dementia".).

Wheaton, M.W., Salamone, A.R., Mosnik, D.M., McDonald, R.O., Appel, S.H., Schmolck, H.I., et al. (2007). Cognitive impairment in familial ALS. *Neurology* 69(14)**,** 1411-1417. doi: 10.1212/01.wnl.0000277422.11236.2c.

Wiese, S., Karus, M., and Faissner, A. (2012). Astrocytes as a source for extracellular matrix molecules and cytokines. *Front Pharmacol* 3**,** 120. doi: 10.3389/fphar.2012.00120.

Wiesenfarth, M., Dorst, J., Brenner, D., Elmas, Z., Parlak, Ö., Uzelac, Z., et al. (2024). Effects of tofersen treatment in patients with *SOD1*-ALS in a "real-world" setting – a 12-month multicenter cohort study from the German early access program. *eClinicalMedicine* 69. doi: 10.1016/j.eclinm.2024.102495.

Winkler, E.A., Sengillo, J.D., Sullivan, J.S., Henkel, J.S., Appel, S.H., and Zlokovic, B.V. (2013). Blood-spinal cord barrier breakdown and pericyte reductions in amyotrophic lateral sclerosis. (1432-0533 (Electronic)).

Winton, M.J., Van Deerlin, V.M., Kwong, L.K., Yuan, W., Wood, E.M., Yu, C.-E., et al. (2008). A90V TDP-43 variant results in the aberrant localization of TDP-43 in vitro. *FEBS Letters* 582(15)**,** 2252-2256. doi: https://doi.org/10.1016/j.febslet.2008.05.024.

Wong, C., Stavrou, M., Elliott, E., Gregory, J.M., Leigh, N., Pinto, A.A., et al. (2021). Clinical trials in amyotrophic lateral sclerosis: a systematic review and perspective. *Brain Commun* 3(4)**,** fcab242. doi: 10.1093/braincomms/fcab242.

Wood, K.C., Blackwell, J.M., and Geffen, M.N. (2017). Cortical inhibitory interneurons control sensory processing. *Current opinion in neurobiology* 46**,** 200-207.

Xiang, X., Werner, G., Bohrmann, B., Liesz, A., Mazaheri, F., Capell, A., et al. (2016). TREM2 deficiency reduces the efficacy of immunotherapeutic amyloid clearance. *EMBO Mol Med* 8(9)**,** 992-1004. doi: 10.15252/emmm.201606370.

Xiao, S., MacNair, L., McGoldrick, P., McKeever, P.M., McLean, J.R., Zhang, M., et al. (2015). Isoform-specific antibodies reveal distinct subcellular localizations of C9orf72 in amyotrophic lateral sclerosis. *Ann Neurol* 78(4)**,** 568-583. doi: 10.1002/ana.24469.

Xiao, S., McLean, J., and Robertson, J. (2006). Neuronal intermediate filaments and ALS: A new look at an old question. *Biochimica et Biophysica Acta (BBA) - Molecular Basis of Disease* 1762(11)**,** 1001-1012. doi: https://doi.org/10.1016/j.bbadis.2006.09.003.

Xie, M., Liu, Y.U., Zhao, S., Zhang, L., Bosco, D.B., Pang, Y.P., et al. (2022). TREM2 interacts with TDP-43 and mediates microglial neuroprotection against TDP-43-related neurodegeneration. *Nat Neurosci* 25(1)**,** 26-38. doi: 10.1038/s41593-021-00975-6.

Xie, Z., Bailey, A., Kuleshov, M.V., Clarke, D.J.B., Evangelista, J.E., Jenkins, S.L., et al. (2021). Gene Set Knowledge Discovery with Enrichr. *Curr Protoc* 1(3)**,** e90. doi: 10.1002/cpz1.90.

Yamanaka, K., Chun, S.J., Boillee, S., Fujimori-Tonou, N., Yamashita, H., Gutmann, D.H., et al. (2008). Astrocytes as determinants of disease progression in inherited amyotrophic lateral sclerosis. *Nature Neuroscience* 11(3)**,** 251-253. doi: 10.1038/nn2047.

Yang, B., Jiang, H., Wang, F., Li, S., Wu, C., Bao, J., et al. (2019). UNC13A variant rs12608932 is associated with increased risk of amyotrophic lateral sclerosis and reduced patient survival: a meta-analysis. *Neurol Sci* 40(11)**,** 2293-2302. doi: 10.1007/s10072-019-03951-y.

Zannas, A.S., Jia, M., Hafner, K., Baumert, J., Wiechmann, T., Pape, J.C., et al. (2019). Epigenetic upregulation of FKBP5 by aging and stress contributes to NF-κB-driven inflammation and cardiovascular risk. *Proc Natl Acad Sci U S A* 116(23)**,** 11370-11379. doi: 10.1073/pnas.1816847116.

Zhang, H., Tan, C.-F., Mori, F., Tanji, K., Kakita, A., Takahashi, H., et al. (2008). TDP-43-immunoreactive neuronal and glial inclusions in the neostriatum in amyotrophic lateral

sclerosis with and without dementia. *Acta Neuropathologica* 115(1)**,** 115-122. doi: 10.1007/s00401-007-0285-7.

Zhang, Q., Mao, C., Jin, J., Niu, C., Bai, L., Dang, J., et al. (2014). Side of limb-onset predicts laterality of gray matter loss in amyotrophic lateral sclerosis. *Biomed Res Int* 2014**,** 473250. doi: 10.1155/2014/473250.

Zhang, S., Li, X., Lin, J., Lin, Q., and Wong, K.C. (2023). Review of single-cell RNA-seq data clustering for cell-type identification and characterization. *Rna* 29(5)**,** 517-530. doi: 10.1261/rna.078965.121.

Zhang, W., Zhang, L., Liang, B., Schroeder, D., Zhang, Z.-w., Cox, G.A., et al. (2016a). Hyperactive somatostatin interneurons contribute to excitotoxicity in neurodegenerative disorders. *Nature neuroscience* 19(4)**,** 557–559. doi: 10.1038/nn.4257.

Zhang, W., Zhang, L., Liang, B., Schroeder, D., Zhang, Z.W., Cox, G.A., et al. (2016b). Hyperactive somatostatin interneurons contribute to excitotoxicity in neurodegenerative disorders. *Nat Neurosci* 19(4)**,** 557-559. doi: 10.1038/nn.4257.

Zhang, Y., Sloan, S.A., Clarke, L.E., Caneda, C., Plaza, C.A., Blumenthal, P.D., et al. (2016c). Purification and Characterization of Progenitor and Mature Human Astrocytes Reveals Transcriptional and Functional Differences with Mouse. *Neuron* 89(1)**,** 37-53. doi: 10.1016/j.neuron.2015.11.013.

Zhang, Y.J., Caulfield, T., Xu, Y.F., Gendron, T.F., Hubbard, J., Stetler, C., et al. (2013a). The dual functions of the extreme N-terminus of TDP-43 in regulating its biological activity and inclusion formation. *Hum Mol Genet* 22(15)**,** 3112-3122. doi: 10.1093/hmg/ddt166.

Zhang, Y.J., Xu, Y.F., Dickey, C.A., Buratti, E., Baralle, F., Bailey, R., et al. (2007). Progranulin mediates caspase-dependent cleavage of TAR DNA binding protein-43. *J Neurosci* 27(39)**,** 10530-10534. doi: 10.1523/jneurosci.3421-07.2007.

Zhang, Z., Almeida, S., Lu, Y., Nishimura, A.L., Peng, L., Sun, D., et al. (2013b). Downregulation of microRNA-9 in iPSC-derived neurons of FTD/ALS patients with TDP-43 mutations. *PLoS One* 8(10)**,** e76055. doi: 10.1371/journal.pone.0076055.

Zhao, M., Kim, J.R., van Bruggen, R., and Park, J. (2018). RNA-Binding Proteins in Amyotrophic Lateral Sclerosis. *Mol Cells* 41(9)**,** 818-829. doi: 10.14348/molcells.2018.0243.

Zhou, Y., Song, W.M., Andhey, P.S., Swain, A., Levy, T., Miller, K.R., et al. (2020). Human and mouse single-nucleus transcriptomics reveal TREM2-dependent and TREM2-independent cellular responses in Alzheimer's disease. *Nat Med* 26(1)**,** 131-142. doi: 10.1038/s41591-019-0695-9.

Ziemann, U., Winter, M., Reimers, C.D., Reimers, K., Tergau, F., and Paulus, W. (1997). Impaired motor cortex inhibition in patients with amyotrophic lateral sclerosis: evidence from paired transcranial magnetic stimulation. *Neurology* 49(5)**,** 1292-1298.

Zinszner, H., Sok, J., Immanuel, D., Yin, Y., and Ron, D. (1997). TLS (FUS) binds RNA in vivo and engages in nucleo-cytoplasmic shuttling. *Journal of cell science* 110(15)**,** 1741-1750.

Zong, B., Yu, F., Zhang, X., Pang, Y., Zhao, W., Sun, P., et al. (2023). Mechanosensitive Piezo1 channel in physiology and pathophysiology of the central nervous system. *Ageing Res Rev* 90**,** 102026. doi: 10.1016/j.arr.2023.102026.

Zou, Z.-Y., Zhou, Z.-R., Che, C.-H., Liu, C.-Y., He, R.-L., and Huang, H.-P. (2017). Genetic epidemiology of amyotrophic lateral sclerosis: a systematic review and meta-analysis. *Journal of Neurology, Neurosurgery & Psychiatry* 88(7)**,** 540-549.

Declaration of Author Contributions

The author produced all the presented results in this thesis, involving experimental design and the collection and analysis of experimental data (see below for exceptions).

Dr. Eduardo Beltrán supported optimization of nuclei sorting and library preparation. **Dr. Eduardo Beltrán** and **Klara Magdalena Eglseer** performed preprocessing of the snRNA-seq raw data and were involved in preliminary analyses.

Dr. med. Thomas Arzberger and technical staff of **Neurobiobank München**, assisted and performed anti-pTDP-43 and anti-HLA-DP+DQ+DR stainings.

Charlene-Annett Hurler performed human cortical tissue fixation, sectioning and scanning of immunohistological stainings.

XiaoQian Ye provided code to help with visualization of GO terms, performed bootstrapping of cell-cell interaction frequency data and implemented its statistical analysis.

Acknowledgements

I would like to express my sincere gratitude to Prof. Dr. Sabine Liebscher, my supervisor, for her extensive guidance and for granting me invaluable opportunities to contribute to numerous exciting projects within the lab and with many collaborators. I am thankful for her effort and support in my personal growth over the past five years not only as an advisor, but also as a mentor. My gratitude extends to the members of my thesis advisory committee, Prof. Dr. Dieter Edbauer, PD Dr. Florence Bareyre, Dr. Christian Mayer and Prof. Dr. Smita Saxena, for their constructive feedback and perspectives.

My thanks go to both present and past members of the Liebscher lab for making this journey exceptional. A special note of appreciation to XiaoQian and Shenyi for consistently being there for me during challenging times. I extend special thanks to Anastasia for her belief in me, and importantly, for always being willing to have a coffee with me.

I am thankful for the privilege of being a part of the Graduate School of Systemic Neurosciences (GSN) and for the invaluable opportunities they have offered. I am deeply appreciative of the unwavering support provided by the GSN staff. In particular, I would like to extend my sincere thanks to Lena Bittl and Stefanie Bosse for their immense help and encouraging presence, which have played a crucial role in my academic and personal development.

Finally, I express my heartfelt gratitude to my family and friends beyond the confines of the lab. My profound thanks go to my parents and sister, unwavering pillars of support who accompanied me at every juncture of this transformative journey. I extend my appreciation to my close friends, Ali and Inanna, steadfast companions throughout my time in Munich, infusing my life with unforgettable moments. Özlem and Merve, my dear friends, thank you for being my confidants and supporting me no matter what. I am profoundly grateful for the love and encouragement you provided.